Ghent University – Faculty of Sciences
Department of Biomedical Molecular Biology
Unit of Developmental Biology

WNT/β-CATENIN SIGNALING IN THE *XENOPUS* HINDBRAIN: DEVELOPMENT AND CANCER

RIVKA NOELANDERS

Thesis submitted in partial fulfillment of the requirements for the degree of
DOCTOR OF SCIENCE: BIOTECHNOLOGY

Promoter: Prof. Dr. Kris Vleminckx
2017-2018

The author of this work has been supported by the Research Foundation Flanders (FWO Vlaanderen) and Ghent University.
Cover photo courtesy of Hong Thi Tran and Eef Parthoens

WNT/β-CATENIN SIGNALING IN THE *XENOPUS* HINDBRAIN: DEVELOPMENT AND CANCER

By Rivka Noelanders

Unit of Developmental Biology
Department of Biomedical Molecular Biology
Faculty of Sciences
Ghent University
Technologiepark 927
BE-9052 Zwijnaarde

Promoter	Prof. Dr. Kris Vleminckx[1]
Examination Committee:	
Chairman	Prof. Dr. Rudi Beyaert[1,2]
Secretary	Prof. Dr. Geert Berx[1,3]
	Dr. Andy Willaert[4]
	Prof. Dr. Frank Speleman[3, 4]
	Prof. Dr. Eric Bellefroid[5]
	Prof. Dr. Ann Huysseune[6]
	Prof. Dr. Beatrice Durand[7]

[1] Department of Biomedical Molecular Biology, Ghent University, Belgium

[2] VIB Center for Inflammation Research, Ghent, Belgium

[3] Cancer Research Institute Ghent, Ghent University, Belgium

[4] Center for Medical Genetics, Ghent University, Belgium

[5] Département de Biologie Moléculaire, Université Libre de Bruxelles, Institute of Neuroscience, Gosselies, Belgium

[6] Evolutionary Developmental Biology Research Group, Department of Biology, Ghent University, Belgium

[7] Institut Curie; UMR 3387, Centre National de la Recherche Scientifique, Paris Sciences et Lettres Research University; Université Paris-Sud, France

DANKWOORD

Ik heb vier jaar lang gedacht dat dit moment nooit zou komen, maar plots was er dan toch licht aan het einde van de tunnel en is het tijd om alle mensen te bedanken zonder wie het afronden van dit doctoraat niet was mogelijk geweest.

Allereerst bedankt Kris om je vooroordelen over Biomedische wetenschappers even op zij te zetten en mij een plaatsje in je labo te geven. Ik heb enorm veel geleerd de voorbije vijf jaar en ben dankzij jou een betere wetenschapper geworden. Mijn lieve collega's waarvan ik de voorbije jaren al afscheid van heb moeten nemen: Griet, Hong en Tom, bedankt om mij met open armen te ontvangen en me op sleeptouw te nemen in het labo. Griet, jij hebt een ongelooflijk talent om iemand zich meteen welkom te doen voelen, bedankt om mij wegwijs te maken in het reilen en zeilan ven het IRC en je luisterend oor. Ik zal de koffiepauzes missen. Hong, thank you for your immensible knowledge about this crazy, frustrating creature called *Xenopus.* Bedankt Tom om al mijn saaie labmeetings met 100-den *in situ* foto's te doorstaan en te luisteren naar mijn eindeloze frustratie over het gebrek aan vooruitgang. Ik wens je veel geluk met je prachtige gezin en je nieuwe job. En dan de nieuwe garde: Thomas, Dionysia, Suzan, Dieter en Marjolein. Thomas, je passie voor wetenschappelijk onderzoek is inspirerend. Veel geluk met de laatste loodjes en hopelijk schop je het tot prof. Naert. Dionysia, I wish you all the best in the lab and especially outside of it. Stop stressing!!! Take it from me, it all works out in the end. Suzan, bedankt om mijn laatste loodje was lichter te maken. Dieter en Marjolein, veel geluk met jullie rit op de PhD rollercoaster. Ik wens jullie vele mooie embryo's, stressloze injectiesessies en absoluut geen onverklaarbare sterfgevallen. Ook een dikke merci aan Gert, voor alle hulp met mijn flow cytometrie experimenten, Marnik voor de statistiche hulp met de medulloblastoma datasets, de bioimaging core, het keukenpersoneel voor de constante aanvoer van RNAse vrije epjes en alle andere mensen die op een of andere manier hebben bijgedragen aan dit eindresultaat.

En dan zijn er ook nog de mensen buiten het labo dankzij wie ik mijn mentale gezondheid de voorbije 5 jaar min of meer heb weten te bewaren. Laurence, Lieselot, Nele, Dorien en Melanie bedankt om mijn studententijd onvergetelijk te maken en genoeg drank, lekker eten en gelach in mijn leven te brengen zodat stress en frustratie nooit de bovenhand kregen! Tim en Evelien bedankt voor de eindeloze jaren vriendschap, dat er nog vele epische Risk battles mogen volgen!

Mama en papa, het is een cliché maar zonder jullie had ik dit nooit kunnen bereiken. Bedankt om mij te steunen in alles wat ik doe en mij af en toe een duwtje in de juiste richting te geven. Mijn liefste Duchan enkel jij weet precies hoeveel bloed, zweet en bij momenten eigenlijk vooral tranen dit doctoraat mij gekost heeft. Bedankt voor je onvoorwaardelijke steun. Ik kijk er naar uit om samen verder de wereld te verkennen. Mijn lieve Lia, zonder dat je het beseft heb ook jij een kleine bijdrage aan dit werk geleverd. Bedankt om mijn zonnetje te zijn.

Rivka

GENERAL SUMMARY

The human body is a highly complex, but also highly robust system. From embryonic development to adult homeostasis, each process is highly regulated through instruction from molecular signaling pathways. Remarkably, there are only a limited number of signaling pathways that are reiteratively used throughout life. Not surprisingly, disruption of their signaling activity is associated with disease. Therefore a good understanding of the physiological function of these signaling pathways is essential as it can guide the search for tailored therapies to treat human disorders.

One of these key developmental signaling pathways is the Wnt/β-catenin signaling pathway. In this work we sought to widen the insight in this important signaling pathway in a specific part of the body, the hindbrain, both during normal embryonic development as during disease, namely cancer.

The hindbrain is a highly conserved part of the brain, responsible for vital functions such as breathing, consciousness and motor coordination. During development the hindbrain is subdivided in eight compartments, so-called rhombomeres. A feature that is highly important for patterning of the hindbrain and organization of its neural circuits. At the boundaries between these compartments a specialized cell population is formed that serves as a signaling center. We found that in *Xenopus* these rhombomere boundaries show highly localized Wnt signaling activity. We show that Wnt signaling activity is important to maintain the rhombomere boundaries as Notch signaling-free zones. Furthermore, we reveal that there is an antagonistic relationship between Notch and Wnt signaling in the hindbrain. These findings contradict a previously described model in zebrafish, which describes a positive feedback loop between both signaling pathways. Furthermore, we performed cell cycle analysis in the hindbrain and show that rhombomere boundary cells are actively cycling. Wnt signaling activity induces G1-to-S-phase transition in these cells and thereby prevents cell-cycle-exit. This confirms recent findings in chick, where rhombomere boundaries were identified as pools of neural stem cells that contribute progenitor cells and differentiating neurons to the rhombomeres.

Wnt signaling is essential for normal brain development and homeostasis. However, uncontrolled, constitutive activity of the pathway is associated with one subtype of the most common pediatric brain malignancy, medulloblastoma. Current treatment consists of optimal surgical resection with adjuvant chemotherapy and craniospinal irradiation. This aspecific and aggressive treatment approach applied to an immature brain has detrimental consequences on neurological function. Large-scale genomic profiling of medulloblastoma has generated vast amounts of data that could guide development of molecular targeted therapies. However, model organisms that accurately reflect the clinical presentation of the disease and that allow functional annotation of the cancer genome are lacking. We generated a *Xenopus tropicalis* model for Wnt-type medulloblastoma through CRISPR/Cas9-mediated gene editing of *apc,* a negative regulator of the Wnt signaling pathway. Tadpoles developed brain tumors that highly resembled the clinical presentation of medulloblastoma. Tumors developed within 6 weeks, however incidence only reached 15%. Further optimization of the model is needed. Nevertheless, we show that our model could provide a straightforward and cost-effective platform for functional analysis of potential tumor modulatory genes. We identified two potential Wnt-type medulloblastoma-specific tumor suppressor genes through CRISPR/Cas9 multiplexing.

We uncovered a new role of Wnt/β-catenin signaling during hindbrain development and generated a new tool to study its role during tumorigenesis. In this way we contributed to the understanding of this multi-facetted signaling pathway.

ALGEMENE SAMENVATTING

Het menselijk lichaam is een zeer complex, maar ook zeer robuust systeem. Elk van de processen in het lichaam, vanaf de embryonale ontwikkeling tot de homeostase in het volwassen lichaam, wordt precies gereguleerd door de instructies van moleculaire signaalwegen. Opmerkelijk genoeg bestaan er slechts een beperkt aantal signaalwegen die tijdens het leven voor verschillende processen worden ingezet. Belemmering van het functioneren van deze signaalwegen is dan ook vaak de aanleiding van ziekte. Het is essentieel dat we het fysiologisch functioneren van deze signaalwegen goed begrijpen, want dit genereert belangrijke inzichten in hoe we deze aandoeningen het best behandelen.

De Wnt/β-catenine signaalweg is één van deze fundamentele signaalwegen. Met dit onderzoek trachtten we de kennis over deze belangrijke signaalweg in een specifieke regio, de achterhersenen, te vergroten, zowel tijdens de embryonale ontwikkeling als in het kader van een pathologie, namelijk kanker.

De achterhersenen zijn een evolutionair zeer geconserveerde regio van de hersenen, verantwoordelijk voor onder andere ademhaling, bewustzijn en de coördinatie van bewegingen. Tijdens de ontwikkeling wordt deze regio onderverdeeld in acht compartimenten, de rhombomeren. Dit is zeer belangrijk om het grondplan van de neuronencircuits in de achterhersenen vast te leggen. Op de compartimentgrenzen ontstaat er een gespecialiseerde celpopulatie die dienst doet als signalisatiecentrum. Deze rhombomeergrenzen tonen specifiek activatie van de Wnt signaalweg. Wij bewijzen dat deze activiteit belangrijk is om activatie van de Notch signaalweg in de rhombomeergrenzen te voorkomen. Bovendien bestaat er een antagonisme van beide signaalwegen. Deze bevindingen ontkrachten een eerdere studie uit zebravis, waarin een positieve feedbacklus tussen Wnt en Notch signalisatie werd beschreven. Voorts voerden we cellcyclusanalyse van de achterhersenen uit en leidden daaruit af dat cellen uit de rhombomeergrenzen actief delen. Wnt signalisatie stimuleert de overgang van de G1- naar de S-fase en voorkomt zo terminale differentiatie. Hiermee bevestigen we de bevindingen uit een recente studie in de kip. Hierin werden de rhombomeergrenzen geïdentificeerd als een bron van neurale stamcellen die voorlopercellen en differentiërende neuronen aanleveren voor de rhombomeren.

Wnt signalisatie is essentieel voor de normale ontwikkeling en homeostase van de hersenen. Ongecontroleerde, constante activatie van de signaalweg ligt echter aan de basis van een subtype van de meest voorkomende hersenkanker bij kinderen, medulloblastoma. De huidige behandeling bestaat uit optimale chirurgische dissectie van de tumor, gecombineerd met chemotherapie en craniospinale bestraling. De aspecifieke en agressieve aard van deze behandelingsmethode, toegepast op een groeiend brein, heeft zware gevolgen voor het verdere neurologisch functioneren van de patiënt. De next-generation-sequencing revolutie heeft een enorme hoeveelheid informatie gegenereerd die de ontwikkeling van moleculair gerichte therapeutica kan aansturen. Hiervoor zijn er modelorganismen nodig die het klinische ziektebeeld accuraat nabootsen en die functionele annotatie van het kankergenoom toelaten. Wij creëerden een *Xenopus tropicalis* model voor Wnt-type medulloblastoma door CRISPR/Cas9-gemedieerde mutatie van *apc,* een negatieve regulator van de Wnt signaalweg. De bekomen hersentumoren reflecteerden het ziektebeeld van medulloblastoma. Slechts 15% van de kikkervisjes ontwikkelden tumoren, maar deze ontstonden wel binnen de zes weken. Optimalisatie van het model is dus vereist. Desondanks tonen onze resultaten aan dat ons model een eenvoudig en economisch alternatief kan zijn voor functiebepaling van

kandidaat tumormodulerende genen. We identificeerden twee nieuwe tumor suppressorgenen in Wnt-type medulloblastoma door CRISPR/Cas9 multiplexing.
We ontrafelden een nieuwe functie voor Wnt/β-catenine signalisatie tijdens de onwikkeling van de achterhersenen en genereerden een nieuw hulpmiddel voor onderzoek naar de rol van Wnt signalisatie tijdens tumorvorming. Op deze manier leverden we een bijdrage aan het doorgronden van deze veelzijdige signaalweg.

TABLE OF CONTENTS

LIST OF ABBREVIATIONS

A

A	anterior
AD	Alzheimer's disease
ADAM	a disintegrin and metalloproteinase
ahSC	adult hippocampal stem cell
AKT	AKT Serine/Threonine Kinase
ALCAR	acetyl-L-carnitine
ALK	anaplastic lymphoma kinase
ANK	ankyrin repeat
APC	adenomatous polyposis coli
ARID	AT-rich interaction domain
ATP	adenosine triphosphate
axin	axis inhibition protein

B

β-cat	beta-catenin
β-gal	beta-galactosidase
β-Trcp	beta-transducin repeat containing E3 ubiquitin protein ligase
BBB	blood brain barrier
BCL9	B-cell chronic lymphocytic leukemia/lymphoma 9
bHLH	basic helix loop helix
bhmt	betaine-homocysteine S-methyltransferase
BIO	6-Bromoindirubin-3'-oxime
Blbp	brain lipid binding protein
BMP	bone morphogenetic protein
Brn	brain
bs	brainstem
BSA	bovine serum albumin

C

c-Cbl	casitas B-lineage lymphoma proto-oncogene
C-terminal	carboxyterminal
Cas9	CRISPR associated protein 9
cb	cerebellum
CBF1	C-promoter binding factor 1
CBP	CREB binding protein
CDH1	cadherin 1
Cdx1	caudal type homeobox 1
CHD7	chromodomain helicase DNA binding protein 7
ChIP	chromatin immunoprecipitation
CK1	casein kinase 1

CNS	central nervous system
crabp2	cellular retinoic acid binding protein 2
Cre	causes recombination
CREB	cAMP responsive element binding protein
CRISPR	clustered regularly interspaced short palindromic repeats
crRNA	CRISPR RNA
CSL	CBF1, Suppressor of Hairless, Lag-1
CSNK2B	casein kinase 2 beta
CSPG	chondroitin sulfate proteoglycan
CtBP	C-terminal binding protein
cyp26a1	cytochrome P450 family 26 subfamily A member 1

D

D	dorsal
D/N	desmoplastic/nodular
DAPI	4',6-diamidino-2-phenylindole
DBM	DNA binding mutant
DDX3	DEAD-box helicase 3
DISC1	disrupted in schizophrenia 1
Dkk	dickkopf
Dll	delta like canonical notch ligand
DMEM	Dulbecco's modified Eagle medium
DMSO	dimethylsulfoxide
dn	dominant negative
DSB	double stranded break
DSL	Delta/Serrate/lag-2
DTT	1,4-dithiothreitol
Dvl	disheveled

E

ECM	extracellular matrix
EDTA	ethylenediaminetetra-acetic acid
eGFP	enhanced green fluorescent protein
emx2	empty spiracles homeobox 2
EnR	engrailed repressor domain
Eph	ephrin receptor
ER	endoplasmatic reticulum
Erk1/2	extracellular signal-regulated kinase 1/2
erm	ETS variant 5
ESC	embryonic stem cell
ezh2	enhancer of zeste homolog 2

F

FAP	familial adenomatous polyposis

FB	forebrain
FGF	fibroblast growth factor
FGFR	FGF receptor
FISH	fluorescent in situ hybridization
fng	fringe
fox	forkhead box
FSC	forward scatter
Fzd	frizzled

G

G1-phase	gap 1 phase
G2-phase	gap 2 phase
g3	group 3
g4	group 4
GABA	gamma-aminobutyric acid
gad1	glutamate decarboxylase 1
GFAP	glial fibrillary acidic protein
GFI1	growth factor independent 1 transcriptional repressor
GL	granule layer
glut1	glucose transporter
GNP	granule neuron precursor
GR	glucocorticoid receptor hormone binding domain
grhl3	grainyhead like transcription factor
gRNA	guideRNA
gSC	glioma stem cell
GSK3	glycogen synthase kinase 3

H

HA	hemagglutinin
HB	hindbrain
hCG	human chorionic gonadotropin
hdac	histone deacetylase
HDR	homology dependent repair
HEPES	4-(2-hydroxyethyl)-1-piperazineethanesulfonic acid
hes1	hairy and enhancer of split 1
hey	hairy/enhancer-of-split related with YRPW motif
hiPSC	human induced pluripotent stem cell
HMA	heteroduplex mobility assay
hox	homeobox
hPSC	human pluripotent stem cell
HSPG	heparan sulfate proteoglycan
hth	hypothalamus

I

id	inhibitor of DNA binding
IdU	5-Iodo-2'-deoxyuridine
indels	insertions and deletions
int1	MMTV integration site 1
IP	intermediate progenitor
isl-1	islet-1
IWP12	inhibitor of wnt production 12
IWR1	inhibitor of wnt response 1
IZ	intermediate zone

J

jag	jagged

K

kdm6a	lysine demethylase 6a
KO	knockout
Kremen	kringle-containing protein marking the eye and the nose

L

L	lateral
LCA	large cell anaplastic
LEF	lymphoid enhancer binding factor
lfng l	unatic fringe
LGR4/5/6	leucine rich repeat containing G protein-coupled receptor 4/5/6
LOF	loss of function
LRL	lower rhombic lip
LRP5/6	low density lipoprotein receptor-related protein

M

M	medial
M-phase	mitotic phase
MafB	musculoaponeurotic fibrosarcoma basic leucine zipper transcription factor B
MAML	mastermind like
MAPK	mitogen-activated protein kinase
mash	achaete-scute family bHLH transcription factor
math	atonal bHLH transcription factor
MB	medulloblastoma
MB	midbrain
MBEN	medulloblastoma with extensive nodularity
meis	myeloid ecotropic viral integration site
mfng	manic fringe
MGMT	O-6-methylguanine-DNA methyltransferase
MHB	midbrain-hindbrain boundary

mib	mindbomb
miR	microRNA
MMR	Marc's modified Ringer's
MO	morpholino
msx	msh homeobox
MyT1	myelin transcription factor 1
MZ	marginal zone

N

N-terminal	aminoterminal
nab1/2	NGFI-A binding protein
NCAM	neural cell adhesion molecule
NF-κB	nuclear factor kappa B
NHEJ	non-homologous end-joining
NI	non-injected
NICD	notch intracellular domain
NLS	nuclear localization signal
nlz1/2	zinc finger protein
NPC	neural progenitor cell
nrarp	notch regulated ankyrin repeat protein
nrp2a	neuropilin 2a
NSC	neural stem cell
NSCL1	nescient helix-loop-helix 1
NTD	neural tube defect

O

olig1	oligodendrocyte transcription factor

P

P	posterior
p21	cyclin dependent kinase inhibitor 1a
PAM	protospacer adjacent motif
pax	paired box
PBS	phosphate buffered saline
pbx	pre-B-cell leukemia homeobox
PCAF	p300/CBP-associated factor
PCR	polymerase chain reaction
PD	Parkinson's disease
pea3	ETS variant 4
PEST	proline/glutamine acid/serine/threonine
PFA	paraformaldehyde
PH3	phospho-histone 3
pik3ca	phosphatidylinositol-4,5-bisphosphate 3-kinase catalytic subunit alpha
PLVAP	plasmalemma vesicle associated protein

plzf	promyelocytic leukaemia zinc finger
ppmd1d	protein phosphatase, Mg2+/Mn2+dependent 1d
PSB	pallial-subpallial boundary
Ptec	pretectum
Pth	prethalamus

R

r	rhombomere
RA	retinoic acid
raldh2	retinaldehyde-specific dehydrogenase type 2
RAM	RBKj association module
RB	rhombomere boundary
RBPjκ	recombination signal binding protein for immunoglobulin kappa J region 2
rest	RE1 silencing transcription factor
rfng	radical fringe
RING	really interesting new gene
RL	rhombic lip
RNF43	ring finger protein 43
RNP	ribonucleoprotein complex
RNS	reactive nitrogen species
ROS	reactive oxygen species
RP	roof plate
RSPO	R-spondin
rUTP	ribonucleotide uridine triphosphate

S

S	serine
s	somite
S-phase	synthesis phase
SC	spinal cord
SCI	spinal cord injury
sema	semaphorin
ser	serrate
sFRP	secreted frizzled related protein
SGZ	subgranular zone
Shh	sonic hedgehog
SLC2A	solute carrier 2a
SMARCA4	SWI/SNF related, matrix associated, actin dependent regulator of chromatin a4
SMRT	silencing mediator of retinoic acid and thyroid hormone receptor
SNAI2	snail family transcriptional repressor 2
SNc	substantia nigra pars compacta
sox9	sex-determining region Y-box 9
spg	spiel ohne grenzen
SSC	side scatter

st	stage
Su(H)	supressor of hairless
SVZ	subventricular zone
SWI/SNF	SWItch/sucrose non-fermentable

T

T	threonine
TA	transcriptional co-activator
TALEN	transcription activator-like effector nuclease
TBI	traumatic brain injury
tbr2	T-box brain 2
TCF	T-cell-specific transcription factor
Tel	telencephalon
TGF_	transforming growth factor beta
Th	thalamus
TLE	transducin like enhancer of split
tmem51	transmembrane protein 51
tnc	tenascin C
tp53	tumor protein p53
TR	transcriptional co-repressor
tracrRNA	trans-activating crRNA
TSG	tumor supressor gene

U

ub	ubiquitin
URL	upper rhombic lip

V

V	ventral
val	valentino
vhnf1	variant hepatic nuclear factor 1
VP16	virus protein 16
VTA	ventral tegmental area
VZ	ventricular zone

W

Wg	wingless
WIF	wnt inhibitory factor
WIP1	wild-type p53-induced phosphatase
WISH	whole mount in situ hybridization
WLS	wntless wnt ligand secretion mediator
Wnt	wingless/int1

Z

ZLI	zona limitans intrathalamica
ZMYM3	zinc finger MYM-type containing 3
ZNRF3	zinc and ring finger 3

PART I
INTRODUCTION

CHAPTER 1

WNT/β-CATENIN SIGNALING

1.1 INTRODUCTION

Wnt is a portmanteau word combining the names of two independently discovered genes, the mammalian proto-oncogene *Int1* and the *Drosophila wingless* gene [1, 2]. Both genes turned out to be homologues of the same gene, leading to them being renamed as *Wnt1* [3, 4]. This was one of the first discoveries linking one gene to both embryonic development and carcinogenesis [5]. It is now established that vertebrates contain a family of 19 Wnt-related genes, each displaying unique patterns of expression [5, 6]. These genes execute a myriad of functions during embryonic development, in adult tissue homeostasis and disease [7-10].

1.2 THE PATHWAY

The key event of the Wnt/β-catenin or canonical Wnt pathway is stabilization of the multifunctional protein β-catenin. Wnt ligands can also signal through β-catenin independent mechanisms, so-called non-canonical signaling, but these are beyond the scope of this thesis.

In the absence of Wnt ligand, β-catenin is phosphorylated and targeted for proteosomal degradation by the destruction complex, keeping cytoplasmic β-catenin levels low [11-16] (Figure 1.1). The destruction complex is composed of two scaffolding proteins, Adenomatous Polyposis Coli (APC) and axis inhibiting protein (axin), and two kinases, Casein Kinase 1α (CK1α) and Glycogen Synthase Kinase 3β (GSK3β) [11, 13, 15-20]. β-catenin contains four serine (S)/Threonine (T) residues at its aminoterminus (S33, S37, T41 and S45). CK1α phosphorylates the S45 residue and thereby primes β-catenin for further phosphorylation in a carboxy- to aminoterminal direction by GSK3β on T41, S37

and S33 [15, 16]. Phosphorylation of S33 and S37 is necessary for β-catenin recognition and ubiquitination by the E3 ubiquitin ligase β-Transducin repeats containing protein (β-Trcp) and subsequent degradation by the proteosome [12, 14, 21, 22]. In the nucleus, transcription factors of the Lymphoid Enhancer-binding Factor (LEF)/ T Cell- specific (TCF) family associate with transcriptional repressor Groucho and histone deacetylases (HDAC), preventing target gene expression [23, 24].

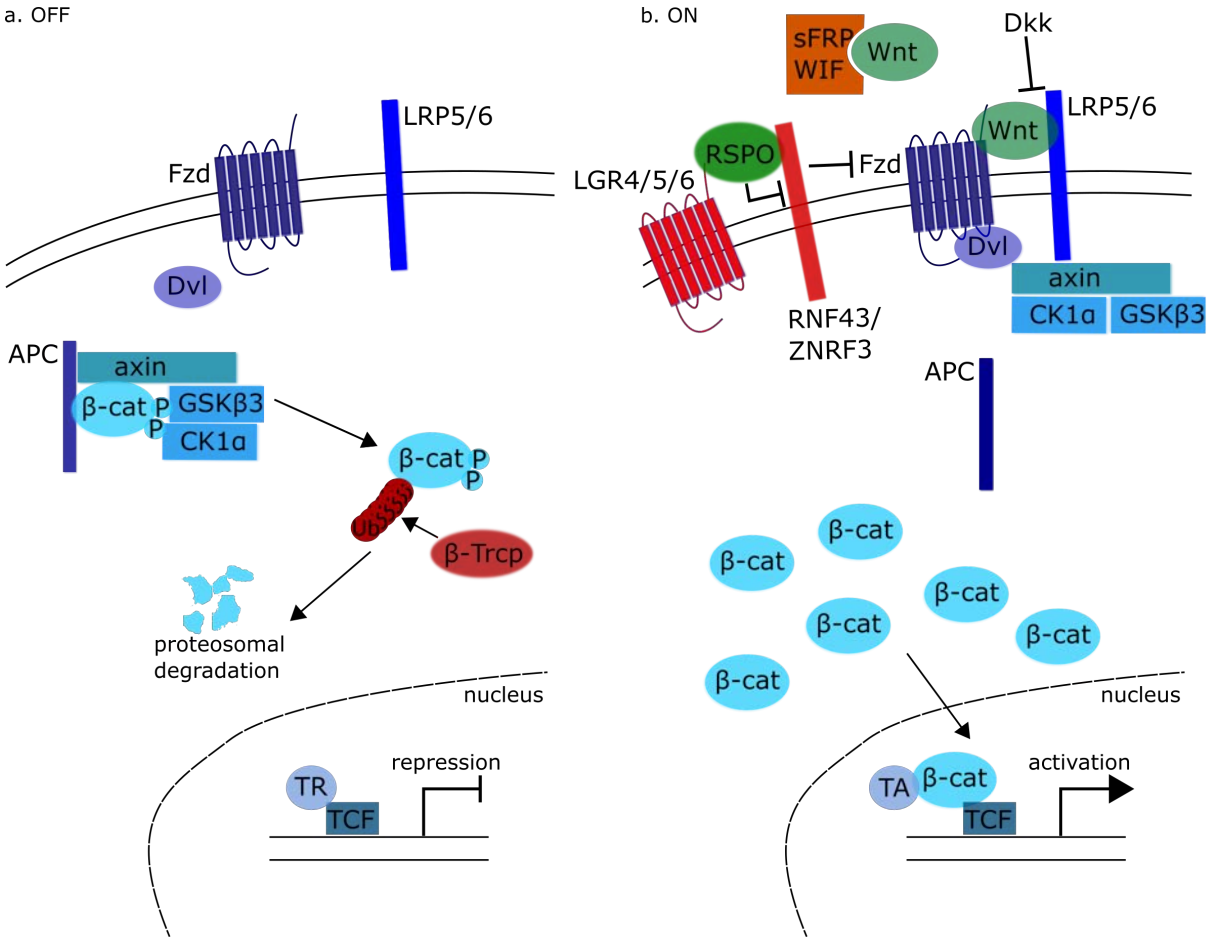

Figure 1.1 The Wnt signaling pathway. (a) In the absence of Wnt ligand, β-catenin is phosphorylated and thereby targeted for proteosomal degradation by the destruction complex composed of APC, axin, GSK3β and CK1α. In the nucleus target gene expression is repressed. (b) In the presence of Wnt ligand and binding to the Frizzled receptor and LRP5/6 coreceptor, the destruction complex falls apart, leading to the accumulation of β-catenin in the cytosol and its subsequent translocation to the nucleus. In the nucleus β-catenin binds transcription factors of the TCF/LEF family and recruits transcriptional activators leading to the expression of target genes. Endogenous antagonists of the pathway are sFRPs/WIF, which bind Wnt preventing it to bind to the receptor, and Dkk, which interacts with the LRP5/6 coreceptor. ZNRF3/RNF43 inhibit the pathway by stimulating Fzd endocytosis. ZNRF3/RNF43 activity is prevented in the presence of R-spondins. TR, transcriptional repressor; TA, transcriptional activator.

Wnt ligands are post-translationally lipid modified by an O-linked palmitoleate on a conserved serine residue making them hydrophobic [25, 26]. This modification is necessary for the secretion of Wnt ligands and thus for activation of the pathway [27]. The ER protein Porcupine, a membrane bound O-acyltransferase, is the single protein responsible for catalyzing the lipid modification of the Wnts [28, 29]. Wnt is subsequently transported from the Golgi apparatus to the cell surface for release by the multipass transmembrane protein Wntless (WLS) [30, 31]. Wnt signaling activation occurs upon binding of Wnt ligand to a Frizzled (Fzd) receptor and its co-receptor, the Low-density lipoprotein receptor-Related Protein 5 or 6 (LRP5/6) [32-35] (Figure 1.1). The scaffolding protein

Dishevelled (Dvl) is recruited and leads to oligomerization of LRP6 initiating the signaling cascade [36, 37]. LRP6 is sequentially phosphorylated by GSK3 and CK1γ leading to the recruitment of axin to the receptor complex [38-40]. Although recruitment of axin to the receptor complex by Dvl and subsequent recruitment of GSK3 by axin has also been suggested [41]. Either way, a positive feedback loop exists in which axin further recruits kinases to the complex and phosphorylated LRP6 provides more binding sites for axin, resulting in amplification of the initial signal [36, 41]. It was long unclear how this leads to dysfunction of the destruction complex. Axin can exist in an open or closed conformation depending on its phosphorylation state. Phosphorylation by GSK3 result is an open conformation of axin, allowing it to execute its scaffolding function in the destruction complex. Upon Wnt activation, activated LRP6 can inhibit this phosphorylation and this results in dephosphorylation of axin by protein phosphatase 1. Axin takes on a closed conformation in which it can no longer associate with β-catenin [42, 43]. Also direct inhibition of GSK3-mediated phosphorylation of β-catenin by activated LRP6 has been proposed [44, 45]. The end result is that β-catenin is no longer phosphorylated and thus no longer degraded. Stabilized β-catenin accumulates in the cytoplasm and will translocate to the nucleus [46]. In the nucleus, dephosphorylated β-catenin displaces Groucho from the LEF/TCF factors and recruits transcriptional activators including B Cell Lymphoma 9 protein (BCL9), Pygopus and histone modifier cAMP response element-binding (CREB)-binding protein (CBP) [47-52]. This leads to transcriptional activation of target genes like *c-myc* and *axin2* [53, 54]. Wnt signaling also promotes the expression of several of its own pathway components, indicating feedback control [10].

Alternative ways in which Wnt signaling activation leads to accumulation of β-catenin have been suggested. One possibility is that Wnt signaling activation leads to internalization of GSK3 into multivesicular bodies thereby decreasing GSK3 activity [55, 56]. This would then lead to decreased phosphorylation-mediated degradation of β-catenin. Another possibility is that Wnt signaling activation does not disrupt β-catenin phosphorylation and that the destruction complex remains intact. Instead ubiquitination of β-catenin and subsequent degradation is prevented resulting in the saturation of the destruction complex. Newly synthesized β-catenin can then no longer be phosphorylated and will activate transcription in the nucleus [57, 58]. Yet another mechanism was shown in *Drosophila* by which LRP6 binds and downregulates axin. Thereby directly releasing β-catenin, independent of the destruction complex, and activating signaling [59].

Wnt signaling is further regulated at the level of the ligand-receptor interaction, mostly by the expression of several agonists and antagonists (Figure 1.1). The secreted Frizzled-Related Proteins (sFRPs) can competitively bind Wnt ligands and prevent their interaction with the receptor or directly interact with Fzd [60-63]. However, activation of Wnt signaling by low concentrations of sFRP has also been suggested [64]. Also Wnt Inhibitory factor-1 (WIF-1) can sequester Wnt ligands [65]. The Dickkopf (Dkk) family of proteins antagonizes Wnt signaling through interaction with the LRP5/6 coreceptor [66-68]. Another mechanism of regulation is control over the abundance of Fzd receptors on the cell surface. Ubiquitination of Fzd by the related transmembrane RING domain-containing E3 ubiquitin ligases RNF43 and ZNRF3 leads to endocytosis of the receptor [69, 70]. RNF43 and ZNRF3 are themselves tightly regulated. R-Spondins (RSPOs) complex with the extracellular domains of the ubiquitin ligases leading to their decreased activity and hence sensitize cells to Wnts by increasing receptor abundance [70, 71]. Presence of RSPOs also potentiates Wnt signaling through binding with the receptors of the Lgr family and subsequent interaction with the LRP5/6 coreceptor [72, 73].

1.3 How Wnt signaling builds the brain: bridging development and disease (adapted version)

Rivka Noelanders and Kris Vleminckx

The Neuroscientist 23(3):314-329 (2016)

The vertebrate embryo is an extremely complex entity; however it arises from a single cell through the instructions of only a handful of signaling pathways. These signaling pathways are highly versatile and can have different effects on a cell's decision, depending on location or developmental time point. Also in the adult, the same signaling pathways are responsible for maintaining homeostasis. Failing of these signaling processes early in life can give rise to developmental defects while disturbance of signaling later in life can lead to the acquirement of various diseases. Knowledge of the normal physiological signaling processes is thus essential for understanding what goes wrong in disease states, and can give insight in possible therapeutic solutions for these diseases. One of the key developmental signaling pathways is the Wnt/β-catenin or canonical Wnt pathway (Figure 1.1). Wnt signaling has many crucial functions during development including cell fate determination and early patterning events. And also in the adult, Wnt has an important role in stem cell renewal and tissue homeostasis [10]. One of the organs in which Wnt/β-catenin signaling is important throughout all stages of life is the brain.

1.3.1 Wnt/β-catenin signaling during brain development

1.3.1.1 Early patterning

One of the earliest events in brain development is the establishment of the anterior-posterior axis. In *Xenopus*, similar to other vertebrates like zebrafish, BMP antagonists secreted from the Spemann organizer initially confer a default anterior identity to the whole neural tube (Figure 1.2). Later on, Wnt/β-catenin, retinoic acid and FGF signaling respecify cells to a more posterior identity forming the midbrain, hindbrain and spinal cord [74, 75]. Mouse embryos lacking Wnt1 mediated Wnt/β-catenin signaling show severe brain malformations with a completely absent midbrain and rostral hindbrain that would normally form the cerebellum [76, 77]. On the anterior side, activity of these signaling pathways is inhibited by the expression of inhibitors preventing caudalization of the forebrain which is essential for head formation [78]. Recently, several new antagonists of anterior Wnt signaling necessary for head induction were discovered [79, 80]. This underscores the importance of Wnt inhibition in this process.

Wnt signaling is also important for dorso-ventral patterning, for example in the telencephalon (Figure 1.2). The telencephalon arises from the most anterior part of the forebrain. One of the first patterning events is the subdivision of the telencephalon in two halves along the dorsoventral axis: the ventral subpallium and dorsal pallium [81]. Wnts are expressed in the dorsal midline of the telencephalon, the so-called "hem", and display a dorsomedial to lateral gradient. They are important for both expansion and patterning of the pallium. Active Wnt/β-catenin signaling maintains dorsal identity in pallial progenitor cells while preventing expression of transcription factors that promote ventral, subpallial fates [82].

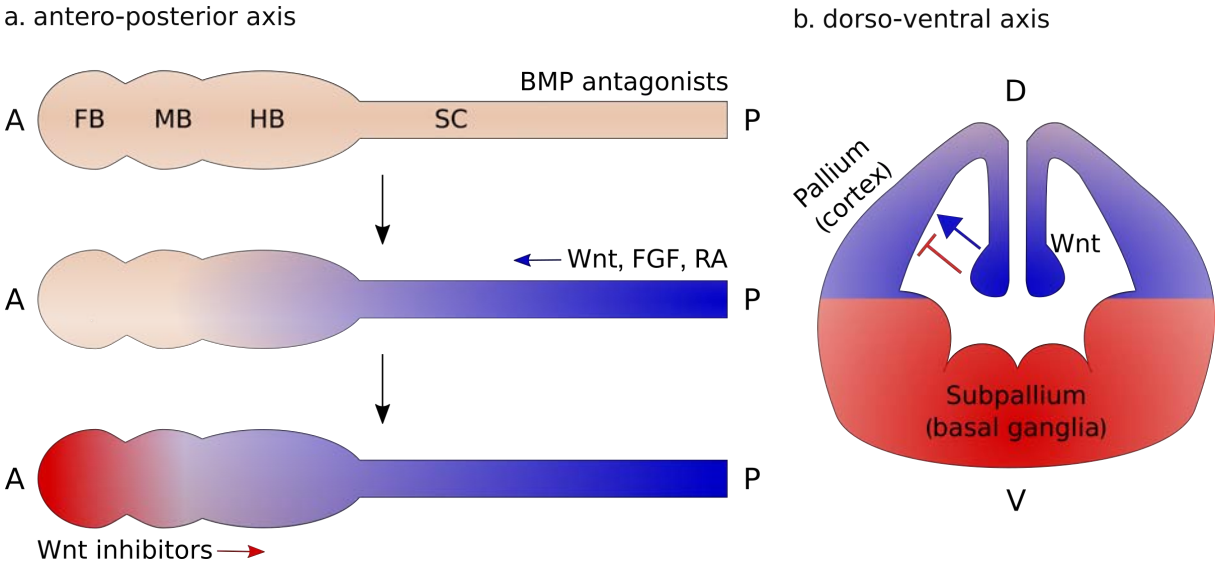

Figure 1.2 Wnt signaling during early patterning. (a) Initially, the neural tube has a default anterior identity. Posterior identity is conferred by a posterior to anterior gradient of Wnt, FGF, and retinoic acid signaling (blue). For head formation inhibition of anterior Wnt signaling is needed (red). (b) Wnts are expressed in the dorsal midline of the telencephalon (blue) and induce and maintain dorsal identity of the pallium (blue arrow) while preventing expression of ventral markers (red inhibition arrow). Ventral identity of the subpallium is induced by Shh signaling (red). FB = forebrain; HB = hindbrain; MB = midbrain; SC = spinal cord.

1.3.1.2 Neurogenesis

A lot of effort has been done to elucidate the role of Wnt/β-catenin signaling in neural progenitor proliferation and neuronal differentiation, with studies often leading to contradictory conclusions. A lot of the differences observed are probably due to differential time windows and locations of Wnt interference. However, most of the studies point towards a common role for Wnt signaling in instructing cell fate decisions.

All neurons and glia cells of the central nervous system arise from the neural precursors cells (NPCs) located in the ventricular zone of the developing brain and spinal cord. The balance between proliferation and differentiation of these cells has to be tightly regulated to ensure proper brain development. Wnt signaling is active in neural progenitors in the ventricular zone during neurogenesis (Figure 1.3). Constitutive activation of Wnt signaling leads to expansion of different neural precursor populations [83] while inhibition of Wnt signaling leads to premature cell cycle exit and depletion of the precursor pool [84, 85]. Wnt signaling thus maintains symmetrical division of NPCs [86]. For neurogenesis, a switch to asymmetrical division is needed (Figure 1.3) [87]. In the cerebral cortex neurogenesis progresses from anterior-lateral to posterior-medial domains [88, 89]. During this time two opposing gradients pattern the major area map of the cortex. Anterolaterally, Fgf8 and Pax6 expression dominate, while Wnt-dependent Emx2 radiates from the posteromedial side [90-93]. Wnt activity gradually regresses away from anterior and lateral zones and is complemented by a progressing wave of neural differentiation (Figure 1.3) [94]. Downregulation of Wnt signaling is needed for the switch to differentiation [86, 95]. However, in a different spatiotemporal context Wnt signaling has also been shown to induce neuronal differentiation. In the *Xenopus* forebrain a switch to active Wnt signaling is needed to initiate neuronal differentiation, while first Wnt inhibition was needed for forebrain fate determination [96]. Moreover, also in mammals Wnt signaling has been shown to drive NPCs to a neuronal fate by upregulation of the proneural factors Neurogenin1 and N-myc [97, 98]. Also in Olig1 positive progenitor cells of the

forebrain, that generally give rise to oligodendrocytes, active Wnt signaling imposes a neuronal fate while suppressing glial fate [99].

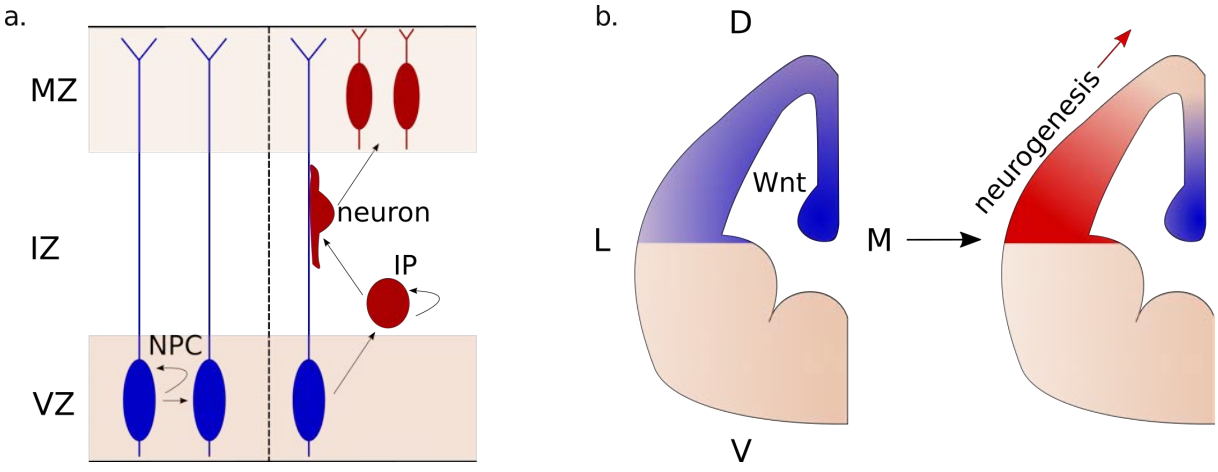

Figure 1.3 Wnt signaling during cortical neurogenesis. (a) Wnt signaling maintains symmetrical divisions of neural progenitor cells in the ventricular zone (blue). For neurogenesis a switch to asymmetrical divisions and reduced Wnt signaling is needed (red). First intermediate progenitor cells are formed that can still self-renew during a limited amount of divisions and will eventually terminally differentiate to form functional neurons. (b) Wnt signaling is active in a posteromedial gradient in the cortex of the telencephalon (blue). Wnt signaling gradually regresses and is complemented by an advancing gradient of neurogenesis (red). IP = intermediate progenitor; IZ = intermediate zone; MZ = marginal zone; NPC = neural progenitor cell; VZ = ventricular zone.

1.3.2 WNT/B-CATENIN SIGNALING IN THE ADULT BRAIN

It is now established that in the adult brain some zones retain the capacity to produce new functional neurons. In the adult neural stem cells (NSCs) of the subventricular zone, Wnt signaling induces cell cycle exit through upregulation of the cell cycle-dependent kinase inhibitor p16INK4a - and subsequent neuronal differentiation [100]. However, upon activation of Wnt signaling, either ectopically or e.g. after injury, adult NSCs still react, similarly as during developmental stages, by induction of proliferation [101-104]. Alternatively, in the hypothalamus Wnt signaling inhibits proliferation of neural stem cells and is required for the differentiation of a specific subset of neurons arising from this population [105].

Adult neurogenesis declines with aging leading also to impairment of neurological function. The diminished formation of neurons is probably linked to a reduction in the number of NPCs. The protein phosphatase Ppmd1d, also known as WT p53-induced phosphatase 1 (Wip1), is normally expressed in NPCs of the subventricular zone where it maintains neuron formation [106]. Ppmd1d/Wip1 expression decreases during aging leading to reduced neuron formation through upregulation of p53 and a p53-dependent upregulation of Dkk3. This Dkk3 upregulation leads to inhibition of canonical Wnt signaling and of Wnt-induced neurogenesis. The increase in Dkk3 expression can be prevented by overexpression of WIP1 leading to increased NSC proliferation, and more importantly, neuronal differentiation. Pharmacological activation of the Wnt pathway also improved neurogenesis to a similar extent [107].

1.3.3 WNT/B-CATENIN SIGNALING AND PLURIPOTENT STEM CELLS

Human pluripotent stem cells (hPSCs), including embryonic stem cells (ESCs) and hiPSCs, hold great promise for cell therapy in neurodegenerative diseases. For the generation of functional neurons from hPSCs in culture the same signaling pathways are important as during normal development. As Wnt/β-catenin signaling is needed during several stages of neural development, tight regulation of this pathway is essential. During early stages, inhibition of Wnt signaling is needed to promote

neurectodermal versus mesendodermal differentiation [108]. Later on, Wnt signaling level is important to drive differentiation according to a desired rostral to caudal identity (Figure 1a). Similar as during formation of the antero-posterior axis in the early embryo, high Wnt signaling leads to more posterior neural fates e.g. hindbrain or spinal cord [109]. Also during differentiation towards neural lineages, a tight regulation of Wnt/β-catenin signaling is needed [110]. Human ESCs differentiate towards a dorsal telencephalic character in the absence of morphogens. This can be explained by endogenous Wnt signaling that is required to infer dorsal identity in the developing telencephalon. Inhibition of Wnt signaling or activation of Shh signaling converts them to ventral telencephalic precursors (Figure 1b). Dorsal and ventral telencephalic progenitors will differentiate further to form functional glutamatergic and GABA-ergic neurons, respectively [111].
Also cultures of NPCs show great therapeutic potential as a renewable cell source for nervous tissue repair [112]. Several studies have demonstrated that active Wnt signaling promotes neuronal differentiation of NPCs in culture, as it does during normal development [113, 114]. Cui et al. found that reduced neuronal differentiation in 3D versus 2D NPC cultures is due to inhibition of Wnt signaling downstream of Rest expression in these cultures [115].

1.3.4 DEVELOPMENTAL DEFECTS GIVE RISE TO DISEASE

A complex interplay between different signaling pathways is responsible for proper development. Deregulation of any of the signaling events during development might give rise to developmental defects that can manifest early or only become apparent later in life.

1.3.4.1 Neural tube defects

Neural tube defects (NTDs) comprise all defects that result from a failure of the neural tube to close properly during early neural development. Mutations in both canonical and non-canonical Wnt genes have been linked to the etiology of NTDs [116, 117]. Four rare single nucleotide variations in the coding region of the LRP6, the Wnt coreceptor, gene were found in infants with spina bifida. However only one of these variants decreased canonical Wnt signaling, while the others increased the non-canonical Wnt/PCP pathway [118].
Prior to neural tube closure, neural ectoderm and surface ectoderm are still joined in a single ectodermal sheet. At the end of neural tube closure the two fates are completely separated. So initially the progenitor cells at the neural plate border are uncommitted to either fate. Expression of the Wnt antagonists Dkk1/Kremen1 maintains the uncommitted character of these progenitor cells. During neurulation, canonical Wnt signaling is needed for the specification of surface ectoderm fate through activation of the Grainyhead-like 3 (Grhl3) transcription factor. Both β-catenin and Grhl3 mutant embryos show neural tube defects indicating that proper fate specification is essential for neural tube closure [119]. Li et al. further showed that impaired neurulation in a mouse model of NTDs is a consequence of reduced Wnt/β-catenin signaling downstream of retinoic acid signaling. Addition of retinoic acid could completely rescue the NTDs through upregulation of Wnt/β-catenin signaling [120].

1.3.4.2 Psychiatric disorders

Abnormal brain development can lead to defective brain circuitry that can later manifest in behavioral disorders of the adult [121]. Dishevelled (Dvl) functions as a positive regulator of the Wnt pathway downstream of Frizzled through a mechanism that is still not completely understood [122]. Dvl1$^{-/-}$ mice exhibit abnormal social interaction behaviors [123]. *Dvl1*$^{-/-}$*3*$^{+/-}$ mice additionally show repetitive patterns of behavior. These symptoms are typically seen in patients with autism spectrum disorders. When looking at brain development, the *Dvl1*$^{-/-}$*3*$^{+/-}$ mice showed a transient increase in

brain size and a reduction of $Brn2^+$ deep layer neurons, indicating premature differentiation. Belinson et al. showed that the observed developmental changes are the result of reduced canonical Wnt signaling which leads to reduced expression of its direct target gene *Pou3f2/Brn2*. The latter normally directly represses Eomes/Tbr2 expression, keeping proliferation of NPCs in check [124, 125]. Moreover, reactivation of Wnt/β-catenin signaling in the $Dvl1^{-/-}3^{+/-}$ mice rescues both the embryonic and adult phenotypes. Precise control of Wnt/β-catenin signaling during development is thus needed for the establishment of normal social and stereotypic behavior in the adult [125]. The findings are consistent with a model that autism may be caused by abnormalities in the development of deep layer glutamatergic projection neurons [126, 127]. Also faults in synaptic connections that lead to an imbalance of excitatory and inhibitory impulses are commonly seen in autism spectrum disorders. GSK3β has been shown to be important in activity dependent synaptic plasticity. This links Wnt signaling to the regulation of excitatory/ inhibitory synapse balance as recently reviewed [128].

Mental illnesses result from a combination of genetic susceptibility and environmental factors. Clinical and genetic studies indicate that altered circuitry as a result of disturbed neurodevelopment might underlie these diseases [129]. One of the rare genes that shows a strong correlation with mental illness is disrupted in schizophrenia 1 (*DISC1*) [130]. Srikanth et al. created disease-relevant DISC1 mutations in human induced pluripotent stem cells (hiPSCs). They showed that all mutations lead to reduced DISC1 protein levels. This lead to a subtle shift of NPCs and neurons to a dorsal identity [131]. As Wnt/β-catenin signaling is important for dorsal fate specification in neural progenitors (Figure 1b) [82, 111] and as DISC1 has been shown to affect Wnt signaling in mice [132], changes in this pathway were investigated. *DISC1* disruption lead to an increase in baseline Wnt signaling in NPCs derived from hiPSCs which altered their identity and their Wnt responsiveness. This ultimately lead to the altered neuronal identity observed in these cells. Antagonism of Wnt signaling during neural progenitor development can reverse the changes in cell fate [131]. In another study employing hiPSCs to model mental illness hiPSCs derived forebrain neural progenitor cells from four schizophrenia patients and control subjects were compared. RNA sequencing revealed a significant enrichment of Wnt signaling pathway genes in the hiPSC NPCs from schizophrenia patients but no difference in formation of neuronal populations was observed [133]. Schizophrenia is often accompanied by deficits in cognitive function. In this subgroup of patients with cognitive deficits Wu et al. found a specific and significant downregulation of Wnt signaling [134].

1.3.5 DEVELOPMENTAL SIGNALING CIRCUITS ARE HIJACKED DURING DISEASE

Processes like cell migration, proliferation and differentiation are tightly regulated during development and in the adult through the coordinated activity of signaling pathways. Sometimes these processes, and the signaling circuits that regulate them, are hijacked in pathogenesis. One of the best known examples is carcinogenesis, during which cells regain the capacity to self-renew and acquire migratory properties leading to metastasis.

1.3.5.1 Medulloblastoma

Medulloblastoma is the most common malignant brain tumor in children. It arises in the posterior fossa, which contains the cerebellum and brain stem. Overactivation of Wnt/β-catenin signaling defines one of four medulloblastoma subtypes [135-137]. Sporadic medulloblastomas show several mutations in the pathway [138-141] and germline mutations of *APC* cause familial adenomatous polyposis or Turcot's syndrome. Besides intestinal malignancies these patients often develop medulloblastoma [142].

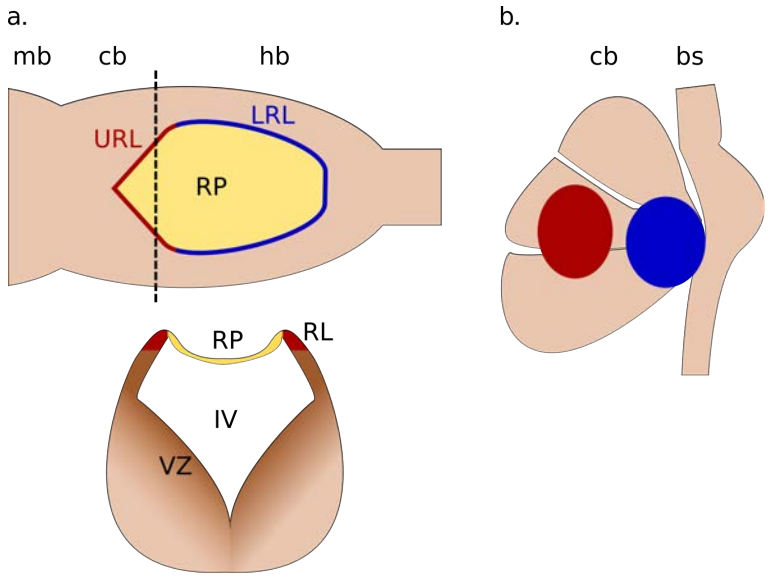

Figure 1.4 The origin of medulloblastoma. (a) The cerebellum arises from two germinal zones: the ventricular zone of the fourth ventricle (dark brown) and the upper rhombic lip (red). The upper rhombic lip gives rise to the granule neurons, the cell of origin of Shh-type medulloblastoma. Wnt-type medulloblastoma arises from the lower rhombic lip (blue) or dorsal brainstem. This is reflected by the anatomical position of both tumor types. (b) Shh-type medulloblastoma (red) occurs in the hemispheres of the cerebellum, while Wnt-type medulloblastoma (blue) is always associated with the brainstem. bs = brainstem; cb = cerebellum; hb = hindbrain; IV = fourth ventricle; LRL = lower rhombic lip; mb = midbrain; RL = rhombic lip; RP = roof plate; URL = upper rhombic lip; VZ = ventricular zone.

There are two distinct germinal zones giving rise to all the cell types of the cerebellum: the ventricular zone (VZ), on the dorsal side of the fourth ventricle, and the upper rhombic lip, at the caudal edge of the cerebellum (Figure 1.4) [143]. The upper rhombic lip gives rise to the granule neurons. These are the cell of origin of Sonic Hedgehog-type medulloblastoma and were for a long time considered to be the cells of origin for all medulloblastomas [144]. However overactivation of the Wnt pathway does not have a mitogenic effect on cerebellar granule neuron precursors. On the contrary, active Wnt signaling in these cells inhibits proliferation and expansion of granule neurons giving rise to a significantly smaller cerebellum [95, 145, 146]. Wnt/β-catenin signaling is active in the ventricular zone of mouse cerebellum from E18.5 onwards [147]. Pei et al showed that Wnt/β-catenin does promote proliferation in NSCs from the ventricular zone, however this is accompanied by a loss of self-renewal capacity and of differentiation [146]. Gibson et al. identified the lower rhombic lip (LRL) and dorsal brainstem as the origin of Wnt-type medulloblastoma (Figure 1.4). Activating β-catenin mutations have no effect on proliferation of progenitor cells in the cerebellum itself. However they lead to aberrant cell collections in the dorsal brainstem due to disturbed migration of progenitor cells of the LRL. Only concomitant mutation of Tp53 leads to the formation of tumors and these are always confined to the dorsal brainstem [148].

From the different medulloblastoma subtypes, Wnt-type medulloblastoma has the best prognosis. Recently it was shown that this is, at least in part, because of a disrupted blood-brain barrier specifically in this subtype. This leads to higher chemotherapy exposure in the tumors and thus higher response rates compared to other subtypes. Activation of the Wnt pathway in the tumor leads to increased expression of secreted Wnt antagonists, e.g. Dkk1, WIF1, resulting in the inhibition of Wnt signaling in adjacent endothelial cells, hence transforming the blood vessels in and around the tumor to a non-brain type of vessel with fenestrations and disturbed tight junctions [149]. Angiogenesis and blood-brain barrier formation are linked during development [150, 151]. Wnt ligands expressed in neural progenitors activate Wnt/β-catenin signaling in the endothelial cells and

this is needed for development of normal vasculature [151]. Wnt signaling also induces expression of some important markers of the blood brain barrier like the glucose transporter glut-1 at these early stages. The blood-brain barrier is an important obstacle for the treatment of neural diseases as many therapeutic compounds cannot cross it. Inhibition of Wnt signaling in the neural vasculature might thus resolve this problem, making the brain accessible for therapeutics.

1.3.5.2 Glioma

Glioblastoma is the most common and malignant primary brain tumor in humans and is very resistant to therapy. The tumor is characterized by the presence of a glioma stem cell (gSC) population that closely resembles adult neural stem cells and that is thought to be responsible for the continuous recurrence of the tumor [152]. Even though Wnt/β-catenin activating mutations are rare in glioblastoma, Wnt signaling was shown to be dysregulated in gSCs [153]. sFRP1, a negative regulator of Wnt/β-catenin signaling is severely downregulated in gSC cultures through promoter methylation [154, 155]. Restoration of sFRP1 expression reduces gSC proliferation by preventing S/G2 transition in the cell cycle. Additionally sFRP1 induces apoptosis in gSCs. However these effects are not permanent [154].

In glioma cell lines, active Wnt signaling is correlated with increased oncogenic properties [156, 157]. Sox9 overexpression is also associated with poor prognosis in malignant glioma [158]. Sox9 promotes epithelial-to-mesenchymal transition, a process important for metastasis, in a glioma cell line. It does so at least in part by activation of Wnt/β-catenin signaling [159]. Recently Wnt/β-catenin signaling was also linked to glioma dissemination. miR-30a-5p, which is upregulated in glioma and is linked with grade of malignancy [160], was shown to be a direct target of Wnt/β-catenin signaling. The microRNA miR-30a-5p is responsible for inhibition of NCAM expression upon Wnt signaling activation thus reducing cell adhesion and promoting the invasive properties of glioma cells [161].

1.3.6 DEVELOPMENTAL SIGNALING AS A CLUE FOR TREATING NEUROLOGICAL DISEASE

Disease is often the result of dysregulation of signaling pathways. Knowledge about the physiological role of these signaling pathways is therefore essential for determining what goes wrong in disease. This is important in the search for possible therapies. In the brain, especially neurodegenerative diseases might benefit from a restoration of neurogenesis.

1.3.6.1 Alzheimer's disease

Alzheimer's disease (AD) is the most common form of dementia in the elderly population. At the molecular level it is characterized by aggregation of amyloid β peptide into plaques and of hyperphosphorylated tau protein in neurofibrillary tangles. AD patients show progressive loss of cholinergic neurons leading to brain atrophy and impaired neurocognition (Figure 1.5). This is first seen in the medial temporal lobe, including the entorhinal cortex and hippocampus. Over the years aberrant Wnt/β-catenin signaling has been proposed to play a role in the onset and progression of AD [162]. Expression of Wnt signaling components at all levels of the pathway was changed in the post-mortem entorhinal cortex and hippocampus of AD patients compared to non-AD controls. At the protein level, the changes were most pronounced in intracellular signaling components (β-catenin, GSK3β, TCF7l1/TCF3) suggestive of changed Wnt pathway activity in AD patients [163].

Wnt signaling is already essential for initial specification of the neuroepithelium that will form the hippocampus. Interference with Wnt signaling during early stages of hippocampal development leads to a dramatic decrease or complete absence of the hippocampal primordium [164-166]. At later stages Wnt signaling has been shown to play a crucial role in neurogenesis. Overexpression of GSK3β, a negative regulator of the pathway, increases proliferation of NPCs leading to an increase in

mature granule cells and dentate gyrus volume in the adult possibly by preventing asymmetric cell divisions [167]. In the adult, Wnt/β-catenin signaling is active in the subgranular zone where adult hippocampal stem cells (ahSCs) reside (Figure 1.5). Wnts secreted by hippocampal astrocytes stimulate Wnt/β-catenin signaling in ahSCs. Wnt/β-catenin signaling promotes neuroblast proliferation and induces the neuronal lineage decision both *in vitro* and *in vivo* (Figure 1.5) [168]. *In vivo* knockdown of Fzd1 leads to impaired neuronal differentiation and migration of new neurons in the granule cell layer [169]. Surprisingly, Overexpression of Lrp6, a coreceptor of canonical Wnt signaling, reduces proliferation of NPCs from the adult hippocampus, however the molecular mechanism still has to be elucidated [170].

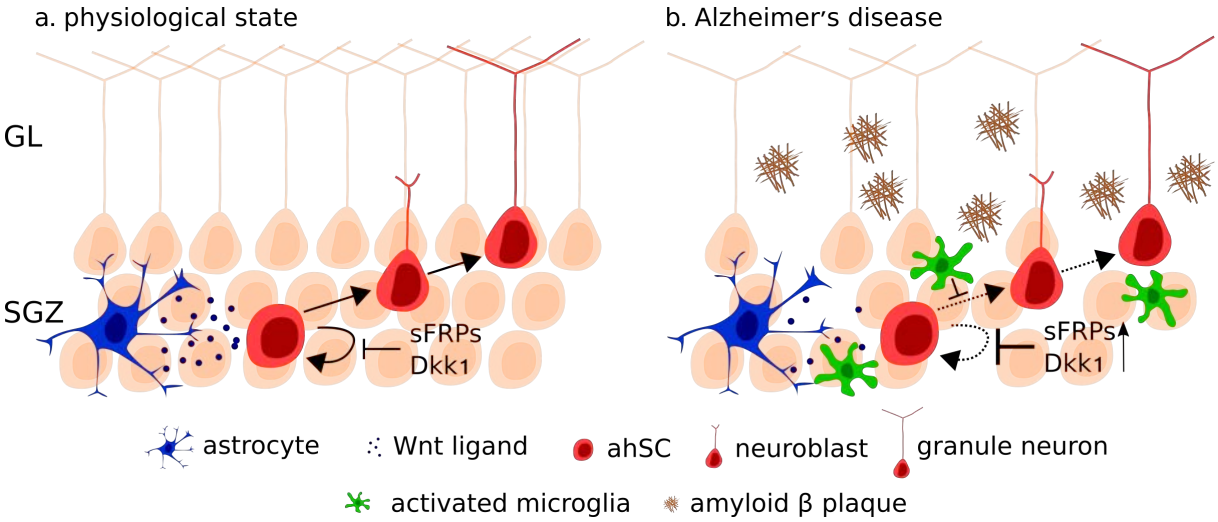

Figure 1.5 Adult neurogenesis in the dentate gyrus in the healthy adult and during Alzheimer's disease. (a) Wnt ligands secreted by astrocytes in the subgranular zone induce Wnt signaling in ahSCs. This leads to proliferation and differentiation to form new neurons which integrate in the granule cell layer. Neurogenesis is regulated by expression of Wnt antagonists (sFRPs, Dkk1) that maintain neighboring ahSCs in a quiescent state. (b) Alzheimer's disease is characterized by formation of amyloid beta plaques and loss of cholinergic neurons. With age Wnt ligand production by astrocytes diminishes and Wnt inhibitor expression increases preventing formation of new neurons. Activated microglia are recruited leading to neuroinflammation. This affects survival of ahSCs and further inhibits neurogenesis. ahSC, adult hippocampal stem cell; GL = granule layer; SGZ = subgranular zone.

Neurogenesis in the subgranular zone is tightly regulated by the expression of Wnt inhibitors by actively proliferating NPCs that counteract the activity of Wnts present in the stem cell niche and thus prevent self-renewal of neighboring quiescent stem cells [171, 172]. Differential expression of Wnt inhibitors is also responsible for regional differences in neurogenesis in the dentate gyrus [173]. With old age, neurogenesis diminishes, leading to a decrease of neurocognitive function (Figure 1.5). Loss of Dkk1 can rescue neurogenesis leading to formation of newborn mature neurons that exhibit complex dendritic morphology, another quality that is normally lost with old age, and that integrate in the dentate gyrus where they show neural activity positively influencing for example memory function [171].

In a mouse model of AD, activation of Wnt/β-catenin signaling via lithium treatment stimulated proliferation and differentiation of ahSCs, reduced amyloid β deposition and improved cognitive function during early stages of the disease. At more advanced stages of the disease lithium treatment also reduced amyloid β deposition but no increase in neurogenesis or amelioration of cognitive function was observed [174]. Recently, a lot of studies reported that compounds that have been shown to confer neuroprotection and promote neurogenesis in various AD models, exert these effects through activation of Wnt/β-catenin signaling [175-178]. The deposition of amyloid β plaques

during AD also leads to the recruitment and activation of microglia. This leads to neuroinflammation and studies have indicated that this may affect survival of NSCs and inhibit neurogenesis (Figure 1.5) [179]. In co-cultures of NSCs with microglia and amyloid β, nicotine treatment rescued proliferation and differentiation and prevented apoptosis of NSCs. Nicotine also activates Wnt/β-catenin signaling, which is repressed by activated microglia in AD, but it was not shown if this activation was solely responsible for the observed neuroprotection [180]. Further investigation is needed to elucidate the full potential of Wnt signaling interference in the treatment of AD.

1.3.6.2 Parkinson's disease

In the ventral midbrain there are two major populations of dopaminergic neurons (DA): the substantia nigra pars compacta (SNc) and the ventral tegmental area (VTA). The SNc DA are important for control over the execution of voluntary movements [181]. It is these neurons that preferentially degenerate during the progression of Parkinson's disease.

DA arise from the midbrain floor plate (Figure 1.6). The floor plate is defined by the expression of sonic hedgehog (Shh) but Shh prevents neurogenesis. In the midbrain, Wnt1 mediated active Wnt/β-catenin signaling is needed to counteract the inhibitory effect of Shh and to induce expression of DA progenitor-specific genes [182]. However constitutive activation of Wnt/β-catenin signaling does not lead to an increase in DA neurons. On the contrary, fewer DA are formed due to an altered DA progenitor identity [183]. Precise control over the level of Wnt/β-catenin signaling is thus needed for proper DA development. The transition of expression of Dickkopf 1/2 (Dkk1/2), secreted inhibitors of Wnt signaling, to expression of Dkk3, which can both positively and negatively modulate the pathway, leads to a switch from inactive to active Wnt/β-catenin signaling in DA progenitors and coincides with peak DA neurogenesis (Figure 1.6). Treatment of mouse pluripotent stem cells (PSCs) with WNT1/DKK3 promoted the formation of SNc DA neurons over VTA DA neurons [184]. This argues for the inclusion of DKK3 in differentiation protocols of PSCs into SNc DA neurons for use in stem cell-based therapies for Parkinson's disease. Another study in human PSCs also showed that precise control of Wnt signaling is essential for differentiation towards a DA fate [185].

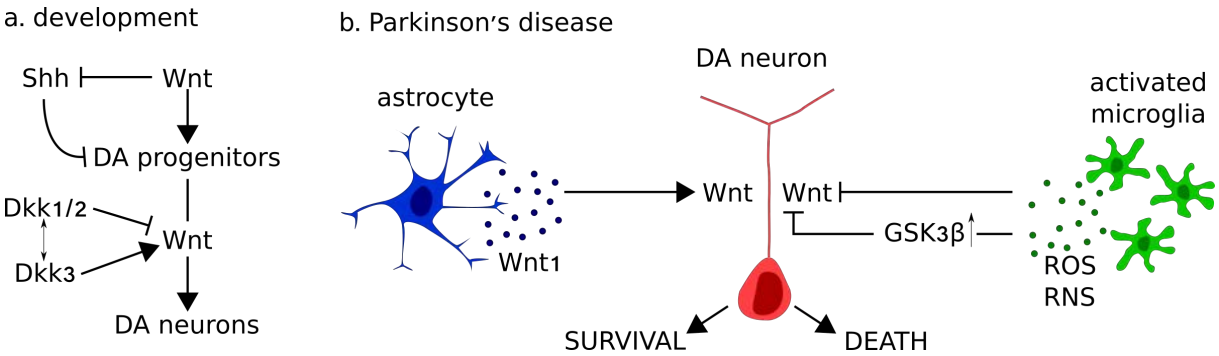

Figure 1.6 Wnt signaling during dopaminergic neuron development and Parkinson's disease. (a) Wnt signaling counteracts inhibitory Shh signaling in the midbrain floor plate to induce DA progenitors. Later a switch from inhibitory Dkk1/2 to Dkk3 expression induces precise levels of active Wnt signaling to induce DA differentiation. (b) During the progression of Parkinson's disease neuroinflammation by activation of microglia occurs. This leads to reduced Wnt signaling activation in DA. Activated microglia also produce reactive oxygen and nitrogen species, leading to an increase in GSK3β expression and further reducing Wnt signaling in DA. This contributes to DA death. Wnt ligand production by astrocytes counteracts the inhibitory effect of neuroinflammation on Wnt signaling in the DAs. However, this ability diminishes with age. DA, dopaminergic neuron; RNS, reactive nitrogen species; ROS, reactive oxygen species.

During the progression of Parkinson's disease, neuroinflammation by activation of microglia occurs (Figure 1.6) [186]. This contributes to degeneration of DA and to impairment of regeneration of these neurons. Activated microglia produce reactive oxygen and nitrogen species, leading to

reduced neurogenesis in part through activation of GSK3β [187]. During aging, expression of antioxidant and anti-inflammatory genes in the SVZ diminishes, contributing to the proinflammatory microenvironment in this region during PD [188]. This is counteracted by astrocytes that promote Wnt/β-catenin signaling by Wnt1 production, however this ability also diminishes with age [188-190]. Pharmacological inhibition of inflammation upregulates β-catenin in the SVZ where it rescues NPC proliferation and neuroblast formation. Moreover exogenous activation of β-catenin could overcome the negative effects on neurogenesis by activated microglia [187]. Pretreatment with acetyl-L-carnitine (ALCAR), a potent antioxidant, leads to improvement of behavioral and motor deficits through prevention of neuronal damage and enhancement of survival of DA neurons in a rat model of PD. This neuroprotective effect is the result of reduced glial activation and increased expression of proneural genes and is at least in part mediated by upregulation of the Wnt/β-catenin signaling pathway [191].

1.3.6.3 Central nervous system injury

Ischemia in the brain, e.g. by the occlusion of an artery, leads to cell death but also triggers a regenerative response. NPCs are induced to proliferate leading to an increase in immature neurons in the subventricular zone. Eventually mature neurons are formed that will repair the induced damage to some extent. However compared to the induction of proliferation of NPCs, differentiation into mature neurons that will restore neurologic function is limited [192]. In line with development inhibition of Wnt signaling leads to reduced proliferation of NPCs, neurogenesis and migration of immature neurons. This ultimately leads to a larger infarct volume [193]. Activation of Wnt signaling at the ischemic site increases neurogenesis and neuroprotection resulting in improved neurological function in mice [194].

Intravenous administration of bone marrow derived mesenchymal stem cells leads to improved neurocognition after traumatic brain injury (TBI). Zhao et al. showed that this is mainly the result of increased serum levels of Wnt3a leading to increased Wnt/β-catenin signaling activation in hippocampal neurons. Furthermore, intravenous injection of recombinant Wnt3a alone leads to neuroprotection in a mouse model of TBI [195]. Also after spinal cord injury (SCI) transplantation of Wnt3a-secreting fibroblasts leads to increased connectivity through axonal regeneration and improved motor function in rats [196]. In zebrafish, Wnt/β-catenin signaling is activated in radial glial neural progenitor cells in response to SCI. Wnt signaling promotes neuronal differentiation but has no effect on proliferation of these cells [197]. Recently it was shown that the neuroprotective effect of two independent drugs in rat models of SCI was due to activation of Wnt/β-catenin signaling [198, 199]. These studies highlight the potential of Wnt signaling activation as a therapeutic strategy to restore neurological function after central nervous system injury.

1.3.6.4 Generation of functional neurons from pluripotent stem cells

The holy grail for treating neurodegenerative diseases is replacement of lost neurons by new functional neurons through cell therapy. Both human pluripotent stem cells (hPSCs) and neural stem cells show great potential as an endless source of new neurons for tissue repair. As discussed above Wnt signaling has an important role in the differentiation of these cells towards various neural fates. In recent years a lot of progress has been made in the generation of specific neuronal cultures. Du et al. described a method to get an almost pure spinal motor neuron population from hPSCs through recapitulation of the developmental program of these neurons in culture. This is partly based on time-dependent regulation of Wnt/β-catenin signaling [200]. And also Cutts et al. described a protocol based on manipulation of Wnt/β-catenin signaling to get more brain region specific, homogenous NPC cultures from hPSCs [201]. Also, as described above, for the generation of

dopaminergic neurons precise control of Wnt signaling is essential [184, 185]. For generation of pure neuron populations precise recapitulation of the developmental program of these cells is needed, underscoring the importance of unraveling the physiological signaling events leading to their generation in the vertebrate embryo.

1.4 Interaction with the Notch signaling pathway

Only a handful of core signaling pathways exist. However, they guide the whole plethora of developmental processes from early cell specification to organogenesis. Cross talk between these pathways is therefore important to expand the amount of possible signaling outcomes. Wnt signaling has been extensively linked to the Notch signaling pathway [202]. Even in the polyp hydra, which belongs to one of the most basal animal phyla, integration of the Wnt and Notch signaling pathways occurs [203]. They are sometimes referred to as "Wntch signaling" [204, 205]. Interaction between both pathways can be both agonistic and antagonistic, depending on the specific context and cell type, and can occur at multiple levels of the pathways [202].

1.4.1 The Notch signaling pathway

The Notch signaling pathway is unique in the fact that it requires physical contact between cells to activate signaling. Notch signals are often used for binary fate decisions, selecting between pre-existing developmental programs [206].

The Notch receptor is a heterodimeric transmembrane protein (Figure 1.7). The Notch precursor is processed by a furin-like protease in the Golgi apparatus yielding the N-terminal extracellular fragment and the C-terminal transmembrane fragment that will associate at the cell surface forming the mature receptor [207, 208]. The extracellular domain contains epidermal growth factor-like repeats that mediate interaction with ligands [206, 208, 209]. The Notch ligands are themselves transmembrane proteins and are characterized by a N-terminal Delta/Serrate/LAG-2 (DSL) motif [206, 208]. Ligand binding triggers a conformational change in the receptor and initiates a sequence of proteolytic events leading to receptor activation [206, 210-213]. A first cleavage is performed by a disintegrin and metalloprotease (ADAM) protease in the extracellular domain just before the transmembrane domain. This creates a membrane-tethered intermediate that functions as substrate for a second and third cleavage by γ-secretase, setting the Notch intracellular domain (NICD) free [206, 211, 214]. The NICD contains a RBPjκ association module (RAM) domain, several nuclear localization signals, seven ankyrin repeats (ANK domain), a transactivation domain and a proline/glutamine acid/serine/threonine-rich motifs (PEST) domain, that harbors degradation signals [206, 208]. NICD translocates to the nucleus where it interacts with the CSL DNA-binding protein, an acronym of NICD binding proteins in different species (CBF1/RBPjκ/Su(H)/Lag-1), through its RAM domain [215, 216]. The ANK domain also associates with CSL and recruits the mastermind (MAML) co-activator, which in turn recruits general transcription activation factors including CBP/p300 and PCAF, leading to transcription of target genes [206, 211, 212, 217]. The CSL proteins thus function as the molecular endpoint of the pathway and determine the specificity of transcriptional activation through binding of CSL motifs in the gene promoters [218]. In the absence of NICD, CSL proteins act as a repressor by recruiting, among others, the transcriptional corepressor proteins hairless/CtBP, Groucho/TLE and the SMRT deacetylase corepressor complex [206, 212, 219].

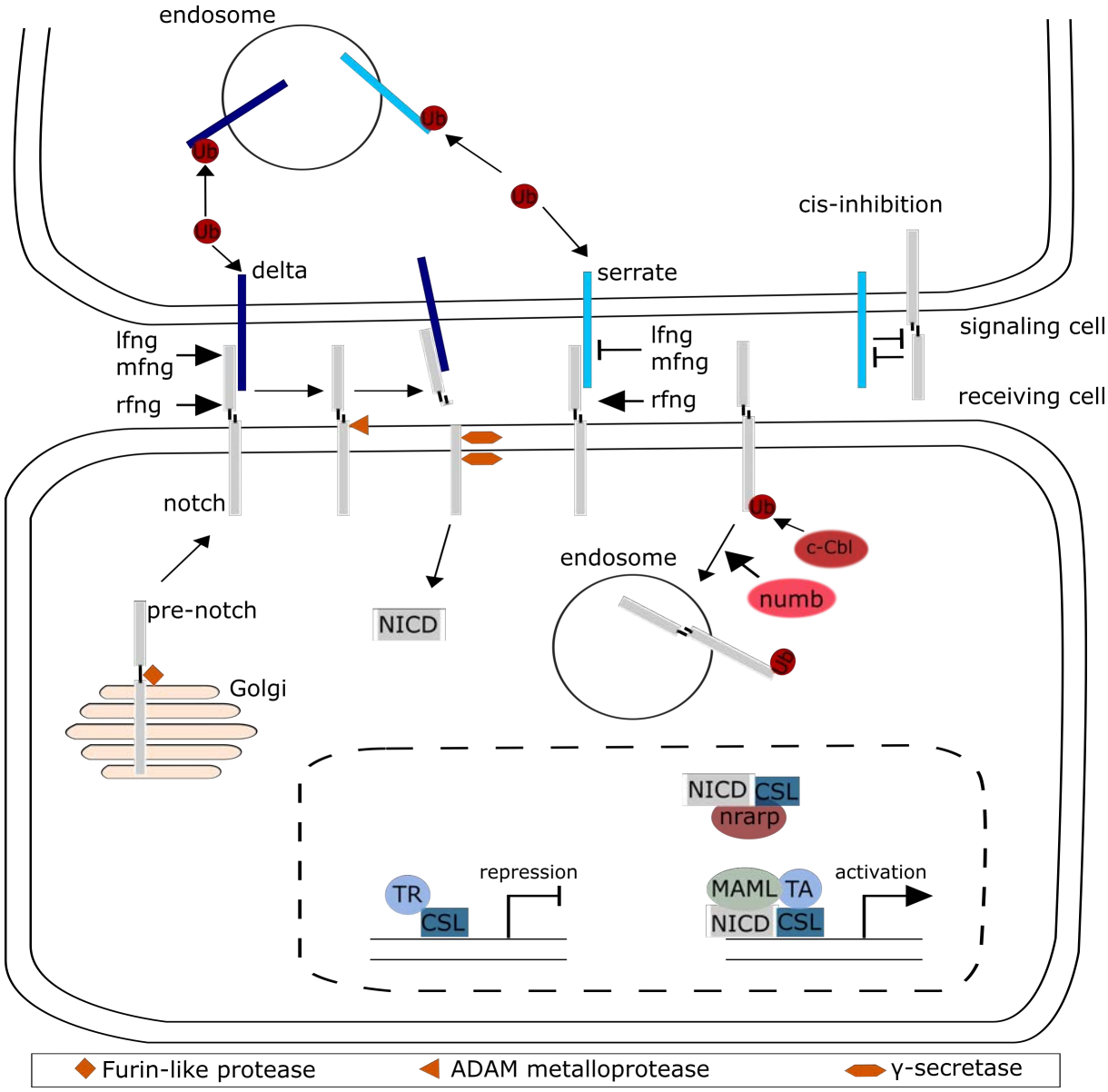

Figure 1.7 The Notch signaling pathway. The pre-Notch receptor is cleaved by a Furin-like protease in the Golgi apparatus. The mature Notch receptor forms a heterodimer at the cell membrane. Both the receptor and its ligands are transmembrane proteins. Upon interaction the receptor undergoes subsequent proteolytic cleavages by an ADAM metalloprotease and γ-secretase, resulting in release of the intracellular domain (NICD). The NICD enters the nucleus where it will bind CSL proteins and thereby removing transcriptional repressors. NICD recruits the Mastermind (MAML) co-activator, which in turn will recruit additional co-activators and induce transcription of target genes. Nrarp sequesters NICD and CSL in the nucleus thereby preventing transcriptional activation. Both receptor and ligand undergo ubiquitin-regulated internalization and are either degraded or recycled. The fringe proteins modulate ligand-receptor interactions. Lfng = lunatic fringe; mfng = manic fringe; rfng = radical fringe; TA = transcriptional activator; TR = transcriptional repressor.

Upon activation of the pathway only a subset of target genes are activated depending on the cellular context [220]. This is mostly achieved through interaction with local transcription factors. Also active maintenance of repression by CSL/co-repressor complexes on specific target gene promoters diversifies the Notch response [220]. Alternatively, interaction of NICD with DNA-binding factors alternative to CSL has been reported [220]. Members of the Hey and Hes family of basic Helix Loop Helix (bHLH) repressor proteins are the most prominent target genes [208, 221-223]. They were shown to be most rapidly upregulated upon Notch activation and shape the Notch signaling response through regulation of late target genes [224]. *Hes* genes generally prevent neural differentiation and maintain progenitors through repression of proneural bHLH activator proteins including *Mash1,*

Math and *Neurogenin* [225-229]. These proneural factors are expressed by differentiating neurons and induce *Delta* expression in these cells. This leads to Notch activation in neighboring cells and thus to the maintenance of these cells as progenitor cells, a process called lateral inhibition [230]. Notch-regulated ankyrin-repeat protein (Nrarp) is another, highly conserved, transcriptional target of Notch signaling [231-233]. Nrarp inhibits Notch signaling in several developmental systems through interference with NICD-mediated transcription [231, 234]. It forms a ternary complex with NICD and CSL protein and leads to a reduction in NICD levels [233].

As each receptor can signal only once, both Notch receptor and DSL ligand levels at the cell surface are tightly regulated (Figure 1.7) [208]. Besides regulation of expression, posttranslational regulatory mechanisms have been unveiled [206]. Endosomal trafficking has emerged as an important component of the Notch pathway, both for its activation as for the limitation of signaling [210, 212, 235]. The Notch receptor is tyrosine phosphorylated and subsequently mono-ubiquitinated by the E3 ubiquitin-ligating enzyme c-Cbl. This serves as a signal for internalization and targeting to the lysosomal degradation machinery [207]. The adaptor protein Numb acts as an inhibitor of Notch signaling by promoting sorting of internalized Notch receptor to late endosomes for degradation. Depletion of Numb promotes trafficking to recycling endosomes [235]. Ligands are internalized through endocytosis after mono-ubiquitination through the E3 ubiquitin ligases Neuralized and Mindbomb and through a poorly characterized process this leads to a more active ligand at the cell surface [206, 212].

Signaling is further regulated by cis-inhibition (Figure 1.7) [236-238]. A phenomenon based on inhibiting interactions between ligand and receptor localized on the same cell. Increased ligand expression in the receiving cell reduces its ability to respond to the ligand, while reciprocally increasing receptor expression in the sending cell reduces its ability to convey signal. If a cell would express more receptor than ligand cis-interactions would remove all ligands, leaving an excess of receptor thus enabling the cell to receive, but not send, Notch signals. On the other hand if more ligand is expressed the cell could only send, but not receive, signals. Cis-inhibition thus results in mutually exclusive signaling states [208, 237, 239]. This is important, as one of the main functions of Notch signaling is to control cell fate choices in adjacent cells that appear developmentally equivalent. One cell will exhibit a small increase of Notch ligand, inducing a certain cell fate, and meanwhile activates Notch signaling in the adjacent cells preventing them from adopting the same fate (similar to lateral inhibition during neurogenesis) [208, 212, 230]. However, in mammals four different Notch receptors (Notch1-4), three Delta family ligands (Dll1, Dll3 and Dll4) and two Serrate family ligands (Jag1 and Jag2) exist. These often have overlapping expression patterns and each receptor-ligand pair has different interaction strength. This makes predicting a cell's signaling state not straightforward [240]. Moreover, Fringe glycosyltransferases modulate the ligand-receptor interactions through glycosylation of the Notch extracellular domain (Figure 1.7) [240-242]. In mammals three homologues exist: *lunatic fringe* (*lfng*), *radical fringe* (*rfng*) and *manic fringe* (*mfng*). Lfng and mfng strengthen Delta signaling while inhibiting Serrate signaling [240, 241]. Rfng increases the signaling response to both ligand families. At the same time all fringe proteins strengthen Delta-Notch cis-interaction, while lfng and mfng, but not rfng, reduce Serrate-Notch cis-interactions [240].

1.4.2 NOTCH-MEDIATED INHIBITION OF WNT SIGNALING

In the supporting cells of the cochlea Notch inhibits Wnt signaling activation thereby preventing their proliferation and the regeneration of hair cells [243]. In intestinal stem cells Notch signaling is required to dampen Wnt signaling output thereby maintaining them as stem cells and preventing

Wnt-induced differentiation to secretory lineages [244]. Also in osteoblasts Notch signaling decreases active Wnt signaling [245]. During myogenesis, a switch from active Notch to Wnt signaling is needed, with Notch initially antagonizing Wnt signaling through activation of GSK3β (Figure 1.8) [246]. In embryonic stem cells and colon cancer cells the Notch receptor can sequester activated β-catenin and lead to its degradation by normal trafficking to the lysosome [247]. A same mechanism was also observed in *Drosophila* [248, 249]. During early patterning of the *Xenopus* embryo Notch antagonizes Wnt signaling through direct interaction between NICD and β-catenin. NICD destabilizes β-catenin protein independent of GSK3β-mediated phosphorylation [250]. In *Drosophila* synergistic downregulation of β-catenin by Notch and axin, independent of the destruction complex, has been described [251]. In colorectal cancer, activated Notch signaling leads to a downregulation of Wnt pathway target genes through epigenetic modification of their promoters [252]. In epidermis expressing a dominant negative MAML, thus preventing transcriptional activation of Notch target genes, nuclear β-catenin accumulates [253]. In cardiac and neural progenitor cells Notch signaling inhibition increases dephosphorylated β-catenin [254, 255]. Also in the epidermis and pancreas Notch1 functions as a tumor suppressor as *Notch1* loss of function induces an increase in activated β-catenin and augmented tumor incidence and progression [256, 257]. A possible mechanism is provided by Devgan et al, who show that the Notch target gene *p21* negatively regulates transcription of *Wnts* downstream of Notch signaling in keratinocytes [258]. Furthermore several Wnt ligand promoters contain binding sites for the Notch effector Hes1, a transcriptional repressor [258].

1.4.3 NOTCH-MEDIATED ACTIVATION OF WNT SIGNALING

In hematopoietic stem cells Notch signaling activates Wnt signaling through direct upregulation of *frizzled* expression, thereby promoting dendritic cell differentiation (Figure 1.8) [259]. In *Drosophila* Notch has been shown to cell-autonomously induce *Wnt* expression [260]. At the dorso-ventral boundary of the *Drosophila* wing disc and in the wing margin Notch signaling induces *Wnt* expression [261, 262]. In melanoma cells activated Notch signaling increases β-catenin protein levels through enhanced stability of the protein leading to augmented proliferation and metastatic capacity [263]. Also in the intestine, Notch and Wnt have a synergistic effect on proliferation and cooperate to trigger tumorigenesis [264, 265]. NICD was shown to interact with β-catenin and thereby promote proliferation through transcriptional activation of both *hes1* and *cyclinD1* [266]. Synergy between Notch and Wnt signaling to induce proliferation is also conserved in the *Drosophila* eye [264]. At high concentrations NICD can function as a co-activator for LEF1 on certain promoters, different from those bound by β-catenin/LEF1 [267]. The Notch target gene and inhibitor of the Notch signaling pathway, Nrarp, is a positive regulator of Wnt signaling. Nrarp blocks ubiquitination and subsequent degradation of LEF1 leading to its increased stability [268]. Last, MAML was also shown to act as a transcriptional co-activator associated with β-catenin to induce expression of Wnt target genes independent of Notch signaling [269].

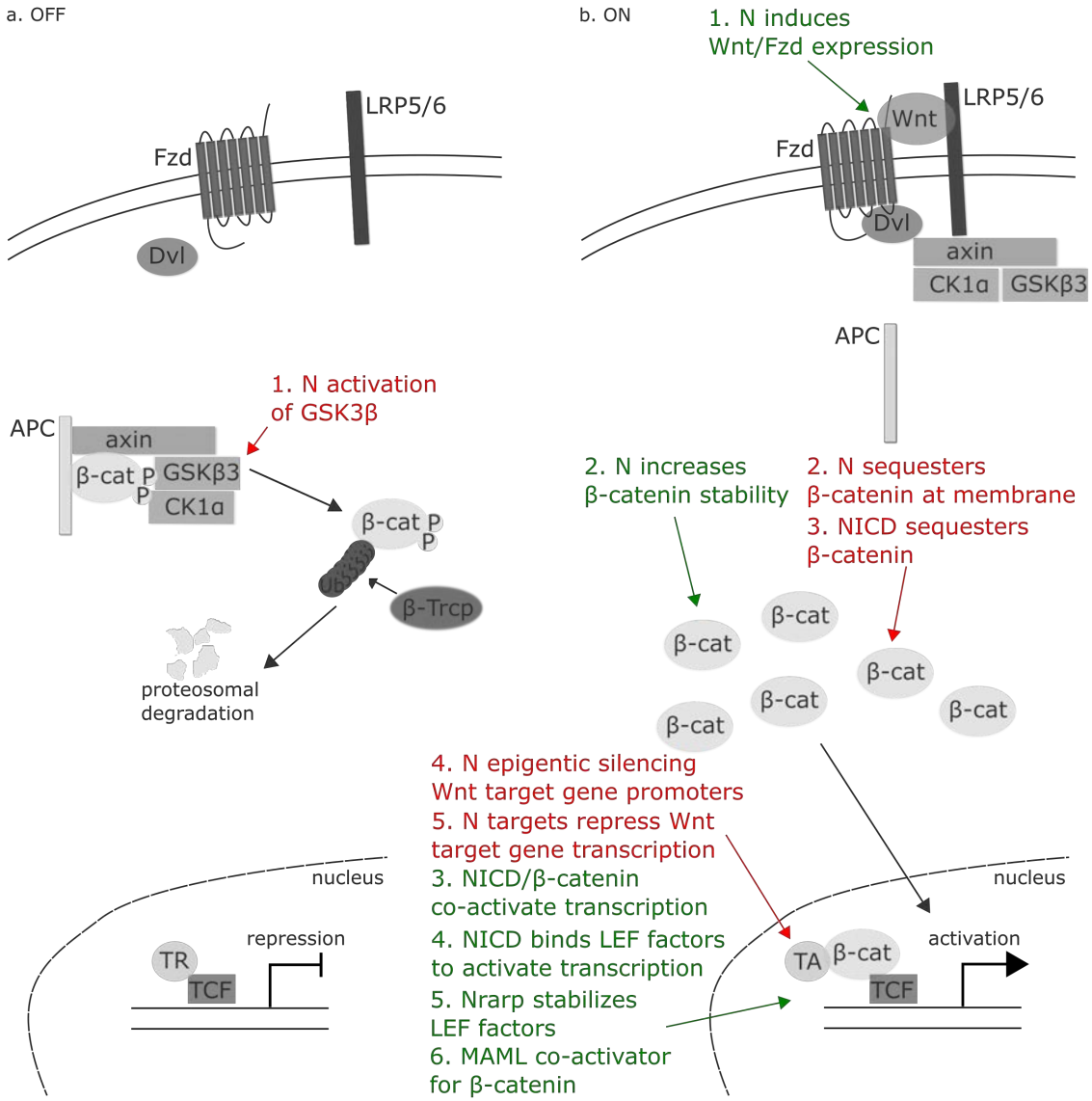

Figure 1.8 Notch mediated activation and inhibition of Wnt signaling. Wnt signaling pathway is depicted as above. Inhibiting and activating interactions with the Notch pathway are indicated in red and green, respectively. N, Notch.

1.4.4 WNT-MEDIATED INHIBITION OF NOTCH SIGNALING

In mammary stem cells Notch signaling is inhibited by active Wnt signaling through recruitment of β-catenin to Notch pathway gene promoters by the histone methylation reader Pygopus2, thereby preventing activation of their transcription [270]. In mammalian cells and the *Xenopus* embryo epidermis, Wnt signaling attenuates Notch signaling activity through direct binding of Dvl to CSL proteins, leading to a reduction of CSL protein in the nucleus (Figure 1.9) [271]. In *Drosophila* bristle development, Dvl was also shown to directly interact with NICD [272]. Dvl binds the PEST domain of NICD and promotes its degradation [273]. Also in *Drosophila,* Wnt signaling mediates the internalization and intracellular trafficking of Notch through Dvl-binding to the NICD [274]. Moreover, in *Drosophila* axin and APC promote the removal of Notch from the cell surface thereby targeting it for degradation [275]. Finally, it was shown that the Notch inhibitor Numb is a direct target gene of Wnt signaling, revealing also transcription-mediated inhibition of the Notch pathway downstream of Wnt signaling [276].

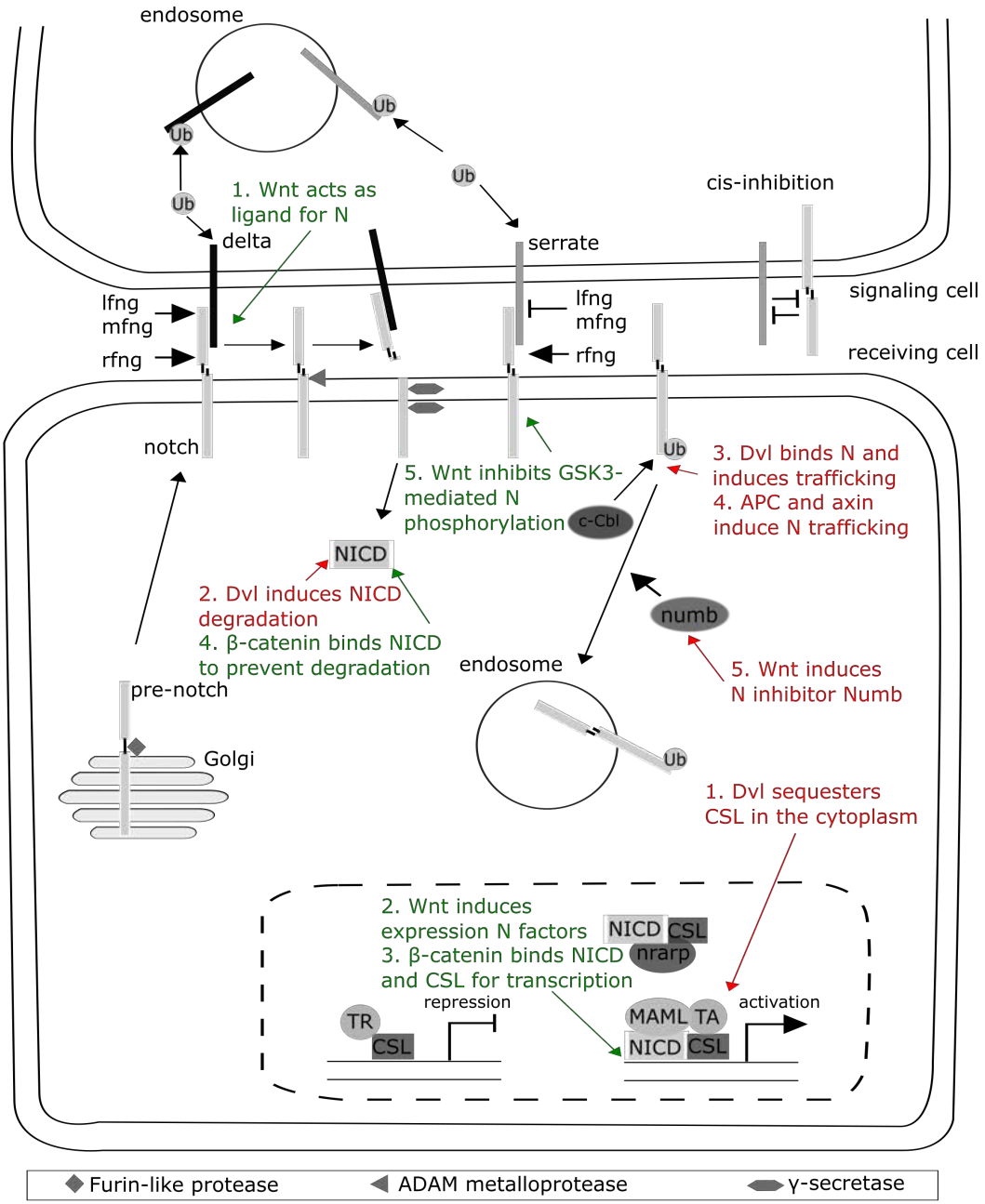

Figure 1.9 Wnt mediated activation and inhibition of Notch signaling. Notch signaling pathway is depicted as above. Inhibiting and activating interactions with the Wnt pathway are indicated in red and green, respectively. N, Notch.

1.4.5 *Wnt-mediated activation of Notch signaling*

Wnt signaling was shown to induce Notch signaling in hematopoietic stem cells [277]. In *Drosophila* Wnt ligand can bind the Notch receptor at a distinct site from the Delta or Serrate binding site and was shown to signal through the Notch receptor, independent of β-catenin (Figure 1.9) [262, 278-280]. In colorectal cancer, activated Wnt signaling, through APC loss of function, induces expression of Notch signaling components [281]. Many Notch pathway genes contain LEF/TCF sites in their promoters [282, 283]. In the mouse otic placode *Jag1, Notch1* and *Hes1* expression is induced by active Wnt signaling and Notch signaling subsequently augments Wnt signaling [284]. Wnt signaling directly induces Delta expression during mouse somitogenesis and *Drosophila* trachea development [283, 285]. *Jagged1* is a direct transcriptional target of Wnt signaling both in colorectal cancer cells and the epidermis, leading to Notch signaling activation [281, 286-288]. Also *Notch2* is a direct

transcriptional target of Wnt signaling in colorectal cancer cells [282]. Wnt signaling induces expression of *Hes1,* independent of Notch signaling activation [230, 252, 289, 290]. The *Hes1* promoter contains two putative LEF/TCF sites and Wnt signaling directly induces *Hes1* expression in colorectal cancer [281]. Furthermore, Wnt signaling can also induce *Hes1* expression through Notch signaling factors. During mouse vasculogenesis β-catenin, NICD and RBP-Jκ form a complex in arterial endothelial cells, where they induce specific target genes for arterial fate specification, including *Hes1* [291]. Other studies confirmed β-catenin/NICD interaction in the nucleus, where they bind, together with transcriptional activators, RBP-Jκ sites in the *Hes1* promoter thereby potentiating Hes1 expression [292, 293]. Moreover, the interaction between NICD and β-catenin was shown to confer mutual protection from proteosomal degradation [293]. GSK3 phosphorylates both Notch1 and Notch2 ICD resulting in downregulation of Notch-dependent *Hes1* transcription [294, 295]. Wnt signaling activation can thus increase Hes1 expression through inhibition of GSK3β [294, 295].

1.5 WNT SIGNALING IN CANCER

Even though the *Wnt1* gene was originally discovered as an initiating gene in mouse mammary carcinogenesis, no mutations in *Wnt* genes, either point mutations or structural rearrangements, could be identified in any kind of human tumor [5]. Later work revealed that downstream components, rather than the Wnt ligands at the upper end of the pathway, are commonly mutated in human cancers. Pioneering insights came from colorectal cancer with the identification of the *APC* gene [296, 297].

1.5.1 CONSTITUTIVE ACTIVATION OF THE PATHWAY

Familial adenomatous polyposis (FAP), an autosomal dominant inherited syndrome of colorectal cancer, is characterized by the development of hundreds to thousands colonic adenomas at a young age. These adenomas have the tendency to undergo malignant transformation leading to colorectal cancer. Patients often also suffer from extracolonic malignancies, like adenomas and adenocarcinomas in other regions of the gastrointestinal system, desmoid tumors and brain tumors [298]. This syndrome was linked to germline mutations of *APC* in 1991 [296, 297, 299]. Somatic mutations in *APC* are also found in most sporadic colorectal cancers (Figure 1.10a) [300]. Mutations are concentrated in the so-called mutation cluster region, resulting in a truncated protein that can no longer bind its interaction partners and thus can no longer execute its function in the destruction complex [301, 302]. This leads to constitutive activation of the Wnt pathway [298, 300, 303]. Interestingly, different mutations in *APC* result in different levels of activated β-catenin protein and are associated with tumor formation in the different tissues [304]. *APC* mutations thus occur not entirely random but are associated with an optimal level of β-catenin signaling to promote tumor formation, described as the "just-right"-signaling hypothesis [302, 304]. Colorectal tumors with an intact *APC* gene often contain activating mutations in *CTNNB1* (encoding β-catenin), through disruption of the N-terminal regulatory phosphorylation sites (Figure 1.10a) [300]. The remainder of colorectal tumors carries mutations in yet other Wnt pathway components like *AXIN* or *RNF43* [305-307]. Gene fusions involving R-spondins were also observed. R-spondins potentiate Wnt signaling and the gene fusions constitute an alternative way to achieve Wnt pathway activation [308].

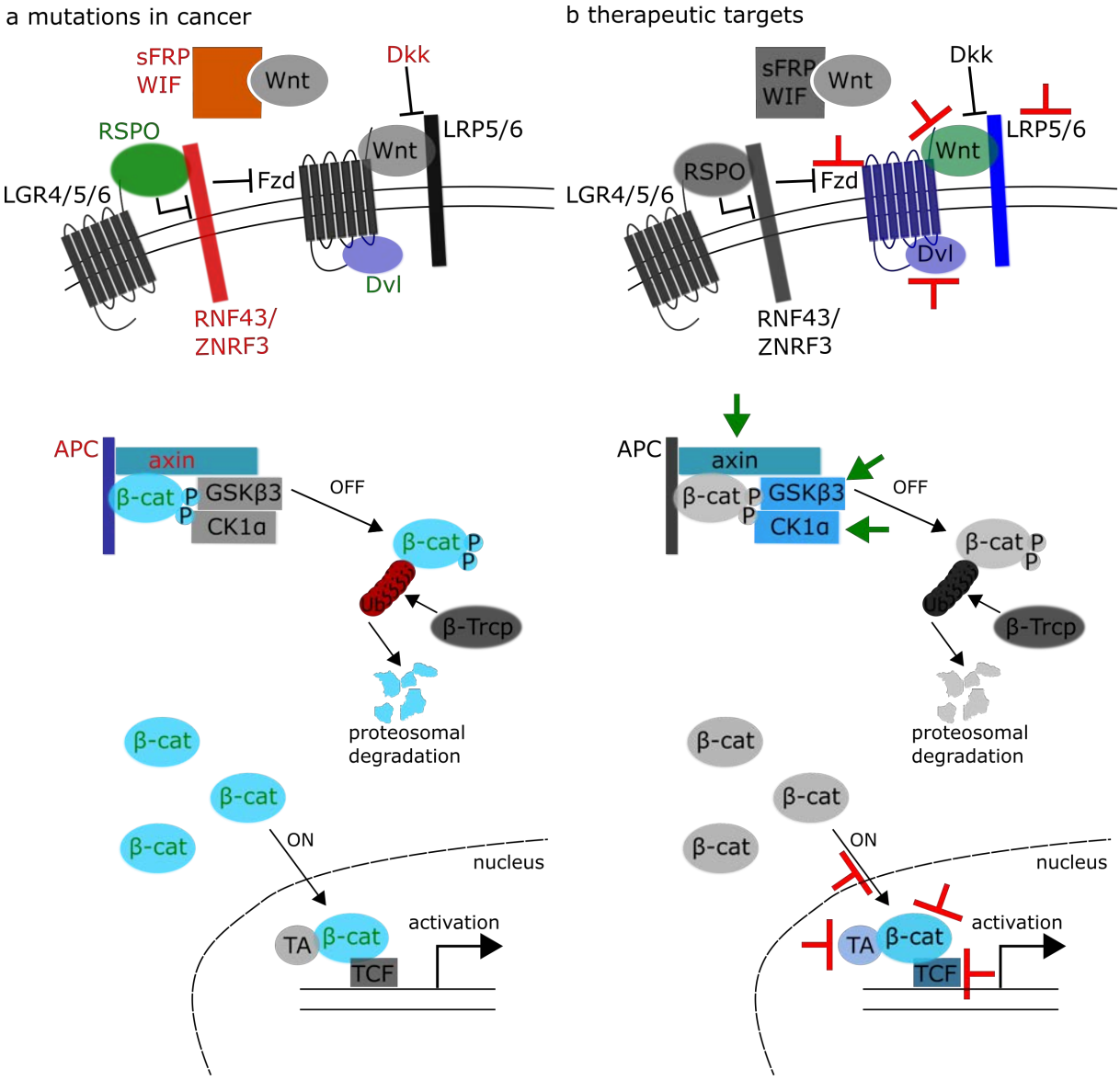

Figure 1.10 Mutations in the Wnt pathway associated with cancer and therapeutic targets. (a) Schematic overview of the Wnt signaling pathway. Signaling factors which are not associated with cancer are depicted in greyscale. Coloured signaling factors represent signaling factors which are associated with constitutive Wnt signaling activation in cancer. Green signaling components show gain of function or overexpression, while red factors show loss of function or reduced expression in malignancies. (b) Schematic overview of the Wnt signaling pathway showing strategies for therapeutic targeting currently under investigation. Currently, no therapeutics are under development against processes in greyscale. Red inhibition arrows represent drugs blocking respective components or processes of the signaling pathway. Green arrows represent drugs that agonize signaling factors. TA, transcriptional activator.

Besides colorectal cancer, constitutive activation of Wnt signaling is involved in multiple other malignancies including, but not limited to, melanoma, non-small cell lung cancer, breast cancer, liver cancer, thyroid cancer and ovarian cancer [307, 309-314]. Mutations in *APC* are rare in cancers outside the gut. Oncogenic mutations in *CTNNB1,* relieving it from negative regulation by the destruction complex, are a more common event in sporadic cancers [302]. Other Wnt signaling factors are linked to specific cancer types (Figure 1.10a). Mutations in *RNF43* are associated with mucinous ovarian cancer and *DVL* overexpression is characteristic for cervical squamous cell cancer and pleural mesothelioma [315-317]. Moreover, epigenetic silencing of Wnt antagonists, for example sFRPs, Dkk proteins and WIF1, is a common event in cancer, further contributing to Wnt signaling hyperactivation [318-327]. Consequence of constitutive Wnt signaling activity is sustained expression

of target genes leading to several pro-tumorigenic events. Induction of Wnt signaling factor expression creates a positive feedback loop, maintaining Wnt activity [298, 328]. CyclinD1 and c-myc induce continuous cell proliferation, while differentiation is inhibited by expression of *ID* and *MSX* genes [54, 298, 328, 329]. Wnt signaling has also been shown to play a role in metastasis for instance by stabilization of the epithelial-to-mesenchymal transition regulator SNAI2 in breast cancer cells [307]. Furthermore, a role for Wnt signaling in immune evasion of cancer cells has recently emerged [307]. Importantly, Wnt signaling activation is not always associated with worse prognosis. In malignant melanoma, increased nuclear β-catenin is associated with reduced proliferation, increased differentiation and improved survival [309, 330]. β-catenin mutations are also associated with a favorable prognosis in endometrioid ovarian cancer [302]. This highlights the importance of studying signaling processes in their proper context.

1.5.2 THERAPEUTIC TARGETING

Interference with Wnt signaling has evidently been explored as a therapeutic strategy in cancer. Therapeutics targeting the Wnt pathway can be divided in four categories based on the level of the signaling pathway where they interact (Figure 1.10b) [331]. A first category focuses on the ligand-receptor interaction with porcupine inhibitors, Wnt5a-mimicking molecules and multiple ligand and receptor blocking antibodies. Wnt1 antibodies induced significant apoptosis in colorectal cancer cells, even in the presence of mutations in downstream factors [332]. Also in head and neck squamous cell carcinoma anti-Wnt1 antibodies inhibited proliferation and induced apoptosis [333]. A second group focuses on β-catenin degradation like DVL inhibitors, axin stabilizing agents and activators of the β-catenin phosphorylating kinases CK1 and GSK3β [331]. As nuclear localization of β-catenin is needed for its transcriptional activity, a third category focuses on subcellular localization of β-catenin and a last category targets transcriptional co-activators of β-catenin in the nucleus like blocking of the β-catenin-CBP interaction [307, 331, 334, 335]. However, due to the involvement of Wnt signaling in so many developmental processes and in adult tissue homeostasis, side effects from targeting such a crucial pathway are an obvious concern. Moreover, due to its complexity, the Wnt pathway is notoriously difficult to target [336]. Despite tremendous efforts, no drugs targeting the Wnt pathway are currently being used in the clinic, however several are in clinical trials, mostly phase I [51, 307, 336].

1.6 SUMMARY

It has been over 30 years since the Wnt/β-catenin signaling pathway was first discovered, but still today new insights into its signaling mechanism are generated. Many different mechanisms for the internal signaling cascades have been proposed while no consensus has been reached about how exactly Wnt signaling activation leads to transcriptional activation by β-catenin. The many different factors involved in the pathway and their involvement in other cellular processes further complicates the unraveling of this multi-purpose signaling pathway. Research into the many Wnt-related processes thus remains valuable to uncover the whole Wnt signaling-picture.

Notch signaling is another key developmental signaling pathway. Wnt and Notch signaling are often simultaneously important during development. Wnt-Notch signaling antagonism instructs cell fate decisions where activity of each pathway drives the cell to a different lineage. Signaling antagonism creates a clear distinction between Wnt ON, Notch OFF and Wnt OFF, Notch ON cells. In other contexts, like cancer, both signaling pathways enhance each other's activity. Interaction occurs

through transcriptional regulation of signaling component of the other pathway and through direct protein-protein interactions between components of both pathways.

More and more evidence confirms the essential role of Wnt signaling during neural development and its involvement in disorders of the central nervous system. As we gain more knowledge in the developmental role of Wnt signaling, we learn more about the molecular mechanisms behind disease. This should bring us closer to new therapeutic strategies for curing these diseases.

1.7 REFERENCES

1. Nusse, R. and H.E. Varmus, *Many tumors induced by the mouse mammary tumor virus contain a provirus integrated in the same region of the host genome.* Cell, 1982. **31**(1): p. 99-109.
2. Sharma, R.P. and V.L. Chopra, *Effect of the Wingless (wg1) mutation on wing and haltere development in Drosophila melanogaster.* Dev Biol, 1976. **48**(2): p. 461-5.
3. Nusse, R., et al., *A new nomenclature for int-1 and related genes: the Wnt gene family.* Cell, 1991. **64**(2): p. 231.
4. Rijsewijk, F., et al., *The Drosophila homolog of the mouse mammary oncogene int-1 is identical to the segment polarity gene wingless.* Cell, 1987. **50**(4): p. 649-57.
5. Nusse, R. and H. Varmus, *Three decades of Wnts: a personal perspective on how a scientific field developed.* EMBO J, 2012. **31**(12): p. 2670-84.
6. Gavin, B.J., J.A. McMahon, and A.P. McMahon, *Expression of multiple novel Wnt-1/int-1-related genes during fetal and adult mouse development.* Genes Dev, 1990. **4**(12B): p. 2319-32.
7. Petersen, C.P. and P.W. Reddien, *Wnt signaling and the polarity of the primary body axis.* Cell, 2009. **139**(6): p. 1056-68.
8. Barker, N., et al., *Identification of stem cells in small intestine and colon by marker gene Lgr5.* Nature, 2007. **449**(7165): p. 1003-7.
9. Clevers, H. and R. Nusse, *Wnt/beta-catenin signaling and disease.* Cell, 2012. **149**(6): p. 1192-205.
10. Logan, C.Y. and R. Nusse, *The Wnt signaling pathway in development and disease.* Annu Rev Cell Dev Biol, 2004. **20**: p. 781-810.
11. Ikeda, S., et al., *Axin, a negative regulator of the Wnt signaling pathway, forms a complex with GSK-3beta and beta-catenin and promotes GSK-3beta-dependent phosphorylation of beta-catenin.* EMBO J, 1998. **17**(5): p. 1371-84.
12. Orford, K., et al., *Serine phosphorylation-regulated ubiquitination and degradation of beta-catenin.* J Biol Chem, 1997. **272**(40): p. 24735-8.
13. Peifer, M., L.M. Pai, and M. Casey, *Phosphorylation of the Drosophila adherens junction protein Armadillo: roles for wingless signal and zeste-white 3 kinase.* Dev Biol, 1994. **166**(2): p. 543-56.
14. Aberle, H., et al., *beta-catenin is a target for the ubiquitin-proteasome pathway.* EMBO J, 1997. **16**(13): p. 3797-804.
15. Liu, C., et al., *Control of beta-catenin phosphorylation/degradation by a dual-kinase mechanism.* Cell, 2002. **108**(6): p. 837-47.
16. Amit, S., et al., *Axin-mediated CKI phosphorylation of beta-catenin at Ser 45: a molecular switch for the Wnt pathway.* Genes Dev, 2002. **16**(9): p. 1066-76.
17. Behrens, J., et al., *Functional interaction of an axin homolog, conductin, with beta-catenin, APC, and GSK3beta.* Science, 1998. **280**(5363): p. 596-9.
18. Rubinfeld, B., et al., *Binding of GSK3beta to the APC-beta-catenin complex and regulation of complex assembly.* Science, 1996. **272**(5264): p. 1023-6.
19. Su, L.K., B. Vogelstein, and K.W. Kinzler, *Association of the APC tumor suppressor protein with catenins.* Science, 1993. **262**(5140): p. 1734-7.

20. Rubinfeld, B., et al., *Association of the APC gene product with beta-catenin.* Science, 1993. **262**(5140): p. 1731-4.
21. Winston, J.T., et al., *The SCFbeta-TRCP-ubiquitin ligase complex associates specifically with phosphorylated destruction motifs in IkappaBalpha and beta-catenin and stimulates IkappaBalpha ubiquitination in vitro.* Genes Dev, 1999. **13**(3): p. 270-83.
22. Liu, C., et al., *beta-Trcp couples beta-catenin phosphorylation-degradation and regulates Xenopus axis formation.* Proc Natl Acad Sci U S A, 1999. **96**(11): p. 6273-8.
23. Cavallo, R.A., et al., *Drosophila Tcf and Groucho interact to repress Wingless signalling activity.* Nature, 1998. **395**(6702): p. 604-8.
24. Billin, A.N., H. Thirlwell, and D.E. Ayer, *Beta-catenin-histone deacetylase interactions regulate the transition of LEF1 from a transcriptional repressor to an activator.* Mol Cell Biol, 2000. **20**(18): p. 6882-90.
25. Willert, K., et al., *Wnt proteins are lipid-modified and can act as stem cell growth factors.* Nature, 2003. **423**(6938): p. 448-52.
26. Takada, R., et al., *Monounsaturated fatty acid modification of Wnt protein: its role in Wnt secretion.* Dev Cell, 2006. **11**(6): p. 791-801.
27. Najdi, R., et al., *A uniform human Wnt expression library reveals a shared secretory pathway and unique signaling activities.* Differentiation, 2012. **84**(2): p. 203-13.
28. Hofmann, K., *A superfamily of membrane-bound O-acyltransferases with implications for wnt signaling.* Trends Biochem Sci, 2000. **25**(3): p. 111-2.
29. Kadowaki, T., et al., *The segment polarity gene porcupine encodes a putative multitransmembrane protein involved in Wingless processing.* Genes Dev, 1996. **10**(24): p. 3116-28.
30. Bartscherer, K., et al., *Secretion of Wnt ligands requires Evi, a conserved transmembrane protein.* Cell, 2006. **125**(3): p. 523-33.
31. Banziger, C., et al., *Wntless, a conserved membrane protein dedicated to the secretion of Wnt proteins from signaling cells.* Cell, 2006. **125**(3): p. 509-22.
32. Yang-Snyder, J., et al., *A frizzled homolog functions in a vertebrate Wnt signaling pathway.* Curr Biol, 1996. **6**(10): p. 1302-6.
33. Bhanot, P., et al., *A new member of the frizzled family from Drosophila functions as a Wingless receptor.* Nature, 1996. **382**(6588): p. 225-30.
34. Wehrli, M., et al., *arrow encodes an LDL-receptor-related protein essential for Wingless signalling.* Nature, 2000. **407**(6803): p. 527-30.
35. Pinson, K.I., et al., *An LDL-receptor-related protein mediates Wnt signalling in mice.* Nature, 2000. **407**(6803): p. 535-8.
36. Bilic, J., et al., *Wnt induces LRP6 signalosomes and promotes dishevelled-dependent LRP6 phosphorylation.* Science, 2007. **316**(5831): p. 1619-22.
37. Noordermeer, J., et al., *dishevelled and armadillo act in the wingless signalling pathway in Drosophila.* Nature, 1994. **367**(6458): p. 80-3.
38. Zeng, X., et al., *A dual-kinase mechanism for Wnt co-receptor phosphorylation and activation.* Nature, 2005. **438**(7069): p. 873-7.
39. Davidson, G., et al., *Casein kinase 1 gamma couples Wnt receptor activation to cytoplasmic signal transduction.* Nature, 2005. **438**(7069): p. 867-72.
40. Mao, J., et al., *Low-density lipoprotein receptor-related protein-5 binds to Axin and regulates the canonical Wnt signaling pathway.* Mol Cell, 2001. **7**(4): p. 801-9.
41. Zeng, X., et al., *Initiation of Wnt signaling: control of Wnt coreceptor Lrp6 phosphorylation/activation via frizzled, dishevelled and axin functions.* Development, 2008. **135**(2): p. 367-75.
42. Willert, K., S. Shibamoto, and R. Nusse, *Wnt-induced dephosphorylation of axin releases beta-catenin from the axin complex.* Genes Dev, 1999. **13**(14): p. 1768-73.
43. Luo, W., et al., *Protein phosphatase 1 regulates assembly and function of the beta-catenin degradation complex.* EMBO J, 2007. **26**(6): p. 1511-21.

44. Cselenyi, C.S., et al., *LRP6 transduces a canonical Wnt signal independently of Axin degradation by inhibiting GSK3's phosphorylation of beta-catenin.* Proc Natl Acad Sci U S A, 2008. **105**(23): p. 8032-7.
45. Wu, G., et al., *Inhibition of GSK3 phosphorylation of beta-catenin via phosphorylated PPPSPXS motifs of Wnt coreceptor LRP6.* PLoS One, 2009. **4**(3): p. e4926.
46. Riggleman, B., P. Schedl, and E. Wieschaus, *Spatial expression of the Drosophila segment polarity gene armadillo is posttranscriptionally regulated by wingless.* Cell, 1990. **63**(3): p. 549-60.
47. Daniels, D.L. and W.I. Weis, *Beta-catenin directly displaces Groucho/TLE repressors from Tcf/Lef in Wnt-mediated transcription activation.* Nat Struct Mol Biol, 2005. **12**(4): p. 364-71.
48. Huber, O., et al., *Nuclear localization of beta-catenin by interaction with transcription factor LEF-1.* Mech Dev, 1996. **59**(1): p. 3-10.
49. Molenaar, M., et al., *XTcf-3 transcription factor mediates beta-catenin-induced axis formation in Xenopus embryos.* Cell, 1996. **86**(3): p. 391-9.
50. Behrens, J., et al., *Functional interaction of beta-catenin with the transcription factor LEF-1.* Nature, 1996. **382**(6592): p. 638-42.
51. Staal, F.J., et al., *Wnt signals are transmitted through N-terminally dephosphorylated beta-catenin.* EMBO Rep, 2002. **3**(1): p. 63-8.
52. Hecht, A., et al., *The p300/CBP acetyltransferases function as transcriptional coactivators of beta-catenin in vertebrates.* EMBO J, 2000. **19**(8): p. 1839-50.
53. Jho, E.H., et al., *Wnt/beta-catenin/Tcf signaling induces the transcription of Axin2, a negative regulator of the signaling pathway.* Mol Cell Biol, 2002. **22**(4): p. 1172-83.
54. He, T.C., et al., *Identification of c-MYC as a target of the APC pathway.* Science, 1998. **281**(5382): p. 1509-12.
55. Vinyoles, M., et al., *Multivesicular GSK3 sequestration upon Wnt signaling is controlled by p120-catenin/cadherin interaction with LRP5/6.* Mol Cell, 2014. **53**(3): p. 444-57.
56. Taelman, V.F., et al., *Wnt signaling requires sequestration of glycogen synthase kinase 3 inside multivesicular endosomes.* Cell, 2010. **143**(7): p. 1136-48.
57. Li, V.S., et al., *Wnt signaling through inhibition of beta-catenin degradation in an intact Axin1 complex.* Cell, 2012. **149**(6): p. 1245-56.
58. Hernandez, A.R., A.M. Klein, and M.W. Kirschner, *Kinetic responses of beta-catenin specify the sites of Wnt control.* Science, 2012. **338**(6112): p. 1337-40.
59. Tolwinski, N.S., et al., *Wg/Wnt signal can be transmitted through arrow/LRP5,6 and Axin independently of Zw3/Gsk3beta activity.* Dev Cell, 2003. **4**(3): p. 407-18.
60. Bafico, A., et al., *Interaction of frizzled related protein (FRP) with Wnt ligands and the frizzled receptor suggests alternative mechanisms for FRP inhibition of Wnt signaling.* J Biol Chem, 1999. **274**(23): p. 16180-7.
61. Rattner, A., et al., *A family of secreted proteins contains homology to the cysteine-rich ligand-binding domain of frizzled receptors.* Proc Natl Acad Sci U S A, 1997. **94**(7): p. 2859-63.
62. Leyns, L., et al., *Frzb-1 is a secreted antagonist of Wnt signaling expressed in the Spemann organizer.* Cell, 1997. **88**(6): p. 747-56.
63. Finch, P.W., et al., *Purification and molecular cloning of a secreted, Frizzled-related antagonist of Wnt action.* Proc Natl Acad Sci U S A, 1997. **94**(13): p. 6770-5.
64. Xavier, C.P., et al., *Secreted Frizzled-related protein potentiation versus inhibition of Wnt3a/beta-catenin signaling.* Cell Signal, 2014. **26**(1): p. 94-101.
65. Hsieh, J.C., et al., *A new secreted protein that binds to Wnt proteins and inhibits their activities.* Nature, 1999. **398**(6726): p. 431-6.
66. Semenov, M.V., et al., *Head inducer Dickkopf-1 is a ligand for Wnt coreceptor LRP6.* Curr Biol, 2001. **11**(12): p. 951-61.
67. Mao, B., et al., *LDL-receptor-related protein 6 is a receptor for Dickkopf proteins.* Nature, 2001. **411**(6835): p. 321-5.

68. Bafico, A., et al., *Novel mechanism of Wnt signalling inhibition mediated by Dickkopf-1 interaction with LRP6/Arrow.* Nat Cell Biol, 2001. **3**(7): p. 683-6.
69. Koo, B.K., et al., *Tumour suppressor RNF43 is a stem-cell E3 ligase that induces endocytosis of Wnt receptors.* Nature, 2012. **488**(7413): p. 665-9.
70. Hao, H.X., et al., *ZNRF3 promotes Wnt receptor turnover in an R-spondin-sensitive manner.* Nature, 2012. **485**(7397): p. 195-200.
71. Zebisch, M., et al., *Structural and molecular basis of ZNRF3/RNF43 transmembrane ubiquitin ligase inhibition by the Wnt agonist R-spondin.* Nat Commun, 2013. **4**: p. 2787.
72. Carmon, K.S., et al., *R-spondins function as ligands of the orphan receptors LGR4 and LGR5 to regulate Wnt/beta-catenin signaling.* Proc Natl Acad Sci U S A, 2011. **108**(28): p. 11452-7.
73. de Lau, W., et al., *Lgr5 homologues associate with Wnt receptors and mediate R-spondin signalling.* Nature, 2011. **476**(7360): p. 293-7.
74. Nordstrom, U., T.M. Jessell, and T. Edlund, *Progressive induction of caudal neural character by graded Wnt signaling.* Nat Neurosci, 2002. **5**(6): p. 525-32.
75. Carron, C. and D.L. Shi, *Specification of anteroposterior axis by combinatorial signaling during Xenopus development.* Wiley Interdiscip Rev Dev Biol, 2016. **5**(2): p. 150-68.
76. Brault, V., et al., *Inactivation of the beta-catenin gene by Wnt1-Cre-mediated deletion results in dramatic brain malformation and failure of craniofacial development.* Development, 2001. **128**(8): p. 1253-64.
77. Thomas, K.R. and M.R. Capecchi, *Targeted disruption of the murine int-1 proto-oncogene resulting in severe abnormalities in midbrain and cerebellar development.* Nature, 1990. **346**(6287): p. 847-50.
78. Houart, C., et al., *Establishment of the telencephalon during gastrulation by local antagonism of Wnt signaling.* Neuron, 2002. **35**(2): p. 255-65.
79. Zhang, X., et al., *Notum is required for neural and head induction via Wnt deacylation, oxidation, and inactivation.* Dev Cell, 2015. **32**(6): p. 719-30.
80. Miyagi, A., et al., *G protein-coupled receptors Flop1 and Flop2 inhibit Wnt/beta-catenin signaling and are essential for head formation in Xenopus.* Dev Biol, 2015. **407**(1): p. 131-44.
81. Danesin, C. and C. Houart, *A Fox stops the Wnt: implications for forebrain development and diseases.* Curr Opin Genet Dev, 2012. **22**(4): p. 323-30.
82. Backman, M., et al., *Effects of canonical Wnt signaling on dorso-ventral specification of the mouse telencephalon.* Dev Biol, 2005. **279**(1): p. 155-68.
83. Chenn, A. and C.A. Walsh, *Regulation of cerebral cortical size by control of cell cycle exit in neural precursors.* Science, 2002. **297**(5580): p. 365-9.
84. Woodhead, G.J., et al., *Cell-autonomous beta-catenin signaling regulates cortical precursor proliferation.* J Neurosci, 2006. **26**(48): p. 12620-30.
85. Zhou, C.J., et al., *Neuronal production and precursor proliferation defects in the neocortex of mice with loss of function in the canonical Wnt signaling pathway.* Neuroscience, 2006. **142**(4): p. 1119-31.
86. Munji, R.N., et al., *Wnt signaling regulates neuronal differentiation of cortical intermediate progenitors.* J Neurosci, 2011. **31**(5): p. 1676-87.
87. Noctor, S.C., et al., *Dividing precursor cells of the embryonic cortical ventricular zone have morphological and molecular characteristics of radial glia.* J Neurosci, 2002. **22**(8): p. 3161-73.
88. Takahashi, T., et al., *Sequence of neuron origin and neocortical laminar fate: relation to cell cycle of origin in the developing murine cerebral wall.* J Neurosci, 1999. **19**(23): p. 10357-71.
89. McSherry, G.M. and I.H. Smart, *Cell production gradients in the developing ferret isocortex.* J Anat, 1986. **144**: p. 1-14.
90. Bishop, K.M., G. Goudreau, and D.D. O'Leary, *Regulation of area identity in the mammalian neocortex by Emx2 and Pax6.* Science, 2000. **288**(5464): p. 344-9.
91. Shimogori, T., et al., *Embryonic signaling centers expressing BMP, WNT and FGF proteins interact to pattern the cerebral cortex.* Development, 2004. **131**(22): p. 5639-47.

92. Fukuchi-Shimogori, T. and E.A. Grove, *Emx2 patterns the neocortex by regulating FGF positional signaling.* Nat Neurosci, 2003. **6**(8): p. 825-31.
93. Fukuchi-Shimogori, T. and E.A. Grove, *Neocortex patterning by the secreted signaling molecule FGF8.* Science, 2001. **294**(5544): p. 1071-4.
94. Machon, O., et al., *A dynamic gradient of Wnt signaling controls initiation of neurogenesis in the mammalian cortex and cellular specification in the hippocampus.* Dev Biol, 2007. **311**(1): p. 223-37.
95. Poschl, J., et al., *Constitutive activation of beta-catenin in neural progenitors results in disrupted proliferation and migration of neurons within the central nervous system.* Dev Biol, 2013. **374**(2): p. 319-32.
96. Zhang, S., et al., *Fezf2 promotes neuronal differentiation through localised activation of Wnt/beta-catenin signalling during forebrain development.* Development, 2014. **141**(24): p. 4794-805.
97. Hirabayashi, Y., et al., *The Wnt/beta-catenin pathway directs neuronal differentiation of cortical neural precursor cells.* Development, 2004. **131**(12): p. 2791-801.
98. Wu, S.X., et al., *Pyramidal neurons of upper cortical layers generated by NEX-positive progenitor cells in the subventricular zone.* Proc Natl Acad Sci U S A, 2005. **102**(47): p. 17172-7.
99. Yang, J., et al., *Predominant neuronal differentiation of Olig1+ neural progenitors in forebrain cortex biased by beta-catenin over-expression.* Neurosci Lett, 2016. **622**: p. 19-23.
100. Marinaro, C., et al., *Wnt signaling has opposing roles in the developing and the adult brain that are modulated by Hipk1.* Cereb Cortex, 2012. **22**(10): p. 2415-27.
101. Adachi, K., et al., *Beta-catenin signaling promotes proliferation of progenitor cells in the adult mouse subventricular zone.* Stem Cells, 2007. **25**(11): p. 2827-36.
102. Alvarez-Buylla, A. and J.M. Garcia-Verdugo, *Neurogenesis in adult subventricular zone.* J Neurosci, 2002. **22**(3): p. 629-34.
103. Imura, T., et al., *Adenomatous polyposis coli is essential for both neuronal differentiation and maintenance of adult neural stem cells in subventricular zone and hippocampus.* Stem Cells, 2010. **28**(11): p. 2053-2064.
104. Piccin, D. and C.M. Morshead, *Wnt signaling regulates symmetry of division of neural stem cells in the adult brain and in response to injury.* Stem Cells, 2011. **29**(3): p. 528-38.
105. Duncan, R.N., et al., *Hypothalamic radial glia function as self-renewing neural progenitors in the absence of Wnt/beta-catenin signaling.* Development, 2016. **143**(1): p. 45-53.
106. Zhu, Y.H., et al., *Wip1 regulates the generation of new neural cells in the adult olfactory bulb through p53-dependent cell cycle control.* Stem Cells, 2009. **27**(6): p. 1433-42.
107. Zhu, Y., et al., *Phosphatase WIP1 regulates adult neurogenesis and WNT signaling during aging.* J Clin Invest, 2014. **124**(7): p. 3263-73.
108. ten Berge, D., et al., *Wnt signaling mediates self-organization and axis formation in embryoid bodies.* Cell Stem Cell, 2008. **3**(5): p. 508-18.
109. Moya, N., et al., *Endogenous WNT signaling regulates hPSC-derived neural progenitor cell heterogeneity and specifies their regional identity.* Stem Cell Reports, 2014. **3**(6): p. 1015-28.
110. Kim, H., et al., *Dual Function of Wnt Signaling during Neuronal Differentiation of Mouse Embryonic Stem Cells.* Stem Cells Int, 2015. **2015**: p. 459301-459311.
111. Li, X.J., et al., *Coordination of sonic hedgehog and Wnt signaling determines ventral and dorsal telencephalic neuron types from human embryonic stem cells.* Development, 2009. **136**(23): p. 4055-63.
112. Temple, S., *The development of neural stem cells.* Nature, 2001. **414**(6859): p. 112-7.
113. Muroyama, Y., H. Kondoh, and S. Takada, *Wnt proteins promote neuronal differentiation in neural stem cell culture.* Biochem Biophys Res Commun, 2004. **313**(4): p. 915-21.
114. Lutolf, M.P., P.M. Gilbert, and H.M. Blau, *Designing materials to direct stem-cell fate.* Nature, 2009. **462**(7272): p. 433-41.

115. Cui, Y., et al., *The miR-20-Rest-Wnt signaling axis regulates neural progenitor cell differentiation.* Sci Rep, 2016. **6**: p. 23300-233013.
116. van Amerongen, R. and A. Berns, *Knockout mouse models to study Wnt signal transduction.* Trends Genet, 2006. **22**(12): p. 678-89.
117. Greco, T.L., et al., *Analysis of the vestigial tail mutation demonstrates that Wnt-3a gene dosage regulates mouse axial development.* Genes Dev, 1996. **10**(3): p. 313-24.
118. Lei, Y., et al., *Rare LRP6 variants identified in spina bifida patients.* Hum Mutat, 2015. **36**(3): p. 342-9.
119. Kimura-Yoshida, C., et al., *Fate Specification of Neural Plate Border by Canonical Wnt Signaling and Grhl3 is Crucial for Neural Tube Closure.* EBioMedicine, 2015. **2**(6): p. 513-27.
120. Li, B.I., et al., *The orphan GPCR, Gpr161, regulates the retinoic acid and canonical Wnt pathways during neurulation.* Dev Biol, 2015. **402**(1): p. 17-31.
121. Normand, E.A., et al., *Temporal and mosaic Tsc1 deletion in the developing thalamus disrupts thalamocortical circuitry, neural function, and behavior.* Neuron, 2013. **78**(5): p. 895-909.
122. Gao, C. and Y.G. Chen, *Dishevelled: The hub of Wnt signaling.* Cell Signal, 2010. **22**(5): p. 717-27.
123. Long, J.M., et al., *Expanded characterization of the social interaction abnormalities in mice lacking Dvl1.* Genes Brain Behav, 2004. **3**(1): p. 51-62.
124. Goodall, J., et al., *Brn-2 expression controls melanoma proliferation and is directly regulated by beta-catenin.* Mol Cell Biol, 2004. **24**(7): p. 2915-22.
125. Belinson, H., et al., *Prenatal beta-catenin/Brn2/Tbr2 transcriptional cascade regulates adult social and stereotypic behaviors.* Mol Psychiatry, 2016.
126. Willsey, A.J., et al., *Coexpression networks implicate human midfetal deep cortical projection neurons in the pathogenesis of autism.* Cell, 2013. **155**(5): p. 997-1007.
127. Courchesne, E., et al., *Neuron number and size in prefrontal cortex of children with autism.* JAMA, 2011. **306**(18): p. 2001-10.
128. Caracci, M.O., M.E. Avila, and G.V. De Ferrari, *Synaptic Wnt/GSK3beta Signaling Hub in Autism.* Neural Plast, 2016. **2016**: p. 9603751-9603761.
129. Weinberger, D.R., *From neuropathology to neurodevelopment.* Lancet, 1995. **346**(8974): p. 552-7.
130. Sullivan, P.F., M.J. Daly, and M. O'Donovan, *Genetic architectures of psychiatric disorders: the emerging picture and its implications.* Nat Rev Genet, 2012. **13**(8): p. 537-51.
131. Srikanth, P., et al., *Genomic DISC1 Disruption in hiPSCs Alters Wnt Signaling and Neural Cell Fate.* Cell Rep, 2015. **12**(9): p. 1414-29.
132. Mao, Y., et al., *Disrupted in schizophrenia 1 regulates neuronal progenitor proliferation via modulation of GSK3beta/beta-catenin signaling.* Cell, 2009. **136**(6): p. 1017-31.
133. Topol, A., et al., *Altered WNT Signaling in Human Induced Pluripotent Stem Cell Neural Progenitor Cells Derived from Four Schizophrenia Patients.* Biol Psychiatry, 2015. **78**(6): p. e29-34.
134. Wu, J.Q., et al., *Altered neural signaling and immune pathways in peripheral blood mononuclear cells of schizophrenia patients with cognitive impairment: A transcriptome analysis.* Brain Behav Immun, 2016. **53**: p. 194-206.
135. Thompson, M.C., et al., *Genomics identifies medulloblastoma subgroups that are enriched for specific genetic alterations.* J Clin Oncol, 2006. **24**(12): p. 1924-31.
136. Northcott, P.A., et al., *Medulloblastoma comprises four distinct molecular variants.* J Clin Oncol, 2011. **29**(11): p. 1408-14.
137. Kool, M., et al., *Integrated genomics identifies five medulloblastoma subtypes with distinct genetic profiles, pathway signatures and clinicopathological features.* PLoS One, 2008. **3**(8): p. e3088.
138. Zurawel, R.H., et al., *Sporadic medulloblastomas contain oncogenic beta-catenin mutations.* Cancer Res, 1998. **58**(5): p. 896-9.

139. Eberhart, C.G., T. Tihan, and P.C. Burger, *Nuclear localization and mutation of beta-catenin in medulloblastomas.* J Neuropathol Exp Neurol, 2000. **59**(4): p. 333-7.
140. Huang, H., et al., *APC mutations in sporadic medulloblastomas.* Am J Pathol, 2000. **156**(2): p. 433-7.
141. Baeza, N., et al., *AXIN1 mutations but not deletions in cerebellar medulloblastomas.* Oncogene, 2003. **22**(4): p. 632-6.
142. Hamilton, S.R., et al., *The molecular basis of Turcot's syndrome.* N Engl J Med, 1995. **332**(13): p. 839-47.
143. Wingate, R.J., *The rhombic lip and early cerebellar development.* Curr Opin Neurobiol, 2001. **11**(1): p. 82-8.
144. Roussel, M.F. and M.E. Hatten, *Cerebellum development and medulloblastoma.* Curr Top Dev Biol, 2011. **94**: p. 235-82.
145. Lorenz, A., et al., *Severe alterations of cerebellar cortical development after constitutive activation of Wnt signaling in granule neuron precursors.* Mol Cell Biol, 2011. **31**(16): p. 3326-38.
146. Pei, Y., et al., *WNT signaling increases proliferation and impairs differentiation of stem cells in the developing cerebellum.* Development, 2012. **139**(10): p. 1724-33.
147. Selvadurai, H.J. and J.O. Mason, *Wnt/beta-catenin signalling is active in a highly dynamic pattern during development of the mouse cerebellum.* PLoS One, 2011. **6**(8): p. e23012.
148. Gibson, P., et al., *Subtypes of medulloblastoma have distinct developmental origins.* Nature, 2010. **468**(7327): p. 1095-9.
149. Phoenix, T.N., et al., *Medulloblastoma Genotype Dictates Blood Brain Barrier Phenotype.* Cancer Cell, 2016. **29**(4): p. 508-22.
150. Daneman, R., et al., *Wnt/beta-catenin signaling is required for CNS, but not non-CNS, angiogenesis.* Proc Natl Acad Sci U S A, 2009. **106**(2): p. 641-6.
151. Stenman, J.M., et al., *Canonical Wnt signaling regulates organ-specific assembly and differentiation of CNS vasculature.* Science, 2008. **322**(5905): p. 1247-50.
152. Suva, M.L., et al., *Reconstructing and reprogramming the tumor-propagating potential of glioblastoma stem-like cells.* Cell, 2014. **157**(3): p. 580-94.
153. Sandberg, C.J., et al., *Comparison of glioma stem cells to neural stem cells from the adult human brain identifies dysregulated Wnt- signaling and a fingerprint associated with clinical outcome.* Exp Cell Res, 2013. **319**(14): p. 2230-43.
154. Kierulf-Vieira, K.S., et al., *Wnt inhibition is dysregulated in gliomas and its re-establishment inhibits proliferation and tumor sphere formation.* Exp Cell Res, 2016. **340**(1): p. 53-61.
155. Gotze, S., et al., *Frequent promoter hypermethylation of Wnt pathway inhibitor genes in malignant astrocytic gliomas.* Int J Cancer, 2010. **126**(11): p. 2584-93.
156. Nager, M., et al., *beta-Catenin Signalling in Glioblastoma Multiforme and Glioma-Initiating Cells.* Chemother Res Pract, 2012. **2012**: p. 192362-192369.
157. Zhang, K., et al., *Wnt/beta-catenin signaling in glioma.* J Neuroimmune Pharmacol, 2012. **7**(4): p. 740-9.
158. Wang, L., et al., *Oncogenic role of SOX9 expression in human malignant glioma.* Med Oncol, 2012. **29**(5): p. 3484-90.
159. Liu, H., et al., *SOX9 Overexpression Promotes Glioma Metastasis via Wnt/beta-Catenin Signaling.* Cell Biochem Biophys, 2015. **73**(1): p. 205-212.
160. Wang, K., et al., *Analysis of hsa-miR-30a-5p expression in human gliomas.* Pathol Oncol Res, 2013. **19**(3): p. 405-11.
161. Wang, Z., et al., *MiR-30a-5p is induced by Wnt/beta-catenin pathway and promotes glioma cell invasion by repressing NCAM.* Biochem Biophys Res Commun, 2015. **465**(3): p. 374-80.
162. Inestrosa, N.C. and L. Varela-Nallar, *Wnt signaling in the nervous system and in Alzheimer's disease.* J Mol Cell Biol, 2014. **6**(1): p. 64-74.
163. Riise, J., et al., *Aberrant Wnt signaling pathway in medial temporal lobe structures of Alzheimer's disease.* J Neural Transm (Vienna), 2015. **122**(9): p. 1303-18.

164. Galceran, J., et al., *Hippocampus development and generation of dentate gyrus granule cells is regulated by LEF1.* Development, 2000. **127**(3): p. 469-82.
165. Lee, S.M., et al., *A local Wnt-3a signal is required for development of the mammalian hippocampus.* Development, 2000. **127**(3): p. 457-67.
166. Solberg, N., O. Machon, and S. Krauss, *Effect of canonical Wnt inhibition in the neurogenic cortex, hippocampus, and premigratory dentate gyrus progenitor pool.* Dev Dyn, 2008. **237**(7): p. 1799-811.
167. Jurado-Arjona, J., et al., *GSK3beta Overexpression in Dentate Gyrus Neural Precursor Cells Expands the Progenitor Pool and Enhances Memory Skills.* J Biol Chem, 2016. **291**(15): p. 8199-213.
168. Lie, D.C., et al., *Wnt signalling regulates adult hippocampal neurogenesis.* Nature, 2005. **437**(7063): p. 1370-5.
169. Mardones, M.D., et al., *Frizzled-1 receptor regulates adult hippocampal neurogenesis.* Mol Brain, 2016. **9**(1): p. 29-41.
170. Kannan, S., et al., *Systems Genetics Analysis of a Recombinant Inbred Mouse Cell Culture Panel Reveals Wnt Pathway Member Lrp6 as a Regulator of Adult Hippocampal Precursor Cell Proliferation.* Stem Cells, 2016. **34**(3): p. 674-84.
171. Seib, D.R., et al., *Loss of Dickkopf-1 restores neurogenesis in old age and counteracts cognitive decline.* Cell Stem Cell, 2013. **12**(2): p. 204-14.
172. Jang, M.H., et al., *Secreted frizzled-related protein 3 regulates activity-dependent adult hippocampal neurogenesis.* Cell Stem Cell, 2013. **12**(2): p. 215-23.
173. Sun, J., et al., *A septo-temporal molecular gradient of sfrp3 in the dentate gyrus differentially regulates quiescent adult hippocampal neural stem cell activation.* Mol Brain, 2015. **8**: p. 52-62.
174. Fiorentini, A., et al., *Lithium improves hippocampal neurogenesis, neuropathology and cognitive functions in APP mutant mice.* PLoS One, 2010. **5**(12): p. e14382.
175. Tiwari, S.K., et al., *Bisphenol-A Mediated Inhibition of Hippocampal Neurogenesis Attenuated by Curcumin via Canonical Wnt Pathway.* Mol Neurobiol, 2015. **53**(5): p. 3010-3029.
176. Tiwari, S.K., et al., *Ethosuximide Induces Hippocampal Neurogenesis and Reverses Cognitive Deficits in an Amyloid-beta Toxin-induced Alzheimer Rat Model via the Phosphatidylinositol 3-Kinase (PI3K)/Akt/Wnt/beta-Catenin Pathway.* J Biol Chem, 2015. **290**(47): p. 28540-58.
177. Varela-Nallar, L., et al., *Andrographolide Stimulates Neurogenesis in the Adult Hippocampus.* Neural Plast, 2015. **2015**: p. 935403-935416.
178. Yao, Y., et al., *Osthole promotes neuronal differentiation and inhibits apoptosis via Wnt/beta-catenin signaling in an Alzheimer's disease model.* Toxicol Appl Pharmacol, 2015. **289**(3): p. 474-81.
179. Meda, L., et al., *Activation of microglial cells by beta-amyloid protein and interferon-gamma.* Nature, 1995. **374**(6523): p. 647-50.
180. Jiang, D.Q., et al., *Nicotine contributes to the neural stem cells fate against toxicity of microglial-derived factors induced by Abeta via the Wnt/beta-catenin pathway.* Int J Neurosci, 2016. **126**(3): p. 257-68.
181. Bjorklund, A. and S.B. Dunnett, *Dopamine neuron systems in the brain: an update.* Trends Neurosci, 2007. **30**(5): p. 194-202.
182. Joksimovic, M., et al., *Wnt antagonism of Shh facilitates midbrain floor plate neurogenesis.* Nat Neurosci, 2009. **12**(2): p. 125-31.
183. Nouri, N., et al., *Excessive Wnt/beta-catenin signaling promotes midbrain floor plate neurogenesis, but results in vacillating dopamine progenitors.* Mol Cell Neurosci, 2015. **68**: p. 131-42.
184. Fukusumi, Y., et al., *Dickkopf 3 Promotes the Differentiation of a Rostrolateral Midbrain Dopaminergic Neuronal Subset In Vivo and from Pluripotent Stem Cells In Vitro in the Mouse.* J Neurosci, 2015. **35**(39): p. 13385-401.

185. Lee, C.T., et al., *Functional consequences of 17q21.31/WNT3-WNT9B amplification in hPSCs with respect to neural differentiation.* Cell Rep, 2015. **10**(4): p. 616-32.
186. F, L.E., et al., *Glia as a turning point in the therapeutic strategy of Parkinson's disease.* CNS Neurol Disord Drug Targets, 2010. **9**(3): p. 349-72.
187. L'Episcopo, F., et al., *Plasticity of subventricular zone neuroprogenitors in MPTP (1-methyl-4-phenyl-1,2,3,6-tetrahydropyridine) mouse model of Parkinson's disease involves cross talk between inflammatory and Wnt/beta-catenin signaling pathways: functional consequences for neuroprotection and repair.* J Neurosci, 2012. **32**(6): p. 2062-85.
188. L'Episcopo, F., et al., *Aging-induced Nrf2-ARE pathway disruption in the subventricular zone drives neurogenic impairment in parkinsonian mice via PI3K-Wnt/beta-catenin dysregulation.* J Neurosci, 2013. **33**(4): p. 1462-85.
189. L'Episcopo, F., et al., *Reactive astrocytes and Wnt/beta-catenin signaling link nigrostriatal injury to repair in 1-methyl-4-phenyl-1,2,3,6-tetrahydropyridine model of Parkinson's disease.* Neurobiol Dis, 2011. **41**(2): p. 508-27.
190. L'Episcopo, F., et al., *A Wnt1 regulated Frizzled-1/beta-Catenin signaling pathway as a candidate regulatory circuit controlling mesencephalic dopaminergic neuron-astrocyte crosstalk: Therapeutical relevance for neuron survival and neuroprotection.* Mol Neurodegener, 2011. **6**: p. 49-78.
191. Singh, S., A. Mishra, and S. Shukla, *ALCAR Exerts Neuroprotective and Pro-Neurogenic Effects by Inhibition of Glial Activation and Oxidative Stress via Activation of the Wnt/beta-Catenin Signaling in Parkinsonian Rats.* Mol Neurobiol, 2015. **53**(7): p. 4286-4301.
192. Arvidsson, A., et al., *Neuronal replacement from endogenous precursors in the adult brain after stroke.* Nat Med, 2002. **8**(9): p. 963-70.
193. Lei, Z.N., L.M. Zhang, and F.Y. Sun, *Beta-catenin siRNA inhibits ischemia-induced striatal neurogenesis in adult rat brain following a transient middle cerebral artery occlusion.* Neurosci Lett, 2008. **435**(2): p. 108-12.
194. Shruster, A., et al., *Wnt signaling enhances neurogenesis and improves neurological function after focal ischemic injury.* PLoS One, 2012. **7**(7): p. e40843.
195. Zhao, Y., et al., *Wnt3a, a protein secreted by Mesenchymal Stem Cells is neuroprotective and promotes neurocognitive recovery following Traumatic Brain Injury.* Stem Cells, 2016.
196. Suh, H.I., et al., *Axonal regeneration effects of Wnt3a-secreting fibroblast transplantation in spinal cord-injured rats.* Acta Neurochir (Wien), 2011. **153**(5): p. 1003-10.
197. Briona, L.K., et al., *Wnt/b-catenin signaling is required for radial glial neurogenesis following spinal cord injury.* Dev Biol, 2015. **403**(1): p. 15-21.
198. Gao, K., et al., *Neuroprotective effect of rapamycin on spinal cord injury via activation of the Wnt/beta-catenin signaling pathway.* Neural Regen Res, 2015. **10**(6): p. 951-7.
199. Gao, K., et al., *Simvastatin inhibits neural cell apoptosis and promotes locomotor recovery via activation of Wnt/beta-catenin signaling pathway after spinal cord injury.* J Neurochem, 2015. **138**(1): p. 139-149.
200. Du, Z.W., et al., *Generation and expansion of highly pure motor neuron progenitors from human pluripotent stem cells.* Nat Commun, 2015. **6**: p. 6626-6635.
201. Cutts, J., N. Brookhouser, and D.A. Brafman, *Generation of Regionally Specific Neural Progenitor Cells (NPCs) and Neurons from Human Pluripotent Stem Cells (hPSCs).* Methods Mol Biol, 2016.
202. Hurlbut, G.D., et al., *Crossing paths with Notch in the hyper-network.* Curr Opin Cell Biol, 2007. **19**(2): p. 166-75.
203. Munder, S., et al., *Notch-signalling is required for head regeneration and tentacle patterning in Hydra.* Dev Biol, 2013. **383**(1): p. 146-57.
204. Hayward, P., T. Kalmar, and A.M. Arias, *Wnt/Notch signalling and information processing during development.* Development, 2008. **135**(3): p. 411-24.
205. Munoz Descalzo, S. and A. Martinez Arias, *The structure of Wntch signalling and the resolution of transition states in development.* Semin Cell Dev Biol, 2012. **23**(4): p. 443-9.

206. Kopan, R. and M.X. Ilagan, *The canonical Notch signaling pathway: unfolding the activation mechanism.* Cell, 2009. **137**(2): p. 216-33.
207. Jehn, B.M., et al., *c-Cbl binding and ubiquitin-dependent lysosomal degradation of membrane-associated Notch1.* J Biol Chem, 2002. **277**(10): p. 8033-40.
208. Artavanis-Tsakonas, S., M.D. Rand, and R.J. Lake, *Notch signaling: cell fate control and signal integration in development.* Science, 1999. **284**(5415): p. 770-6.
209. Rebay, I., et al., *Specific EGF repeats of Notch mediate interactions with Delta and Serrate: implications for Notch as a multifunctional receptor.* Cell, 1991. **67**(4): p. 687-99.
210. Fortini, M.E. and D. Bilder, *Endocytic regulation of Notch signaling.* Curr Opin Genet Dev, 2009. **19**(4): p. 323-8.
211. Kidd, S., T. Lieber, and M.W. Young, *Ligand-induced cleavage and regulation of nuclear entry of Notch in Drosophila melanogaster embryos.* Genes Dev, 1998. **12**(23): p. 3728-40.
212. Fortini, M.E., *Notch signaling: the core pathway and its posttranslational regulation.* Dev Cell, 2009. **16**(5): p. 633-47.
213. Schroeter, E.H., J.A. Kisslinger, and R. Kopan, *Notch-1 signalling requires ligand-induced proteolytic release of intracellular domain.* Nature, 1998. **393**(6683): p. 382-6.
214. Mumm, J.S., et al., *A ligand-induced extracellular cleavage regulates gamma-secretase-like proteolytic activation of Notch1.* Mol Cell, 2000. **5**(2): p. 197-206.
215. Tamura, K., et al., *Physical interaction between a novel domain of the receptor Notch and the transcription factor RBP-J kappa/Su(H).* Curr Biol, 1995. **5**(12): p. 1416-23.
216. Honjo, T., *The shortest path from the surface to the nucleus: RBP-J kappa/Su(H) transcription factor.* Genes Cells, 1996. **1**(1): p. 1-9.
217. Fryer, C.J., et al., *Mastermind mediates chromatin-specific transcription and turnover of the Notch enhancer complex.* Genes Dev, 2002. **16**(11): p. 1397-411.
218. Bailey, A.M. and J.W. Posakony, *Suppressor of hairless directly activates transcription of enhancer of split complex genes in response to Notch receptor activity.* Genes Dev, 1995. **9**(21): p. 2609-22.
219. Kao, H.Y., et al., *A histone deacetylase corepressor complex regulates the Notch signal transduction pathway.* Genes Dev, 1998. **12**(15): p. 2269-77.
220. Cave, J.W., *Selective repression of Notch pathway target gene transcription.* Dev Biol, 2011. **360**(1): p. 123-31.
221. Nakagawa, O., et al., *Members of the HRT family of basic helix-loop-helix proteins act as transcriptional repressors downstream of Notch signaling.* Proc Natl Acad Sci U S A, 2000. **97**(25): p. 13655-60.
222. Krejci, A., et al., *Direct response to Notch activation: signaling crosstalk and incoherent logic.* Sci Signal, 2009. **2**(55): p. ra1.
223. Iso, T., et al., *HERP, a new primary target of Notch regulated by ligand binding.* Mol Cell Biol, 2001. **21**(17): p. 6071-9.
224. Housden, B.E., et al., *Transcriptional dynamics elicited by a short pulse of notch activation involves feed-forward regulation by E(spl)/Hes genes.* PLoS Genet, 2013. **9**(1): p. e1003162.
225. Taelman, V., et al., *Sequences downstream of the bHLH domain of the Xenopus hairy-related transcription factor-1 act as an extended dimerization domain that contributes to the selection of the partners.* Dev Biol, 2004. **276**(1): p. 47-63.
226. Kobayashi, T., et al., *The cyclic gene Hes1 contributes to diverse differentiation responses of embryonic stem cells.* Genes Dev, 2009. **23**(16): p. 1870-5.
227. Wall, D.S., et al., *Progenitor cell proliferation in the retina is dependent on Notch-independent Sonic hedgehog/Hes1 activity.* J Cell Biol, 2009. **184**(1): p. 101-12.
228. Ohtsuka, T., et al., *Hes1 and Hes5 as notch effectors in mammalian neuronal differentiation.* EMBO J, 1999. **18**(8): p. 2196-207.
229. Hatakeyama, J., et al., *Hes genes regulate size, shape and histogenesis of the nervous system by control of the timing of neural stem cell differentiation.* Development, 2004. **131**(22): p. 5539-50.

230. Kageyama, R., et al., *Roles of bHLH genes in neural stem cell differentiation.* Exp Cell Res, 2005. **306**(2): p. 343-8.
231. Yun, T.J. and M.J. Bevan, *Notch-regulated ankyrin-repeat protein inhibits Notch1 signaling: multiple Notch1 signaling pathways involved in T cell development.* J Immunol, 2003. **170**(12): p. 5834-41.
232. Krebs, L.T., et al., *The Nrarp gene encodes an ankyrin-repeat protein that is transcriptionally regulated by the notch signaling pathway.* Dev Biol, 2001. **238**(1): p. 110-9.
233. Lamar, E., et al., *Nrarp is a novel intracellular component of the Notch signaling pathway.* Genes Dev, 2001. **15**(15): p. 1885-99.
234. Mizeracka, K., C.R. DeMaso, and C.L. Cepko, *Notch1 is required in newly postmitotic cells to inhibit the rod photoreceptor fate.* Development, 2013. **140**(15): p. 3188-97.
235. McGill, M.A., et al., *Numb regulates post-endocytic trafficking and degradation of Notch1.* J Biol Chem, 2009. **284**(39): p. 26427-38.
236. Jacobsen, T.L., et al., *Cis-interactions between Delta and Notch modulate neurogenic signalling in Drosophila.* Development, 1998. **125**(22): p. 4531-40.
237. Sprinzak, D., et al., *Cis-interactions between Notch and Delta generate mutually exclusive signalling states.* Nature, 2010. **465**(7294): p. 86-90.
238. Sakamoto, K., et al., *Intracellular cell-autonomous association of Notch and its ligands: a novel mechanism of Notch signal modification.* Dev Biol, 2002. **241**(2): p. 313-26.
239. Becam, I., et al., *A role of receptor Notch in ligand cis-inhibition in Drosophila.* Curr Biol, 2010. **20**(6): p. 554-60.
240. LeBon, L., et al., *Fringe proteins modulate Notch-ligand cis and trans interactions to specify signaling states.* Elife, 2014. **3**: p. e02950.
241. Hicks, C., et al., *Fringe differentially modulates Jagged1 and Delta1 signalling through Notch1 and Notch2.* Nat Cell Biol, 2000. **2**(8): p. 515-20.
242. Moloney, D.J., et al., *Fringe is a glycosyltransferase that modifies Notch.* Nature, 2000. **406**(6794): p. 369-75.
243. Li, W., et al., *Notch inhibition induces mitotically generated hair cells in mammalian cochleae via activating the Wnt pathway.* Proc Natl Acad Sci U S A, 2015. **112**(1): p. 166-71.
244. Tian, H., et al., *Opposing activities of Notch and Wnt signaling regulate intestinal stem cells and gut homeostasis.* Cell Rep, 2015. **11**(1): p. 33-42.
245. Deregowski, V., et al., *Notch 1 overexpression inhibits osteoblastogenesis by suppressing Wnt/beta-catenin but not bone morphogenetic protein signaling.* J Biol Chem, 2006. **281**(10): p. 6203-10.
246. Brack, A.S., et al., *A temporal switch from notch to Wnt signaling in muscle stem cells is necessary for normal adult myogenesis.* Cell Stem Cell, 2008. **2**(1): p. 50-9.
247. Kwon, C., et al., *Notch post-translationally regulates beta-catenin protein in stem and progenitor cells.* Nat Cell Biol, 2011. **13**(10): p. 1244-51.
248. Sanders, P.G., et al., *Ligand-independent traffic of Notch buffers activated Armadillo in Drosophila.* PLoS Biol, 2009. **7**(8): p. e1000169.
249. Hayward, P., et al., *Notch modulates Wnt signalling by associating with Armadillo/beta-catenin and regulating its transcriptional activity.* Development, 2005. **132**(8): p. 1819-30.
250. Acosta, H., et al., *Notch destabilises maternal beta-catenin and restricts dorsal-anterior development in Xenopus.* Development, 2011. **138**(12): p. 2567-79.
251. Hayward, P., T. Balayo, and A. Martinez Arias, *Notch synergizes with axin to regulate the activity of armadillo in Drosophila.* Dev Dyn, 2006. **235**(10): p. 2656-66.
252. Kim, H.A., et al., *Notch1 counteracts WNT/beta-catenin signaling through chromatin modification in colorectal cancer.* J Clin Invest, 2012. **122**(9): p. 3248-59.
253. Proweller, A., et al., *Impaired notch signaling promotes de novo squamous cell carcinoma formation.* Cancer Res, 2006. **66**(15): p. 7438-44.
254. Kwon, C., et al., *A regulatory pathway involving Notch1/beta-catenin/Isl1 determines cardiac progenitor cell fate.* Nat Cell Biol, 2009. **11**(8): p. 951-7.

255. Shi, F., et al., *Beta-catenin up-regulates Atoh1 expression in neural progenitor cells by interaction with an Atoh1 3' enhancer.* J Biol Chem, 2010. **285**(1): p. 392-400.
256. Nicolas, M., et al., *Notch1 functions as a tumor suppressor in mouse skin.* Nat Genet, 2003. **33**(3): p. 416-21.
257. Hanlon, L., et al., *Notch1 functions as a tumor suppressor in a model of K-ras-induced pancreatic ductal adenocarcinoma.* Cancer Res, 2010. **70**(11): p. 4280-6.
258. Devgan, V., et al., *p21WAF1/Cip1 is a negative transcriptional regulator of Wnt4 expression downstream of Notch1 activation.* Genes Dev, 2005. **19**(12): p. 1485-95.
259. Zhou, J., et al., *Notch and wingless signaling cooperate in regulation of dendritic cell differentiation.* Immunity, 2009. **30**(6): p. 845-59.
260. Rulifson, E.J. and S.S. Blair, *Notch regulates wingless expression and is not required for reception of the paracrine wingless signal during wing margin neurogenesis in Drosophila.* Development, 1995. **121**(9): p. 2813-24.
261. Diaz-Benjumea, F.J. and S.M. Cohen, *Serrate signals through Notch to establish a Wingless-dependent organizer at the dorsal/ventral compartment boundary of the Drosophila wing.* Development, 1995. **121**(12): p. 4215-25.
262. Brennan, K., et al., *Wingless modulates the effects of dominant negative notch molecules in the developing wing of Drosophila.* Dev Biol, 1999. **216**(1): p. 210-29.
263. Balint, K., et al., *Activation of Notch1 signaling is required for beta-catenin-mediated human primary melanoma progression.* J Clin Invest, 2005. **115**(11): p. 3166-76.
264. Fre, S., et al., *Notch and Wnt signals cooperatively control cell proliferation and tumorigenesis in the intestine.* Proc Natl Acad Sci U S A, 2009. **106**(15): p. 6309-14.
265. van Es, J.H., et al., *Notch/gamma-secretase inhibition turns proliferative cells in intestinal crypts and adenomas into goblet cells.* Nature, 2005. **435**(7044): p. 959-63.
266. Gopalakrishnan, N., et al., *Colocalization of beta-catenin with Notch intracellular domain in colon cancer: a possible role of Notch1 signaling in activation of CyclinD1-mediated cell proliferation.* Mol Cell Biochem, 2014. **396**(1-2): p. 281-93.
267. Ross, D.A. and T. Kadesch, *The notch intracellular domain can function as a coactivator for LEF-1.* Mol Cell Biol, 2001. **21**(22): p. 7537-44.
268. Ishitani, T., et al., *Nrarp functions to modulate neural-crest-cell differentiation by regulating LEF1 protein stability.* Nat Cell Biol, 2005. **7**(11): p. 1106-12.
269. Alves-Guerra, M.C., C. Ronchini, and A.J. Capobianco, *Mastermind-like 1 Is a specific coactivator of beta-catenin transcription activation and is essential for colon carcinoma cell survival.* Cancer Res, 2007. **67**(18): p. 8690-8.
270. Gu, B., et al., *Chromatin effector Pygo2 mediates Wnt-notch crosstalk to suppress luminal/alveolar potential of mammary stem and basal cells.* Cell Stem Cell, 2013. **13**(1): p. 48-61.
271. Collu, G.M., et al., *Dishevelled limits Notch signalling through inhibition of CSL.* Development, 2012. **139**(23): p. 4405-15.
272. Axelrod, J.D., et al., *Interaction between Wingless and Notch signaling pathways mediated by dishevelled.* Science, 1996. **271**(5257): p. 1826-32.
273. Ramain, P., et al., *Novel Notch alleles reveal a Deltex-dependent pathway repressing neural fate.* Curr Biol, 2001. **11**(22): p. 1729-38.
274. Munoz-Descalzo, S., et al., *Wingless modulates the ligand independent traffic of Notch through Dishevelled.* Fly (Austin), 2010. **4**(3): p. 182-93.
275. Munoz-Descalzo, S., et al., *Modulation of the ligand-independent traffic of Notch by Axin and Apc contributes to the activation of Armadillo in Drosophila.* Development, 2011. **138**(8): p. 1501-6.
276. Liu, X.H., et al., *Androgens up-regulate transcription of the Notch inhibitor Numb in C2C12 myoblasts via Wnt/beta-catenin signaling to T cell factor elements in the Numb promoter.* J Biol Chem, 2013. **288**(25): p. 17990-8.

277. Duncan, A.W., et al., *Integration of Notch and Wnt signaling in hematopoietic stem cell maintenance.* Nat Immunol, 2005. **6**(3): p. 314-22.
278. Wesley, C.S., *Notch and wingless regulate expression of cuticle patterning genes.* Mol Cell Biol, 1999. **19**(8): p. 5743-58.
279. Couso, J.P. and A. Martinez Arias, *Notch is required for wingless signaling in the epidermis of Drosophila.* Cell, 1994. **79**(2): p. 259-72.
280. Langdon, T., et al., *Notch receptor encodes two structurally separable functions in Drosophila: a genetic analysis.* Dev Dyn, 2006. **235**(4): p. 998-1013.
281. Peignon, G., et al., *Complex interplay between beta-catenin signalling and Notch effectors in intestinal tumorigenesis.* Gut, 2011. **60**(2): p. 166-76.
282. Ungerback, J., et al., *The Notch-2 gene is regulated by Wnt signaling in cultured colorectal cancer cells.* PLoS One, 2011. **6**(3): p. e17957.
283. Galceran, J., et al., *LEF1-mediated regulation of Delta-like1 links Wnt and Notch signaling in somitogenesis.* Genes Dev, 2004. **18**(22): p. 2718-23.
284. Jayasena, C.S., et al., *Notch signaling augments the canonical Wnt pathway to specify the size of the otic placode.* Development, 2008. **135**(13): p. 2251-61.
285. Chihara, T. and S. Hayashi, *Control of tracheal tubulogenesis by Wingless signaling.* Development, 2000. **127**(20): p. 4433-42.
286. Rodilla, V., et al., *Jagged1 is the pathological link between Wnt and Notch pathways in colorectal cancer.* Proc Natl Acad Sci U S A, 2009. **106**(15): p. 6315-20.
287. Katoh, M. and M. Katoh, *Notch ligand, JAG1, is evolutionarily conserved target of canonical WNT signaling pathway in progenitor cells.* Int J Mol Med, 2006. **17**(4): p. 681-5.
288. Estrach, S., et al., *Jagged 1 is a beta-catenin target gene required for ectopic hair follicle formation in adult epidermis.* Development, 2006. **133**(22): p. 4427-38.
289. Issack, P.S. and E.B. Ziff, *Genetic elements regulating HES-1 induction in Wnt-1-transformed PC12 cells.* Cell Growth Differ, 1998. **9**(10): p. 827-36.
290. Kubo, F. and S. Nakagawa, *Hairy1 acts as a node downstream of Wnt signaling to maintain retinal stem cell-like progenitor cells in the chick ciliary marginal zone.* Development, 2009. **136**(11): p. 1823-33.
291. Yamamizu, K., et al., *Convergence of Notch and beta-catenin signaling induces arterial fate in vascular progenitors.* J Cell Biol, 2010. **189**(2): p. 325-38.
292. Shimizu, T., et al., *Stabilized beta-catenin functions through TCF/LEF proteins and the Notch/RBP-Jkappa complex to promote proliferation and suppress differentiation of neural precursor cells.* Mol Cell Biol, 2008. **28**(24): p. 7427-41.
293. Jin, Y.H., et al., *Beta-catenin modulates the level and transcriptional activity of Notch1/NICD through its direct interaction.* Biochim Biophys Acta, 2009. **1793**(2): p. 290-9.
294. Espinosa, L., et al., *Phosphorylation by glycogen synthase kinase-3 beta down-regulates Notch activity, a link for Notch and Wnt pathways.* J Biol Chem, 2003. **278**(34): p. 32227-35.
295. Jin, Y.H., et al., *Regulation of Notch1/NICD and Hes1 expressions by GSK-3alpha/beta.* Mol Cells, 2009. **27**(1): p. 15-9.
296. Kinzler, K.W., et al., *Identification of FAP locus genes from chromosome 5q21.* Science, 1991. **253**(5020): p. 661-5.
297. Groden, J., et al., *Identification and characterization of the familial adenomatous polyposis coli gene.* Cell, 1991. **66**(3): p. 589-600.
298. Clements, W.M., A.M. Lowy, and J. Groden, *Adenomatous polyposis coli/beta-catenin interaction and downstream targets: altered gene expression in gastrointestinal tumors.* Clin Colorectal Cancer, 2003. **3**(2): p. 113-20.
299. Nishisho, I., et al., *Mutations of chromosome 5q21 genes in FAP and colorectal cancer patients.* Science, 1991. **253**(5020): p. 665-9.
300. Morin, P.J., et al., *Activation of beta-catenin-Tcf signaling in colon cancer by mutations in beta-catenin or APC.* Science, 1997. **275**(5307): p. 1787-90.

301. Rubinfeld, B., et al., *Loss of beta-catenin regulation by the APC tumor suppressor protein correlates with loss of structure due to common somatic mutations of the gene.* Cancer Res, 1997. **57**(20): p. 4624-30.
302. Polakis, P., *The many ways of Wnt in cancer.* Curr Opin Genet Dev, 2007. **17**(1): p. 45-51.
303. Korinek, V., et al., *Constitutive transcriptional activation by a beta-catenin-Tcf complex in APC-/- colon carcinoma.* Science, 1997. **275**(5307): p. 1784-7.
304. Bakker, E.R., et al., *beta-Catenin signaling dosage dictates tissue-specific tumor predisposition in Apc-driven cancer.* Oncogene, 2013. **32**(38): p. 4579-85.
305. Satoh, S., et al., *AXIN1 mutations in hepatocellular carcinomas, and growth suppression in cancer cells by virus-mediated transfer of AXIN1.* Nat Genet, 2000. **24**(3): p. 245-50.
306. Liu, W., et al., *Mutations in AXIN2 cause colorectal cancer with defective mismatch repair by activating beta-catenin/TCF signalling.* Nat Genet, 2000. **26**(2): p. 146-7.
307. Zhan, T., N. Rindtorff, and M. Boutros, *Wnt signaling in cancer.* Oncogene, 2017. **36**(11): p. 1461-1473.
308. Seshagiri, S., et al., *Recurrent R-spondin fusions in colon cancer.* Nature, 2012. **488**(7413): p. 660-4.
309. Chien, A.J., et al., *Activated Wnt/beta-catenin signaling in melanoma is associated with decreased proliferation in patient tumors and a murine melanoma model.* Proc Natl Acad Sci U S A, 2009. **106**(4): p. 1193-8.
310. Uematsu, K., et al., *Activation of the Wnt pathway in non small cell lung cancer: evidence of dishevelled overexpression.* Oncogene, 2003. **22**(46): p. 7218-21.
311. Wong, S.C., et al., *Expression of frizzled-related protein and Wnt-signalling molecules in invasive human breast tumours.* J Pathol, 2002. **196**(2): p. 145-53.
312. Han, Z.G., *Functional genomic studies: insights into the pathogenesis of liver cancer.* Annu Rev Genomics Hum Genet, 2012. **13**: p. 171-205.
313. Sastre-Perona, A. and P. Santisteban, *Role of the wnt pathway in thyroid cancer.* Front Endocrinol (Lausanne), 2012. **3**: p. 31.
314. Gatcliffe, T.A., et al., *Wnt signaling in ovarian tumorigenesis.* Int J Gynecol Cancer, 2008. **18**(5): p. 954-62.
315. Ryland, G.L., et al., *RNF43 is a tumour suppressor gene mutated in mucinous tumours of the ovary.* J Pathol, 2013. **229**(3): p. 469-76.
316. Okino, K., et al., *Up-regulation and overproduction of DVL-1, the human counterpart of the Drosophila dishevelled gene, in cervical squamous cell carcinoma.* Oncol Rep, 2003. **10**(5): p. 1219-23.
317. Uematsu, K., et al., *Wnt pathway activation in mesothelioma: evidence of Dishevelled overexpression and transcriptional activity of beta-catenin.* Cancer Res, 2003. **63**(15): p. 4547-51.
318. Suzuki, H., et al., *Epigenetic inactivation of SFRP genes allows constitutive WNT signaling in colorectal cancer.* Nat Genet, 2004. **36**(4): p. 417-22.
319. Marsit, C.J., et al., *Epigenetic inactivation of SFRP genes and TP53 alteration act jointly as markers of invasive bladder cancer.* Cancer Res, 2005. **65**(16): p. 7081-5.
320. Aguilera, O., et al., *Epigenetic inactivation of the Wnt antagonist DICKKOPF-1 (DKK-1) gene in human colorectal cancer.* Oncogene, 2006. **25**(29): p. 4116-21.
321. Urakami, S., et al., *Epigenetic inactivation of Wnt inhibitory factor-1 plays an important role in bladder cancer through aberrant canonical Wnt/beta-catenin signaling pathway.* Clin Cancer Res, 2006. **12**(2): p. 383-91.
322. Sato, H., et al., *Frequent epigenetic inactivation of DICKKOPF family genes in human gastrointestinal tumors.* Carcinogenesis, 2007. **28**(12): p. 2459-66.
323. Nojima, M., et al., *Frequent epigenetic inactivation of SFRP genes and constitutive activation of Wnt signaling in gastric cancer.* Oncogene, 2007. **26**(32): p. 4699-713.
324. Taniguchi, H., et al., *Frequent epigenetic inactivation of Wnt inhibitory factor-1 in human gastrointestinal cancers.* Oncogene, 2005. **24**(53): p. 7946-52.

325. Wu, D., et al., *Suppression of WIF-1 through promoter hypermethylation causes accelerated proliferation of the aryl hydrocarbon receptor (AHR) overexpressing MCF10AT1 breast cancer cells.* Toxicology, 2011. **285**(3): p. 97-103.
326. Fukui, T., et al., *Transcriptional silencing of secreted frizzled related protein 1 (SFRP 1) by promoter hypermethylation in non-small-cell lung cancer.* Oncogene, 2005. **24**(41): p. 6323-7.
327. Mazieres, J., et al., *Wnt inhibitory factor-1 is silenced by promoter hypermethylation in human lung cancer.* Cancer Res, 2004. **64**(14): p. 4717-20.
328. Willert, J., et al., *A transcriptional response to Wnt protein in human embryonic carcinoma cells.* BMC Dev Biol, 2002. **2**: p. 8.
329. Tetsu, O. and F. McCormick, *Beta-catenin regulates expression of cyclin D1 in colon carcinoma cells.* Nature, 1999. **398**(6726): p. 422-6.
330. Bachmann, I.M., et al., *Importance of P-cadherin, beta-catenin, and Wnt5a/frizzled for progression of melanocytic tumors and prognosis in cutaneous melanoma.* Clin Cancer Res, 2005. **11**(24 Pt 1): p. 8606-14.
331. Shang, S., F. Hua, and Z.W. Hu, *The regulation of beta-catenin activity and function in cancer: therapeutic opportunities.* Oncotarget, 2017. **8**(20): p. 33972-33989.
332. He, B., et al., *Blockade of Wnt-1 signaling induces apoptosis in human colorectal cancer cells containing downstream mutations.* Oncogene, 2005. **24**(18): p. 3054-8.
333. Rhee, C.S., et al., *Wnt and frizzled receptors as potential targets for immunotherapy in head and neck squamous cell carcinomas.* Oncogene, 2002. **21**(43): p. 6598-605.
334. Oren, O. and B.D. Smith, *Eliminating Cancer Stem Cells by Targeting Embryonic Signaling Pathways.* Stem Cell Rev, 2017. **13**(1): p. 17-23.
335. Lyou, Y., et al., *Inhibition of nuclear Wnt signalling: challenges of an elusive target for cancer therapy.* Br J Pharmacol, 2017.
336. Kahn, M., *Can we safely target the WNT pathway?* Nat Rev Drug Discov, 2014. **13**(7): p. 513-32.

CHAPTER 2

HINDBRAIN

2.1 INTRODUCTION

The central nervous system is one of the most complex organs in vertebrates. However, it arises from a homogenous neuroepithelium. Numerous patterning events transform a simple tubular structure, the neural tube, into a highly organized combination of functional units responsible for all information processing. One of the most striking features of patterning in the prospective brain is the subdivision in so-called neuromeres (Figure 2.1). Sequential segmentation events occur, separating cells with different developmental fates. The first subdivision occurs with the appearance of the primary brain vesicles: the forebrain or prosencephalon, the midbrain or mesencephalon and the hindbrain or rhombencephalon. These primary brain regions are patterned further and subdivided through the establishment of different signaling centers at the boundaries between segments. The mid- and hindbrain are separated by the midbrain-hindbrain boundary (MHB) [1, 2]. The anterior neural plate is subdivided into telencephalon, hypothalamus, diencephalon and eye field [3]. The hindbrain is subdivided in 8 segments, called rhombomeres, separated by rhombomere boundaries (RBs) [1].

The hindbrain is an evolutionary conserved brain region responsible for most vital functions. Neuronal networks with rhythmic, pacemaker-like activity control breathing, swallowing and vocalization. Eight out of twelve cranial nerves have their origin in the hindbrain and relay sensory information from the cranial sensory organs to the brain and motor inputs to the head muscles. Furthermore, a network of reticulospinal neurons integrates sensory input and motor impulses from the cortex to coordinate locomotion and posture [4].

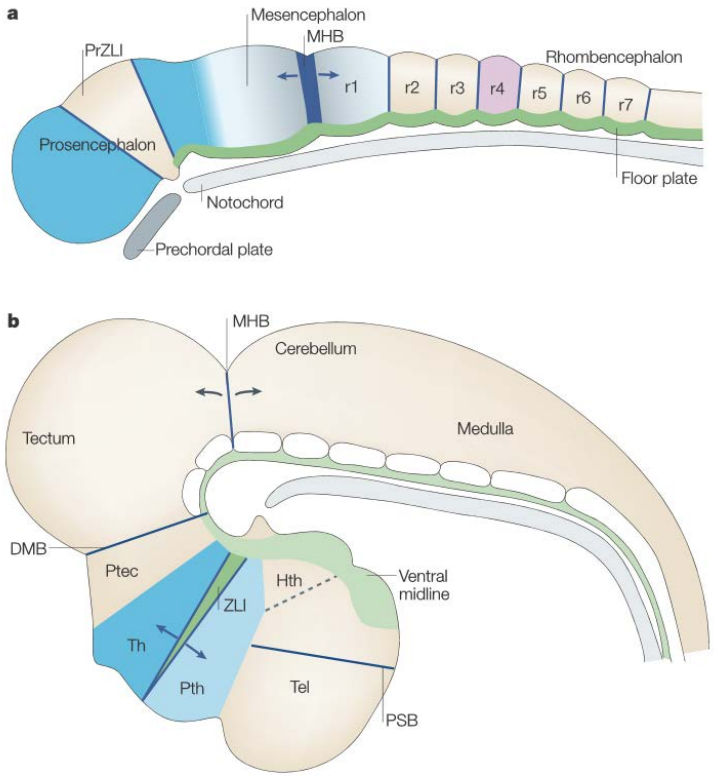

Figure 2.1 Subdivisions of the vertebrate brain. Lateral view of embryonic avian brain at Hamburger-Hamilton stage 13 (a) and 24 (b), anterior to the left, dorsal to the top. Initially the brain is subdivided in three primary vesicles: prosencephalon, mesencephalon and rhombencephalon. As development progresses further compartmentalization is induced under the influence of signaling pathways. Dark blue lines represent lineage restriction border. Major signaling centers are the midbrain-hindbrain boundary (MHB), rhombomere boundaries, floor plate/ ventral midline and the zona limitans intrathalamica (ZLI). DMB, diencephalon-midbrain boundary; Hth, hypothalamus; PSB, pallial-subpallial boundary; Ptec, pretectum; Pth, prethalamus; Tel, telencephalon; Th, thalamus. (Reproduced from Kiecker and Lumsden, 2005 [1])

2.2 SEGMENTATION

The hindbrain is one of the best-characterized examples of lineage restriction. During the course of development the hindbrain is subdivided in 7 to 8 compartments, called rhombomeres (Figure 2.1). The boundary between r7 and r8 is not morphologically visible. The different compartments are only defined by distinct neuronal nuclei and as a result are considered as one rhombomere by some [5]. Before boundary formation, cells can move freely between segments, but afterwards no cell movements across boundaries occur thus maintaining rhombomeres as lineage-restricted compartments [6]. In mouse embryos restriction of cell movements across boundaries happens even before boundaries are molecularly and morphologically defined [7]. However, lineage restriction is not complete as a small proportion of cells seems to be able to violate the RBs [6].

Compartments are defined as adjacent cell populations. Cells can migrate freely within a compartment, but cannot migrate from one compartment to another. This is usually achieved through differential identity of the cells in each compartment [8]. Segmentation enables regional diversity, as the adjacent rhombomeric cell populations will diverge independently along distinct developmental pathways [4].

The acquirement of segmental identity is a complex process. The following sections are therefore not a reflection of the chronological order in which segmentation occurs. They are descriptions of different processes that happen more or less at the same time, but which have been split up for simplicity.

2.2.1 *RESTRICTED EXPRESSION OF TRANSCRIPTION FACTORS*

The rhombomeres acquire a different identity through the unique combination of genes expressed in each segment. However, expression patterns in the hindbrain are temporally dynamic, as many feed forward and feedback loops exist between the different factors. This results in a complex gene regulatory network from which no straightforward gene hierarchy can be deduced (Figure 2.2) [4].

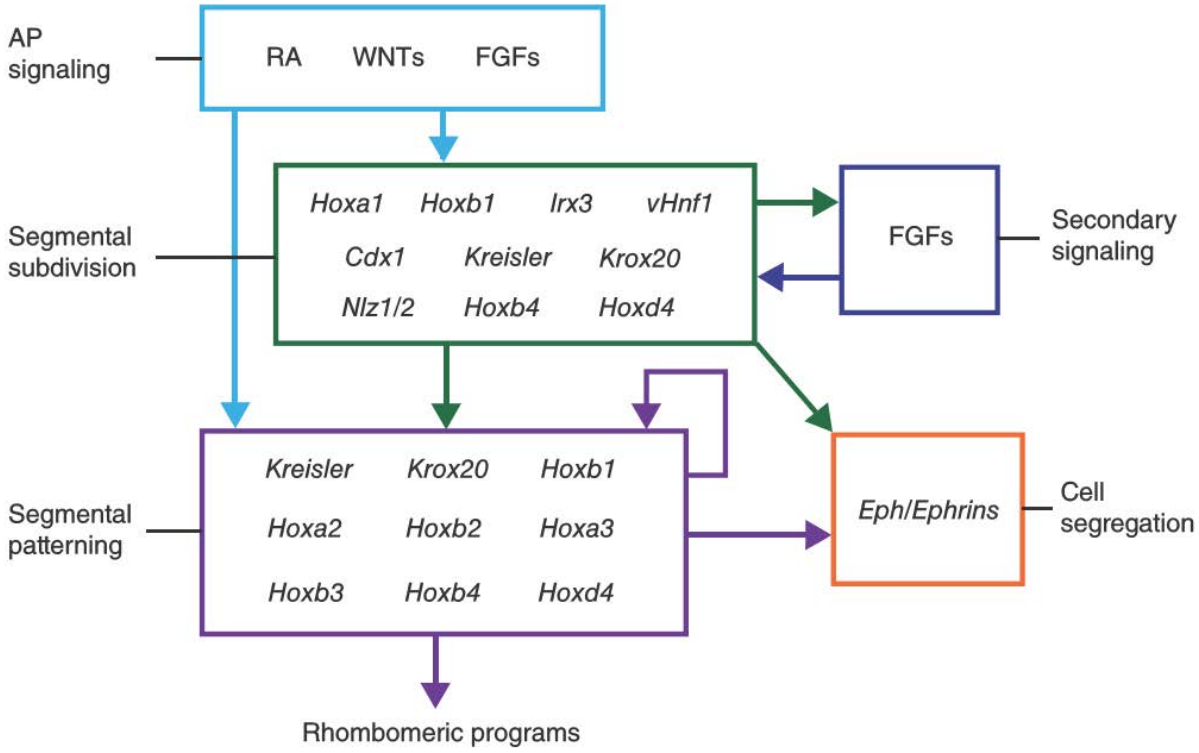

Figure 2.2 Gene regulatory network of the hindbrain. Schematic representation of the hierarchical structure of gene expression in the hindbrain and the key factors of each layer. Different groups of genes are mainly linked to distinct aspects of hindbrain development: AP signaling, segmental subdivision, segmental patterning, secondary signaling and cell segregation. Together these key genes and signaling molecules drive rhombomeric identity. (Reproduced from Parker and Krumlauf, 2017 [9])

Fibroblast growth factor 3 (FGF3), FGF19, the FGF receptors (FGFRs) and downstream components of the MAPK signaling pathway are all dynamically expressed in specific segments of the hindbrain throughout its development, indicating a role for FGF signaling in hindbrain segmentation [10]. Rhombomere 4 (r4) is the first rhombomere to form [11]. FGF3 and FGF8 form a signaling center in presumptive r4 and from there induce segmental expression of patterning genes in the other rhombomeres [11, 12]. The Bone Morphogenetic Protein (BMP) inhibitor follistatin shows a similar spatial and temporal expression pattern as FGF3 in the hindbrain and inhibition of BMPs by follistatin is necessary for segmental expression of *FGF3* [13]. FGF signaling establishes expression of the earliest segmentation markers: *Krox20* in r3 and r5 and *MafB* in r5-r6 [14]. FGF3 induces expression of *Pea3* through the MAPK pathway and downstream *Pea3* then induces *Krox20* expression in r3 and r5 [10]. Even though FGF signaling is not restricted to r3 and r5 only these rhombomeres express *Krox20*. Krox20 controls the expression of genes essential for r3 and r5 fate (see further). Krox20 levels are tightly regulated. In a positive feedback loop krox20 binds it own promoter. On the other hand precise *Krox20* transcript levels are assured through induction of expression of its own antagonists *Nab1* and *Nab2* [15, 16]. Furthermore, *Nab1* expression is induced by Pax6, another target of FGF signaling in r3 and r5, revealing another mechanism by which *Krox20* expression is

restricted [17]. Krox20 was the first gene discovered to have a segmental expression pattern and thereby was the first proof of a patterning function of neuromeres [18]. *Krox20*$^{LacZ/LacZ}$ mice lack r3 and r5. The cells normally giving rise to these rhombomeres are incorporated in the adjacent even-numbered rhombomeres leading to a reduction in the amount of segments formed [19, 20]. Furthermore, FGF signals synergize with *variant hepatocyte nuclear factor 1* (*vhnf1*) to specify r5 and r6. Both are needed to induce expression of *mafB* and *Krox20* in r5. Vhnf1 also represses *Hoxb1* expression, indepently of FGF signaling, thereby limiting its expression to r4 [21].
Next to FGF signaling, a posterior-to-anterior gradient of retinoic acid (RA) exists in the hindbrain. RA is synthesized in the presomitic mesoderm by RALDH2 and diffuses along the neural tube to the anterior hindbrain, where it is degraded by the expression of RA-degrading enzymes [4, 22-24]. Many *hox* genes contain RA response elements in their promoters, including the paralogues of *hox4* and *hox1* [22-24]. Early activation of *Hoxa1* and *Hoxb1* expression by RA precedes rhombomere formation and expression of all other segmentation factors that will later induce expression of other *Hox* genes [4]. Since RA concentration is high in the posterior hindbrain, patterning of this region is mostly RA-dependent [25-27]. Treatment of mouse embryos with ectopic RA induces duplication of the *Hox* genes normally expressed in r4 to r2 and of r5 to r3 resulting in a homeotic transformation of identity in anterior rhombomeres [28]. In r5-r6 *mafB* is expressed under the influence of specific concentrations of RA [29]. *Kreisler* (*mafB*) mutant mice lack r5, instead there is a fusion between r4 and r6. As mafB is also responsible for induction of *Hox* gene expression in r6, defects in segmental patterning of r6 are seen later in development [30]. Mafb activates expression of *Hoxa3* in r5-r6 and of *Hoxb3* in r5 [31]. Moens et al characterized a zebrafish *valentine* (*mafB*) mutant. They describe loss of segmental organization of neurogenesis and an absence of rhombomere boundaries posterior to the r3/r4 boundary due to a lack of specification of r5 and r6 [32]. Also *vhnf1*, which specifies r5-r6 identity, is, besides induction by FGF signaling and a positive feedback loop with *mafB,* under direct control of RA [24]. Anterior to r5 *vhnf1* expression is inhibited by the *iroquois* genes [21, 24].
Another transcription factor, Pou2, seems to function during early hindbrain regionalization, even upstream of Krox20 and MafB. The zebrafish *spiel ohne grenzen* (*spg*) mutant, that has *pou2* loss of function, does not have rhombomere boundaries and expression of *Krox20* and *MafB* is greatly reduced. Pou2 can rescue this expression, but cannot drive ectopic expression of both genes. *Hox* gene expression is disturbed in *spg* mutants indicating altered segmentation [33].

2.2.2 SEGMENTAL IDENTITY: THE HOX CODE

Combined activity of all segmentally expressed transcription factors in the hindbrain leads to localized expression of homeobox-containing transcription factors, *Hox* genes, along the anterior-posterior axis [34]. Krox20 directly induces *Hoxa2* and *Hoxb2* expression in r3 and r5 [35, 36] (and see 2.2.1 for additional examples). The anterior boundaries of different *Hox* genes are separated by two segments, conferring a two-segment periodicity to the rhombomeres [37]. The *Hoxb* cluster genes *Hoxb2, Hoxb3, Hoxb4* and *Hoxb5* have anterior expression limits at the r2/r3, r4/r5, r6/r7 and r8/spinal cord boundary, respectively [38]. The combination of *Hox* genes expressed in a given rhombomere, the so-called Hox code, determines its positional identity [4]. *Hox* knockouts in mouse lead to loss of individual rhombomeres or transformation to more anterior identities [24]. *Hoxa1* is normally expressed caudal to the r3/r4 boundary. In *Hoxa1*$^{-/-}$ embryos r4 and r5 are greatly reduced and fused to r6 [39]. *Hoxb1* expression is, as opposed to other *hox* genes, confined to a single rhombomere, r4, where it maintains its own expression through an auto-regulatory loop [38, 40]. *Hoxb1*$^{-/-}$ mice show normal initial segmentation, but fail to upregulate r4 specific genes at later

stages indicating that r4 identity is not maintained. As a result mutant embryos show defects in migration behavior of r4 specific neuron populations [40]. On the other hand, overexpression of *Hoxb1* in r2 transforms this rhombomere to r4 identity [41]. Transplantation of rhombomeres to a more rostral position does not lead to a change in identity and *Hox* expression correlated to the original position is maintained. However, when rhombomeres are transplanted to a more caudal position *Hox* gene expression changes to match the new position, suggesting the presence of posterior inducing signals responsible for *Hox* gene expression [37, 42]. This is in line with the establishment of *Hox* gene expression from posterior to anterior [38].

Hox proteins cooperate with the Pbx and Meis homeobox containing transcription factors for DNA binding specificity. Their interaction is responsible for auto- and crossregulation of Hox factors in the hindbrain [24]. In zebrafish lacking both *pbx4* and *pbx2* r2-r6 are transformed to r1 identity. Pbx transcription factors cooperate with hoxa1 and hoxb1 to induce *fgf3* expression in r4 and *vhnf1* expression in r5-r6. These induce *mafB* expression in r5-r6 and mafB is needed to establish initial expression of group 3 *hox* genes (*Hoxa3* and *Hoxb3*) in these segments [43]. *Hoxa3* expression is maintained in r5-r6 after *MafB* expression disappears through an autoregulatory loop, while *Hoxb3* expression is only maintained posterior to the r6/r7 boundary [44]. Downstream of the Hox genes segmental expression of several genes is induced that confer a specific identity to each rhombomere or that can drive cell segregation in adjacent rhombomeres, for example genes of the Eph receptor/ephrin family [45, 46].

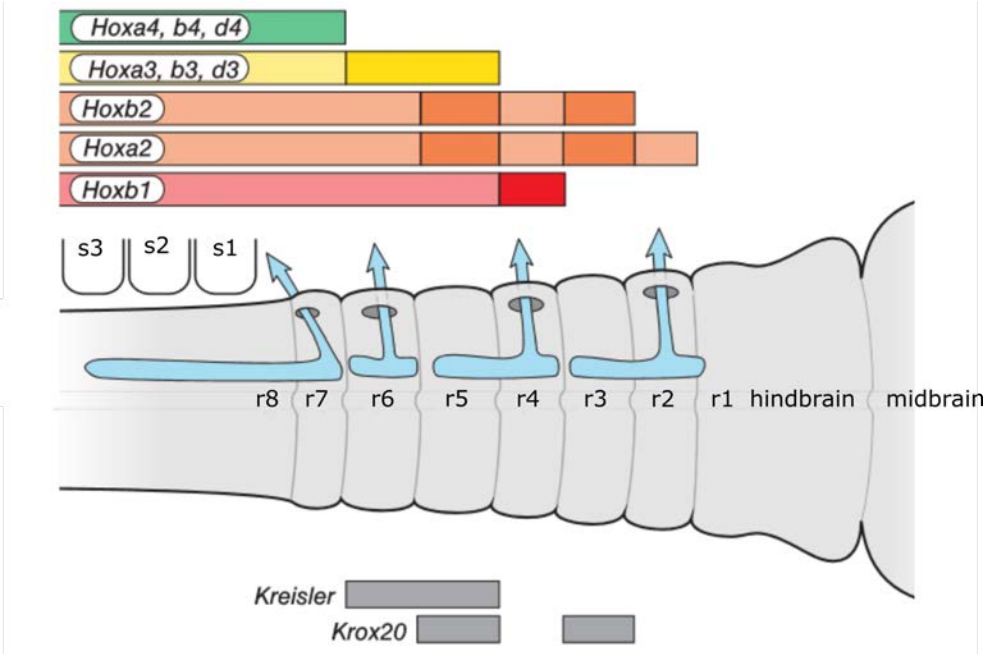

Figure 2.3 Hox gene expression in the vertebrate hindbrain. Dorsal view of the mouse embryonic hindbrain. Rhombomeric expression domains of different Hox genes and the segmental regulators Kreisler (mafB) and Krox20 is shown. Darker shading of Hox domains indicates higher levels of expression in those rhombomeres. Neuronal pools contributing to cranial nerves are depicted in light blue. Somites (s1-3) are shown only on the left side. r = rhombomere. (Reproduced from Parker and Krumlauf, 2017 [9])

2.2.3 *Cell segregation*

The expression boundaries of the transcription factors in the hindbrain are initially diffuse, but eventually sharpen giving rise to distinct rhombomere boundaries (RBs) [47]. This sharpening can occur by at least two mechanisms: through cell sorting of cells with different identities or through changing a cells identity according to the compartment in which it is localized (cell plasticity) (Figure

2.4). A recent study revealed that neither mechanism leads to sharp boundaries on its own, but together they work synergistically to achieve well-defined compartments [48]. At the same time that gene expression sharpens, RBs also become morphologically visible and the rhombomeres appear as a series of bulges. This indicates the existence of a mechanical force constricting the neural tissue at the boundaries. In the avian embryo RBs start to emerge immediately after neural tube closure and are completely visible before the onset of neurogenesis [49].

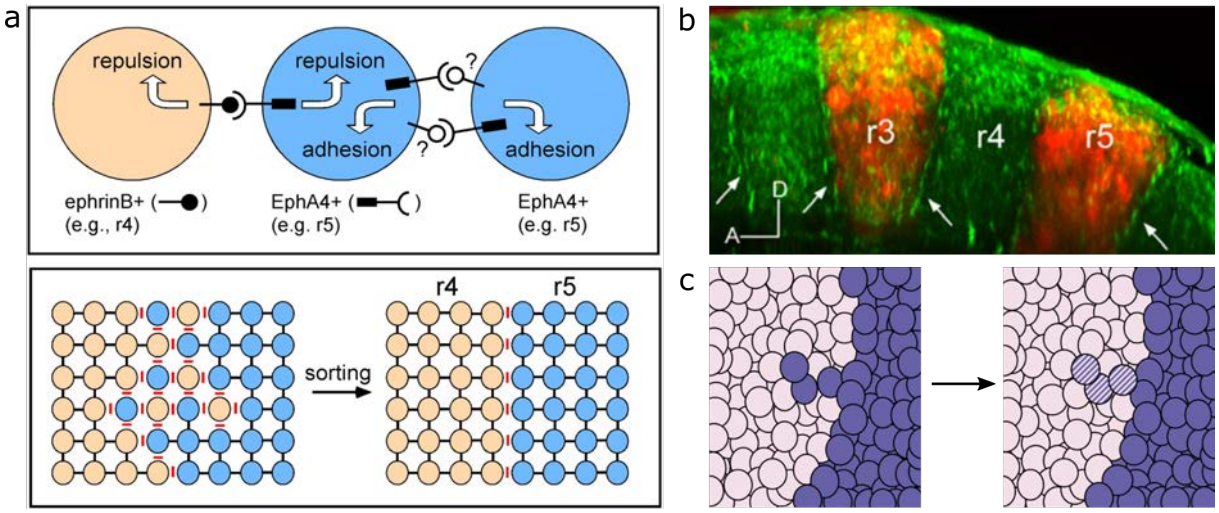

Figure 2.4 Different mechanism to reach cell segregation in the hindbrain. (a) Sharp boundaries are achieved through differential adhesion properties of cells in different compartments, leading to active sorting of cells to the right compartment. In the hindbrain cell sorting occurs through Eph receptor-ephrin mediated repulsion between compartments and adhesion within one compartment. (Figure reproduced from Cooke et al., 2005 [50]) (b) Sagittal-optical sections through the zebrafish hindbrain showing actomyosin cables in the rhombomere boundaries (arrows). These cables form a mechanical barrier for cell movements across the boundary. Green and red fluorescent signal represents myosin II and krox20 expression, respectively. (Figure reproduced from Calzolari et al., 2014 [51]) (c) Cell plasticity is a final mechanism to reach sharp boundaries. Cells change gene expression profile to match the identity of their neighbors. (Figure adapted from Cooke and Moens, 2002 [52])

2.2.3.1 Cell sorting

Cell sorting in the hindbrain occurs through differential adhesion properties of adjacent cell populations [53]. Transplantation experiments in chick revealed that juxtaposition of two odd- or even-numbered rhombomeres does not lead to formation of a boundary, similar to when two identical rhombomeres are juxtaposed. However, juxtaposition of an odd-numbered to an even-numbered rhombomere does lead to boundary formation and no cell mixing is observed. This implicates a two segment periodicity in the expression of a cell-surface factor leading to boundary formation [54, 55]. *Krox20*-null cells from r3 and r5 intermingle with cells from adjacent even-numbered rhombomeres indicating that early segmentation genes confer differential properties to neighboring segments [19]. Ectopic *Krox20* expression can induce odd-numbered segment identity in even-numbered rhombomeres [56, 57].

The restriction in migration between compartments relies at least in part on signaling via ephrins and the Ephrin family of receptor tyrosine kinases (Eph) (Figure 2.4). Both Eph receptors and their ligands are attached to the plasma membrane and are often expressed in complementary domains. They bind each other directly thereby eliciting bi-directional signaling. This leads to repulsion between the interacting cells and can thus restrict intermingling of adjacent cell populations [58]. Besides preventing cell mixing once boundaries have been established, this mechanism could also drive initial sharpening of gene expression boundaries through cell sorting. In the vertebrate hindbrain Ephs and ephrins are expressed in complementary, segment-specific domains such that

the RBs colocalize with an interface between an Eph receptor and its ligand [45, 50, 59-62]. *MafB* induces expression of *ephB4* and represses *ephrinB2a* in r5-r6 [63]. Krox20 induces expression of *EphA4* in r3 and r5 in mice, zebrafish and *Xenopus* [50, 56, 57, 64]. In the zebrafish hindbrain ephrinB2a is expressed in r1, r4 and r7. Morpholino (MO) mediated knockdown of EphA4 leads to fuzzy *krox20* expression boundaries and a loss or disorganization of expression of boundary markers. EphrinB2a knockdown has little effect, but knockdown of both EphA4 and ephrinB2a leads to a more severe disorganization of the hindbrain. Due to a failure in cell sorting, specialized boundary cells do not seem to form. This leads to defects in neural patterning with the fusion of neuronal populations that are normally separated by RBs [50]. Expression of a dominant negative truncated EphA4 receptor disrupts segmental *krox20* expression both in *Xenopus* and zebrafish. Furthermore expression of the boundary marker *pax6* is diminished and neuronal patterning disturbed [64]. Mosaic overexpression of ephrinB2 results in a normal distribution of ephrinB2 expressing cells in even-numbered rhombomeres, but in odd-numbered rhombomeres these cells sort out to the RB. However identity of the ephrinB2 expressing cells complies with the rhombomere they are in [65]. Next to repulsion between segments Eph receptors and ephrins also independently promote cell-cell affinity within their respective segments thereby contributing to the separation of segments. EphA4 MO and ephrin2B MO injected cells sort out from EPhA4 and ephrin2B expressing cells, respectively [50, 66].

2.2.3.2 Mechanical barrier

Next to differential adhesion, mechanical barriers formed by actomyosin cables have been described to prevent intercompartmental cell mixing [67, 68]. In *Drosophila* differential expression of Hox genes in adjacent compartments has been shown to induce expression of non-muscle myosin II and thereby control cell segregation [69]. In zebrafish, actomyosin cables form at RBs the moment they become morphologically visible and these restrict cell movement between rhombomeres (Figure 2.4). Formation of actomyosin cables occurs downstream of ephrin/Eph-signaling [51].

2.2.3.3 Cell plasticity

A third mechanism to sharpen expression boundaries that has been observed in the hindbrain, is cell plasticity (Figure 2.4) [66]. This is most pronounced during early segmentation as indicated by cell transplantations in the zebrafish hindbrain and is progressively lost [70]. In zebrafish, *hoxb1a* and *krox20* both positively regulate their own expression, while downregulating expression of the other. This can give rise to an alternating gene expression pattern with sharp boundaries. Furthermore, it has been shown that the initial noise in both expression of segmental markers and morphogen gradients like the RA gradient, can be a trigger to drive sharpening of expression domains [71, 72]. The initial fluctuations are thought to actually help cells switch between different profiles of gene expression thereby sharpening the RBs, a mechanism called noise-induced switching [71, 72]. Sosnik et al. recently showed that the RA-binding protein crabp2a and the RA-degrading enzyme cyp26a1 are essential to modulate noise in the RA gradient and to drive sharpening of the RBs [72].

2.2.4 SEGMENTAL ORGANIZATION OF NEURAL CIRCUITRY

Together the segment-specific expression of transcription factors and the restriction of cell movement form a spatial framework for patterning of the hindbrain circuitry and as a result the different hindbrain neuronal populations, such as motor, reticular and vestibular nuclei, will be arranged in a segmental pattern [5, 73-76]. This segmental organization is highly conserved in all vertebrates (Figure 2.5) [5]. Reticulospinal neurons, neurons of the reticular formation that relay information to the spinal cord mainly controlling posture, are formed first and locate to rhombomere

centers. Only later neurons appear adjacent to RBs, like commissural neurons which have their axons aligned to the RBs [77]. Also oligodendrocytes show regional identity as a result of segmental *hox* gene expression [78]. Loss or misexpression of segmental genes leads to defects in the timing or spatial organization of neurogenesis, resulting in mispatterned hindbrain circuitry [56]. All this is consistent with rhombomeres being autonomous units. However, some suggestions of interrhombomeric signaling exist. Projection neurons, excitatory neurons connecting to the cortex, and motorneurons appear first in even-numbered rhombomeres followed by the odd-numbered rhombomeres. When individual rhombomeres are separated this timing difference is no longer observed suggesting crosstalk between different rhombomeres [79].

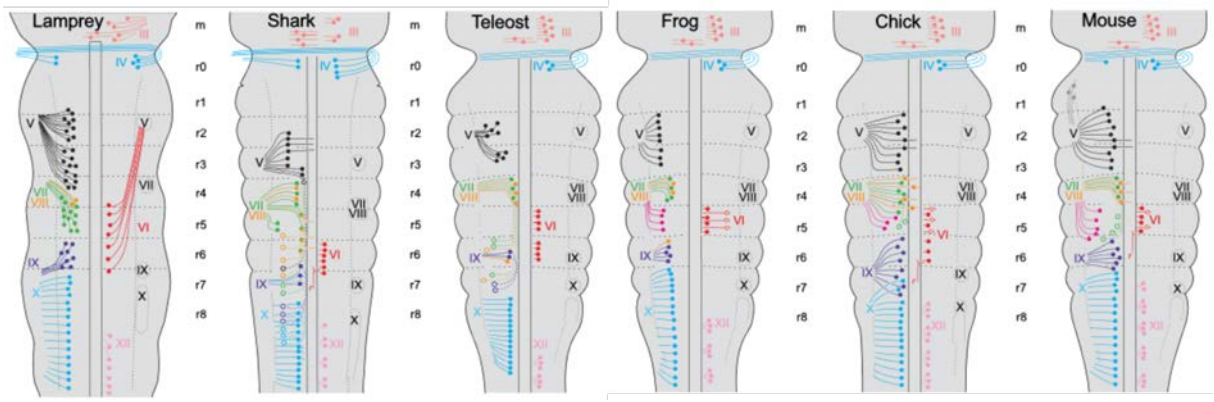

Figure 2.5 Conservation of segmental organization of cranial nerve nuclei across vertebrates. Dorsal view on the hindbrain of different vertebrates. Different colors depict efferent neurons from different cranial nerves (III-XII). (Figure reproduced from Gilland and Baker, 2005 [5])

2.3 RHOMBOMERE BOUNDARIES AS SIGNALING CENTERS

Boundaries are formed where cells of different identity are juxtaposed. However, their function is not only to keep cells with different expression patterns separate. Interaction between these differential cell types establishes a new signaling center at their boundary that will further pattern the adjacent tissue [80]. Proof that RBs only form between segments with different identity is provided by zebrafish that lack *pbx* expression. In these embryos all rhombomeres show r1 identity and no RBs are formed [43]. Furthermore, RBs reform after they have been ablated, indicating that boundary formation is an intrinsic property of two opposing cell populations [54].

2.3.1 RHOMBOMERE BOUNDARIES

During early stages, expression of segment specific genes meets exactly at the center of the RBs. Later, boundary cells form a separate cell population with distinct characteristics. They show a decreased rate of cell division and interkinetic nuclear migration, positioning of the nucleus according to the cell cycle phase [81]. Cell divisions require cell rearrangements and this might challenge boundaries. In *Drosophila* imaginal discs, a zone of non-proliferating cells has been proposed to function as a lineage restriction boundary [82]. However, Amoyel et al. observed elevated expression of the Wnt target gene *cyclinD1,* a known marker of cell proliferation, at the RBs [83, 84]. Boundary cells express *foxj1,* a master regulator of ciliogenesis, in *Xenopus* from stage 40 and bear elongated monocilia [85]. They also show increased extracellular space and expression of specific extracellular matrix (ECM) proteins like laminin and chondroitin sulphate proteoglycan (CSPG) in chick [86, 87]. Furthermore, they have reduced junctional permeability [88]. RBs have been shown to prevent spreading of morphogenetic signals in chick [89]. Next to this, boundary cells are

characterized by the specific expression of a myriad of genes like *fgf3*, the zinc-finger gene *plzf* and *pax6* [86, 90]. RBs also contain radial glia positive for the markers vimentin and DMγ, while radial glia in rhombomere centers can be labeled with GFAP [86, 91]. Recently, in chick RBs were shown to be composed of Sox2-positive neural progenitor cells (NPCs), while NPCs disappear from rhombomere centers at later stages. The Sox2-positive NPCs showed a slow division rate compatible with them constituting a NSC population that can give rise to transit amplifying progenitors that will in turn give rise to differentiating neurons that will migrate to the rhombomere centers. RBs thus act as a reservoir of NSCs [92].
RB cells are thus considered to be an immobile, quiescent cell population thereby forming a mechanical barrier between rhombomeres and retaining its signaling function. Interestingly, upon application of retinoic acid to the chick hindbrain, the posterior RBs, both morphological and molecular, are lost. The loss of boundary cells is preceded by loss of *krox20* and *EphA4* expression and followed by changes in the expression pattern of *Hox* genes. However, no cell mixing was seen and only small changes in the organization of motor nuclei were observed [93].

2.3.2 NOTCH SIGNALING

During early hindbrain development, the Notch signaling modulatory genes *manic* and *lunatic fringe* are expressed in presumptive r3 and r5 creating opposing fields of *fringe* expressing and non-expressing cells. This situation has been linked to the establishment of compartment boundaries (see box1) [94]. Cheng et al. described a segmental expression pattern of Notch signaling components in the zebrafish hindbrain. *Radical fringe* (*Rfng*) is expressed in the rhombomere boundaries, while the ligands *DeltaA* and *DeltaD* are expressed in stripes adjacent to the boundaries (Figure 2.6) [95]. This expression pattern suggests Notch signaling activation at the RB [96, 97]. Moreover, mosaic overexpression of Notch intracellular domain (NICD), which activates Notch signaling in these cells, lead to the preferential localization of these cells at the RBs (Figure 2.6). This effect is dependent on Notch signaling mediated activation of transcription as a dominant active form of the pathways endpoint, the transcription factor Su(H), had the same effect. Time lapse tracking of these cells revealed that they actively move to the RB and take on the elongated morphology of boundary cells. Notch signaling thus seems to influence the affinity properties of hindbrain cells. However, Notch signaling is not required for boundary cell specification. Ectopic activation of the pathway could not induce the expression of boundary markers in non-boundary cells [95]. *Mind bomb* (*mib*) encodes an E3 ubiquitin ligase that is required for Delta function. *Mib* mutant embryos have a Notch pathway deficiency leading to excess production of early neurons due to reduced lateral inhibition. In the zebrafish hindbrain this precocious neural differentiation results in a severe reduction of later-born neuron types, like commissural neurons and branchiomotor neurons. Furthermore, a loss of segmental gene expression and RBs at these late stages was described (Figure 2.6) [98, 99]. However, Cheng et al. showed that *mib* mutants still express boundary markers except for *rfng.* Moreover, Notch activated and inhibited cells still migrated to and away from the RBs, respectively [95].
Also in zebrafish, another Notch signaling modulator, lfng, is expressed in stripes adjacent to the RBs, similar to markers of neuronal differentiation of the neurogenin, neuroD, achaete-scute and delta families. MO mediated knockdown of lfng had no effect on boundary formation, but lead to an increase in neuronal differentiation. This resulted in a depletion of progenitor cells at late stages, indicating that lfng is important for Notch-mediated lateral inhibition of neurogenesis. Proneural genes induce lfng expression and lfng then cell autonomously inhibits neurogenesis [100].

The Notch effector Hes1, a repressor-type bHLH transcription factor, inhibits proneural bHLH factors. *Hes1* expression normally oscillates thereby contributing to regulated neuronal differentiation [101, 102]. However, at neuromeric boundaries *Hes1* expression is persistently high and these cells are shown to proliferate more slowly. Sustained *Hes1* expression is thought to be responsible for the absence of expression of proneural factors like Notch ligands and cell cycle regulators like *cyclinD1.* This leads to inhibited neuronal differentiation and reduced cell cycle progression expression, thus maintaining boundary regions as neuron-free zones and signaling centers [102, 103].

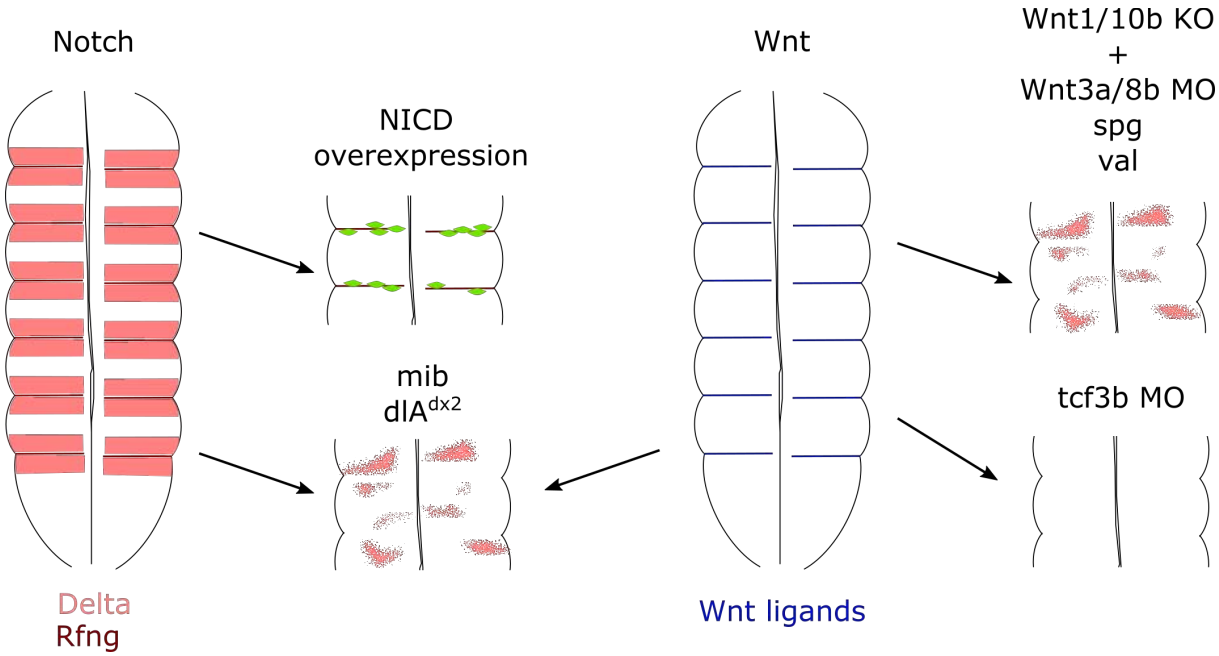

Figure 2.6 Notch and Wnt signaling in the rhombomere boundaries. Simplified scheme representing current knowledge about Notch and Wnt signaling in the zebrafish rhombomere boundaries (RBs). Radical fringe (Rfng) is expressed in the RBs, delta ligands are expressed adjacent to the RBs (left panel). Cells overexpressing the Notch intracellular domain (NICD, bright green) sort to the RBs. In *mib* and *dlA*^{dx2} mutants, which both have deficient Notch signaling, boundary marker expression is lost and Delta expression pattern is chaotic. Several Wnt ligands are expressed in the RBs. In *wnt 1/10b* knockout zebrafish combined with wnt3a and 8b morpholino mediated knock down (MO) and in *spg* and *val* mutants, which have lost RBs, Wnt ligand expression is lost and Delta expression pattern is chaotic. Tcf3b MO leads to loss of boundary marker expression.

2.3.3 WNT SIGNALING

In zebrafish, MO mediated knockdown of *tcf3b,* which functions as a transcriptional repressor of Wnt target genes, leads to a loss of RBs, both physical, as indicated by phalloidin staining, and molecular, indicated by loss of *foxb1a* expression (Figure 2.6). *Wnt1* is normally exclusively expressed at the RBs, but shows uniform expression at the dorsal margin of the hindbrain after *tcf3b* MO injection. However, segmental organization is normal [104].

Two research groups tried to clarify the role of Wnt signaling in the zebrafish RBs. Amoyel et al. found that *Wnt1* is expressed in the dorsal half of the RBs, while markers of neuronal differentiation are expressed in stripes adjacent to the RBs. MO mediated knockdown of Wnt1 lead to a broadening of the expression domain of the boundary markers *rfng* and *foxb1a,* while the sharp expression domain of the segment markers *krox20* and *hoxb1a* was maintained. Furthermore, expression of proneural markers was decreased, as was the number of differentiated neurons [83]. In rfng MO embryos *wnt1* expression in the RB was lost [83, 95]. In this study both *rfng* and *tcf3b* knockdown had similar effects as *wnt1* knockdown [83, 95]. This is counterintuitive as tcf3b has a repressive

effect on Wnt signaling. MO mediated knockdown of proneural genes also lead to a broadening of *rfng* and *foxb1.2* expression. Activation of Wnt signaling, either through overexpression of *wnt1* or of a stabilized form of β-catenin, increased the number of differentiated neurons. The authors conclude that Wnt signaling is necessary to prevent spreading of boundary marker expression to non-boundary cells and to induce differentiation of neurons adjacent to boundaries [83]. They propose a signaling network similar to the dorso-ventral boundary of the *Drosophila* wing imaginal disc where Notch is specifically activated at the boundary and induces Wnt ligand expression at the boundary. Wnt signaling, in turn, induces Notch ligand expression adjacent to the boundary, thereby creating a positive feedback loop that maintains the boundary signaling center (see box 1). Importantly, these authors later retracted their findings. They found that the reduction in proneural marker expression and the spreading of boundary marker expression was due to off-target effects of the MOs, inducing the Tp53-mediated cell death pathway. They found that pro-apoptotic genes can induce gene expression revealing a previously unknown effect of MO-mediated toxicity [105].

Riley et al. observed expression of *Wnt1, Wnt10b, Wnt3a* and *Wnt8b* in the RBs, again flanked by thin stripes of proneural gene expression. *Wnt1, Wnt10b* double knock out embryos were injected with MO against *Wnt3a* and *Wnt8b.* This resulted in a disorganized expression pattern of *Delta* genes and several neuronal defects at later stages, while segment identity was maintained (Figure 2.6) [106]. *Tcf3b* MO embryos showed similar disorganization of the hindbrain, however *tcf3b* MO was shown to have off target effects [105]. *Spiel-ohne-grenzen* (spg) mutants (*pou2* loss of function), that fail to form RBs, and *valentino* (*MafB*) mutants, that do not form RBs after r4, don't show boundary-specific *Wnt1* expression, have chaotic *Delta* expression and show disorganized neuronal pattern at later stages (Figure 2.6). All this indicates a role for Wnt signaling in maintaining metameric patterning. Embryos with defective Delta-Notch signaling, dlA^{dx2} and *mib* mutants, show disorganization of the hindbrain. Expression of *Wnt1* is lost and *deltaA* expression is chaotic and decreased (Figure 2.6). Heat shock-mediated overexpression of *Wnt1* could partially rescue hindbrain organization. However, if induction of *Wnt1* expression was only started after boundaries were already lost, hindbrain organization could not be rescued anymore. They conclude that Wnt signaling is required for normal hindbrain patterning and that expression of *Wnts* in the RBs is maintained by *Delta* expression in neighboring cells [106]. They also point towards an analogy with the *Drosophila* wing disc.

BOX1 THE DORSO-VENTRAL BOUNDARY OF THE DROSOPHILA WING DISC

In the *Drosophila* wing disc the Notch receptor is ubiquitously expressed. The Serrate ligand is only expressed in dorsal cells (blue), while ventral cells express Delta ligand (red). The dorsal cells also express Fringe, which cell-autonomously potentiates Delta-Notch signaling, but inhibits Serrate-Notch signaling. Fringe expression thus prevents Notch activation in all cells that express Serrate. As a result, Serrate can only activate the Notch receptor at the dorso-ventral boundary in the ventral boundary cells that neither express Fringe nor Serrate [107]. At the same time, the Delta-expressing ventral cells preferentially activate the Notch receptor in the dorsal, Fringe-expressing cells, as in these cells the Notch receptor is modified to potentiate Notch signaling activation [107]. Notch signaling activation in the ventral wing disc is prevented by cis-inhibition, as these cells express both ligand and receptor. As a result, the Notch receptor is only activated symmetrically at each side of the border between dorsal and ventral cells. Notch activation induces the expression of *Wingless* (Wg (Wnt)) at the boundary (green) [108]. Wg maintains its own expression at the dorso-ventral boundary through a positive feedback loop. It diffuses to adjacent dorsal and ventral cells in which it

induces expression of both Notch ligands. Notch ligand expression is thus maintained in a narrow band next to the boundary. These ligands signal back to the boundary where they maintain Notch signaling activation and subsequent Wg expression [107].

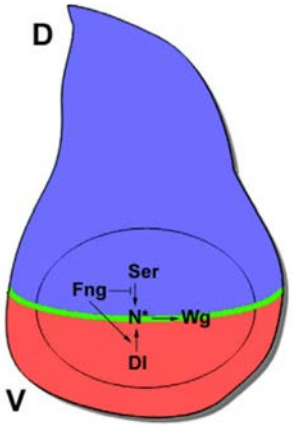

2.3.4 *FGF SIGNALING*

In chick, FGF signaling has also been shown in the RBs [10]. *FGF3* is expressed in the ventral half of the RBs and all four FGF receptors, *FGFR1-4,* and the signal transducer dual phosphorylated Erk1/2 also show specific boundary expression (Figure 2.7) [109, 110]. Proteoglycans of the ECM are important cofactors for FGF signaling. Heparan sulfate proteoglycan (HSPG) and chondroitin sulfate proteoglycan (CSPG) are also both present in RBs.

Expression of several boundary markers was assessed upon FGF signaling disruption. The ECM proteins CSPG and laminin, the bHLH transcription factor Neuronal Stem Cell Leukemia 1 (NSCL1), the transcription factor Brn3a and the neurofilament-associated antigen 3A10 all showed a clear decrease upon chemical inhibition of FGF signaling or after MO-mediated knockdown of FGF3 (Figure 2.7). The boundary marker follistatin, a TGFβ inhibitor, which is not regulated by FGFs, remained expressed in the RBs indicating that disruption of FGF signaling does not cause a general defect in boundary maintenance or formation [110]. Expression of a dominant negative truncated EphA4 (dnEphA4) receptor in the chick hindbrain lead to a loss of RBs with a consequent loss of sharp expression domains of segmental markers. *FGF3* expression occurs first in specific hindbrain centers and is only later confined to the RBs. Upon expression of dnEphA4 and when boundary cells were surgically removed FGF3 was not downregulated in hindbrain centers. This indicates that boundary cells regulate gene expression in rhombomere centers [111].

At late stages, neurogenesis in the hindbrain is spatially restricted. Neuronal differentiation is limited to the zones flanking the RB and is absent in the rhombomere centers and at the RBs. In segment centers a subset of neurons express *fgf20a* leading to the local activation of FGF signaling (Figure 2.7). Activated FGF signaling is needed to prevent neurogenesis and maintain a population of neural progenitors. It does so, at least in part, through induction of the RA metabolizing enzyme cyp26b1 thus preventing RA-induced neuronal differentiation [112]. In zebrafish, Notch signaling inhibits FGF signaling activation in the RBs through repression of *fgf20a,* preventing the subsequent upregulation of the FGF signaling effector *erm.* The expression domain of *erm* broadens in *mib* mutants (Figure 2.7). On the other hand, hdac1 is needed to maintain *fgf20a* expression and FGF signaling activity in the rhombomere centers as *erm* expression is lost in *hdac1* mutant embryos [113]. Also in zebrafish, MO mediated knockdown of ephrin signaling components or rfng, which result in boundary marker

downregulation, leads to a relocation of fgf20a expressing neurons. They appear more dispersed or closer to RBs, while their numbers are unchanged, indicating that boundary cells are required to maintain their positioning at rhombomere centers. Boundary cells express two semaphorins, which are known repellent cues, sema3fb and sema3gb, while fgf20a expressing neurons also express the semaphorin receptor nrp2a. These are responsible for the positioning of the fgf20a expressing neurons in the rhombomere centers and, as fgf20a represses neurogenesis, this maintains the correct patterning of neurogenesis (Figure 2.7) [114]. FGF signaling is also important for the expression of key genes underlying neural subtype specification and thus underlies neural cell diversity in the hindbrain [115].

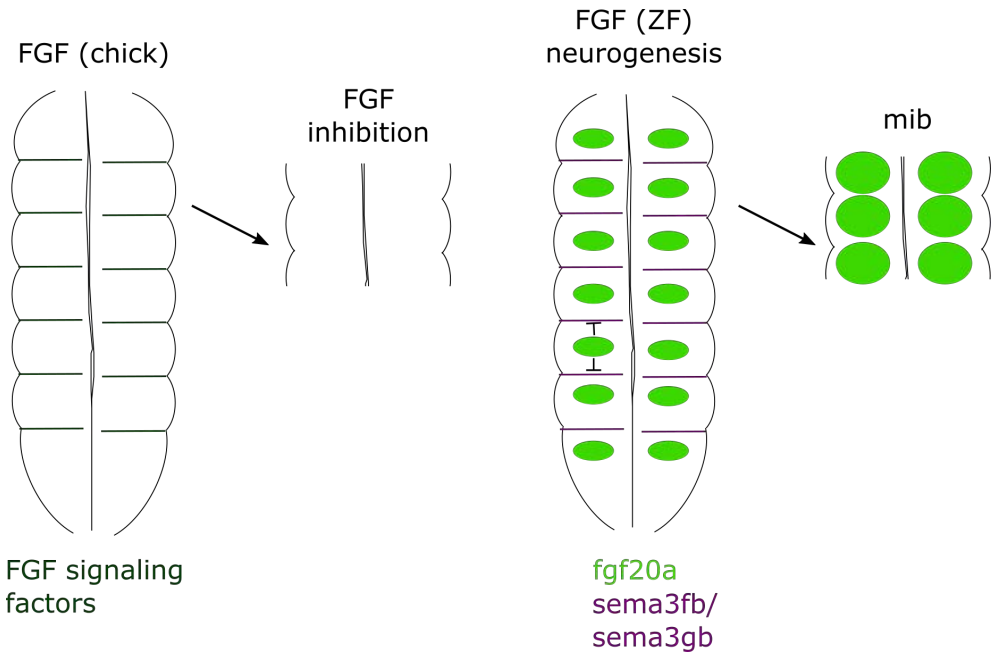

Figure 2.7 FGF signaling in the rhombomere boundaries. Simplified scheme representing current knowledge about FGF signaling in the rhombomere boundaries. In chick, FGF signaling factors are expressed in the rhombomere boundaries. Inhibition of FGF leads to loss of boundary marker expression. In zebrafish, at late developmental stages, neurogenesis is spatially restricted. Fgf20a positive neurons in the rhombomere centers inhibit neurogenesis and maintain neural progenitors. These neurons are kept in position through repellent semaphorin signals coming from the RBs. In Notch signaling deficient embryos FGF signaling is no longer inhibited around the RBs and FGF signaling activity via fgf20a expands.

2.4 Summary

One of the most striking features of the developing hindbrain is its subdivision in eight compartments called rhombomeres. This subdivision is required for proper patterning and stays apparent in the organization of the neural circuitry long after visible segmentation has disappeared.

At the interfaces of the successive segments a specific population of boundary cells is formed that has distinct characteristics from the other hindbrain cells. Depending on the species, these cells express specific markers and show activity of key developmental signaling pathways like Notch, Wnt and FGF signaling. However, the exact function of this signaling activity remains incompletely understood.

2.5 References

1. Kiecker, C. and A. Lumsden, *Compartments and their boundaries in vertebrate brain development.* Nat Rev Neurosci, 2005. **6**(7): p. 553-64.
2. Rhinn, M., et al., *Positioning of the midbrain-hindbrain boundary organizer through global posteriorization of the neuroectoderm mediated by Wnt8 signaling.* Development, 2005. **132**(6): p. 1261-72.
3. Houart, C., et al., *Establishment of the telencephalon during gastrulation by local antagonism of Wnt signaling.* Neuron, 2002. **35**(2): p. 255-65.
4. Parker, H.J., M.E. Bronner, and R. Krumlauf, *The vertebrate Hox gene regulatory network for hindbrain segmentation: Evolution and diversification: Coupling of a Hox gene regulatory network to hindbrain segmentation is an ancient trait originating at the base of vertebrates.* Bioessays, 2016. **38**(6): p. 526-38.
5. Gilland, E. and R. Baker, *Evolutionary patterns of cranial nerve efferent nuclei in vertebrates.* Brain Behav Evol, 2005. **66**(4): p. 234-54.
6. Fraser, S., R. Keynes, and A. Lumsden, *Segmentation in the chick embryo hindbrain is defined by cell lineage restrictions.* Nature, 1990. **344**(6265): p. 431-5.
7. Jimenez-Guri, E., et al., *Clonal analysis in mice underlines the importance of rhombomeric boundaries in cell movement restriction during hindbrain segmentation.* PLoS One, 2010. **5**(4): p. e10112.
8. Blair, S.S., *Developmental biology: Notching the hindbrain.* Curr Biol, 2004. **14**(14): p. R570-2.
9. Parker, H.J. and R. Krumlauf, *Segmental arithmetic: summing up the Hox gene regulatory network for hindbrain development in chordates.* Wiley Interdiscip Rev Dev Biol, 2017.
10. Weisinger, K., et al., *Analysis of expression and function of FGF-MAPK signaling components in the hindbrain reveals a central role for FGF3 in the regulation of Krox20, mediated by Pea3.* Dev Biol, 2010. **344**(2): p. 881-95.
11. Maves, L., W. Jackman, and C.B. Kimmel, *FGF3 and FGF8 mediate a rhombomere 4 signaling activity in the zebrafish hindbrain.* Development, 2002. **129**(16): p. 3825-37.
12. Walshe, J., et al., *Establishment of hindbrain segmental identity requires signaling by FGF3 and FGF8.* Curr Biol, 2002. **12**(13): p. 1117-23.
13. Weisinger, K., D.G. Wilkinson, and D. Sela-Donenfeld, *Inhibition of BMPs by follistatin is required for FGF3 expression and segmental patterning of the hindbrain.* Dev Biol, 2008. **324**(2): p. 213-25.
14. Marin, F. and P. Charnay, *Hindbrain patterning: FGFs regulate Krox20 and mafB/kr expression in the otic/preotic region.* Development, 2000. **127**(22): p. 4925-35.
15. Mechta-Grigoriou, F., S. Garel, and P. Charnay, *Nab proteins mediate a negative feedback loop controlling Krox-20 activity in the developing hindbrain.* Development, 2000. **127**(1): p. 119-28.
16. Bouchoucha, Y.X., et al., *Dissection of a Krox20 positive feedback loop driving cell fate choices in hindbrain patterning.* Mol Syst Biol, 2013. **9**: p. 690.
17. Kayam, G., et al., *A novel role for Pax6 in the segmental organization of the hindbrain.* Development, 2013. **140**(10): p. 2190-202.
18. Wilkinson, D.G., et al., *Segment-specific expression of a zinc-finger gene in the developing nervous system of the mouse.* Nature, 1989. **337**(6206): p. 461-4.
19. Voiculescu, O., et al., *Hindbrain patterning: Krox20 couples segmentation and specification of regional identity.* Development, 2001. **128**(24): p. 4967-78.
20. Schneider-Maunoury, S., et al., *Segmental and neuronal architecture of the hindbrain of Krox-20 mouse mutants.* Development, 1997. **124**(6): p. 1215-26.
21. Wiellette, E.L. and H. Sive, *vhnf1 and Fgf signals synergize to specify rhombomere identity in the zebrafish hindbrain.* Development, 2003. **130**(16): p. 3821-9.
22. White, R.J., et al., *Complex regulation of cyp26a1 creates a robust retinoic acid gradient in the zebrafish embryo.* PLoS Biol, 2007. **5**(11): p. e304.
23. Hernandez, R.E., et al., *Cyp26 enzymes generate the retinoic acid response pattern necessary for hindbrain development.* Development, 2007. **134**(1): p. 177-87.

24. Alexander, T., C. Nolte, and R. Krumlauf, *Hox genes and segmentation of the hindbrain and axial skeleton.* Annu Rev Cell Dev Biol, 2009. **25**: p. 431-56.
25. Linville, A., et al., *Independent roles for retinoic acid in segmentation and neuronal differentiation in the zebrafish hindbrain.* Dev Biol, 2004. **270**(1): p. 186-99.
26. Papalopulu, N., et al., *Retinoic acid causes abnormal development and segmental patterning of the anterior hindbrain in Xenopus embryos.* Development, 1991. **113**(4): p. 1145-58.
27. Gavalas, A. and R. Krumlauf, *Retinoid signalling and hindbrain patterning.* Curr Opin Genet Dev, 2000. **10**(4): p. 380-6.
28. Marshall, H., et al., *Retinoic acid alters hindbrain Hox code and induces transformation of rhombomeres 2/3 into a 4/5 identity.* Nature, 1992. **360**(6406): p. 737-41.
29. Grapin-Botton, A., et al., *Defined concentrations of a posteriorizing signal are critical for MafB/Kreisler segmental expression in the hindbrain.* Development, 1998. **125**(7): p. 1173-81.
30. Manzanares, M., et al., *The role of kreisler in segmentation during hindbrain development.* Dev Biol, 1999. **211**(2): p. 220-37.
31. Giudicelli, F., et al., *Novel activities of Mafb underlie its dual role in hindbrain segmentation and regional specification.* Dev Biol, 2003. **253**(1): p. 150-62.
32. Moens, C.B., et al., *valentino: a zebrafish gene required for normal hindbrain segmentation.* Development, 1996. **122**(12): p. 3981-90.
33. Hauptmann, G., et al., *spiel ohne grenzen/pou2 is required for zebrafish hindbrain segmentation.* Development, 2002. **129**(7): p. 1645-55.
34. Janssens, S., et al., *Direct control of Hoxd1 and Irx3 expression by Wnt/beta-catenin signaling during anteroposterior patterning of the neural axis in Xenopus.* Int J Dev Biol, 2010. **54**(10): p. 1435-42.
35. Nonchev, S., et al., *Segmental expression of Hoxa-2 in the hindbrain is directly regulated by Krox-20.* Development, 1996. **122**(2): p. 543-54.
36. Sham, M.H., et al., *The zinc finger gene Krox20 regulates HoxB2 (Hox2.8) during hindbrain segmentation.* Cell, 1993. **72**(2): p. 183-96.
37. Itasaki, N., et al., *Reprogramming Hox expression in the vertebrate hindbrain: influence of paraxial mesoderm and rhombomere transposition.* Neuron, 1996. **16**(3): p. 487-500.
38. Wilkinson, D.G., et al., *Segmental expression of Hox-2 homoeobox-containing genes in the developing mouse hindbrain.* Nature, 1989. **341**(6241): p. 405-9.
39. Mark, M., et al., *Two rhombomeres are altered in Hoxa-1 mutant mice.* Development, 1993. **119**(2): p. 319-38.
40. Studer, M., et al., *Altered segmental identity and abnormal migration of motor neurons in mice lacking Hoxb-1.* Nature, 1996. **384**(6610): p. 630-4.
41. Bell, E., R.J. Wingate, and A. Lumsden, *Homeotic transformation of rhombomere identity after localized Hoxb1 misexpression.* Science, 1999. **284**(5423): p. 2168-71.
42. Grapin-Botton, A., et al., *Plasticity of transposed rhombomeres: Hox gene induction is correlated with phenotypic modifications.* Development, 1995. **121**(9): p. 2707-21.
43. Waskiewicz, A.J., H.A. Rikhof, and C.B. Moens, *Eliminating zebrafish pbx proteins reveals a hindbrain ground state.* Dev Cell, 2002. **3**(5): p. 723-33.
44. Manzanares, M., et al., *Independent regulation of initiation and maintenance phases of Hoxa3 expression in the vertebrate hindbrain involve auto- and cross-regulatory mechanisms.* Development, 2001. **128**(18): p. 3595-607.
45. Taneja, R., et al., *The expression pattern of the mouse receptor tyrosine kinase gene MDK1 is conserved through evolution and requires Hoxa-2 for rhombomere-specific expression in mouse embryos.* Dev Biol, 1996. **177**(2): p. 397-412.
46. Prin, F., et al., *Hox proteins drive cell segregation and non-autonomous apical remodelling during hindbrain segmentation.* Development, 2014. **141**(7): p. 1492-502.
47. Irving, C., et al., *Progressive spatial restriction of Sek-1 and Krox-20 gene expression during hindbrain segmentation.* Dev Biol, 1996. **173**(1): p. 26-38.

48. Wang, Q., et al., *Cell Sorting and Noise-Induced Cell Plasticity Coordinate to Sharpen Boundaries between Gene Expression Domains.* PLoS Comput Biol, 2017. **13**(1): p. e1005307.
49. Lumsden, A., *Segmentation and compartition in the early avian hindbrain.* Mech Dev, 2004. **121**(9): p. 1081-8.
50. Cooke, J.E., H.A. Kemp, and C.B. Moens, *EphA4 is required for cell adhesion and rhombomere-boundary formation in the zebrafish.* Curr Biol, 2005. **15**(6): p. 536-42.
51. Calzolari, S., J. Terriente, and C. Pujades, *Cell segregation in the vertebrate hindbrain relies on actomyosin cables located at the interhombomeric boundaries.* EMBO J, 2014. **33**(7): p. 686-701.
52. Cooke, J.E. and C.B. Moens, *Boundary formation in the hindbrain: Eph only it were simple.* Trends Neurosci, 2002. **25**(5): p. 260-7.
53. Wizenmann, A. and A. Lumsden, *Segregation of rhombomeres by differential chemoaffinity.* Mol Cell Neurosci, 1997. **9**(5-6): p. 448-59.
54. Guthrie, S. and A. Lumsden, *Formation and regeneration of rhombomere boundaries in the developing chick hindbrain.* Development, 1991. **112**(1): p. 221-9.
55. Guthrie, S., V. Prince, and A. Lumsden, *Selective dispersal of avian rhombomere cells in orthotopic and heterotopic grafts.* Development, 1993. **118**(2): p. 527-38.
56. Giudicelli, F., et al., *Krox-20 patterns the hindbrain through both cell-autonomous and non cell-autonomous mechanisms.* Genes Dev, 2001. **15**(5): p. 567-80.
57. Theil, T., et al., *Segmental expression of the EphA4 (Sek-1) receptor tyrosine kinase in the hindbrain is under direct transcriptional control of Krox-20.* Development, 1998. **125**(3): p. 443-52.
58. Mellitzer, G., Q. Xu, and D.G. Wilkinson, *Eph receptors and ephrins restrict cell intermingling and communication.* Nature, 1999. **400**(6739): p. 77-81.
59. Helbling, P.M., et al., *Comparative analysis of embryonic gene expression defines potential interaction sites for Xenopus EphB4 receptors with ephrin-B ligands.* Dev Dyn, 1999. **216**(4-5): p. 361-73.
60. Henkemeyer, M., et al., *Immunolocalization of the Nuk receptor tyrosine kinase suggests roles in segmental patterning of the brain and axonogenesis.* Oncogene, 1994. **9**(4): p. 1001-14.
61. Nieto, M.A., et al., *A receptor protein tyrosine kinase implicated in the segmental patterning of the hindbrain and mesoderm.* Development, 1992. **116**(4): p. 1137-50.
62. Becker, N., et al., *Several receptor tyrosine kinase genes of the Eph family are segmentally expressed in the developing hindbrain.* Mech Dev, 1994. **47**(1): p. 3-17.
63. Cooke, J., et al., *Eph signalling functions downstream of Val to regulate cell sorting and boundary formation in the caudal hindbrain.* Development, 2001. **128**(4): p. 571-80.
64. Xu, Q., et al., *Expression of truncated Sek-1 receptor tyrosine kinase disrupts the segmental restriction of gene expression in the Xenopus and zebrafish hindbrain.* Development, 1995. **121**(12): p. 4005-16.
65. Xu, Q., et al., *In vivo cell sorting in complementary segmental domains mediated by Eph receptors and ephrins.* Nature, 1999. **399**(6733): p. 267-71.
66. Kemp, H.A., J.E. Cooke, and C.B. Moens, *EphA4 and EfnB2a maintain rhombomere coherence by independently regulating intercalation of progenitor cells in the zebrafish neural keel.* Dev Biol, 2009. **327**(2): p. 313-26.
67. Monier, B., et al., *An actomyosin-based barrier inhibits cell mixing at compartmental boundaries in Drosophila embryos.* Nat Cell Biol, 2010. **12**(1): p. 60-5; sup pp 1-9.
68. Major, R.J. and K.D. Irvine, *Influence of Notch on dorsoventral compartmentalization and actin organization in the Drosophila wing.* Development, 2005. **132**(17): p. 3823-33.
69. Curt, J.R., L.F. de Navas, and E. Sanchez-Herrero, *Differential activity of Drosophila Hox genes induces myosin expression and can maintain compartment boundaries.* PLoS One, 2013. **8**(2): p. e57159.

70. Schilling, T.F., V. Prince, and P.W. Ingham, *Plasticity in zebrafish hox expression in the hindbrain and cranial neural crest.* Dev Biol, 2001. **231**(1): p. 201-16.
71. Zhang, L., et al., *Noise drives sharpening of gene expression boundaries in the zebrafish hindbrain.* Mol Syst Biol, 2012. **8**: p. 613.
72. Sosnik, J., et al., *Noise modulation in retinoic acid signaling sharpens segmental boundaries of gene expression in the embryonic zebrafish hindbrain.* Elife, 2016. **5**: p. e14034.
73. Straka, H., R. Baker, and E. Gilland, *The frog as a unique vertebrate model for studying the rhombomeric organization of functionally identified hindbrain neurons.* Brain Res Bull, 2002. **57**(3-4): p. 301-5.
74. Straka, H., R. Baker, and E. Gilland, *Rhombomeric organization of vestibular pathways in larval frogs.* J Comp Neurol, 2001. **437**(1): p. 42-55.
75. Metcalfe, W.K., B. Mendelson, and C.B. Kimmel, *Segmental homologies among reticulospinal neurons in the hindbrain of the zebrafish larva.* J Comp Neurol, 1986. **251**(2): p. 147-59.
76. Lumsden, A. and R. Keynes, *Segmental patterns of neuronal development in the chick hindbrain.* Nature, 1989. **337**(6206): p. 424-8.
77. Trevarrow, B., D.L. Marks, and C.B. Kimmel, *Organization of hindbrain segments in the zebrafish embryo.* Neuron, 1990. **4**(5): p. 669-79.
78. Miguez, A., et al., *Opposing roles for Hoxa2 and Hoxb2 in hindbrain oligodendrocyte patterning.* J Neurosci, 2012. **32**(48): p. 17172-85.
79. Eickholt, B.J., et al., *Rhombomere interactions control the segmental differentiation of hindbrain neurons.* Mol Cell Neurosci, 2001. **18**(2): p. 141-8.
80. Meinhardt, H., *Cell determination boundaries as organizing regions for secondary embryonic fields.* Dev Biol, 1983. **96**(2): p. 375-85.
81. Guthrie, S., M. Butcher, and A. Lumsden, *Patterns of cell division and interkinetic nuclear migration in the chick embryo hindbrain.* J Neurobiol, 1991. **22**(7): p. 742-54.
82. O'Brochta, D.A. and P.J. Bryant, *A zone of non-proliferating cells at a lineage restriction boundary in Drosophila.* Nature, 1985. **313**(5998): p. 138-41.
83. Amoyel, M., et al., *Wnt1 regulates neurogenesis and mediates lateral inhibition of boundary cell specification in the zebrafish hindbrain.* Development, 2005. **132**(4): p. 775-85.
84. Shimizu, T., et al., *Stabilized beta-catenin functions through TCF/LEF proteins and the Notch/RBP-Jkappa complex to promote proliferation and suppress differentiation of neural precursor cells.* Mol Cell Biol, 2008. **28**(24): p. 7427-41.
85. Hagenlocher, C., et al., *Ciliogenesis and cerebrospinal fluid flow in the developing Xenopus brain are regulated by foxj1.* Cilia, 2013. **2**(1): p. 12.
86. Heyman, I., A. Faissner, and A. Lumsden, *Cell and matrix specialisations of rhombomere boundaries.* Dev Dyn, 1995. **204**(3): p. 301-15.
87. Heyman, I., A. Kent, and A. Lumsden, *Cellular morphology and extracellular space at rhombomere boundaries in the chick embryo hindbrain.* Dev Dyn, 1993. **198**(4): p. 241-53.
88. Martinez, S., et al., *Reduced junctional permeability at interrhombomeric boundaries.* Development, 1992. **116**(4): p. 1069-76.
89. Martinez, S., et al., *Induction of ectopic engrailed expression and fate change in avian rhombomeres: intersegmental boundaries as barriers.* Mech Dev, 1995. **51**(2-3): p. 289-303.
90. Cook, M., et al., *Expression of the zinc-finger gene PLZF at rhombomere boundaries in the vertebrate hindbrain.* Proc Natl Acad Sci U S A, 1995. **92**(6): p. 2249-53.
91. Yoshida, M. and D.R. Colman, *Glial-defined rhombomere boundaries in developing Xenopus hindbrain.* J Comp Neurol, 2000. **424**(1): p. 47-57.
92. Peretz, Y., et al., *A new role of hindbrain boundaries as pools of neural stem/progenitor cells regulated by Sox2.* BMC Biol, 2016. **14**: p. 57.
93. Nittenberg, R., et al., *Cell movements, neuronal organisation and gene expression in hindbrains lacking morphological boundaries.* Development, 1997. **124**(12): p. 2297-306.
94. Johnston, S.H., et al., *A family of mammalian Fringe genes implicated in boundary determination and the Notch pathway.* Development, 1997. **124**(11): p. 2245-54.

95. Cheng, Y.C., et al., *Notch activation regulates the segregation and differentiation of rhombomere boundary cells in the zebrafish hindbrain.* Dev Cell, 2004. **6**(4): p. 539-50.
96. Sakamoto, K., et al., *Intracellular cell-autonomous association of Notch and its ligands: a novel mechanism of Notch signal modification.* Dev Biol, 2002. **241**(2): p. 313-26.
97. LeBon, L., et al., *Fringe proteins modulate Notch-ligand cis and trans interactions to specify signaling states.* Elife, 2014. **3**: p. e02950.
98. Bingham, S., et al., *Neurogenic phenotype of mind bomb mutants leads to severe patterning defects in the zebrafish hindbrain.* Dev Dyn, 2003. **228**(3): p. 451-63.
99. Qiu, X., et al., *Temporal Notch activation through Notch1a and Notch3 is required for maintaining zebrafish rhombomere boundaries.* Dev Genes Evol, 2009. **219**(7): p. 339-51.
100. Nikolaou, N., et al., *Lunatic fringe promotes the lateral inhibition of neurogenesis.* Development, 2009. **136**(15): p. 2523-33.
101. Bonev, B., P. Stanley, and N. Papalopulu, *MicroRNA-9 Modulates Hes1 ultradian oscillations by forming a double-negative feedback loop.* Cell Rep, 2012. **2**(1): p. 10-8.
102. Shimojo, H., T. Ohtsuka, and R. Kageyama, *Oscillations in notch signaling regulate maintenance of neural progenitors.* Neuron, 2008. **58**(1): p. 52-64.
103. Baek, J.H., et al., *Persistent and high levels of Hes1 expression regulate boundary formation in the developing central nervous system.* Development, 2006. **133**(13): p. 2467-76.
104. Dorsky, R.I., et al., *Two tcf3 genes cooperate to pattern the zebrafish brain.* Development, 2003. **130**(9): p. 1937-47.
105. Gerety, S.S. and D.G. Wilkinson, *Morpholino artifacts provide pitfalls and reveal a novel role for pro-apoptotic genes in hindbrain boundary development.* Dev Biol, 2011. **350**(2): p. 279-89.
106. Riley, B.B., et al., *Rhombomere boundaries are Wnt signaling centers that regulate metameric patterning in the zebrafish hindbrain.* Dev Dyn, 2004. **231**(2): p. 278-91.
107. Troost, T. and T. Klein, *Sequential Notch signalling at the boundary of fringe expressing and non-expressing cells.* PLoS One, 2012. **7**(11): p. e49007.
108. Irvine, K.D. and C. Rauskolb, *Boundaries in development: formation and function.* Annu Rev Cell Dev Biol, 2001. **17**: p. 189-214.
109. Mahmood, R., et al., *Multiple roles for FGF-3 during cranial neural development in the chicken.* Development, 1995. **121**(5): p. 1399-410.
110. Weisinger, K., et al., *Expression of hindbrain boundary markers is regulated by FGF3.* Biol Open, 2012. **1**(2): p. 67-74.
111. Sela-Donenfeld, D., G. Kayam, and D.G. Wilkinson, *Boundary cells regulate a switch in the expression of FGF3 in hindbrain rhombomeres.* BMC Dev Biol, 2009. **9**: p. 16.
112. Gonzalez-Quevedo, R., et al., *Neuronal regulation of the spatial patterning of neurogenesis.* Dev Cell, 2010. **18**(1): p. 136-47.
113. Lightman, E.G., M.R. Harrison, and V.T. Cunliffe, *Opposing actions of histone deacetylase 1 and Notch signalling restrict expression of erm and fgf20a to hindbrain rhombomere centres during zebrafish neurogenesis.* Int J Dev Biol, 2011. **55**(6): p. 597-602.
114. Terriente, J., et al., *Signalling from hindbrain boundaries regulates neuronal clustering that patterns neurogenesis.* Development, 2012. **139**(16): p. 2978-87.
115. Esain, V., et al., *FGF-receptor signalling controls neural cell diversity in the zebrafish hindbrain by regulating olig2 and sox9.* Development, 2010. **137**(1): p. 33-42.

CHAPTER 3

MEDULLOBLASTOMA

3.1 INTRODUCTION

Medulloblastoma (MB) is the most common malignant brain tumor in children with an annual incidence of ten children per million [1-3]. It is a highly aggressive, undifferentiated tumor and it is always located in the posterior cranial fossa, which includes the cerebellum, brainstem and IVth ventricle (Figure 3.1). The cerebellum arises from dorsal rhombomere 1 (r1), anterior in the hindbrain [4]. Patients present with symptoms of cerebellar dysfunction, including balance problems and incoordination of movements, and also often with hydrocephalus [5].

Treatment protocols are aggressive and aspecific and include optimal surgical removal with adjuvant craniospinal radiation- and chemotherapy [5, 6]. Response to therapy and overall survival are variable, but the current treatment protocol results in overall 5-year survival rates around 70% [2, 3, 6, 7]. However, treatment has detrimental effects on the intellect of treated children [8, 9]. A large proportion of survivors suffer from therapy-induced side effects including neurocognitive, endocrinological and developmental disorders [10]. Furthermore, in the long term, there is a significant risk for disease recurrence and development of treatment-related secondary malignancies [2, 3, 11]. As longterm survival rates have significantly improved, a new focus is needed on how to minimize treatment-related toxicity [12].

For a long time, patient stratification schemes were based on age at diagnosis, remaining tumor after resection and leptomeningeal dissemination. However, prognosis differed greatly between patients with similar characteristics according to these criteria [1, 3]. In an attempt to find a better correlation between MB characteristics and prognosis, differential histology of MBs was taken into account [3]. Two thirds of the cases display classic histology with undifferentiated, blue, round or oval cells and

often presence of Homer Wright rosettes (Figure 3.1). Besides this classic histology, 3 variants exist: desmoplastic-nodular, large cell-anaplastic and MB with extensive nodularity [2, 3, 6]. Desmoplastic histology indicates good prognosis, while large cell-anaplastic MB correlates with poor prognosis [13]. In 2010 large scale genomics and transcriptomics efforts from several research groups have identified four MB subtypes based on the molecular alterations underlying tumor formation: Wnt-type MB, Shh-type MB, group 3 (g3) and group 4 (g4) (Figure 3.1) [1, 3, 14-16]. Moreover, this subdivision based on genetic signatures correlates well with prognosis. Wnt-type MB show the best prognosis with cure rates of over 90%, while g3 MB show the worst prognosis with cure rates of only 40-60% [2, 16]. However, due to the retrospective nature of the subgroup allocation studies this may also reflect sensitivity to the current nonspecific treatment scheme [3].

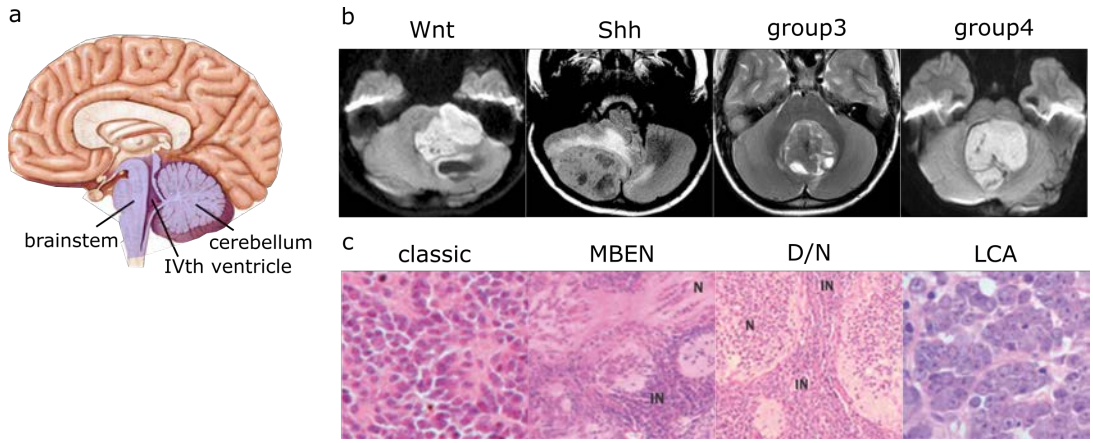

Figure 3.1 Localization and histology of medulloblastoma. (a) Sagittal section through the human brain. The posterior fossa is colored in blue and contains the brainstem, cerebellum and fourth ventricle. (b) MRI images showing localization of the different molecular medulloblastoma subtypes in the posterior fossa. (c) Haematoxylin/eosin staining of medulloblastoma samples showing different histology subtypes. Medulloblastoma is a small, blue round cell tumor and the majority of cases show classic histology. Other possible histological subtypes are medulloblastoma with extensive nodularity (MBEN), desmoplastic/ nodular medulloblastoma (D/N) and large cell/anaplastic medulloblastoma (LCA). (b adapted from Raybaud et al., 2015 [17]; c adapted from Gajjar et al., 2014 [18])

3.2 Demographic and genetic landscape of medulloblastoma subtypes

The subtypes display significant differences in the age of onset and male-to-female ratios as illustrated in Figure 3.2 [1, 3]. Since the identification of the four subtypes, studies have focused on further characterization of their genetic signature. Several additional mutations, copy number variations and chromosomal aberrations associated with specific subtypes have been identified [19-23]. Wnt-type MB are characterized by constitutive activation of the Wnt pathway, nuclear β-catenin accumulation and express several known Wnt target genes (*WIF1, DKK1, DKK2*) [1, 3]. Shh-type MB show hyperactivation of the Shh pathway [1, 3]. G3 and g4 MB are characterized by *MYC* and *MYCN* amplifications, respectively [23]. A molecular pathway underlying g3 and g4 MB has not been identified, but they often carry mutations in genes that regulate histone methylation, for example *KDM6A, EZH2, CHD7* and *ZMYM3,* conferring a stem-like epigenetic status to these tumors [3, 21, 24]. Furthermore, copy number aberrations of and mutations in genes encoding histone-modifying proteins seem to be a common feature of all MB subgroups [13, 25]. Recently, it has been suggested that TGFβ signaling might be driving g3 MB and that g4 MB is linked to NF-κB signaling [20, 23]. Also structural variations leading to *DDX3* enhancer hijacking by *GFI1* or *GFI1B* are specifically linked to g3 and g4 MB. Xenotransplants of neural stem cells with combined overexpression of *MYC* and *GFI1/GFI1B* represent the most accurate g3 MB model to date [26]. The

identification of these different subtypes and their molecular background has kick-started the search for targeted therapies, that could greatly diminish treatment-associated morbidity. For Shh-type MB, several small molecules targeting the Shh pathway have shown efficacy both in mice and human [27, 28].

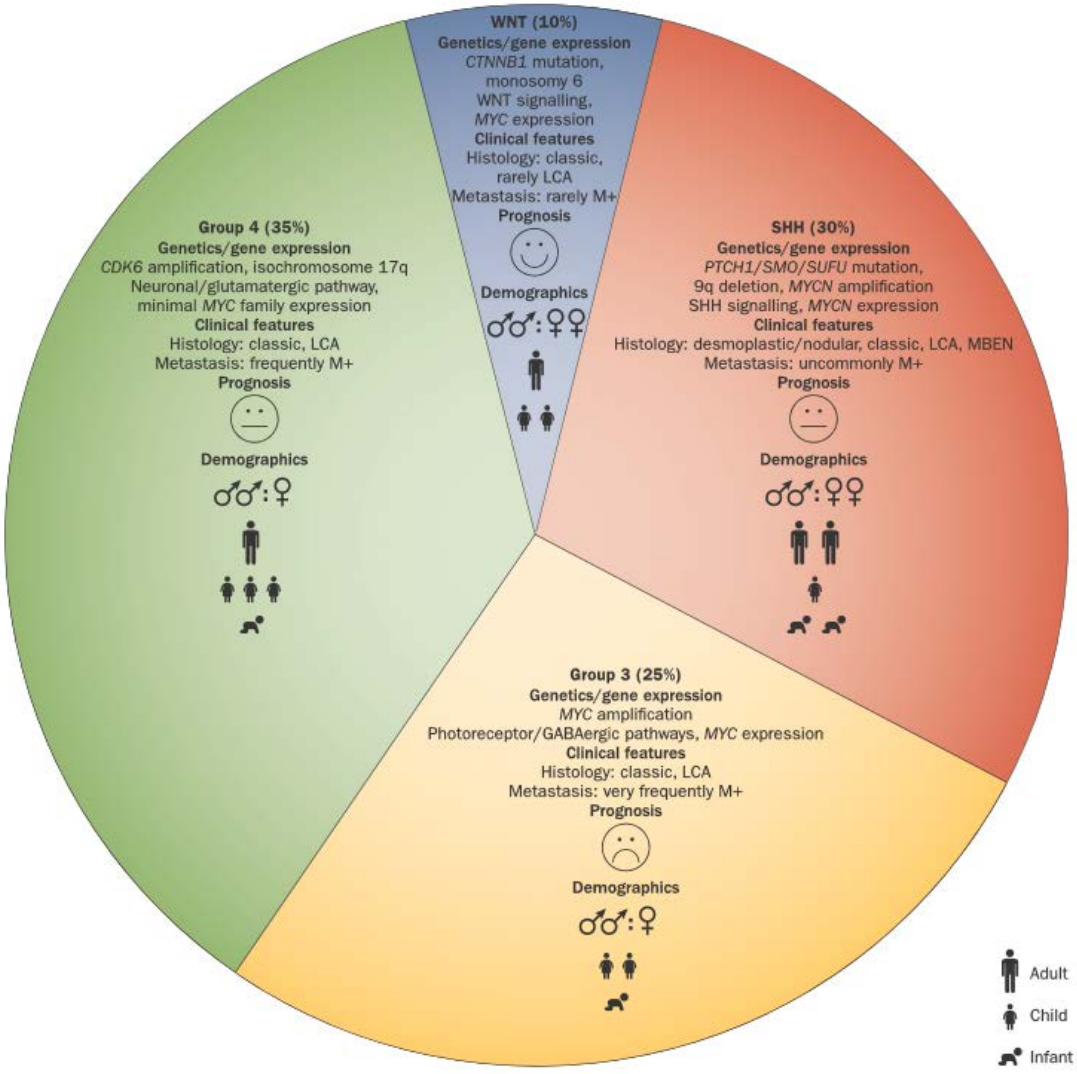

Figure 3.2 Demographic and genetic landscape of medulloblastoma subtypes. Pie chart representing prevalence of different MB subtypes. For each subtypes most common genetic features, histology, prognosis and demographics are listed. LCA, large cell/anaplastic; MBEN, medulloblastoma with extensive nodularity. (Figure reproduced from Northcott et al., 2012 [3])

Even though the identification of the MB subtypes has greatly improved prediction of prognosis for individual patients, within each subgroup heterogeneity in mutational spectrum and clinical outcome still exists. As the power of genomics studies increases, additional driver genes and more detailed molecular processes underlying the different MB subgroups are continuously revealed [29]. Moreover, it has become clear that even within the subtypes, different variants exist [30-33]. One possible explanation is that the same oncogenic event transforms different tumor-initiating cells, indicating that tumor heterogeneity is largely determined by the cell of origin (see also 3.3.3) [30]. Recent efforts have lead to the proposal of further subdivision of the MB subgroups based on clinical risk stratification and distinct biological features [34, 35]. Cavalli et al. describe 12 MB subtypes: two Wnt-type MB, four Shh-type MB, three g3 MB and three g4 MB (Figure 3.3). This refined subdivision

takes into account both gene expression data and DNA methylation profiles. Both sets of data are necessary to robustly identify MB subtypes [35].

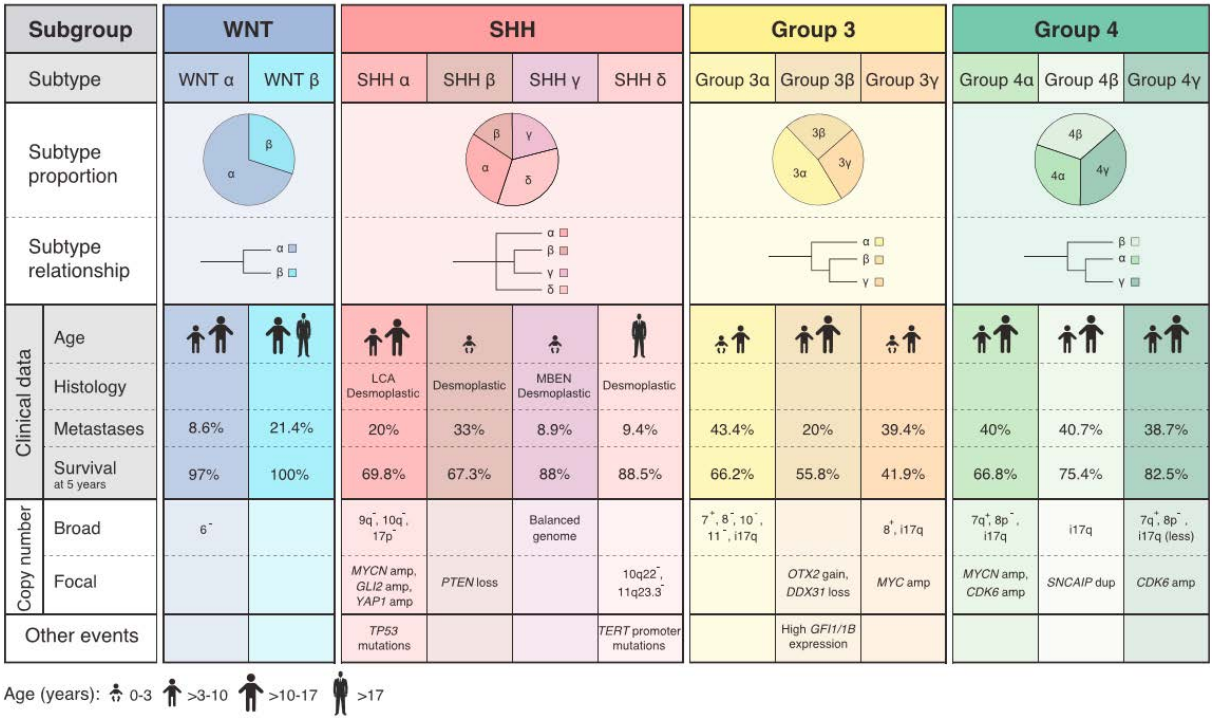

Figure 3.3 12 subtypes of medulloblastoma. Most recent proposal for the subdivision of medulloblastoma based on gene expression and DNA methylation data. Wnt-type MB is divided in two subtypes, Shh-type MB is divided in four subtypes and g3 and g4 MB each count three subtypes. For each subtype prevalence, demographics, clinical presentation, prognosis and most common genetic features are listed. (Figure reproduced from Cavalli et al., 2017 [35]).

3.3 WNT-TYPE MEDULLOBLASTOMA

Wnt-type MB have classic histology, account for 10% of all MB cases and typically occur in older children and adolescents (Figure 3.3) [2, 3]. Metastasis is rare [2, 3].

3.3.1 GENETIC SIGNATURE

Most tumors arise sporadically, although around 5% occurs in the context of an inherited cancer syndrome, FAP, characterized by loss of function mutations in *APC* [2, 5, 36]. However, in sporadic MB *APC* mutations are rare [5, 37]. Instead, oncogenic mutations in *CTNNB1* account for most Wnt-type MB cases [5, 21, 38, 39]. Mutations in *AXIN1* and *CDH1,* which normally sequesters β-catenin at the cell membrane, have also been observed [5, 24, 40]. Next to gene disruptions that lead to constitutive activation of the Wnt pathway multiple other genetic changes are linked to Wnt-type MB. More or less 85% of Wnt-type MB show monosomy 6, but further somatic copy number aberrations are rare (Figure 3.3) [1, 3, 21, 23, 29, 41]. Mutations in the RNA helicase gene *DDX3X* are often concurrent with mutation of *CTNNB1* [19, 21, 24]. Moreover, mutations in *DDX3X* were shown to increase mutant, but not wild type, β-catenin induced transcriptional activation [19]. Furthermore, mutations are found in *PIK3CA, ALK* and several epigenetic regulators, although different from those in g3 and g4, for example *SMARCA4* and *CREBBP* [24, 42]. Variants in *CSNK2B, EPHA7* and subunits of the SWI/SNF nucleosome-remodeling complex (*SMARCA4, ARID1A* and *ARID2*) were also detected in a recent extensive screen combining different next-generation sequencing datasets [29].

3.3.2 *Clinical presentation*

Wnt-type MB has a favorable prognosis with cure rates reaching over 90% [2, 16, 41, 43]. Expression of stabilized β-catenin in a MB cell line revealed that activated Wnt signaling leads to increased differentiation, decreased cell growth and increased sensitivity to irradiation with increased cell death and decreased invasion capability. This indicates that the better prognosis can, at least partly, be attributed to increased response to current treatment [44].

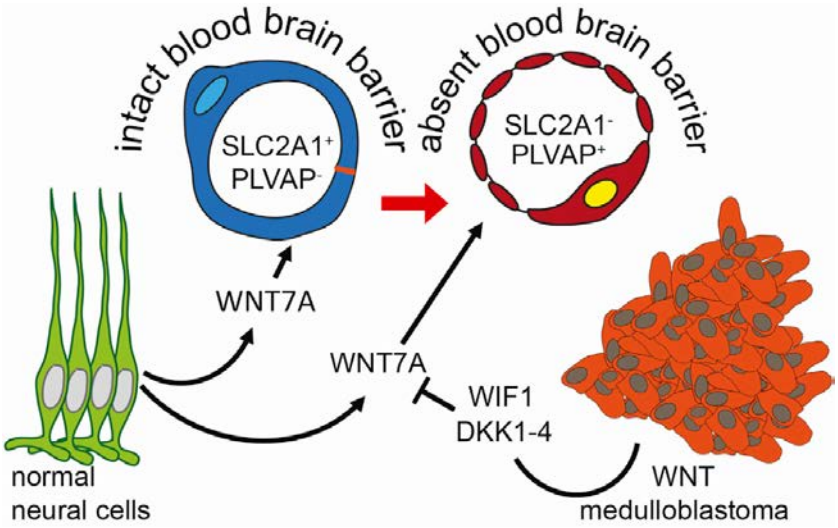

Figure 3.4 Defective blood-brain barrier in Wnt-type medulloblastoma. Normal brain tissue secretes Wnt ligands inducing Wnt signaling activation in brain endothelial cells. Wnt signaling activity induces and maintains blood-brain barrier function of these cells. Wnt-type medulloblastoma produce large amount of Wnt signaling antagonists. Wnt signaling activity is inhibited in surrounding endothelial cells leading to a loss of blood-brain barrier function. Blood vessels lose tight junctions and become fenestrated resulting in increased permeability. (Figure reproduced from Phoenix et al., 2016 [45])

In a mouse model of Wnt-type MB, tumors showed an aberrant vasculature (Figure 3.4) [45]. Recently, this finding was confirmed in human. A patient diagnosed with Wnt-type MB showed abnormal vascularization and hemorrhaging [46]. The vasculature of the CNS is characterized by a tightly sealed endothelium, forming the blood-brain barrier (BBB). The BBB fulfills a critical neuroprotective role by preventing the free passage of molecules from the blood to the brain. Unfortunately, the BBB also blocks the passage of potential therapeutic molecules [47, 48]. Wnt signaling is specifically activated in CNS blood vessels during development through Wnt ligand expression by neural progenitors in the ventricular zone [49]. *Wnt7a/b* double mutant mice display a severe CNS-specific hemorrhaging phenotype, dependent on β-catenin-mediated Wnt signaling activation in the vascular precursors [47, 49]. Also mouse embryos knockout for β-catenin specifically in endothelial cells show a normal vascular pattern in non-neural tissues, but display major vascular defects in the CNS with reduced vessel number, loss of capillary beds and hemorrhagic malformations that remain adjacent to the meningae [49]. In the adult Wnt ligands, secreted by brain tissue, signal to neighboring endothelial cells thereby maintaining the BBB [47, 49, 50]. Wnt signaling also drives expression of the BBB marker glucose transporter 1 (GLUT-1) [47, 49]. The vascular endothelium of Wnt-type MB in mice is positive for PLVAP and negative for SLC2A1, typical for non-CNS endothelial cells. Furthermore, these tumors lack a functional BBB with fenestrated pores, reduced endothelial tight junctions and pericyte coverage and increased permeability (Figure 3.4) [45]. Wnt-type MB produce large amounts of Wnt antagonists, e.g. WIF1 and Dkk1. This leads to inhibition of Wnt signaling in endothelial cells and disrupts the BBB [45]. Moreover, Wnt signaling disruption affects the cerebellum BBB more severely than other brain regions [50]. As a result, in

mouse models, Wnt-type MB were rendered porous for systemic chemotherapies, as opposed to Shh-type MB. Even though *in vitro,* cells from both tumor types are equally sensitive to chemotherapeutics [45]. The observed survival advantage of Wnt-type MB patients can thus, at least in part, be attributed to increased BBB permeability thereby increasing tumor exposure to chemotherapeutics. This opens up new possibilities for the treatment of these tumors with e.g. small-molecule inhibitors and immunotherapy and indicates that disruption of the BBB might be an interesting avenue for treatment of other MB subtypes [48].

Because of its better prognosis a lot of preclinical studies are currently investigating de-escalation of therapy for Wnt-type MB by omission of radiotherapy. However, an important concern is Wnt-induced overexpression of the DNA repair enzyme O6-methylguanine-DNA methyltransferase (MGMT) in several cancers, including MB [51]. MGMT expression is significantly higher in Wnt-type MB compared to all other subtypes and normal cerebellum [51]. Overexpression of MGMT is linked to the development of chemoresistance and Wnt inhibition has been shown to augment efficacy of chemotherapy [51].

3.3.3 Cell of origin

It is now established that the different MB subtypes cannot only be distinguished through different oncogenic events but that these also reflect differential cellular origins [20, 52]. Subgroup identity is maintained in recurrent tumors and in metastasis, indicating distinct cells of origin [52]. However, for g3 MB a recent report shows that the same oncogenic insult can drive this MB subtype in different cerebellar cell lineages [53].

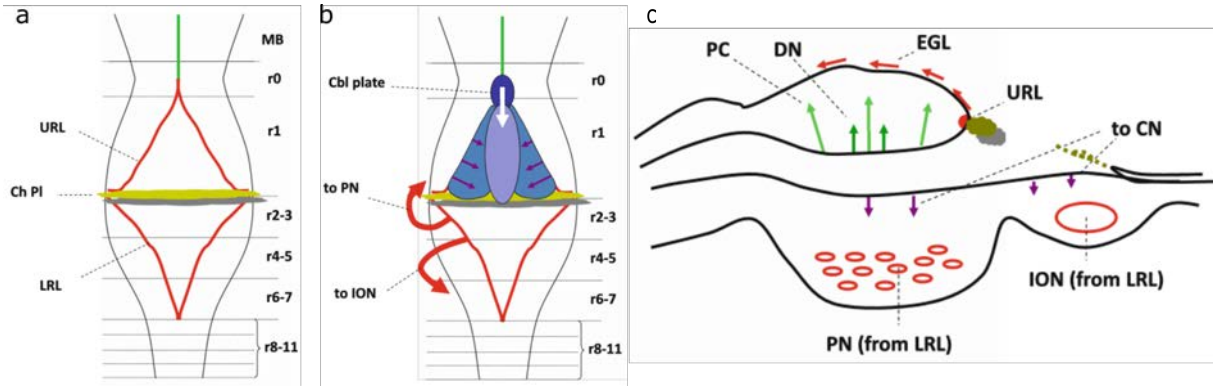

Figure 3.5 Germinal zones during hindbrain development. (a) Dorsal view on the hindbrain. The choroid plexus divides the roof plate of the hindbrain in two halves: r1 on the cranial side and r2-7 on the caudal side. The edges of the roof plate correspond to the upper and lower rhombic lip, respectively. (b) The vermis of the cerebellum (dark blue) develops from the cerebellar plate (white arrow). The cerebellar hemispheres (light blue) develop from the upper rhombic lip (small red arrows). The lower rhombic lip gives rise to the neurons of brainstem nuclei (big red arrows). (c) Sagittal section showing the migration routes of hindbrain neurons: cranial nerve nuclei from the subventricular zone (purple arrows); Purkinje cells and dentate neurons from the cerebellar subventricular zone (green arrows) and granule neuron precursor from the external granular layer migrate from the upper rhombic lip (red arrows). Cbl plate, cerebellar plate; Ch Pl, choroid plexus; CN, cranial nerve nuclei; DN, dentate neurons; EGL, external granular layer; ION, inferior olivary nuclei; LRL, lower rhombic lip; PC, purkinje cell; PN, pontine nuclei; r, rhombomere; URL, upper rhombic lip. (Figure adapted from Raybaud et al., 2015 [17]).

MB is a pediatric tumor and MB cells differentiate along neural and glial fates *in vitro,* indicative of a primitive cell of origin. Hence, a lot of research has been invested in cerebellar development to uncover the molecular mechanism behind MB tumorigenesis [6, 54, 55]. There are two major germinal zones in the embryonic cerebellum: the rhombic lip, giving rise to the granule neurons and other glutamatergic neurons, and the ventricular zone, lining the IVth ventricle and giving rises to all GABA-ergic cerebellar cell types (Figure 3.5) [2, 4, 6, 56]. The granule neurons of the cerebellum are

the most prevalent cell type in the whole brain. Granule neuron precursors (GNPs) undergo massive expansion and differentiation in the external granular layer of the cerebellum, a secondary germinal matrix derived from the rhombic lip [4, 6, 56]. Shh, secreted by the Purkinje cells, serves as a potent mitogen for GNPs [4-6]. GNPs are the cell of origin for Shh-type MB. Moreover, commitment to the granule neuron lineage was shown to be necessary for Shh-induced tumor formation [31, 57]. Originally, GNPs were even considered to be the cell of origin for all MB subtypes [6, 31, 58]. However, Wnt signaling activation does not induce proliferation of GNPs [59]. Moreover, Wnt signaling attenuates GNP proliferation and antagonizes Shh-induced proliferation of GNPs both through the canonical and non-canonical pathways [60, 61]. Constitutive activation of Wnt signaling in GNPs leads to cerebellar hypoplasia due to cell-autonomous inhibition of proliferation and premature differentiation of GNPs [62, 63]. Active Wnt signaling thus does not induce transformation of GNPs, as opposed to Shh signaling [57, 62]. Moreover, activation of Wnt signaling has been shown to have therapeutic potential in Shh-type MB through Shh signaling inhibition [60, 61, 64]. However, a recent report also showed a tumor-promoting role for Wnt signaling in Shh-type MB [65]. The FDA-approved smoothened inhibitor vismodegib was shown to be effective for Shh-type MB treatment in mice. Unfortunately, this initial response is often rapidly followed by recurrence of aggressive MB growth both in mice and human [65]. Recurrence of *tp53* null Shh-type MB in mice was linked to a small population of tumor propagating cells resistant to Shh inhibition, but dependent on active Wnt signaling. Moreover, inhibition of Wnt signaling significantly reduced the amount of these cancer stem cells and decreased tumor burden in graft experiments [65].

Since constitutive Wnt signaling activation is unable to induce transformation of GNPs, the oncogenic potential of Wnt signaling activation in other precursor populations in the cerebellum was investigated. In zebrafish Wnt3 has a positive influence on cerebellar growth during embryonic development [66]. In a cerebellar progenitor cell line, immortalized by stable expression of myc*,* Wnt activation was achieved through stable expression of Wnt1*.* These cells resembled stem cells from the cerebellar ventricular zone, failed to undergo neural differentiation and became tumorigenic [67]. However, it is doubtful that these findings recapitulate the *in vivo* situation. *In vivo* experiments in mice revealed that Wnt signaling can promote proliferation of neural stem cells in the ventricular zone of the cerebellum, although this effect was transient and lead to a concomitant impairment of their potential for self-renewal [59, 61]. Gibson et al. confirmed the differential origins of Shh- and Wnt-type MB (Figure 3.6) [68]. Gene signatures of each MB subtype correlate with different regions of the developing hindbrain. This is also reflected by the differential localization of both tumor types with Wnt-type MB located in the IVth ventricle and infiltrating the dorsal brainstem and Shh-type MB located in the cerebellar hemispheres [68, 69]. Furthermore, mutations in *DDX3X,* which are common in Wnt-type MB, were shown to increase proliferation of progenitors in the lower rhombic lip, giving rise to the future dorsal brain stem [24]. Gibson et al. also generated the first mouse model for Wnt-type MB. These mice carry a Cre-dependent allele encoding stabilized β-catenin, together with homozygous loss of the tumor suppressor *Tp53,* that is activated specifically in progenitor populations of the hindbrain (*Blbp-Cre*$^{+/-}$*;Ctnnb1*$^{+/lox(ex3)}$*;Tp53*$^{flx/flx}$). 15% of these mice developed MB after 500 days and these tumors were always connected to the brainstem. Mice with intact Tp53 function only showed aberrant cell collection in the dorsal brainstem, expressing markers of post mitotic mossy-fibre neurons indicating disrupted migration of these cells, but no tumors were observed [68]. *Tp53* mutations are common in Wnt-type MB, but are not associated with worse prognosis [19, 70, 71]. *Tp53* loss of function has also been shown to increase incidence and reduce latency in a mouse model of Shh-type MB [72]. Importantly, even though *Tp53* loss accelerated

tumor formation, it was not required for tumorigenesis itself. Most likely the increased genomic instability associated with *Tp53* loss synergizes with the oncogenic mutation in *Ptch1* - encoding patched1, the Shh receptor - to increase tumor incidence [72]. Tumor incidence in the Wnt-type MB model was further increased by additional mutation of *Pik3ca* (*Blbp-Cre*$^{+/-}$*;Ctnnb1*$^{+/lox(ex3)}$*;Tp53*$^{flx/+}$*;Pik3ca*^{E545K}) to 100% by 3 months. Activation of the AKT pathway downstream of mutated *Pik3ca* promotes tumor progression, rather than Wnt-type MB initiation [24].

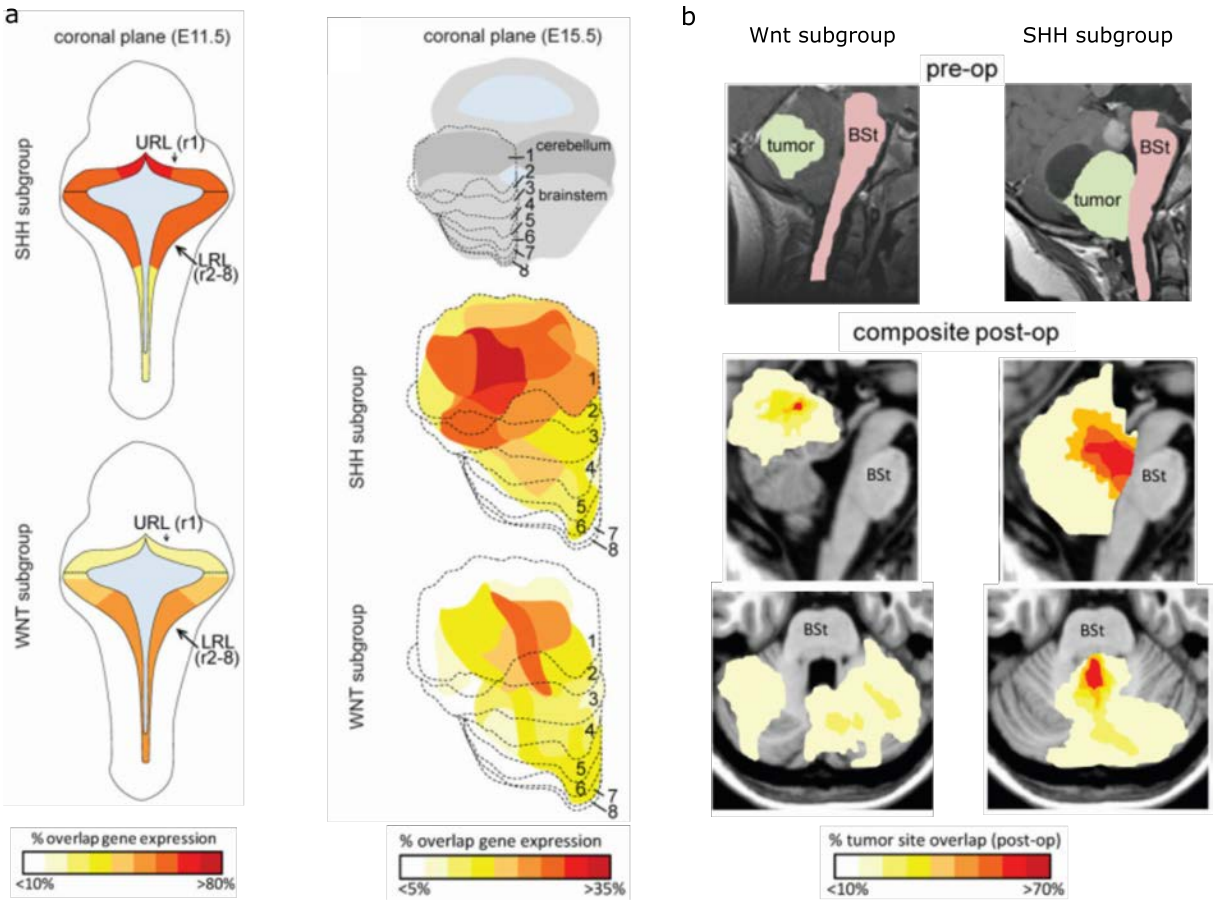

Figure 3.6 Different cell of origin for Wnt-type and Shh-type medulloblastoma. (a) Dorsal view on the mouse hindbrain at embryonic day 11.5 and 15.5. Expression distribution of genes characteristic for Wnt-type and Shh-type medulloblastoma is shown. Numbers in the right panel indicate the rhombomeric origin of the different regions of the brainstem and cerebellum. (b) MRI images showing localization of Wnt-type and Shh-type medulloblastoma. Top panel shows pre-operation images of exemplary Wnt-type and Shh-type medulloblastoma. Lower panel shows heat map representing localization of each tumor type based on cavities after surgical resection (n=6 for each subtype). BSt, brainstem; LRL, lower rhombic lip; URL, upper rhombic lip. (Figure adapted from Gibson et al., 2010 [68])

3.4 Summary

Current treatment protocols for MB are aspecific and aggressive. Even though overall survival rates are around 70%, chemo- and radiotherapy applied to the immature brain severely affects quality of life through neurocognitive impairment. In recent years, knowledge about the etiology and molecular features of MB has increased tremendously. This has instigated the search for translation of this newly acquired knowledge to the adjustment of treatment protocols for the different MB subtypes. Especially molecular targeted therapies could greatly improve clinical outcome.

3.5 REFERENCES

1. Northcott, P.A., et al., *Medulloblastoma comprises four distinct molecular variants.* J Clin Oncol, 2011. **29**(11): p. 1408-14.
2. Coluccia, D., et al., *Medulloblastoma: Tumor Biology and Relevance to Treatment and Prognosis Paradigm.* Curr Neurol Neurosci Rep, 2016. **16**(5): p. 43.
3. Northcott, P.A., et al., *The clinical implications of medulloblastoma subgroups.* Nat Rev Neurol, 2012. **8**(6): p. 340-51.
4. Millen, K.J. and J.G. Gleeson, *Cerebellar development and disease.* Curr Opin Neurobiol, 2008. **18**(1): p. 12-9.
5. Raffel, C., *Medulloblastoma: molecular genetics and animal models.* Neoplasia, 2004. **6**(4): p. 310-22.
6. Roussel, M.F. and M.E. Hatten, *Cerebellum development and medulloblastoma.* Curr Top Dev Biol, 2011. **94**: p. 235-82.
7. Gajjar, A., et al., *Risk-adapted craniospinal radiotherapy followed by high-dose chemotherapy and stem-cell rescue in children with newly diagnosed medulloblastoma (St Jude Medulloblastoma-96): long-term results from a prospective, multicentre trial.* Lancet Oncol, 2006. **7**(10): p. 813-20.
8. Mulhern, R.K., et al., *Neurocognitive consequences of risk-adapted therapy for childhood medulloblastoma.* J Clin Oncol, 2005. **23**(24): p. 5511-9.
9. Moxon-Emre, I., et al., *Intellectual Outcome in Molecular Subgroups of Medulloblastoma.* J Clin Oncol, 2016. **34**(34): p. 4161-4170.
10. Uday, S., et al., *Endocrine sequelae beyond 10 years in survivors of medulloblastoma.* Clin Endocrinol (Oxf), 2015. **83**(5): p. 663-70.
11. Ning, M.S., et al., *Evidence of high mortality in long term survivors of childhood medulloblastoma.* J Neurooncol, 2015. **122**(2): p. 321-7.
12. Weil, A.G., et al., *Survival in pediatric medulloblastoma: a population-based observational study to improve prognostication.* J Neurooncol, 2017. **132**(1): p. 99-107.
13. Northcott, P.A., et al., *Molecular subgroups of medulloblastoma.* Expert Rev Neurother, 2012. **12**(7): p. 871-84.
14. Thompson, M.C., et al., *Genomics identifies medulloblastoma subgroups that are enriched for specific genetic alterations.* J Clin Oncol, 2006. **24**(12): p. 1924-31.
15. Kool, M., et al., *Integrated genomics identifies five medulloblastoma subtypes with distinct genetic profiles, pathway signatures and clinicopathological features.* PLoS One, 2008. **3**(8): p. e3088.
16. Cho, Y.J., et al., *Integrative genomic analysis of medulloblastoma identifies a molecular subgroup that drives poor clinical outcome.* J Clin Oncol, 2011. **29**(11): p. 1424-30.
17. Raybaud, C., et al., *Posterior fossa tumors in children: developmental anatomy and diagnostic imaging.* Childs Nerv Syst, 2015. **31**(10): p. 1661-76.
18. Gajjar, A.J. and G.W. Robinson, *Medulloblastoma-translating discoveries from the bench to the bedside.* Nat Rev Clin Oncol, 2014. **11**(12): p. 714-22.
19. Pugh, T.J., et al., *Medulloblastoma exome sequencing uncovers subtype-specific somatic mutations.* Nature, 2012. **488**(7409): p. 106-10.
20. Lin, C.Y., et al., *Active medulloblastoma enhancers reveal subgroup-specific cellular origins.* Nature, 2016. **530**(7588): p. 57-62.
21. Jones, D.T., et al., *Dissecting the genomic complexity underlying medulloblastoma.* Nature, 2012. **488**(7409): p. 100-5.
22. Northcott, P.A., et al., *Medulloblastomics: the end of the beginning.* Nat Rev Cancer, 2012. **12**(12): p. 818-34.
23. Northcott, P.A., et al., *Subgroup-specific structural variation across 1,000 medulloblastoma genomes.* Nature, 2012. **488**(7409): p. 49-56.

24. Robinson, G., et al., *Novel mutations target distinct subgroups of medulloblastoma.* Nature, 2012. **488**(7409): p. 43-8.
25. Jones, D.T., et al., *The role of chromatin remodeling in medulloblastoma.* Brain Pathol, 2013. **23**(2): p. 193-9.
26. Deibert, C.P., B.M. Zussman, and J.A. Engh, *A novel mechanism of oncogenesis in type 3 and 4 medulloblastomas.* Neurosurgery, 2014. **75**(6): p. N16-7.
27. Romer, J.T., et al., *Suppression of the Shh pathway using a small molecule inhibitor eliminates medulloblastoma in Ptc1(+/-)p53(-/-) mice.* Cancer Cell, 2004. **6**(3): p. 229-40.
28. Rudin, C.M., et al., *Treatment of medulloblastoma with hedgehog pathway inhibitor GDC-0449.* N Engl J Med, 2009. **361**(12): p. 1173-8.
29. Northcott, P.A., et al., *The whole-genome landscape of medulloblastoma subtypes.* Nature, 2017. **547**(7663): p. 311-317.
30. Chow, K.H., et al., *Epigenetic states of cells of origin and tumor evolution drive tumor-initiating cell phenotype and tumor heterogeneity.* Cancer Res, 2014. **74**(17): p. 4864-74.
31. Yang, Z.J., et al., *Medulloblastoma can be initiated by deletion of Patched in lineage-restricted progenitors or stem cells.* Cancer Cell, 2008. **14**(2): p. 135-45.
32. Taylor, M.D., et al., *Molecular subgroups of medulloblastoma: the current consensus.* Acta Neuropathol, 2012. **123**(4): p. 465-72.
33. Northcott, P.A., et al., *Pediatric and adult sonic hedgehog medulloblastomas are clinically and molecularly distinct.* Acta Neuropathol, 2011. **122**(2): p. 231-40.
34. Schwalbe, E.C., et al., *Novel molecular subgroups for clinical classification and outcome prediction in childhood medulloblastoma: a cohort study.* Lancet Oncol, 2017. **18**(7): p. 958-971.
35. Cavalli, F.M.G., et al., *Intertumoral Heterogeneity within Medulloblastoma Subgroups.* Cancer Cell, 2017. **31**(6): p. 737-754 e6.
36. Hamilton, S.R., et al., *The molecular basis of Turcot's syndrome.* N Engl J Med, 1995. **332**(13): p. 839-47.
37. Huang, H., et al., *APC mutations in sporadic medulloblastomas.* Am J Pathol, 2000. **156**(2): p. 433-7.
38. Eberhart, C.G., T. Tihan, and P.C. Burger, *Nuclear localization and mutation of beta-catenin in medulloblastomas.* J Neuropathol Exp Neurol, 2000. **59**(4): p. 333-7.
39. Zurawel, R.H., et al., *Sporadic medulloblastomas contain oncogenic beta-catenin mutations.* Cancer Res, 1998. **58**(5): p. 896-9.
40. Baeza, N., et al., *AXIN1 mutations but not deletions in cerebellar medulloblastomas.* Oncogene, 2003. **22**(4): p. 632-6.
41. Clifford, S.C., et al., *Wnt/Wingless pathway activation and chromosome 6 loss characterize a distinct molecular sub-group of medulloblastomas associated with a favorable prognosis.* Cell Cycle, 2006. **5**(22): p. 2666-70.
42. Trubicka, J., et al., *Identification of a novel inherited ALK variant M1199L in the WNT type of medulloblastoma.* Folia Neuropathol, 2016. **54**(1): p. 23-30.
43. Ellison, D.W., et al., *beta-Catenin status predicts a favorable outcome in childhood medulloblastoma: the United Kingdom Children's Cancer Study Group Brain Tumour Committee.* J Clin Oncol, 2005. **23**(31): p. 7951-7.
44. Salaroli, R., et al., *Wnt activation affects proliferation, invasiveness and radiosensitivity in medulloblastoma.* J Neurooncol, 2015. **121**(1): p. 119-27.
45. Phoenix, T.N., et al., *Medulloblastoma Genotype Dictates Blood Brain Barrier Phenotype.* Cancer Cell, 2016. **29**(4): p. 508-22.
46. Di Giannatale, A., et al., *Anomalous vascularization in a Wnt medulloblastoma: a case report.* BMC Neurol, 2016. **16**: p. 103.
47. Stenman, J.M., et al., *Canonical Wnt signaling regulates organ-specific assembly and differentiation of CNS vasculature.* Science, 2008. **322**(5905): p. 1247-50.

48. Parrish, K.E., J.N. Sarkaria, and W.F. Elmquist, *Improving drug delivery to primary and metastatic brain tumors: strategies to overcome the blood-brain barrier.* Clin Pharmacol Ther, 2015. **97**(4): p. 336-46.
49. Daneman, R., et al., *Wnt/beta-catenin signaling is required for CNS, but not non-CNS, angiogenesis.* Proc Natl Acad Sci U S A, 2009. **106**(2): p. 641-6.
50. Zhou, Y., et al., *Canonical WNT signaling components in vascular development and barrier formation.* J Clin Invest, 2014. **124**(9): p. 3825-46.
51. Wickstrom, M., et al., *Wnt/beta-catenin pathway regulates MGMT gene expression in cancer and inhibition of Wnt signalling prevents chemoresistance.* Nat Commun, 2015. **6**: p. 8904.
52. Wang, X., et al., *Medulloblastoma subgroups remain stable across primary and metastatic compartments.* Acta Neuropathol, 2015. **129**(3): p. 449-57.
53. Kawauchi, D., et al., *Novel MYC-driven medulloblastoma models from multiple embryonic cerebellar cells.* Oncogene, 2017.
54. Hatten, M.E. and M.F. Roussel, *Development and cancer of the cerebellum.* Trends Neurosci, 2011. **34**(3): p. 134-42.
55. Gilbertson, R.J. and D.W. Ellison, *The origins of medulloblastoma subtypes.* Annu Rev Pathol, 2008. **3**: p. 341-65.
56. Goldowitz, D. and K. Hamre, *The cells and molecules that make a cerebellum.* Trends Neurosci, 1998. **21**(9): p. 375-82.
57. Schuller, U., et al., *Acquisition of granule neuron precursor identity is a critical determinant of progenitor cell competence to form Shh-induced medulloblastoma.* Cancer Cell, 2008. **14**(2): p. 123-34.
58. Marino, S., *Medulloblastoma: developmental mechanisms out of control.* Trends Mol Med, 2005. **11**(1): p. 17-22.
59. Pei, Y., et al., *WNT signaling increases proliferation and impairs differentiation of stem cells in the developing cerebellum.* Development, 2012. **139**(10): p. 1724-33.
60. Anne, S.L., et al., *WNT3 inhibits cerebellar granule neuron progenitor proliferation and medulloblastoma formation via MAPK activation.* PLoS One, 2013. **8**(11): p. e81769.
61. Poschl, J., et al., *Wnt/beta-catenin signaling inhibits the Shh pathway and impairs tumor growth in Shh-dependent medulloblastoma.* Acta Neuropathol, 2014. **127**(4): p. 605-7.
62. Lorenz, A., et al., *Severe alterations of cerebellar cortical development after constitutive activation of Wnt signaling in granule neuron precursors.* Mol Cell Biol, 2011. **31**(16): p. 3326-38.
63. Poschl, J., et al., *Constitutive activation of beta-catenin in neural progenitors results in disrupted proliferation and migration of neurons within the central nervous system.* Dev Biol, 2013. **374**(2): p. 319-32.
64. Zinke, J., et al., *beta-Catenin-Gli1 interaction regulates proliferation and tumor growth in medulloblastoma.* Mol Cancer, 2015. **14**: p. 17.
65. Rodriguez-Blanco, J., et al., *Inhibition of WNT signaling attenuates self-renewal of SHH-subgroup medulloblastoma.* Oncogene, 2017.
66. Teh, C., et al., *Modulating the expression level of secreted Wnt3 influences cerebellum development in zebrafish transgenics.* Development, 2015. **142**(21): p. 3721-33.
67. Rogers, H.A., et al., *WNT/beta-catenin pathway activation in Myc immortalised cerebellar progenitor cells inhibits neuronal differentiation and generates tumours resembling medulloblastoma.* Br J Cancer, 2012. **107**(7): p. 1144-52.
68. Gibson, P., et al., *Subtypes of medulloblastoma have distinct developmental origins.* Nature, 2010. **468**(7327): p. 1095-9.
69. Patay, Z., et al., *MR Imaging Characteristics of Wingless-Type-Subgroup Pediatric Medulloblastoma.* AJNR Am J Neuroradiol, 2015. **36**(12): p. 2386-93.
70. Zhukova, N., et al., *Subgroup-specific prognostic implications of TP53 mutation in medulloblastoma.* J Clin Oncol, 2013. **31**(23): p. 2927-35.

71. Pfaff, E., et al., *TP53 mutation is frequently associated with CTNNB1 mutation or MYCN amplification and is compatible with long-term survival in medulloblastoma.* J Clin Oncol, 2010. **28**(35): p. 5188-96.
72. Wetmore, C., D.E. Eberhart, and T. Curran, *Loss of p53 but not ARF accelerates medulloblastoma in mice heterozygous for patched.* Cancer Res, 2001. **61**(2): p. 513-6.

CHAPTER 4

CRISPR/CAS9

4.1 INTRODUCTION

While zinc fingers and transcription activator-like effector nucleases (TALENs) enabled targeted genome editing, there remain some important drawbacks to these systems. Clustered regularly interspaced short palindromic repeats (CRISPR)/CRISPR-associated (Cas) 9 provides easy-to-engineer precision genome engineering at a lower cost, reaching similar or higher mutagenesis efficiencies [1, 2]. Using the CRISPR/Cas9 system, mutagenesis can be directed to diverse genomic loci by simply exchanging the used guide RNA (gRNA) while the Cas9 endonuclease remains constant. Generation of gRNAs is fast, taking only 1-2 days and does not require cloning [3, 4]. Furthermore multiplexing is straightforward by the simultaneous application of multiple sgRNAs [1, 5-7]. This way, also larger deletions or inversions can be achieved [8]. CRISPR/Cas9 has been successfully applied in a number of organisms, including zebrafish, mouse, *Caenorhabditis elegans, Xenopus* and human cell lines [2, 5-7, 9-11].

4.2 THE ORIGINAL CRISPR/CAS9 SYSTEM

CRISPR/Cas9 is an adaptation of the prokaryotic CRISPR adaptive immune system that protects organisms from invading viruses and plasmids (Figure 4.1). Small RNAs are used to recognize and silence specific foreign nucleic acids. Upon a first challenge, bacteria and archaea integrate short fragments of foreign sequence (protospacer) into their own genome between short CRISPR repeat sequences in CRISPR arrays (spacer). The repeat-spacer element is transcribed into precursor CRISPR RNA (pre-crRNA), followed by enzymatic digestion generating a short crRNA that will recognize its

complementary protospacer sequence upon reinvasion of the viruses or plasmids [12, 13]. Cas proteins are recruited to the complex and will silence the foreign sequences [13].

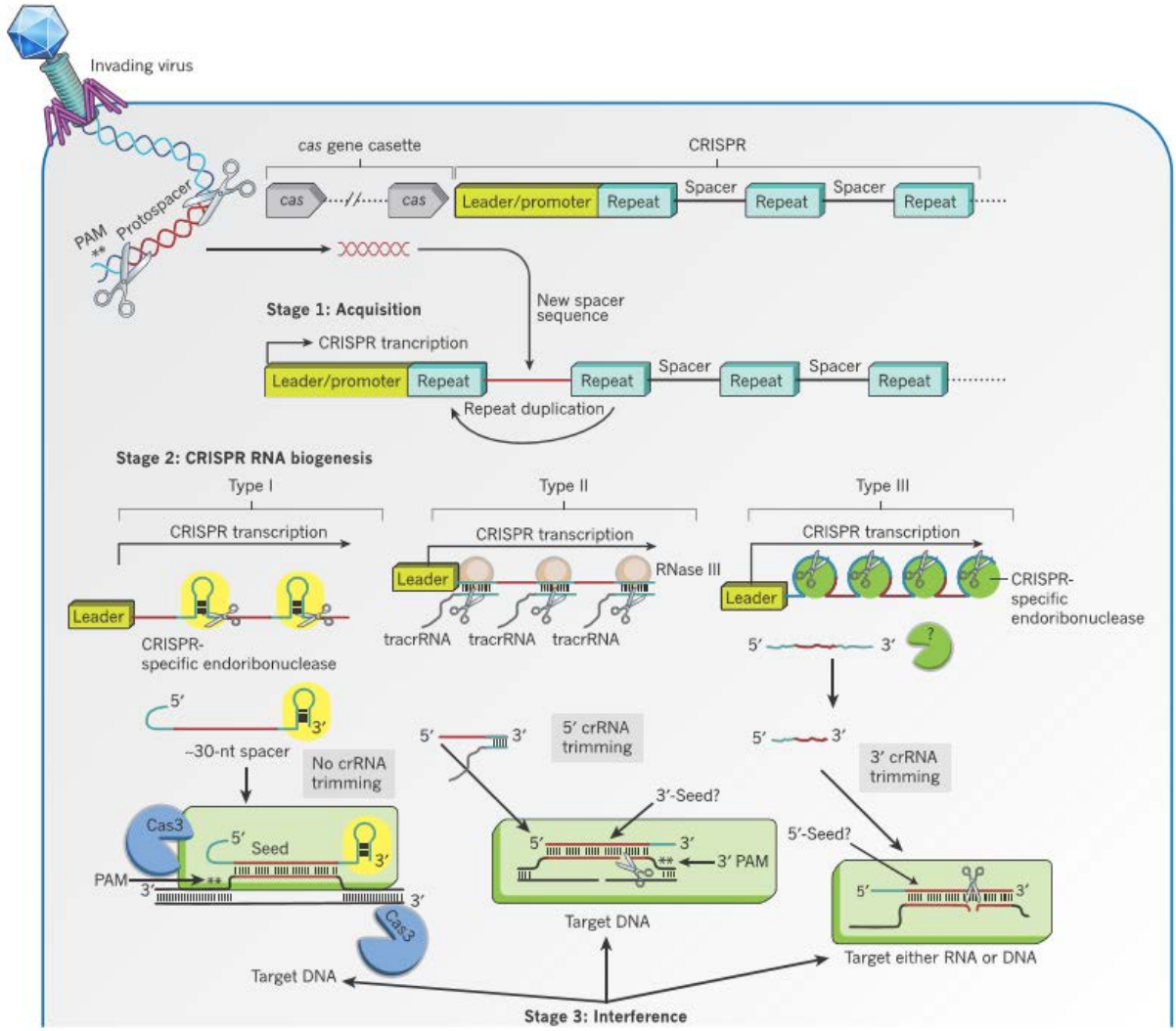

Figure 4.1 The bacterial CRISPR/Cas9 system. The CRISPR locus consists of a series of repeats separated by unique spacer sequences acquired from invading genetic elements (stage 1). Long CRISPR transcripts are processed in to short crRNA by different mechanisms according to the bacterial CRISPR system. In type II systems complementary base pairing with the trans-activating RNA induces cleavage by the ribonuclease RNAseIII. The mature crRNA associates with Cas protein(s) to form a surveillance complex (green rectangles) (stage 2). Upon re-entry of the invading sequence, this will be recognized and cleaved by the Cas protein(s) (stage 3). (Figure reproduced from Wiedenheft et al., 2012 [13]).

There are three types of CRISPR/Cas systems [12, 13]. In type II systems, a trans-activating crRNA (tracrRNA) complementary to the repeat sequence in pre-crRNA triggers pre-crRNA processing by the double-stranded RNA-specific ribonuclease RNAse III in the presence of Cas9 protein (Figure 4.1) [13, 14]. TracrRNA also facilitates crRNA binding, which in turn regulates stability and conformation of the RNA-DNA heteroduplex for cleavage [15]. Furthermore, Cas9 requires base pairing between the tracrRNA and the crRNA for target DNA recognition and cleavage [16, 17]. The tracrRNA-Cas9 interaction allows a conformational rearrangement in Cas9 from an inactive to an active form by reducing the energy state of the active form [15]. Cleavage occurs at a specific site determined by the complementarity between the crRNA and the target protospacer followed by a short motif, the protospacer adjacent motif (PAM), a prerequisite for Cas9 binding [16, 18-20]. The *Streptococcus pyogenes* PAM consists of a NGG consensus sequence [16]. A double stranded break (DSB) creating blunt ends is introduced at a position three base pairs upstream of the PAM. Cas9

contains both HNH and RuvC endonuclease domains and each domain cleaves one DNA strand [16, 18]. In nearly all cell types and organisms DSBs are repaired by nonhomologous end joining (NHEJ) (Figure 4.2). This is an error prone process that induces small insertion/deletion mutations (indels). These can disrupt the translational reading frame of a coding sequence leading to the production of a truncated, nonfunctional protein or to degradation of the mutant mRNA due to nonsense-mediated decay [21]. This thus ultimately leads to a loss of function of the affected gene.

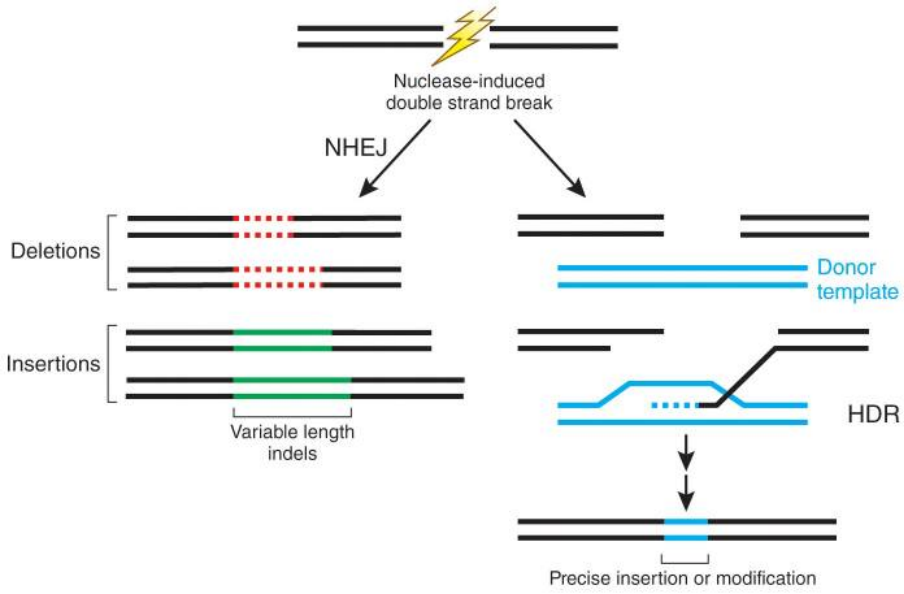

Figure 4.2 Nuclease-induced genome editing. Cas9 induces a double strand break at the target site. This is either repaired by non-homologous end-joining (NHEJ), an error-prone process, leading to small insertions or deletions (indels) at the target site. These can cause a shift in the reading frame leading to loss of function (left). When a DNA donor template is present, double strand breaks can also be repaired by homology-directed repair (HDR). This way precise insertions or modifications can be introduced (right). (Figure reproduced from Sander and Joung, 2014 [22]).

4.3 Adjustment of the system for programmed genome editing

The simple modular composition of the system held great promise for its application in targeted genome editing in eukaryotes. Jinek et al. found that a single chimeric gRNA containing the target recognition sequence at its 5' end and a hairpin structure mimicking the base pairing between the tracrRNA and the crRNA linked to the 5' end of the tracrRNA was able to guide Cas9-catalyzed DNA cleavage [16]. This confirmed the applicability of the system for programmed DNA cleavage and genome editing. The sequence of the gRNA was further optimized by additional tracrRNA-derived sequences at the 3' end (Figure 4.3) [2]. Furthermore, the *S. pyogenes* endonuclease Cas9 was engineered, including the addition of nuclear localization signals (NLS), to ensure nuclear translocation and functioning in mammalian cells [1, 5]. The gRNA and Cas9 were cloned in vectors enabling T7 RNA polymerase-mediated transcription of a capped, polyadenylated Cas9 mRNA and a customizable gRNA containing a 20 nt target recognition sequence [2]. This enabled direct injection and thus further expanded the applications of the system. However, the use of the T7 promoter constrained the possible target sequence by the requirement of a GG at the 5' end. Thereby making only sequences of the form 5'-GG-N_{18}-NGG-3' targetable. This sequence occurs once every 128 bp [2]. Later it was shown that this constraint can simply be overcome by adding two Gs 5' of the target sequence generating one possible target site every 8 bp [23]. Nowadays, recombinant Cas9

protein, instead of mRNA, is used for a lot of applications. *In vitro* assembly of gRNA/Cas9 protein complexes can increase gene editing efficiency because of its immediate activity upon injection [24].

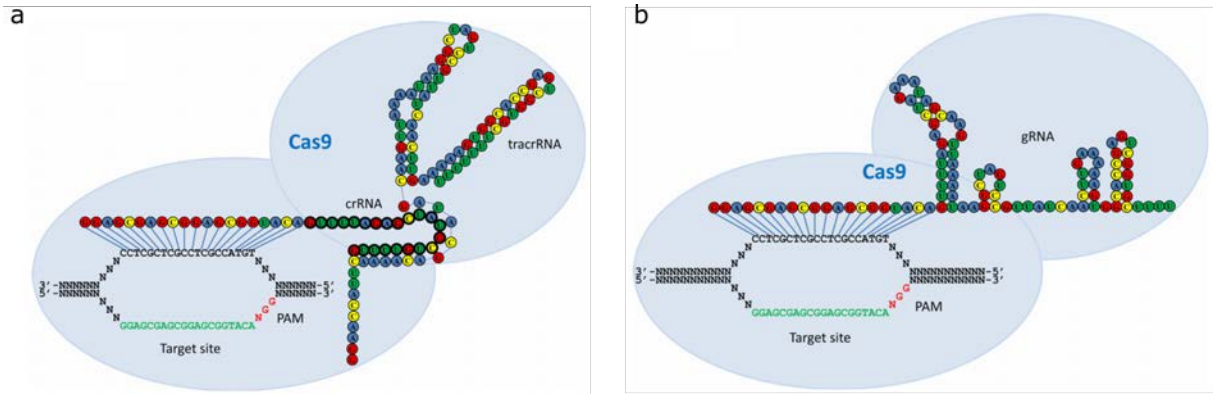

Figure 4.3 Original and chimeric guideRNA composition and structure. Schematic representing the naturally occurring and chimeric, engineered CRISPR/Cas9 system. (a) The original, *Streptococcus pyogenes* bacterial system is based on a dual RNA-guided Cas9. The crRNA interacts with the complementary strand of the target site (green) upstream of the PAM site (red). The tracrRNA is partly complimentary to the crRNA. TracrRNA basepairs with the crRNA and forms secondary structures. The complex is recognized by Cas9, which is recruited and will cleave the target site. (b) Engineered chimeric gRNA molecule containing portions of the crRNA and tracrRNA is shown interacting with the target site and Cas9. (Figure adapted from Hwang et al., 2013 [2]).

As the CRISPR/Cas9 technique became widely used, it revealed that not all genomic loci are susceptible to genome editing to the same degree. A lot of effort has been invested in identifying factors contributing to the efficiency of a given gRNA to induce mutations at a specific genomic location. These efforts have resulted in the development of several prediction tools that claim to predict the mutagenesis efficiency of each candidate gRNA. A first comparative screen of gRNAs targeting 122 loci in zebrafish was performed by Gagnon et al. indicating that G/C content over 50% and a guanine on position 20 adjacent to the PAM ensure high mutagenesis rates [4]. Doench et al. evaluated the activity of 1841 gRNAs in mammalian cells. Sequence features of the different gRNAs were correlated with their mutagenesis efficiency and used for the development of an algorithm predicting activity of different gRNAs [25]. Finally, CRISPRscan takes into account molecular features that influence *in vivo* gRNA stability, activity and Cas9 loading based on the mutagenesis efficiency of 1280 *in vitro* transcribed gRNAs targeting 128 genes in zebrafish. This revealed that the genomic locus does not influence sgRNA efficiency. However, stability of the gRNA is an important determinant of efficiency with high guanine count and depletion of adenine resulting in more stable gRNAs [26]. Moreno-Mateos et al. also identified alternative gRNAs that are 1-2 nucleotides shorter or contain mismatches at the 5'-end, while maintaining high mutagenesis efficiency, increasing the number of possible target sites by 8-fold [26]. Besides these prediction tools, modifications to the Cas9 coding sequence and gRNA sequence have been shown to increase gene editing efficiency. A C-terminal NLS sequence attached with a flexible linker to the Cas9 protein and an additional HA-tag ensures high activity. Most likely through enforced interaction and stabilization of the Cas9/gRNA/DNA ternary complex [27]. A structurally optimized gRNA, gRNA$^{(F+E)}$ contains two modifications leading to higher efficacy. The "F"-modification constitutes an U-to-A base flip that destroys a potential RNA-polymerase stop site (UUUU), while the "E"-modification is a 5 bp extension of the Cas9-binding hairpin that is thought to improve gRNA/Cas9 complex formation [27, 28].

Under physiological conditions DSBs introduced by the Cas9 are repaired by NHEJ (Figure 4.2). The resulting indels that are introduced in exons can lead to frame shifts and consequent loss of function

of the targeted gene. Alternatively, when a DNA donor template is supplied a DSB can be repaired through homology-directed repair (HDR) (Figure 4.2). Through homologous recombination specific mutations or sequences can be inserted at the targeted location further expanding the applicability of the system [22]. However, this is a rare event. A possible strategy to improve HDR rate is the use of Cas9 nickase. A D10A substitution in the RuvC I domain of Cas9 converts the endonuclease into a DNA nickase. Nicked DNA is not repaired by NHEJ, but instead is repaired seamlessly or through HDR [1]. Alternatively, homology-independent target integration is based upon the more efficient NHEJ for creating DNA knock-in [29]. At present, multiple other variations of the system are available that instead of gene disruption provoke a different effect at the target site, including reversible transcriptional activation and silencing, reporter gene integration, fluorescent labeling for live imaging, localized base substitution and induction of point mutations [30-34].

4.4 SPECIFICITY

An important issue to consider when using genome-editing techniques is potential disruption of off-target genomic loci [35]. Since gRNA binding to the target site induces formation of secondary structures important for DNA cleavage, the entire 20 bp target site contributes to target specificity, albeit with varying significance for each position [36]. A so-called seed sequence was identified at 8-12 bp 5' of the PAM. Single-base mismatches in this region completely abolish cleavage by Cas9. However mismatches further at the 5' side of the spacer are tolerated and thus need to be considered to exclude off-target cleavage [1, 16]. However, exceptions to this rule were shown to exist [37]. Zheng et al. identified a short "core" sequence from position +4 to +7 of the PAM sequence. Cas9 was shown to be highly sensitive to single mismatches in this region, probably because of their essential role in secondary structure formation at the target site [36]. Hsu et al. determined that both the identity of mismatched base pairs and the combination of mismatch number and position is important. Furthermore they showed that a NAG PAM can be tolerated albeit at lower efficiency [37]. However, it remains impossible to predict how many mismatches can be tolerated for a given target site, in the same way that it is not completely clear why some target sites are more readily cleaved than others. Off-target prediction tools have been developed based on the above findings. These are generally integrated in the target prediction tools.

Besides *in silico* prediction of possible off-target sites, also practical adaptations have been made to the system to reduce off-target effects. An easy adjustment is the downward titration of the amount of Cas9/gRNA complex used. This has been shown to significantly increase the ratio of on- to off-target cleavage [37]. Moreover, the Cas9/gRNA ribonucleoprotein complex is subject to endogenous degradation mechanisms thereby limiting its potential cleavage time [38]. Genetic engineering of the CRISPR/Cas9 system to increase its specificity has also been explored. One system involves the use of paired nickases. Point mutations were introduced in each nuclease domain of Cas9 thereby transforming it to a nickase that can only cleave one DNA strand. Paired use of two gRNAs and Cas9 nickases can generate two off-set nicks at the target site. By using this system the length of the recognition site is doubled to 40 bp thus increasing the specificity [39, 40]. However, the individual gRNAs can still guide the nickases to off-target sites where they have been shown to induce indels [22, 40]. An important improvement would be to make the activity of the nickases co-dependent for genome editing activity, as has been applied in the TALEN system [22]. Indeed, a similar approach to the nickase system uses a catalytically deactivated version of Cas9 fused to FokI monomers. FokI is the endonuclease used by the TALEN technology and is an obligatory dimer i.e.

DNA cleavage only occurs upon dimerization of the FokI monomers [32]. Another strategy is the use of 5' truncated gRNAs. These 17-18 bp gRNAs maintain on-target efficiency but show reduced off-target mutagenesis [41].
Detection of off-target mutagenesis is laborious and expensive [38]. This is usually done by deep sequencing of expected possible off-target sites or by whole-exome sequencing. However, rare events remain hard to detect. It seems more feasible to exclude possible off-target effects on an observed phenotype by either performing a rescue by reintroducing the wild type gene or by using a different gRNA to target the same gene. As each gRNA is expected to have different off-target effects, observing the same phenotype with both gRNAs most likely excludes confounding effects of undesired off-target mutations [22].

4.5 SUMMARY

CRISPR/Cas9 has rapidly evolved to a widely used technique for genetic engineering of a number of organisms. Its ease-of-use and the short time frame required for designing and constructing new gRNAs makes it a useful technique to replicate human genetic defects in model organisms. Moreover, the multiple variations on the system that are constantly being developed continuously expand the scope of the system.

4.6 REFERENCES

1. Cong, L., et al., *Multiplex genome engineering using CRISPR/Cas systems.* Science, 2013. **339**(6121): p. 819-23.
2. Hwang, W.Y., et al., *Efficient genome editing in zebrafish using a CRISPR-Cas system.* Nat Biotechnol, 2013. **31**(3): p. 227-9.
3. Bassett, A.R., et al., *Highly efficient targeted mutagenesis of Drosophila with the CRISPR/Cas9 system.* Cell Rep, 2013. **4**(1): p. 220-8.
4. Gagnon, J.A., et al., *Efficient mutagenesis by Cas9 protein-mediated oligonucleotide insertion and large-scale assessment of single-guide RNAs.* PLoS One, 2014. **9**(5): p. e98186.
5. Mali, P., et al., *RNA-guided human genome engineering via Cas9.* Science, 2013. **339**(6121): p. 823-6.
6. Wang, H., et al., *One-step generation of mice carrying mutations in multiple genes by CRISPR/Cas-mediated genome engineering.* Cell, 2013. **153**(4): p. 910-8.
7. Guo, X., et al., *Efficient RNA/Cas9-mediated genome editing in Xenopus tropicalis.* Development, 2014. **141**(3): p. 707-14.
8. Seruggia, D., et al., *Functional validation of mouse tyrosinase non-coding regulatory DNA elements by CRISPR-Cas9-mediated mutagenesis.* Nucleic Acids Res, 2015. **43**(10): p. 4855-67.
9. Friedland, A.E., et al., *Heritable genome editing in C. elegans via a CRISPR-Cas9 system.* Nat Methods, 2013. **10**(8): p. 741-3.
10. Nakayama, T., et al., *Simple and efficient CRISPR/Cas9-mediated targeted mutagenesis in Xenopus tropicalis.* Genesis, 2013. **51**(12): p. 835-43.
11. Blitz, I.L., et al., *Biallelic genome modification in F(0) Xenopus tropicalis embryos using the CRISPR/Cas system.* Genesis, 2013. **51**(12): p. 827-34.
12. Brouns, S.J., et al., *Small CRISPR RNAs guide antiviral defense in prokaryotes.* Science, 2008. **321**(5891): p. 960-4.
13. Wiedenheft, B., S.H. Sternberg, and J.A. Doudna, *RNA-guided genetic silencing systems in bacteria and archaea.* Nature, 2012. **482**(7385): p. 331-8.
14. Deltcheva, E., et al., *CRISPR RNA maturation by trans-encoded small RNA and host factor RNase III.* Nature, 2011. **471**(7340): p. 602-7.

15. Lim, Y., et al., *Structural roles of guide RNAs in the nuclease activity of Cas9 endonuclease.* Nat Commun, 2016. **7**: p. 13350.
16. Jinek, M., et al., *A programmable dual-RNA-guided DNA endonuclease in adaptive bacterial immunity.* Science, 2012. **337**(6096): p. 816-21.
17. Jinek, M., et al., *Structures of Cas9 endonucleases reveal RNA-mediated conformational activation.* Science, 2014. **343**(6176): p. 1247997.
18. Gasiunas, G., et al., *Cas9-crRNA ribonucleoprotein complex mediates specific DNA cleavage for adaptive immunity in bacteria.* Proc Natl Acad Sci U S A, 2012. **109**(39): p. E2579-86.
19. Mojica, F.J., et al., *Short motif sequences determine the targets of the prokaryotic CRISPR defence system.* Microbiology, 2009. **155**(Pt 3): p. 733-40.
20. Garneau, J.E., et al., *The CRISPR/Cas bacterial immune system cleaves bacteriophage and plasmid DNA.* Nature, 2010. **468**(7320): p. 67-71.
21. Luo, J., *CRISPR/Cas9: From Genome Engineering to Cancer Drug Discovery.* Trends Cancer, 2016. **2**(6): p. 313-324.
22. Sander, J.D. and J.K. Joung, *CRISPR-Cas systems for editing, regulating and targeting genomes.* Nat Biotechnol, 2014. **32**(4): p. 347-55.
23. Hwang, W.Y., et al., *Heritable and precise zebrafish genome editing using a CRISPR-Cas system.* PLoS One, 2013. **8**(7): p. e68708.
24. Burger, A., et al., *Maximizing mutagenesis with solubilized CRISPR-Cas9 ribonucleoprotein complexes.* Development, 2016. **143**(11): p. 2025-37.
25. Doench, J.G., et al., *Rational design of highly active sgRNAs for CRISPR-Cas9-mediated gene inactivation.* Nat Biotechnol, 2014. **32**(12): p. 1262-7.
26. Moreno-Mateos, M.A., et al., *CRISPRscan: designing highly efficient sgRNAs for CRISPR-Cas9 targeting in vivo.* Nat Methods, 2015. **12**(10): p. 982-8.
27. Zhao, P., et al., *One-step homozygosity in precise gene editing by an improved CRISPR/Cas9 system.* Cell Res, 2016. **26**(5): p. 633-6.
28. Chen, B., et al., *Dynamic imaging of genomic loci in living human cells by an optimized CRISPR/Cas system.* Cell, 2013. **155**(7): p. 1479-91.
29. Suzuki, K., et al., *In vivo genome editing via CRISPR/Cas9 mediated homology-independent targeted integration.* Nature, 2016. **540**(7631): p. 144-149.
30. Hilton, I.B., et al., *Epigenome editing by a CRISPR-Cas9-based acetyltransferase activates genes from promoters and enhancers.* Nat Biotechnol, 2015. **33**(5): p. 510-7.
31. Komor, A.C., et al., *Programmable editing of a target base in genomic DNA without double-stranded DNA cleavage.* Nature, 2016. **533**(7603): p. 420-4.
32. Doudna, J.A. and E. Charpentier, *Genome editing. The new frontier of genome engineering with CRISPR-Cas9.* Science, 2014. **346**(6213): p. 1258096.
33. Ota, S., et al., *Functional visualization and disruption of targeted genes using CRISPR/Cas9-mediated eGFP reporter integration in zebrafish.* Sci Rep, 2016. **6**: p. 34991.
34. Hess, G.T., et al., *Directed evolution using dCas9-targeted somatic hypermutation in mammalian cells.* Nat Methods, 2016. **13**(12): p. 1036-1042.
35. Fu, Y., et al., *High-frequency off-target mutagenesis induced by CRISPR-Cas nucleases in human cells.* Nat Biotechnol, 2013. **31**(9): p. 822-6.
36. Zheng, T., et al., *Profiling single-guide RNA specificity reveals a mismatch sensitive core sequence.* Sci Rep, 2017. **7**: p. 40638.
37. Hsu, P.D., et al., *DNA targeting specificity of RNA-guided Cas9 nucleases.* Nat Biotechnol, 2013. **31**(9): p. 827-32.
38. Zischewski, J., R. Fischer, and L. Bortesi, *Detection of on-target and off-target mutations generated by CRISPR/Cas9 and other sequence-specific nucleases.* Biotechnol Adv, 2017. **35**(1): p. 95-104.
39. Cho, S.W., et al., *Analysis of off-target effects of CRISPR/Cas-derived RNA-guided endonucleases and nickases.* Genome Res, 2014. **24**(1): p. 132-41.

40. Mali, P., et al., *CAS9 transcriptional activators for target specificity screening and paired nickases for cooperative genome engineering.* Nat Biotechnol, 2013. **31**(9): p. 833-8.
41. Fu, Y., et al., *Improving CRISPR-Cas nuclease specificity using truncated guide RNAs.* Nat Biotechnol, 2014. **32**(3): p. 279-84.

PART II
AIMS AND OBJECTIVES

CHAPTER 5

AIMS AND OBJECTIVES

The human brain is a highly complex, but also highly structured organ composed of many different functional units, which are perfectly integrated to perform all cognitive functions. The hindbrain is an evolutionary conserved region of the brain responsible for most vital functions like breathing, heartbeat, consciousness and balance. It is also where ten out of twelve cranial nerves originate.
The Wnt/β-catenin pathway is one of only a handful of key developmental signaling pathways. In the central nervous system, Wnt signaling is responsible for patterning, neural progenitor maintenance, neuronal differentiation and a myriad of other processes depending on the timing and localization of signaling activity [1]. Deregulation of Wnt signaling activity is associated with neurological disease. With this research I aimed to expand knowledge about Wnt/β-catenin signaling function in the hindbrain during physiological conditions, embryological development, and disease, tumor formation.

5.1 WNT SIGNALING IN THE HINDBRAIN: DEVELOPMENT

Most neuron populations in the hindbrain are laid out in a reiterative pattern. The basis of this pattern is determined very early during embryonic development with the subdivision of the embryonic hindbrain in eight rhombomeres. Hindbrain segmentation is achieved through differential gene expression along the anterior-posterior axis. At the borders between the rhombomeres, a specialized population of boundary cells is formed that shows activity of different signaling pathways. While much is known about the early establishment of segmental identity and the maintenance of lineage restriction [2, 3], little is known about the function of these signaling centers at the rhombomere boundaries. Especially their function during later embryonic stages, when the layout of neuronal circuits is mostly complete, remains obscure.

In the host lab, a transgenic Wnt reporter line in *Xenopus* was constructed [4]. The reporter construct contains a destabilized enhanced green fluorescent protein (eGFP) downstream of seven LEF/TCF sites, the Wnt responsive element. The GFP signal thus reflects the spatio-temporal dynamic of Wnt activity in the *Xenopus* embryos. These embryos confirmed some well-known Wnt signaling dependent developmental processes like gastrulation, neural tube closure and intestinal crypt proliferation [4]. Moreover, also some new Wnt signaling activity domains were revealed like the ventral blood island [5]. The transgenic Wnt reporter line also revealed Wnt signaling activity in the rhombomere boundaries in Nieuwkoop stage 44 tadpoles [4]. The main goal of this project was to determine the function of Wnt/β-catenin signaling in the rhombomere boundaries and thereby contribute to the unraveling of rhombomere boundary signaling center function.
In zebrafish a signaling network between Wnt and Notch signaling at the rhombomere boundaries was described [6, 7]. A first goal was to characterize Wnt-Notch signaling interaction at the *Xenopus* rhombomere boundaries. This interaction can be both agonistic and antagonistic depending on the context (see 1.4). To assess expression pattern of multiple factors simultaneously a fluorescent *in situ* hybridization procedure was introduced in the host lab.
Furthermore, I aimed to determine the function of Wnt signaling activity specifically in the rhombomere boundaries. Three different, possible functions were postulated: cell sorting, cell proliferation or cell death and hindbrain patterning. Since adhesion and migration properties are mostly linked to non-canonical Wnt signaling, I focused on patterning and proliferation characteristics of the hindbrain. These analyses again required the introduction of some new techniques in the host lab, like halogen-conjugated deoxyuridine labeling and cell cycle analysis via flow cytometry.

5.2 WNT SIGNALING IN THE HINDBRAIN: CANCER

Medulloblastoma (MB) is the most common brain tumor in children [8]. In recent years, overall 5-year survival rates have risen to 70% [8]. However, the applied treatment protocols consist of optimal surgical resection combined with chemotherapy and craniospinal irradiation [9]. The aggressiveness of the current treatment leads to the eradication of the malignancy in a high number of patients, but also has detrimental side effects when applied to the immature brain. This leads to severe disease sequelae like neurocognitive impairment and neuro-endocrinological defects [10]. Moreover, treatment-associated secondary malignancies have been described [8].
In 2010 large-scale genomics efforts identified four different MB subtypes: Wnt-type MB, Shh-type MB, g3 MB and g4 MB [11-14]. Molecular characterization of the different subtypes continues to improve and molecular characteristics are being linked to clinical outcome. Recently, this resulted in a further subdivision of the 4 MB types to 12 subtypes [15]. However, this huge amount of knowledge is only very slowly being translated to clinical practice. Current clinical trials mainly focus on dose de-escalation in patient groups with good prognosis, like Wnt-type MB patients [16]. Even though radiation dose reduction was shown to improve long-term quality of life, substantial improvements could still be reached by applying molecularly targeted therapies. Moreover, current treatment methods are insufficient for other patient groups, like g3 MB, which only have a 35% 5-year survival rate [8]. These patients are in desperate need of the next generation of cancer medicines specifically targeting the molecular characteristics of the tumor type.
The main need in the field is representative model organisms for the different MB subtypes that accurately reflect the clinical presentation. The emergence of the targetable nucleases, including

CRISPR/Cas9, made it possible for the first time to perform actual reverse genetics in *Xenopus*. My host lab embarked upon a mission to establish clinically relevant tumor models that can be employed for semi-high throughput therapeutic target identification through gRNA multiplexing [17]. The first *Xenopus tropicalis* tumor model phenocopied the cancer syndrome FAP through TALEN-mediated knockout of *apc* [18]. One of the tumor types associated with this syndrome is medulloblastoma and some brain tumors were observed in the original experiments. Since *apc* loss of function causes constitutive activation of the Wnt pathway these brain tumors might be a good model for Wnt-type MB. A first goal was to establish and characterize a *Xenopus tropicalis* model for Wnt-type MB. Wnt signaling has several important developmental functions in the brain and Wnt signaling disruption from embryonic stages might lead to reduced survival [1]. Indeed, *apc* mosaic knockout in the whole embryo gives rise to multiple malignancies affecting survival. Therefore, apc gRNA/Cas9 ribonucleoprotein complex (RNP) injections were targeted to the brain according to the *Xenopus* fate map. Moreover, we employed another strategy to induce Wnt-driven tumor formation in the brain: electroporation-mediated delivery of RNPs directly to the brain.

In the clinic, over 90% of patients presenting with Wnt-type MB carry activating mutations in *CTNNB1* [19-22]. Even though the end result achieved by *APC* inactivation, constitutive activation of the Wnt pathway, is the same, a second objective was to more closely mimic the patient population by targeting the β-catenin encoding gene. This might entails some problems as usually the indels induced by CRISPR/Cas9- mediated gene-editing result in a loss of function of the protein. However, small in frame deletions might still give rise to functional proteins but can remove essential functional amino acids. Here we decided to target the phosphorylation sites in exon 3 of *ctnnb1*, creating a stabilized β-catenin, thereby mimicking the clinical mutations.

A final aim was to commence the identification of new therapeutic targets for Wnt-type MB. Expression profiles of human medulloblastoma samples are publicly available [12, 23]. Comparison of expression data between the different MB subtypes can give clues about possible oncogenic drivers. Current Wnt-type MB mouse models have complicated genetic backgrounds, making them less suitable for quick functional analysis of potential tumor modulatory genes [23, 24]. The simplicity of CRISPR/Cas9 multiplexing through injection of multiple RNPs in *Xenopus* could provide a suitable platform to assess function of tumor modulatory genes and identify potential therapeutic targets.

5.3 References

1. Noelanders, R. and K. Vleminckx, *How Wnt Signaling Builds the Brain: Bridging Development and Disease.* Neuroscientist, 2016.
2. Parker, H.J. and R. Krumlauf, *Segmental arithmetic: summing up the Hox gene regulatory network for hindbrain development in chordates.* Wiley Interdiscip Rev Dev Biol, 2017.
3. Kiecker, C. and A. Lumsden, *Compartments and their boundaries in vertebrate brain development.* Nat Rev Neurosci, 2005. **6**(7): p. 553-64.
4. Tran, H.T. and K. Vleminckx, *Design and use of transgenic reporter strains for detecting activity of signaling pathways in Xenopus.* Methods, 2014. **66**(3): p. 422-32.
5. Tran, H.T., et al., *Wnt/beta-catenin signaling is involved in the induction and maintenance of primitive hematopoiesis in the vertebrate embryo.* Proc Natl Acad Sci U S A, 2010. **107**(37): p. 16160-5.
6. Amoyel, M., et al., *Wnt1 regulates neurogenesis and mediates lateral inhibition of boundary cell specification in the zebrafish hindbrain.* Development, 2005. **132**(4): p. 775-85.
7. Riley, B.B., et al., *Rhombomere boundaries are Wnt signaling centers that regulate metameric patterning in the zebrafish hindbrain.* Dev Dyn, 2004. **231**(2): p. 278-91.

8. Coluccia, D., et al., *Medulloblastoma: Tumor Biology and Relevance to Treatment and Prognosis Paradigm.* Curr Neurol Neurosci Rep, 2016. **16**(5): p. 43.
9. Roussel, M.F. and M.E. Hatten, *Cerebellum development and medulloblastoma.* Curr Top Dev Biol, 2011. **94**: p. 235-82.
10. Uday, S., et al., *Endocrine sequelae beyond 10 years in survivors of medulloblastoma.* Clin Endocrinol (Oxf), 2015. **83**(5): p. 663-70.
11. Cho, Y.J., et al., *Integrative genomic analysis of medulloblastoma identifies a molecular subgroup that drives poor clinical outcome.* J Clin Oncol, 2011. **29**(11): p. 1424-30.
12. Kool, M., et al., *Integrated genomics identifies five medulloblastoma subtypes with distinct genetic profiles, pathway signatures and clinicopathological features.* PLoS One, 2008. **3**(8): p. e3088.
13. Thompson, M.C., et al., *Genomics identifies medulloblastoma subgroups that are enriched for specific genetic alterations.* J Clin Oncol, 2006. **24**(12): p. 1924-31.
14. Northcott, P.A., et al., *Medulloblastoma comprises four distinct molecular variants.* J Clin Oncol, 2011. **29**(11): p. 1408-14.
15. Cavalli, F.M.G., et al., *Intertumoral Heterogeneity within Medulloblastoma Subgroups.* Cancer Cell, 2017. **31**(6): p. 737-754 e6.
16. Clifford, S.C., et al., *Wnt/Wingless pathway activation and chromosome 6 loss characterize a distinct molecular sub-group of medulloblastomas associated with a favorable prognosis.* Cell Cycle, 2006. **5**(22): p. 2666-70.
17. Naert, T., T. Van Nieuwenhuysen, and K. Vleminckx, *TALENs and CRISPR/Cas9 fuel genetically engineered clinically relevant Xenopus tropicalis tumor models.* Genesis, 2017. **55**(1-2).
18. Van Nieuwenhuysen, T., et al., *TALEN-mediated apc mutation in Xenopus tropicalis phenocopies familial adenomatous polyposis.* Oncoscience, 2015. **2**(5): p. 555-66.
19. Eberhart, C.G., T. Tihan, and P.C. Burger, *Nuclear localization and mutation of beta-catenin in medulloblastomas.* J Neuropathol Exp Neurol, 2000. **59**(4): p. 333-7.
20. Jones, D.T., et al., *Dissecting the genomic complexity underlying medulloblastoma.* Nature, 2012. **488**(7409): p. 100-5.
21. Raffel, C., *Medulloblastoma: molecular genetics and animal models.* Neoplasia, 2004. **6**(4): p. 310-22.
22. Zurawel, R.H., et al., *Sporadic medulloblastomas contain oncogenic beta-catenin mutations.* Cancer Res, 1998. **58**(5): p. 896-9.
23. Robinson, G., et al., *Novel mutations target distinct subgroups of medulloblastoma.* Nature, 2012. **488**(7409): p. 43-8.
24. Gibson, P., et al., *Subtypes of medulloblastoma have distinct developmental origins.* Nature, 2010. **468**(7327): p. 1095-9.

PART III
RESULTS

PART IIIA

RESULTS

WNT SIGNALING IN THE HINDBRAIN: DEVELOPMENT

CHAPTER 6

WNT/β-CATENIN SIGNALING ANTAGONIZES NOTCH SIGNALING AND INDUCES PROLIFERATION IN THE *XENOPUS* RHOMBOMERE BOUNDARIES

Rivka Noelanders, Bart Dequeker, Andrzej Kozlowski, Gert Van Isterdael and Kris Vleminckx

BMC Biology, under review

6.1 ABSTRACT

6.1.1 BACKGROUND

The vertebrate embryonic hindbrain is transiently subdivided in seven or eight repetitive units, called rhombomeres. At the boundaries between these segments, signaling centers are established. In zebrafish, a Wnt and Notch signaling network was proposed to be active at the rhombomere boundaries. However, the role of this signaling network has remained ambiguous and the proposed Wnt-Notch positive feedback model has not been confirmed in other vertebrates.

6.1.2 RESULTS

Wnt signaling activation in the *Xenopus* hindbrain, specifically at the rhombomere boundaries was revealed in transgenic Wnt reporter embryos. Surprisingly, in conflict with the proposed zebrafish model, expression of Notch signaling factors was excluded from the rhombomere boundaries in the

hindbrain. Furthermore, experimental Wnt signaling activation suppressed expression of Notch signaling factors, while Wnt inhibition lead to narrowing of the boundary regions. Conversely, experimental Notch signaling activation almost completely eradicated Wnt signaling activity in the hindbrain, while inhibition of endogenous Notch signaling lead to an increase of local Wnt signaling activity. Cell cycle analysis revealed that the hindbrain boundary cells with active Wnt signaling are actively proliferating. Moreover, Wnt signaling activation induces G_1- to S-phase transition in rhombomere boundary cells.

6.1.3 CONCLUSIONS

We show Wnt-Notch signaling antagonism at the *Xenopus* rhombomere boundaries. This antagonism separates Notch signaling mediated neurogenesis within the rhombomeres from zones of active Wnt signaling maintaining a population of proliferating neural stem cells in the rhombomere boundaries.

6.2 BACKGROUND

The human brain is a highly complex, but also highly organized structure composed of specialized functional units. However, during embryonic development the central nervous system starts out as a simple tube composed of a homogenous neuro-epithelium. The eventual complexity is achieved through sequential subcompartmentalization in so-called neuromeres. Initially, the anterior tube thickens and is subdivided to form the primary brain vesicles: prosencephalon (forebrain), mesencephalon (midbrain) and rhombencephalon (hindbrain). These regions are in turn further subdivided and the different regions will develop into specialized functional units under the combinatorial influence of developmental signaling pathways. This subdivision is most apparent in the hindbrain with the emergence of eight subcompartments: the rhombomeres. Separation between the different compartments is first achieved on a molecular level with differential expression of various transcription factors resulting in segmental expression of Hox genes that drive a different transcriptional program in each rhombomere [1]. Later, the different rhombomeres can also be distinguished visibly as a series of bulges in the hindbrain. No cell mixing occurs between the rhombomeres as a result of ephrin-Ephrin receptor mediated repulsion between cells of adjacent compartments and mechanical separation through actomyosin cable formation [2-4]. On the interface between the different rhombomeres, cells show typical characteristics like increased extracellular space and decreased junctional permeability [5-7]. These boundary cells also show specific activity of different signaling pathways. Signaling centers are established on the borders between different compartments that are thought to drive patterning of the adjacent tissue. Each rhombomere thus forms a separate functional unit with specific neuronal populations and neural organization [8-10].

The rhombomere boundaries (RBs) show localized activity of FGF signaling in the chick and Wnt signaling in zebrafish [11, 12]. RBs are considered to contain a static, quiescent cell population thereby functioning as a mechanical barrier to prevent cell mixing and maintaining its signaling function to pattern adjacent tissue. However, upon addition of retinoic acid to the chick hindbrain, both morphological and molecular features of RBs in the posterior hindbrain were lost, but no cell mixing and only minor changes in the neuronal organization were observed [13]. Recently, Peretz et al. described a role for the RBs as a reservoir of neural stem cells (NSCs) [14]. The function of the rhombomere boundaries, especially their signaling activity, is thus still not completely understood.

In zebrafish a signaling network between Notch and Wnt signaling was described. In the canonical Wnt pathway, cytoplasmic β-catenin protein is phosphorylated and thereby targeted for proteosomal degradation by the so-called destruction complex when Wnt ligands are absent or not engaged. When Wnts are binding their receptors, the destruction complex falls apart resulting in an accumulation of β-catenin in the cytoplasm. β-catenin will then translocate to the nucleus where it will bind transcription factors of the LEF/TCF family and recruit transcriptional co-activators to activate transcription. Wnt signaling regulates a myriad of processes including stem cell proliferation and differentiation [15], also in the central nervous system [16]. Both the Notch receptors and their ligands are transmembrane proteins. Ligand binding leads to a series of proteolytic cleavages in the receptor releasing the Notch intracellular domain (NICD) that will bind a CSL (CBF1/RBPjκ/Su(H)/Lag-1) DNA-binding protein and associate with transcriptional co-activators to activate transcription in the nucleus. Notch signaling is mainly important in binary fate decisions [17]. In zebrafish the Notch ligands *DeltaA* and *DeltaD* are expressed in stripes adjacent to the RBs and cells overexpressing NICD sort out to the RBs leading to the conclusion of the authors that Notch signaling is activated in the RBs [18]. Also several Wnt ligands are expressed in the zebrafish RBs [11, 19]. Riley et al. proposed a role for Wnt signaling in organization of neuronal differentiation and patterning of the hindbrain [11]. Another study also showed a role for Wnt signaling in organizing localized neuronal differentiation, but they later retracted their findings attributing them to off-target effects of the used morpholinos [20, 21]. Both groups propose a signaling network at the RBs similar to the dorso-ventral boundary of the *Drosophila* wing disc where Notch is specifically activated at the boundary through complementary expression of its ligands in the flanking cells and is proposed to induce Wnt ligand expression in the boundary. Wnt signaling, in turn, induces Notch ligand expression adjacent to the boundary, thereby creating a positive feedback loop that maintains the boundary signaling center [22].
We here show Wnt signaling activity at the RBs also in the *Xenopus* hindbrain. Our findings call the proposed Notch-Wnt signaling network into question and instead show a role for Wnt signaling in proliferation of RB cells.

6.3 RESULTS

6.3.1 WNT SIGNALING ACTIVITY IN THE XENOPUS RHOMBOMERE BOUNDARIES

Wnt reporter *X. tropicalis* were generated in our lab [23]. These animals express a destabilized eGFP under the control of seven putative LEF/TCF sites, the Wnt responsive element. Expression of eGFP thus reflects the dynamic pattern of Wnt signaling activity throughout embryonic development. In the brain Wnt signaling is highly active in the midbrain-hindbrain boundary, but no Wnt signaling activity is observed in the hindbrain before Nieuwkoop stage 40 (st 40). However, from st 41 onwards Wnt signaling is specifically activated in the RBs, where it is maintained until at least st 45 (Figure 6.1). Wnt signaling activity is restricted to the dorsal 2/3rd of the hindbrain and to the ventricular side of the hindbrain as can be observed from a lateral view of the brain and transverse section through a boundary region (Figure 6.1).
To confirm Wnt signaling activity, we also checked expression of Wnt ligands in the *Xenopus* hindbrain. The *X. tropicalis* genome contains 24 Wnt genes [24]. Of these some were excluded based on previously described expression patterns [24]. We designed RNA-probes for 12 Wnt ligands (wnt1, wnt2b, wnt3, wnt3a, wnt4, wnt5a, wnt5b, wnt8a, wnt8b, wnt10b, wnt11 and wnt11b) and checked

their expression pattern in the hindbrain at stage 41 by whole mount *in situ* hybridization (WISH). Of these only wnt3, wnt3a and wnt4 showed a segmented expression pattern in the hindbrain (Figure 6.2). Signal specificity was checked by comparison to WISH using sense RNA-probes (Figure 6.2).

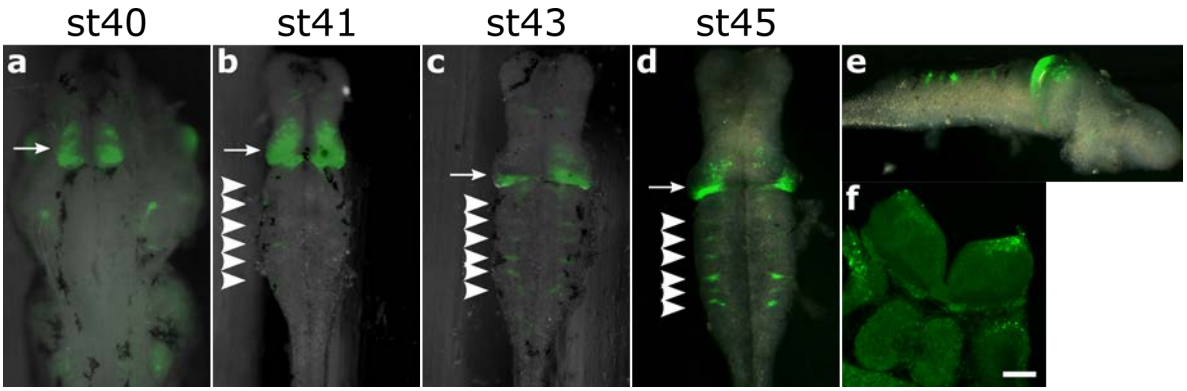

Figure 6.1 Wnt signaling activity in the *Xenopus tropicalis* hindbrain. GFP expression represents active Wnt signaling activity in a transgenic *Xenopus* Wnt reporter line. (a-d) Wnt signaling is highly active in the midbrain-hindbrain boundary (arrow). Wnt signaling activity in the rhombomere boundaries is only visible from stage 41 onwards (arrowheads). (e-f) Wnt activity is confined to the ventricular area of the dorsal hindbrain. (a-d) show a dorsal view with anterior to the top, (e) shows a lateral view with anterior to the right and (f) shows a transversal section through a rhombomere boundary with dorsal to the top. Scale bar = 200 µm.

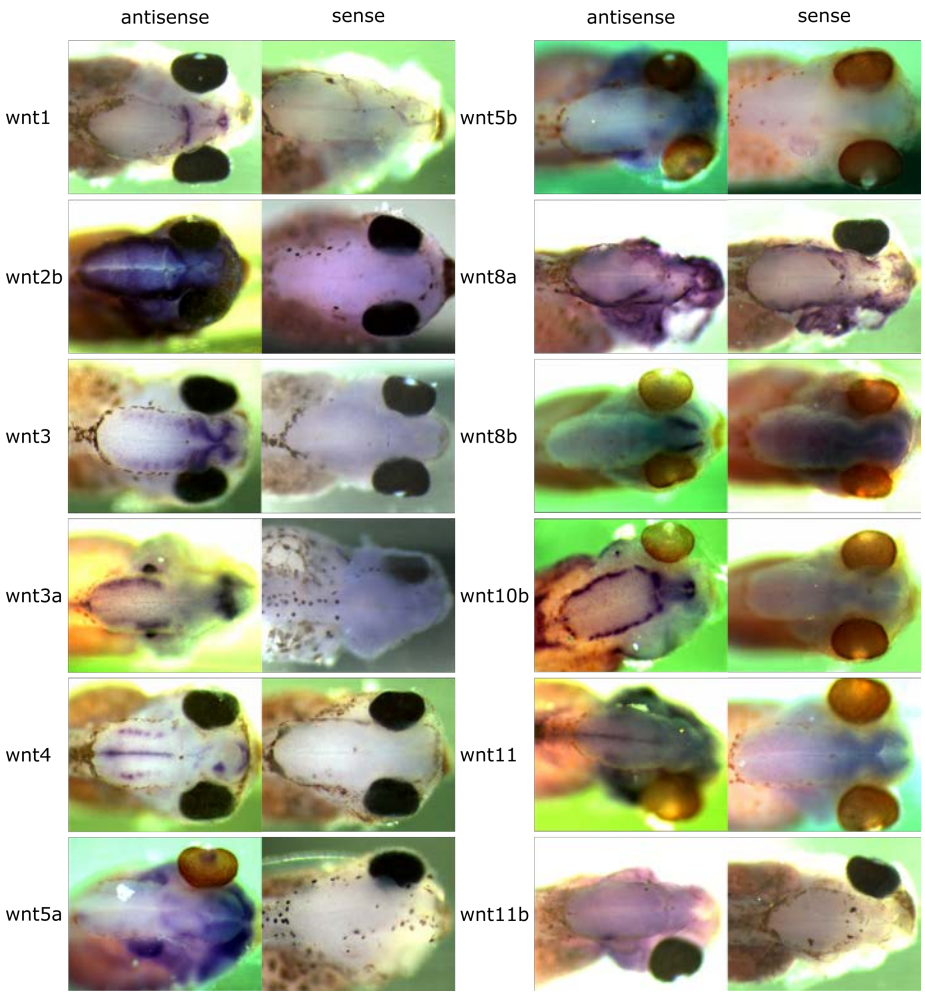

Figure 6.2 Wnt ligand expression in the hindbrain. Dorsal view of the *X. tropicalis* brain at stage 41. Expression pattern of the different Wnt ligands is revealed by WISH. Only wnt3, wnt3a and wnt4 show a segmented expression pattern in the hindbrain. Sense probes were used as a negative control.

Further determination of the responsible ligand is not straightforward as redundancy and compensation mechanisms are known to exist after Wnt ligand knockout [25]. In zebrafish simultaneous knockout of *wnt1* and *wnt10b* and morpholino-mediated knockdown of *wnt3a* and *wnt8b* was needed to elicit a hindbrain phenotype [11]. We attempted to identify the responsible wnt ligand by CRISPR/Cas9-mediated knockout of *wnt3, wnt3a* or *wnt4*. Preassembled gRNA/Cas9 complexes were injected in both animal-dorsal blastomeres of Wnt reporter embryos at the eight-cell stage. These blastomeres will give rise to most neural structures including the hindbrain leading to a mosaic wnt ligand knockout in the hindbrain. High to moderate gene editing efficiencies were achieved (18% for *wnt3,* 14.5% for *wnt3a* and 5.5% for *wnt4* out of possible 25% maximum gene editing efficiency (1/4th of embryo injected)). However, no clear decrease in Wnt signaling activity in the RBs was observed (Figure 6.3). Moreover, in most embryos an increase in Wnt signaling activity was clear. Wnt signaling activity even expanded in the rhombomere centers. These results point towards a compensation mechanism upon knockout of a single wnt ligand. As a result we were not able to identify the responsible Wnt ligand.

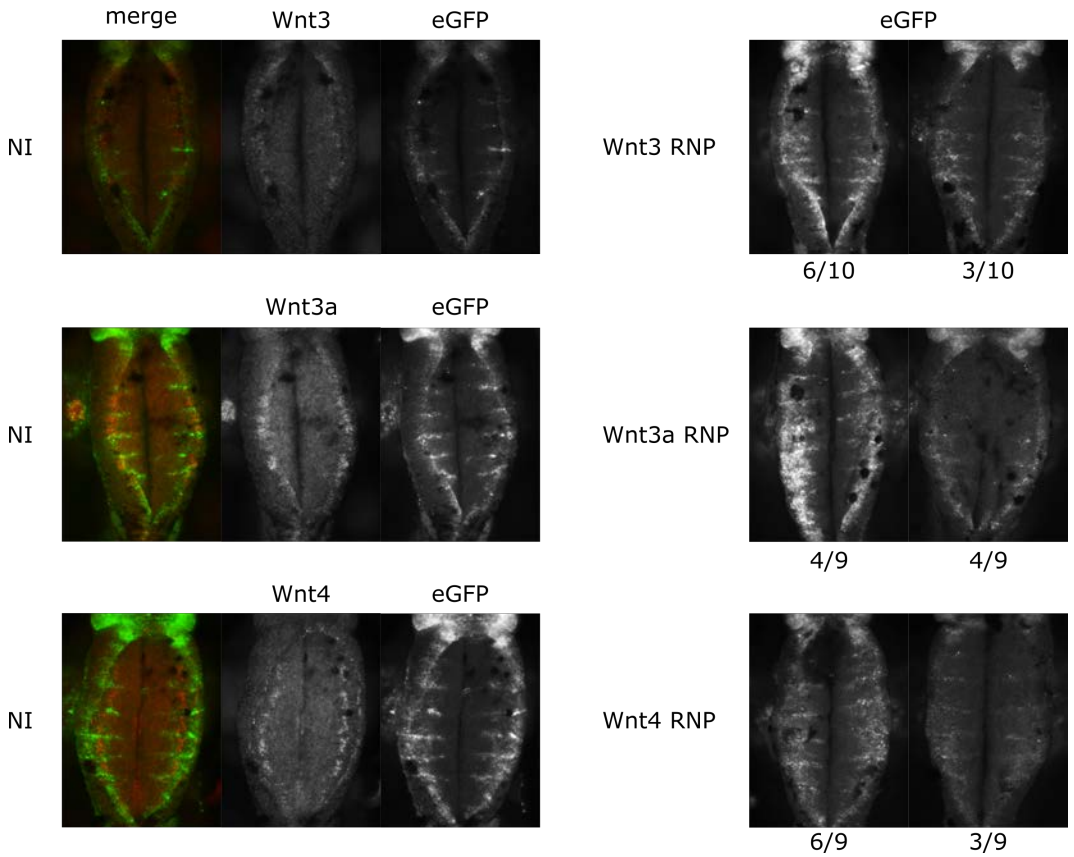

Figure 6.3 Compensation upon CRISPR/Cas9-mediated wnt ligand knockout. Left panels show wnt ligand expression (red) and Wnt activity (green) in non-injected tadpoles (NI). All wnt ligands are expressed in the dorsal hindbrain and Wnt signaling activity is confined to the rhombomere boundaries. Upon injection of wnt ligand gRNA/Cas9 ribonucleoprotein complexes (RNPs) Wnt signaling activity is increased in the majority of injected tadpoles (right panel). Numbers are indicated below the pictures.

6.3.2 NOTCH SIGNALING FACTORS SHOW A METAMERIC EXPRESSION PATTERN

In the zebrafish hindbrain a Notch-Wnt signaling network at the rhombomere boundaries was proposed, analogous to the dorso-ventral boundary of the *Drosophila* wing disc [11, 20]. We wanted to confirm the Notch-Wnt interaction in *Xenopus.* RNA-probes for different Notch signaling factors were designed: the Notch receptor and its ligands (*delta* and *jagged* family), the signaling modulators

lunatic fringe (*lfng*), that influences receptor-ligand affinity [26], and *nrarp*, a negative regulator [27], and two putative Notch target genes *hes1* and *hes5*. Whole mount (fluorescent) *in situ* hybridization showed a metameric expression pattern for all Notch signaling factors (Figure 6.4). *Notch1, delta1, nrarp* and *hes5* show a punctuate expression throughout the rhombomere centers. Expression of *jagged1* is confined to two longitudinal stripes in the ventral hindbrain, interrupted by the RBs. *Lfng* is weakly expressed throughout the rhombomere centers with three zones of higher expression from dorsal to ventral. *Jagged1* and *lfng* expression is complementary, with the stripes of *jagged1* expression colocalizing with the *lfng*-free zones creating alternating expression of both genes form dorsal to ventral (Figure 6.4). *Notch3* showed a similar expression pattern as *notch1.* No specific expression of *notch2, delta2* and *jagged2* was observed in the hindbrain (Figure S6.1). Finally, *hes1* is expressed in the RBs and in a continuous longitudinal stripe in the dorsal hindbrain (Figure 6.4). The proposed model postulates that Notch signaling is active in the RBs [11, 18]. However, all Notch signaling factors, except *hes1*, are excluded from the RBs. The observed expression pattern of the Notch signaling factors thus argues against Notch signaling activation in the RBs.

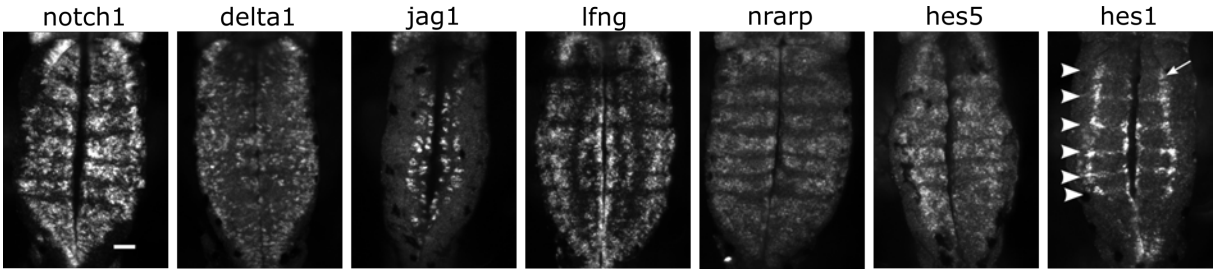

Figure 6.4 Expression of Notch factors in the hindbrain. Maximal projection of confocal scans through the hindbrain after whole mount fluorescent *in situ* hybridization. All Notch signaling factors show a metameric expression pattern. Expression of Notch signaling factors is excluded from the RBs, except for *hes1*, which is only expressed in the RBs (arrowheads) and in a longitudinal stripe in the dorsal hindbrain (arrow). Scale bar = 200 μm.

6.3.3 Hes1 expression in the RBs is induced by Wnt signaling

Throughout development Hes1 expression is mostly linked to active Notch signaling. However, several studies have reported Notch-independent regulation of the *Hes1* gene, with both Sonic Hedgehog and Wnt signaling capable of inducing Hes1 expression independent of Notch signaling activity [28-30]. Moreover, Notch signaling induced Hes1 expression often shows an oscillatory dynamic, for example during neurogenesis [31]. Baek et al. showed that in neural boundary regions in the mouse, Hes1 is continuously expressed at a high level, indicating a different induction mechanism [32]. Given the potential overlap between *hes1* expression and the expression of eGFP in the transgenic Wnt reporter line, we wondered whether in *Xenopus hes1* expression in the RBs might be regulated by Wnt signaling.

We checked the *X. tropicalis* promoter for Wnt-responsive elements. *In silico* analysis identified four LEF/TCF sites. However, β-catenin ChIP (performed by S. Janssens) revealed β-catenin binding to only one site about 3 kb upstream of the transcription start site (Figure 6.5a). A luciferase reporter construct containing a 3.5 kb *X. tropicalis hes1* promoter was made (pGL3b-XtHes1p) and used for *in vitro* assessment of Wnt induced *hes1* expression. HEKT293 cells were transfected with the reporter plasmid, an internal control plasmid expressing β-galactosidase and plasmids expressing dominant active or dominant negative constructs for either Wnt or Notch signaling (Figure 6.5b). Empty vector (pCS2+) was used as a negative control. Effectiveness of signaling interference was checked on Wnt and Notch reporter plasmids respectively (Topflash and 4xCSL-luc, not shown). As expected, Notch signaling activation through expression of NICD-GR lead to a 2-fold increase in *hes1* reporter

expression compared to empty vector (NICD/pCS2+ 2.36; p<0.001). Wnt signaling activation through expression of a dominant active form of β-catenin (β-cateninS33A) resulted in a similar increase in *hes1* reporter expression (β-catS33A/pCS2+ 2.56; p<0.001) proving that Wnt signaling activation can induce *hes1* expression. Combined activation of both Wnt and Notch signaling showed a further increase in *hes1* reporter activity, but no synergistic effect was observed (NICD+β-catS33A/pCS2+ 3,13; p<0.001). Expression of dominant negative TCF4 (DN TCF4) to inhibit Wnt signaling or of a DNA binding mutant of Suppressor of Hairless (DBM) to inhibit Notch signaling had little effect (DN TCF4/pCS2+ 0.87; DBM/pCS2+ 1.03). This is possibly due to low endogenous Wnt and Notch signaling activity in HEKT293 cells.

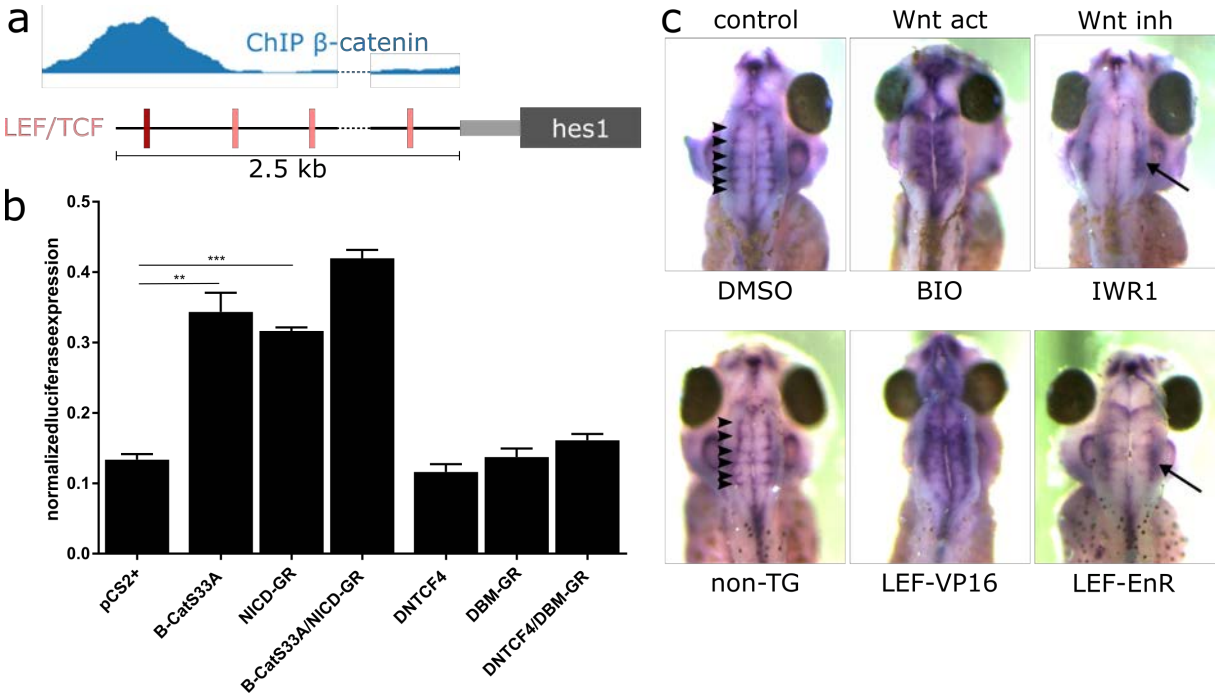

Figure 6.5 Wnt signaling induces *hes1* expression in the rhombomere boundaries. (a) The *X. tropicalis hes1* promoter contains four LEF/TCF sites from which one binds β-catenin *in vivo* as demonstrated by β-catenin ChIP. (b) Luciferase reporter assay showing Wnt signaling induces expression from the *X. tropicalis hes1* promoter to a similar extent as Notch signaling *in vitro.* (c) Wnt signaling activation induced by either LEF-VP16 transgene activation or BIO treatment results in widening of *hes1* expression around the RBs (arrowheads) and ectopic expression in the rhombomere centers. Wnt signaling inhibition leads to almost complete disappearance of *hes1* expression in the hindbrain. Only the continuous band in the dorsal hindbrain is maintained (arrow).

Having shown that Wnt signaling can induce the *X. tropicalis hes1* promoter *in vitro,* we checked if Wnt signaling activity is responsible for *hes1* expression in the RBs. We made use of *X. tropicalis* embryos transgenic for hormone-inducible Wnt activating or inhibiting constructs (LEFΔN-VP16-GR or LEFΔN-EnR-GR) to avoid aspecific effects of interfering with early Wnt-related patterning processes [33]. Next to this we also treated embryos with validated chemical compounds: the GSK3 inhibitor BIO to activate signaling and the axin stabilizing agent IWR1 to inhibit Wnt signaling [34]. Control embryos were treated with DMSO. Signaling interference was started at st 37 by addition of dexamethasone to activate transgenes or by addition of BIO/IWR1, and expression of *hes1* was assessed at st 41 (~ 8 hours) by WISH (Figure 6.5c). Wnt activation by both methods induced widening of the *hes1* expression domain around the RBs and induced ectopic *hes1* expression in the rhombomere centers. On the other hand, Wnt inhibition almost completely abolished *hes1* expression in the RBs. However, *hes1* expression was maintained in the continuous dorsal band,

indicating that both expression domains are induced by different mechanisms. We conclude that Wnt signaling maintains continuous high *hes1* expression in the RBs.

6.3.4 *Wnt signaling prevents expression of Notch signaling factors in the rhombomere boundaries*

Riley et al. proposed induction of Notch ligand expression adjacent to the RBs and subsequent maintenance of Notch signaling activity in the RBs downstream of Wnt signaling [11]. However, since the observed expression profile of the different Notch signaling factors did not match this hypothesis, we checked how Wnt signaling interference affects expression of the other Notch signaling factors besides *hes1*. Chemical Wnt activation and inhibition was performed by addition of BIO and IWR1, respectively, to the rearing medium of st 37 tadpoles. Notch signaling factor expression was checked at st 41 by WISH. Contrary to what was expected based on the model, we observed a reduction in expression of Notch ligand expression (*delta1* and *jagged1* (jag1)) when Wnt signaling was activated (Figure 6.6). Also downstream Notch signaling factors, *nrarp* and *hes5*, showed lower expression compared to DMSO treated embryos (Figure 6.6). These results were confirmed in the LEFΔN-VP16-GR transgenic tadpoles (Figure S6.2).

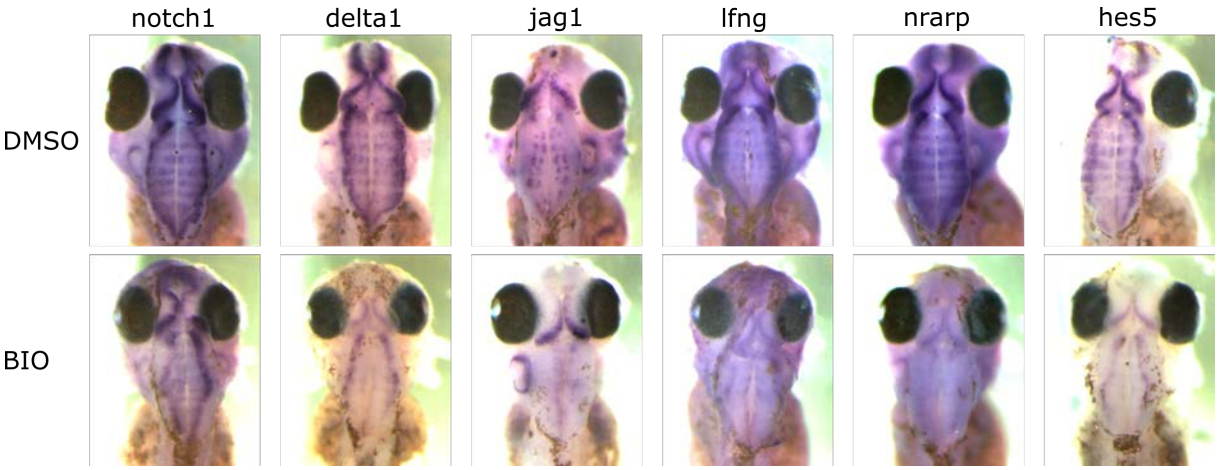

Figure 6.6 Pharmacological activation of Wnt signaling leads to reduced expression of Notch signaling factors. *Notch1, delta1, jagged1* (jag1)*, lunatic fringe* (lfng), *nrarp* and *hes5* show a reduction in expression in the hindbrain after BIO-induced Wnt signaling activation.

Upon Wnt signaling inhibition by IWR1 treatment and in LEFΔN-EnR-GR transgenic tadpoles we could not discern big differences in expression of the Notch signaling factors (Figure S6.2). To increase resolution of the WISH we performed fluorescent *in situ* hybridization (FISH) with tyramide signal amplification. Experiments were performed in Wnt reporter animals to confirm Wnt signaling inhibition. Loss of GFP expression was obvious upon treatment with IWR1 (Figure 6.7). The RBs, devoid of Notch signaling factor expression in untreated embryos, were narrowed upon IWR1 treatment, leading to an almost continuous expression of the different Notch signaling factors throughout the hindbrain (Figure 6.7). Wnt signaling thus restricts Notch signaling in the hindbrain and Wnt signaling activation is needed to maintain the RBs as Notch signaling-free zones.

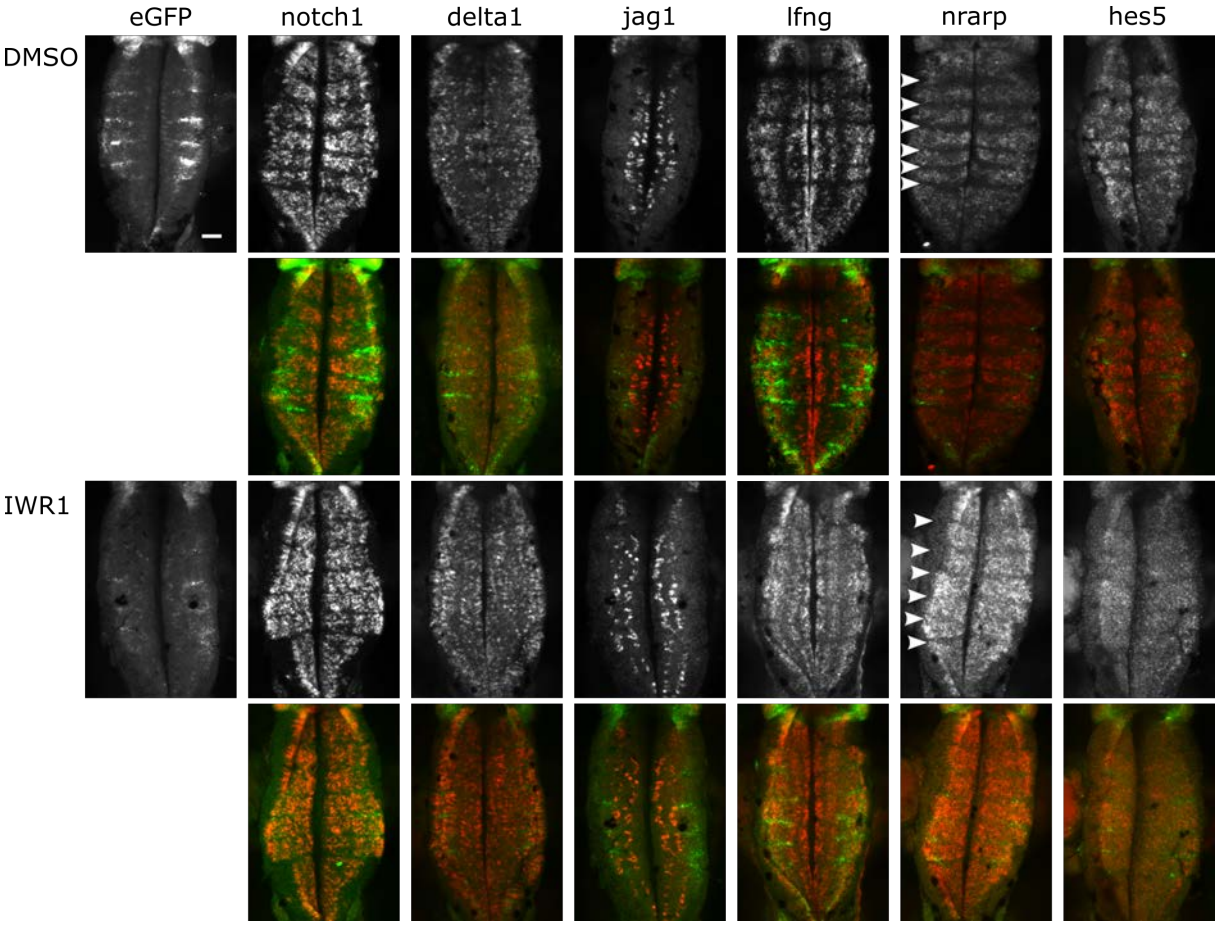

Figure 6.7 Pharmacological Wnt signaling inhibition leads to narrowing of the rhombomere boundaries. In control treated embryos the RBs are devoid of expression of Notch signaling factors. Upon Wnt signaling inhibition these Notch signaling-free zones narrow, leading to an almost uniform expression pattern of Notch signaling factors throughout the hindbrain (arrowheads (for *nrarp*)). Scalebar = 200 µm.

6.3.5 *Notch signaling activation antagonizes Wnt signaling in the rhombomere boundaries*

A final implication of the current zebrafish model [11] is the proposed induction of Wnt signaling activity at the RBs downstream of Notch signaling, creating a positive feedback loop. Hence, we interfered with Notch signaling by injection of hormone-inducible dominant active or dominant negative forms of Suppressor of Hairless (Su(H)). For Notch signaling activation we employed a fusion construct of Su(H) and the ankyrin repeats of the NICD, coupled to the hormone-binding domain of the glucocorticoid receptor (ANK-GR) [35]. Notch signaling inhibition was achieved through a DNA-binding mutant of Su(H) (DBM-GR) [36]. Constructs were injected in Wnt reporter embryos (2-cell stage, whole embryo) and again activated at st 37 through addition of dexamethasone to the rearing medium. Wnt signaling activity in the RBs was assessed at st 41 by fluorescent WISH for eGFP (Figure 6.8). Notch signaling activation lead to almost complete disappearance of eGFP expression. On the other hand, Notch signaling inhibition lead to an increase and broadening of eGFP expression. The effect on Wnt signaling activity was confirmed by looking at the expression pattern of the different Notch signaling factors. Notch activation mimicked Wnt inhibition with narrowed RBs while Notch signaling inhibition had a similar effect as Wnt activation with reduced expression of most Notch associated factors and broadening of the RBs (Figure 6.8). Taken together, in contrast to the model proposed in zebrafish hindbrain, rather than a positive feedback there seems to be an antagonistic relationship between Wnt and Notch signaling in the RBs.

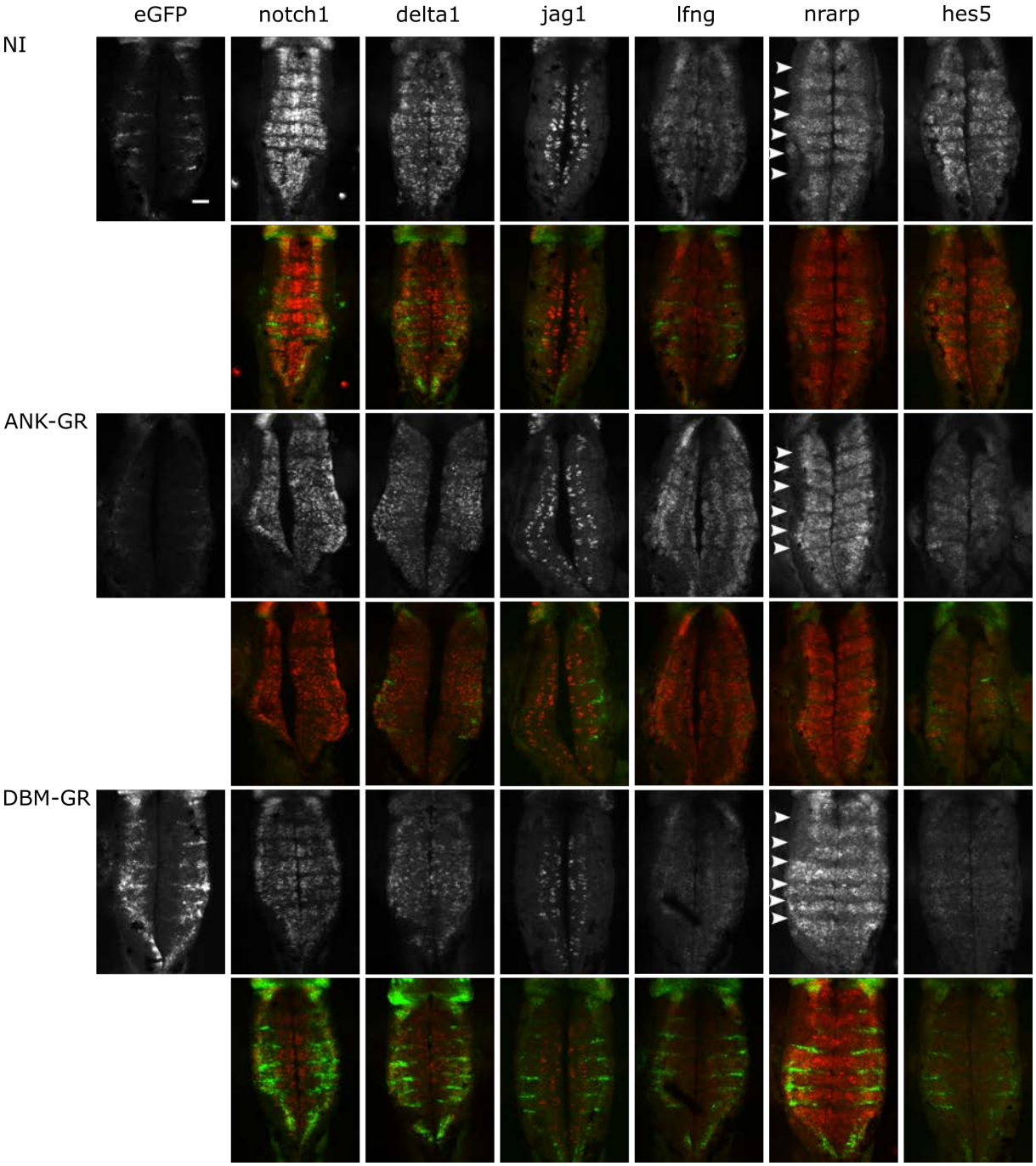

Figure 6.8 Wnt-Notch signaling antagonism in the rhombomere boundaries. Notch signaling activation through injection of synthetic mRNA encoding ANK-GR leads to reduced Wnt signaling activity, narrowing of RBs and expansion of Notch signaling factor expression domains (arrowhead (for *nrarp*)). Notch signaling inhibition, via injection of DBM-GR, leads to increased Wnt signaling activity and widening of the RBs (arrowheads (for *nrarp*)). Concomitantly, expression of several Notch signaling factors is downregulated. Scalebar = 200 µm.

6.3.6 Wnt signaling does not influence neuronal pattern formation in the hindbrain

The function of specific Wnt signaling activation in the RBs remains unclear. Boundary regions are thought to function as signaling centers to further pattern the adjacent tissue. However, Wnt signaling at the RBs is activated quite late during development when coarse patterning is already completed. We checked if Wnt signaling interference disturbed neuronal pattern formation. Several neuronal populations in the hindbrain, including cranial motorneurons, show a specific segmental

pattern [8-10]. We checked organization of cranial motor nerve nuclei by WISH for *Islet-1*. Wnt signaling interference from st 37 onwards had no effect on cranial motor nerve nuclei pattern (Figure 6.9).

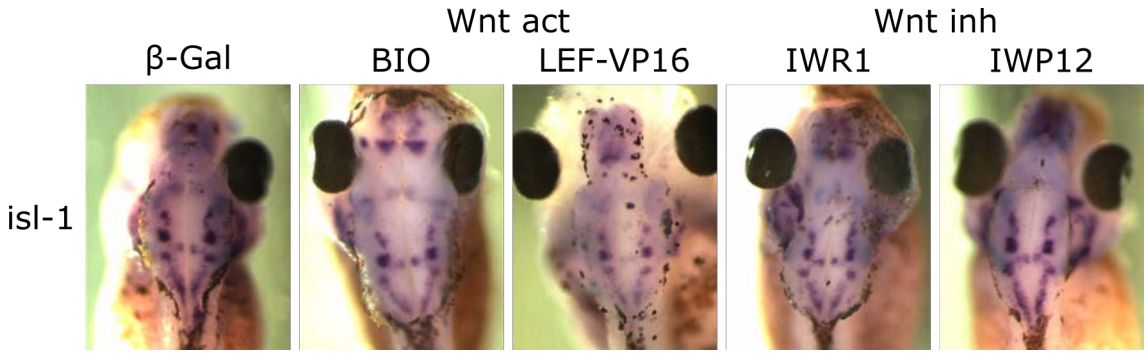

Figure 6.9 Normal organization of cranial motor nerve nuclei upon Wnt signaling interference. Pattern of cranial motor nerve nuclei was unchanged after Wnt signaling activation through BIO treatment or in LEF-VP16 transgenic embryos as revealed by WISH for *isl-1*. No effect was also observed after Wnt signaling inhibition through treatment with either IWR1 or IWP12.

6.3.7 WNT SIGNALING INFLUENCES PROLIFERATION IN THE HINDBRAIN

Another possible role for Wnt signaling in the RBs is regulation of proliferation. We checked proliferation in the hindbrain both through immunofluorescence for the M-phase marker phospho-Histone3 (PH3) and through S-phase labeling with 5-iodo-deoxyuridine (IdU). Imaging was done on a macroconfocal microscope allowing us to scan through the entire depth of the hindbrain. M-phase nuclei seemed stochastically scattered with no clear enrichment in the RBs (Figure 6.10a). However, immunofluorescent detection of IdU-positive nuclei did show clear enrichment at the RBs. Moreover, IdU-positive cells colocalized with GFP^+ boundary cells in hindbrains from Wnt reporter tadpoles (Figure 6.10b). This indicates that Wnt positive boundary cells are actively cycling cells.

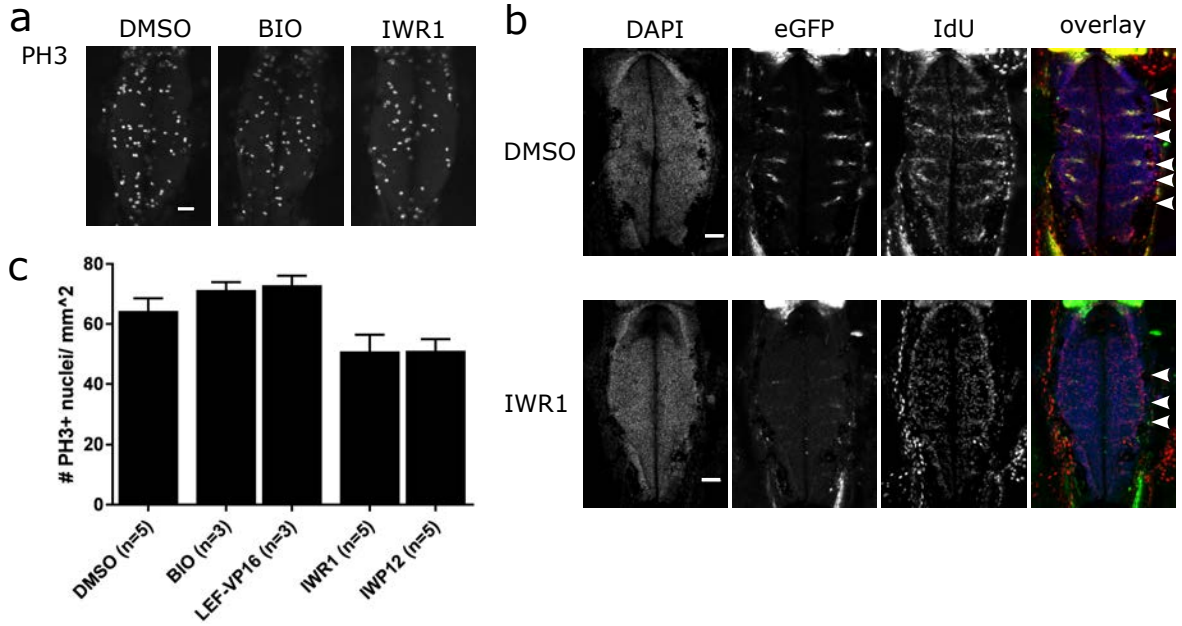

Figure 6.10 Effect of Wnt signaling interference on cellular proliferation in the hindbrain. (a) PH3+ nuclei are scattered throughout the hindbrain. No change is observed upon Wnt signaling interference. (b) RBs are enriched for IdU positive cells, which mostly colocalize with GFP+ cells (arrowheads). Upon pharmacological Wnt inhibition the enrichment in the RBs is lost and IdU positive cells show a stochastic pattern (arrowheads). (c) Graph shows the number of nuclei per surface area for the different treatment conditions. Wnt signaling interference leads to a slight increase of PH3+ nuclei, while Wnt signaling inhibition has the opposite effect. Scalebar = 200 µm.

We again interfered with Wnt signaling during the same time frame (st 37 – 41) through treatment with chemical compounds or transgene activation and checked if proliferation characteristics were affected (Figure 6.10). $PH3^+$ nuclei were manually counted in the different z-stacks. Wnt activation by treatment with BIO or injection of LEF-VP16 transgene activation lead to a slight increase in PH3+ nuclei in the hindbrain (73.71 and 75.33 $PH3^+$ nuclei/ mm^2 respectively vs 64.34 $PH3^+$ nuclei/ mm^2, p = 0.14 and p = 0.14 respectively), while inhibition by treatment with either IWR1 or IWP12 [37] lead to a decrease of PH3+ nuclei (48.5 and 54.2 $PH3^+$ nuclei/ mm^2 respectively vs 64.34 $PH3^+$ nuclei/ mm^2, p = 0.095 and p = 0.056 respectively) (Figure 6.10c). These changes were not significant, but indicate a proliferation inducing effect of Wnt signaling in the hindbrain. Wnt inhibition also lead to a loss of the enrichment of IdU^+ cells at the RBs, instead these showed a more stochastic pattern (Figure 6.10b). The specific activation of Wnt signaling at the RBs may thus serve to limit proliferation to specific zones of the hindbrain.

To look in further detail at proliferation in the hindbrain we turned to cell cycle analysis by flow cytometry. Hindbrains from st 41 Wnt reporter tadpoles were dissected, dissociated and cellular DNA content was revealed by Hoechst staining (20 hindbrains, 3 replicates). Cells were first gated to limit analysis to single cells (Figure S6.3). GFP^- sibling tadpoles were used to set the GFP gate. GFP^+ cells, which in Wnt reporter hindbrains correspond to boundary cells, showed significantly less cells in G_0/G_1 phase compared to GFP^- cells, which correspond to rhombomere center cells (47.53% vs 82.03%; p<0.0001). Furthermore significantly more cells were in S- and G_2/M-phase in the GFP+ population compared to GFP^- cells (S: 35.70% vs 8.53%; p<0.0001 and G_2/M: 15.10% vs 4.80%; p<0.0001) (Figure 6.11). This confirms that RB cells are actively cycling cells.

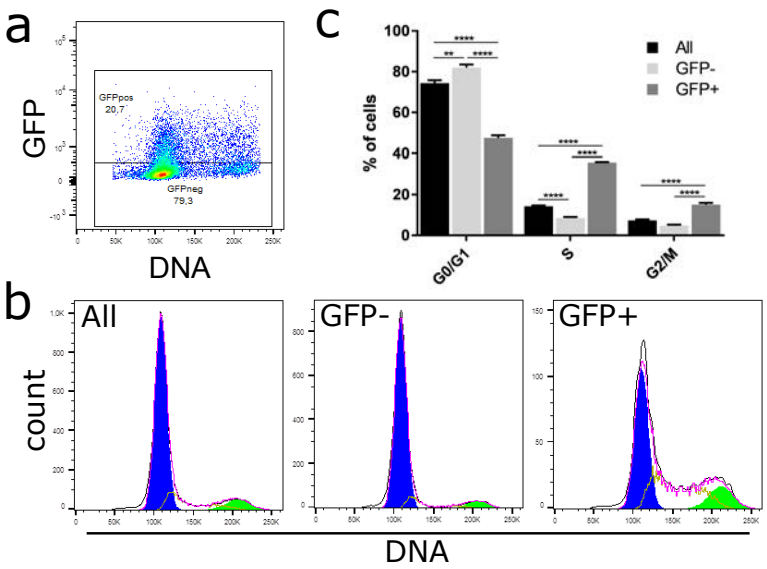

Figure 6.11 Rhombomere boundary cells are actively cycling. (a) GFP positive RB hindbrain cells from a transgenic Wnt reporter *Xenopus* line were gated out from GFP negative hindbrain cells. (b) Histograms showing cell cycle phase distribution of the different cell populations. Pink line represents the optimal histogram deduced by the FlowJo Cell Cycle Analysis algorithm. Blue peak and grean peak represent cells in G0/G1- and G2/M-phase, respectively. Yellow line represents cells in S-phase. (c) Quantification of cell cycle phase distribution. GFP+ cells contain significantly less cells in G0/G1 and more in S- and G2/M- phase.

The GFP^+ cells correspond to cells with active Wnt signaling. However, the GFP^+ signal is confined to RB cells in which other signaling pathways might also be active. To validate that Wnt signaling is responsible for the enhanced proliferation in RB cells we again interfered with Wnt signaling by treatment with BIO or IWR1 and checked for cell cycle phase distribution in the hindbrain. Wnt activation and inhibition resulted in respectively an increase and a decrease of both the amount of

GFP$^+$ cells and the signal intensity, proving the efficacy of the treatments (Figure 6.12). Wnt signaling activation induced ectopic GFP+ cells in the rhombomere centers. If Wnt signaling is not responsible for the enhanced proliferation these GFP$^+$ rhombomere center cells should maintain the same cell cycle kinetics as before and no change in overall cell cycle phase distribution should be observed. However, upon Wnt activation there was a reduction of cells in G_0/G_1 and an increase of cells in S-phase, compared to DMSO treated tadpoles (G_0/G_1: 68.37% vs 74.40%; p = 0.0096 and S: 19.07% vs 14.27%; p = 0.031). We also observed an increase in G_2/M-phase cells, but this was not significant (9.93% vs 7.40%; p = 0.22) (Figure 6.12). Even though there was approximately a 10% drop in GFP$^+$ cells in the tadpoles treated with IWR1 and the expected trend in phase distribution with fewer cells in S- and G_2/M-phase was observed, there was again no significant difference in cell cycle phase distribution compared to DMSO treated tadpoles (G_0/G_1: 75.03% vs 74.40%; p = 0.66, S: 12.97% vs 14.27%; p = 0.38 and G_2/M: 7.21% vs 7.40%; p = 0.89) (Figure 6.12). In conclusion, our data strongly suggest that active Wnt signaling is responsible for increased proliferation in RB cells.

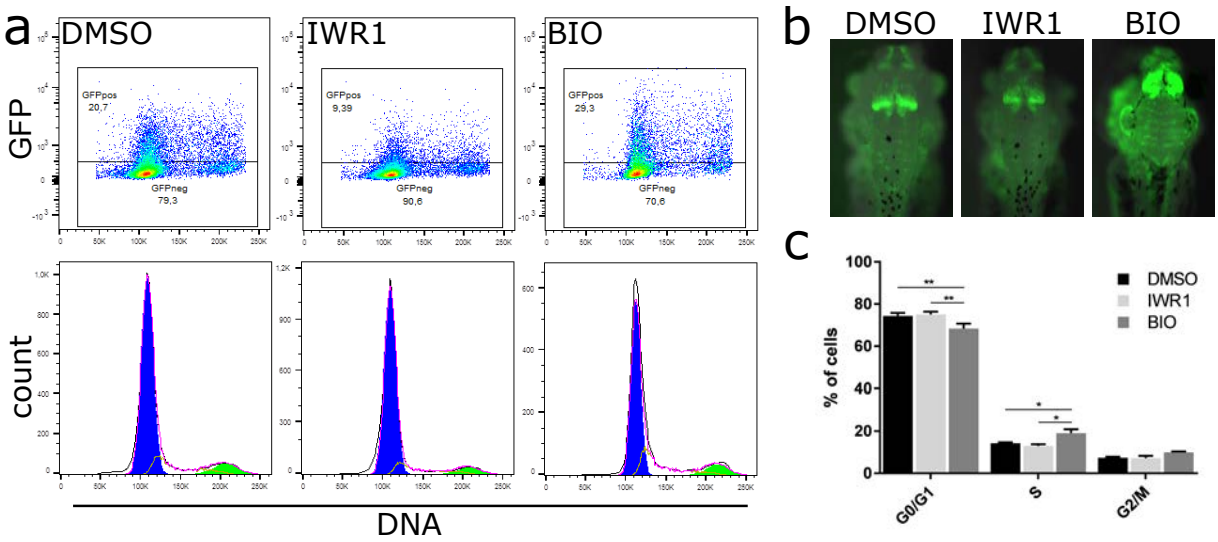

Figure 6.12 Wnt signaling drives rhombomere boundary cell proliferation. (a) GFP positive versus GFP negative cells in the hindbrain (upper panels) and histograms showing cell cycle phase distribution in the hindbrain after the different pharmacological Wnt-interfering treatments (lower panels). (b) Endogenous GFP signal in Wnt reporter embryos after the different treatments showing efficacy of the treatment. (c) Quantification of cell cycle phase distribution after the different treatments showing reduction of cells in G_0/G_1 and increase of cells in S-phase after Wnt activation.

6.3.8 Increase in cell cycle exit upon Wnt signaling inhibition

If Wnt signaling activity in the rhombomere boundaries prevents cell cycle exit, we would expect an increase in cell cycle exit and neural differentiation upon Wnt signaling inhibition. We performed FISH for a neural progenitor marker, sox3, and an immature neuron marker, MyT1, combined with eGFP detection in Wnt reporter embryos. After whole mount staining, embryos were sectioned with a vibratome generating transversal sections through the hindbrain. RBs could be identified through the presence of eGFP expression. In untreated embryos, neural progenitor cells are located at the ventricular area of the brain (Figure 6.13). Upon cell cycle exit, immature neurons migrate away from the ventricular area towards the more lateral mantle zone. Chemical Wnt signaling interference introduced no changes in *sox3* expression (Figure 6.13). However, upon Wnt signaling inhibition there was a clear increase in expression of *myt1*, especially around the ventricular area, indicating that Wnt signaling inhibition leads to increased cell cycle exit (Figure 6.13). No clear downregulation of *myt1* expression was observed upon Wnt signaling activation. Together, these results confirm the

observations made through cell cycle analysis and indicate a role for Wnt signaling in preventing cell cycle exit at the RBs.

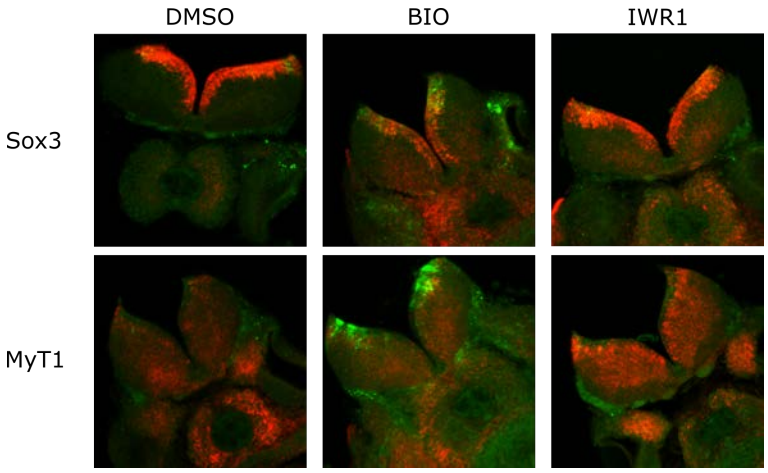

Figure 6.13 Wnt signaling inhibition induces cell cycle exit. Transversal sections through the hindbrain after FISH for sox3 (red, upper panels) or MyT1 (red, lower panels) combined with eGFP (green). Sox3 marks neural progenitor cells and expression is confined to the ventricular area of the hindbrain. MyT1 is a marker for immature neurons and its expression pattern shows migrating immature neurons from the ventricular area to more lateral brain areas. Wnt signaling interference causes no changes in sox3 expression. Wnt signaling inhibition leads to an increase in MyT1 expression.

6.4 DISCUSSION

The role of the establishment of signaling centers at boundary regions between neuromeres has remained unclear. Here we show that Wnt signaling is induced in the *Xenopus* rhombomere boundaries from st 41 onwards. We revealed an antagonistic signaling network between Wnt and Notch in the *Xenopus* hindbrain at this stage. Furthermore, we showed that Wnt activation induces proliferation of rhombomere boundary cells.

6.4.1 WNT-NOTCH SIGNALING ANTAGONISM IN THE RHOMBOMERE BOUNDARIES

6.4.1.1 Wnt signaling activity in Xenopus rhombomere boundaries

Wnt and Notch signaling are highly linked during vertebrate development. Numerous interactions between both pathways at various levels have been described [38, 39]. A previous research paper about Notch-Wnt signaling in the zebrafish hindbrain suggested the existence of a signaling network analogous to the dorso-ventral boundary in the *Drosophila* wing disc [40]. According to this model Notch signaling is active in the RBs and induces Wnt ligand expression. As a result, the Wnt pathway is activated in the cells immediately flanking the boundary. Moreover, a positive feedback loop is proposed to exist between both pathways whereby the RB flanking Wnt-responsive cells express the Notch ligand delta [11]. In conflict with this model, the *Xenopus* Wnt reporter embryos show active Wnt signaling within the RBs, disqualifying a similar signaling network. Moreover, we found that in *Xenopus*, Notch responsive genes such as *nrarp* and *hes5* are expressed in the rhombomeres but are excluded from the boundaries. As a note of caution, it is unclear how the developmental stages in both species compare and some of the observed differences might be due to a discrepancy between developmental time points that were analyzed.

In zebrafish at least four Wnt ligands are expressed in the RBs [11]. We checked expression of all Wnt ligands based on published literature and our own WISH experiments (Figure 6.2) [24]. No Wnt ligands were found to be specifically expressed in the RBs in *Xenopus*, and *wnt3, wnt3a* and *wnt4* showed a segmented expression pattern in the hindbrain while others such as *wnt2b* showed more

uniform expression across the boundaries (Figure 6.2). We attempted to identify the ligand responsible for Wnt signaling activity in the RBs via CRISPR/Cas9 mediated mosaic knock out of the different Wnt ligands and assessment of remaining Wnt activity in reporter tadpoles (Figure 6.3). However, results were inconclusive probably due to redundancy of different Wnt ligands. In zebrafish knockout and knock down of four different Wnt ligands was needed to elicit disturbance of Wnt signaling at the RBs [11]. Another possible mechanism interfering with ligand identification is genetic compensation upon knockout of specific Wnt genes as has been documented in zebrafish studies [25].

6.4.1.2 Notch signaling factors are excluded from the rhombomere boundaries

Since the observed pattern of Wnt signaling activity did not comply with the proposed model in zebrafish, we decided to also assess Notch signaling activity in the *Xenopus* hindbrain. We performed a broader screen of the Notch signaling pathway in the hindbrain and showed that, except for *hes1,* all Notch signaling factors are expressed in the rhombomeres, but are actually excluded from the RBs.

While Hes1 is mainly considered to be a Notch signaling target, Notch independent transcription of Hes1 has been described. In the mouse retina Sonic Hedgehog induces Hes1 expression, and also Wnt signaling has been shown to induce its expression [28-30]. We show here that *hes1* is a direct target gene of Wnt/β-catenin signaling. The *Xenopus tropicalis hes1* promoter is responsive to Wnt/β-catenin signaling *in vitro* and β-catenin directly binds to one of four LEF/TCF sites in the *hes1* promoter. *Hes1* is continuously expressed at high levels in boundary regions as opposed to its normal oscillating expression profile [31]. In the midbrain-hindbrain boundary in the mouse, which is characterized by active Wnt signaling, it was shown that *Wnt1* expressing cells co-express *Hes1* [32]. *Hes1* is also highly expressed in the RBs of the *Xenopus* hindbrain, where, as demonstrated here, Wnt signaling is also active. Moreover, we show that active Wnt signaling at the RBs is necessary for maintaining *hes1* expression in the RBs. Hence, there might be a general role for Wnt-induced *hes1* expression at boundary regions in the developing central nervous system.

Expression of all other Notch signaling factors was confined to the rhombomeres and was excluded from the RBs. Peres et al. already showed exclusion of *delta2* from the RBs in *Xenopus* [41]. Also in zebrafish the *hes5* orthologue *her4* is not expressed in the RBs [42]. In embryonic stem cells, sustained Hes1 expression leads to inhibition of Notch signaling and reduced expression of Notch signaling factors *delta, jagged, notch1* and *hes5* [43]. All this argues against Notch signaling activation in the RBs. In the mouse, *fringe* genes show the same expression pattern in the hindbrain we observed here in *Xenopus* with three longitudinal stripes from dorsal to ventral. Also similarly, *delta* expression coincided with *fringe* expression, while *jagged* was expressed in the complementary region, between the longitudinal stripes. This expression pattern has been linked to neurogenesis [44]. This indicates that Notch signaling activity in the hindbrain is involved in neurogenesis at this stage of development and argues against a role in further patterning of the hindbrain like suggested before [11].

6.4.1.3 Antagonistic signaling network between Wnt and Notch signaling

Our observations reveal an antagonistic relationship between both signaling pathways in the RBs. Wnt signaling activation leads to reduced expression of all Notch signaling factors in the hindbrain. Wnt inhibition leads to a narrowing of the RBs and almost continuous expression of Notch signaling factors throughout the hindbrain. Conversely, Notch signaling activation leads to almost complete disappearance of Wnt signaling activity in the RBs and Notch inhibition leads to a broadening of Wnt signaling activity at the RBs and ectopic foci of Wnt signaling activity in the hindbrain. How the

signaling antagonism is achieved requires further investigation. Wnt-Notch signaling antagonism in other systems is often associated with a transcription-independent mechanism, by direct interaction between signaling components of both pathways [45-47]. This direct antagonism would ensure clear separation of Wnt active versus Notch active cells and thus binary cell fate decisions, which is required in many systems, such as the intestinal epithelium [48]. In addition, the antagonism could also be important for transitions in cell state within one cell lineage, as observed during myogenesis [45]. In the intestinal epithelium, Tian et al. showed that Notch functions as a brake on Wnt signaling activation and that inhibition of the Notch pathway is needed for high Wnt signaling activity [49]. This indicates that the Wnt ON, Notch OFF signature of the RBs might define these cells and guarantee a different fate than the neighboring hindbrain cells.

6.4.2 WNT SIGNALING INDUCES PROLIFERATION OF RHOMBOMERE BOUNDARY CELLS

The actual function of active Wnt signaling in the RBs remained unclear. A role in hindbrain patterning was unlikely, as Wnt signaling is activated in the RBs only at later stages in development when crude patterning is complete. Indeed, we did not observe any defects in segmental organization of cranial motor nuclei upon Wnt signaling interference.

Since Wnt signaling is highly linked to neural progenitor proliferation and differentiation in the brain [16, 50-53], we hypothesized that Wnt signaling in the RBs might influence cell proliferation in the hindbrain. We show that Wnt positive boundary cells are actively dividing. More Wnt active cells are in S- or G2/M-phase compared to Wnt negative cells, which are more likely to be in G0/G1-phase. Furthermore, upon experimental Wnt signaling activation significantly more cells were found in S-phase and less in G0/G1-phase compared to control hindbrains. This indicates that active Wnt signaling is specifically important for the G1-S-phase transition and thus shortens the G1 phase. This is further supported by our observation that IdU-labeled cells are enriched at the RBs. In the chick spinal cord, only Wnts specifically expressed at the dorsal midline, but not more widely expressed Wnts, were shown to have a mitogenic effect on neural progenitor cells through promotion of cell cycle progression from G1- to S-phase and inhibition of cell cycle exit [54]. The mitogenic effect of Wnt signaling was a consequence of upregulation of the G1-to-S-phase-promoting cyclins, *CyclinD1* and *CyclinD2* [54, 55]. *CyclinD1* is a well-known direct target gene of Wnt/β-catenin signaling [56, 57]. Moreover, in zebrafish *cyclinD1* is expressed in the RBs [20]. Regulation of G1 length determines the balance between neural progenitor self-renewal and cell cycle exit and concomitant differentiation. An increase in G1 length leads to differentiation and reduction of the NSC pool [58]. Hence, Wnt signaling in the RBs might be important for NSC maintenance by promoting cell cycle progression from G1- to S-phase. In support of this, we show that Wnt signaling inhibition leads to increased expression of MyT1, a marker for immature neurons, indicating increased cell cycle exit.

A recent paper identified the RBs in chick as pools of $Sox2^+$ neural progenitor/stem cells, which are multipotent and self-renewing [14]. In general, neural stem cells (NSCs) are considered to be slow-proliferating and quiescent cells in the central nervous system [59]. Peretz et al. found non-dividing $Sox2^+$ cells in the center of the RBs, while immediately adjacent to the RBs $Sox2^+$ cells are dividing. They showed that RBs actively contribute cells to the adjacent rhombomeres by cell division and migration [14]. This indicates that RBs as being a reservoir of either quiescent or proliferating NSCs, might be a conserved feature across amniotes and anamniotes. Wnt signaling has been shown to induce proliferation of quiescent NSCs in the adult brain in different contexts like physiological neurogenesis and injury [60-62]. In chick no Wnt signaling at the RBs has been described. In *Xenopus* we observe active Wnt signaling mainly in the ventricular area. This could mean that active Wnt

signaling characterizes either activated NSCs that will divide and contribute new neurons to the adjacent rhombomeres upon activation of Notch signaling or alternatively, based on the G1 shortening, active Wnt signaling characterizes a subgroup of rhombomere boundary NSC that still undergo active self-renewal and are not yet quiescent. Further research is needed to distinguish between both options.

6.5 Conclusions

With this research we provide insight into Wnt-Notch signaling interaction at the rhombomere boundaries and describe a novel role for Wnt/β-catenin signaling at neuromere boundaries. In conclusion, we show here that Wnt signaling is active in the dorsal-ventricular area of the rhombomere boundaries in the *Xenopus* hindbrain. We propose a model in which active Wnt signaling marks a subpopulation of self-renewing neural stem cells in the rhombomere boundaries. Moreover, Wnt signaling is needed to maintain the boundaries as Notch signaling-free zones, while Notch signaling induces neurogenesis in the rhombomere centers through prevention of Wnt signaling.

6.6 Materials and Methods

6.6.1 Transgenic lines and DNA constructs

Wnt reporter, LEF-VP16 and LEF-EnR transgenic lines were constructed in our lab and are described elsewhere [23, 63]. pGL3b-xtHes1p was constructed by ligating the PCR amplified *X. tropicalis hes1* promoter between the SacI and HindIII sites of the pGL3basic vector. The pCS2+-β-CatS33A and pCDNA3-DNTCF4 plasmids were kindly provided by Dr. Barry Gumbiner and Dr. Frank McCormick and Dr. Osamu Tetsu, respectively. The pCS2-NICD-GR and pCS2-DBM-GR plasmids were a kind gift from Dr. Kelly McLaughlin and Dr. Eric Bellefroid kindly provided the pCS2-Su(H)ANK-GR plasmid. All constructs have been described before [35, 36].

6.6.2 Wnt reporter activity detection

Wnt reporter embryos were obtained via natural mating. Wnt reporter embryos were selected based on presence of GFP signal and raised in 0.1x MMR until the desired developmental stage was reached. For endogenous GFP signal detection embryos were fixed with GFP-fixative (4% paraformaldehyde/ 80 mM Na_2HPO_4/ 20 mM NaH_2PO_4). After fixation either the skin above the brain and roof plate was removed or the brain was dissected out.

6.6.3 Whole mount in situ hybridization

Probes for wnt1, wnt2b, wnt3, wnt3a, wnt4, wnt5a, wnt5b, wnt8a, wnt8b, wnt10b, wnt11, wnt11b, notch1, notch2, notch3, delta1, delta2, jagged1, jagged2, lfng, nrarp, hes5, hes1, sox3 and myt1 were made by picking up the coding sequence by PCR with primers linked to RNA-polymerase sites. Primer sequences can be found in supplemental table 1. The islet-1 probe was a kind gift from Dr. Petra Pandur [64]. Sense and antisense RNA probes were generated by transcription with the appropriate RNA polymerase and digoxigenin-rUTP-label. Enhanced GFP probe was made using fluorescein-rUTP-label. Whole mount in situ hybridization was carried out according to [65]. Between fixation and dehydration the skin above the brain was removed. Images were taken using a Zeiss stereomicroscope Lumar-V12 with an AxioCam MRc camera using the Axiovision software package.

6.6.4 WHOLE MOUNT FLUORESCENT IN SITU HYBRIDIZATION

Whole mount fluorescent *in situ* hybridization with tyramide signal amplification for eGFP was performed according to [66]. For all other probes, the same protocol was used except for the fluorogenic reaction which was performed according to [67] with addition of 4-iodophenol in the reaction buffer. Between fixation and dehydration the skin above the brain and roof plate was removed. For vibratome sectioning, stained embryos were first incubated in 3% low melting agarose/PBS at 37°C and then embedded in 5% low melting agarose/PBS. 50 µm sections were made using a Leica VT1000S vibratome. Imaging was done with a Leica TCS LSI macroconfocal microscope. Maximal projection images were made using ImageJ software.

6.6.5 CRISPR/CAS9 MEDIATED DISRUPTION OF WNT LIGANDS

Design of gRNAs was performed with the CRISPRScan algorithm [68]. Generation of DNA templates was done with a PCR-based method departing from one common oligonucleotide and one partly complementary oligonucleotide containing the target site according to [69]. Hanging ends were filled in with a standard PCR reaction using Phusion high-fidelity polymerase (Thermo scientific). Oligonucleotide sequences for the different Wnt ligands are shown in Supplemental table 6.2. Purification was done through phenol/chloroform extraction and sodiumacetate precipitation followed by dilution in RNAse-free water. RNA transcription was performed using HiScribe™ T7 High Yield RNA Synthesis Kit (New England Biolabs) and gRNAs were purified by phenol-chloroform extraction/ammoniumacetate precipitation and diluted in RNAse-free water. Concentrations were determined by Nanodrop (Thermo-Scientific). 400 ng/µl gRNA is combined with 900 ng/µl recombinant NLS-Cas9-NLS protein [70] and incubated at 37°C for 1 minute for ribonucleoprotein complex assembly. 1 nl of the injection mixture is injected in each animal-dorsal blastomere of an 8-cell stage embryo. For analyzing the genome editing efficiency a minimum of 5 stage 56 tadpoles were lysed overnight at 55 °C in lysis buffer containing proteinase K (50 mM Tris pH 8.8, 1 mM EDTA, 0.5% Tween-20, 200 µg/ml proteinase K). The locus of interest was amplified by PCR with the respective primer pairs as shown in Supplemental table 6.2. Targeted deep sequencing of PCR products was performed using a previously described workflow [71, 72].

6.6.6 LUCIFERASE ASSAY

HEK T293 cells were seeded in a 24-well plate in DMEM medium supplemented with 10% fetal calf serum. The next day $CaCl_2$ cotransfection of reporter plasmids, a β-galactosidase plasmid for normalization and the various Wnt and Notch interfering constructs (described above) was performed in triplicate. Luciferase assay was performed 48 hours later. Lysates were prepared using the lysis buffer provided with the Galacto-Star kit (Applied Biosystems). 10 µl of lysate was combined with 100 µl of the β-gal substrate provided in the same kit and 50 µl of the lysate was combined with 100 µl luciferase substrate (40 mM Tricine, 2.14 mM $(MgCO_3)4Mg(OH)_2$, 5.34 mM $MgSO_4$, 66.6 mM DTT, 0.2mM EDTA, 521 µM coenzyme A, 734 µM ATP and 940 µM luciferin). Plates were read out using a Roche luminometer. pCS2 transfected cells were used as a negative control.

6.6.7 WNT AND NOTCH SIGNALING INTERFERENCE

Wild type *X. tropicalis* embryos were injected at the 2-cell stage in both blastomeres with inducible Wnt activating (100 pg) /inhibiting (300 pg) or Notch activating (800 pg) /inhibiting (1400 pg) constructs (described above). Transgenic Wnt reporter, Wnt activating and Wnt inhibiting embryos were obtained by natural mating and selected based on presence of GFP fluorescence. Embryos were

raised in 0.1x MMR at 25°C. Transgenes or injected constructs were activated by the addition of dexamethasone (10 µM) to the rearing medium at st 37. For chemical disruption of Wnt signaling, interfering compounds were dissolved in DMSO and added to the rearing medium at st 37: BIO (2 µM), IWR1 (10 µM) and IWP12 (25 µM). As a negative control non-injected dexamethasone treated, non-transgenic or DMSO-treated embryos were used. All embryos were fixed at st 41. Fixative was dependent on the downstream application. The skin above the brain and roof plate was removed after fixation.

6.6.8 WHOLE MOUNT IMMUNOFLUORESCENCE

For IdU labeling of proliferating cells st 41 embryos were incubated for 30' in rearing medium containing 3.8 mM IdU before fixation in 4%PFA/PBS and dehydrated in methanol. After rehydration antigen retrieval was performed by 15' incubation in 150 mM Tris-HCl buffer (pH 9.0) at 70°C followed by 20' incubation in acetone at -20°C for tissue permeabilization. For IdU detection embryos were incubated in 2N HCl for 1h at room temperature. Blocking was performed in PBS containing 10% goat serum, 0.8% TritonX-100 and 1% BSA followed by primary antibody incubation in the blocking buffer: rabbit polyclonal anti-phospho-Histone H3 (Ser10) (1/250, cat# IHC-00061, Bethyl Laboratories) or mouse monoclonal anti-BrdU (1/400, 347580, BD Biosciences) and rabbit polyclonal anti-GFP (1/100, cat# 632376, Clontech). After washing embryos were incubated with an appropriate Dylight fluorochrome conjugated secondary antibody (1/500, Thermo Fisher Scientific). Nuclear counterstaining was performed by incubation with DAPI (100 µM). Imaging was done with a Leica TCS LSI macroconfocal microscope. Maximal projection images were made using ImageJ software. For quantification of $PH3^+$ nuclei all stained nuclei in the hindbrain were counted with the PointPicker plugin for ImageJ and normalized against the hindbrain area.

6.6.9 CELL CYCLE ANALYSIS

Hindbrains from st 41 Wnt reporter *X. tropicalis* embryos were dissected out and pooled per 20 in 70% L15 medium on ice. For each treatment 3 replicates were made. To dissociate hindbrains, they were incubated in 0.033% Trypsin/0.021% EDTA at room temperature for 8' followed by mechanical dissociation in Ca^{2+}-free medium (116.6 mM NaCl, 0.67 mM KCl, 4.62 mM Tris-HCl, 0.4 mM EDTA, pH 7.8) after which an equal volume of Ca^{2+}-free medium containing 2% BSA was added. Cells were collected by centrifugation at 200 g and resuspended in 0.66x PBS. An equal volume of ice cold 2% paraformaldehyde/0.66x PBS was added and the cell suspension was incubated on ice for 30'. Cells were collected by centrifugation at 700 g, washed with PBS containing 1% BSA, centrifuged, resuspended in ice-cold 70% ethanol/PBS while sitting on a vortex and incubated overnight at 4°C. The next day cells were collected by centrifugation, washed and incubated in 2 µg/ml Hoechst 33342 in PBS for 30' at room temperature. Acquisition was done in the staining solution on a FACSVerse (BD Biosciences). Cell cycle analysis was performed using the embedded algorithm in the FlowJo software.

6.6.10 STATISTICAL METHODS

For evaluation of expression patterns 6-8 embryos per probe/ treatment were used and experiments were repeated at least twice. Representative images are shown. Luciferase assays and cell cycle analysis were performed at least 3 times (biological replicates) and each treatment was performed in triplicate. Error bars represent standard error to the mean. For luciferase assay non-parametric unpaired t-tests using Mann-Whitney were performed to determine statistical significance. For cell

cycle analysis multiple t-tests analysis was performed to determine statistical significance. Statistical significance was set at *p<0.05, **p<0.01, ***p<0.001 and ****p<0.0001.

6.7 Author contributions

RN and KV designed and conceived the study and wrote the manuscript. RN performed all the experiments. BD performed WISH for Wnt ligands. AK performed IdU and PH3 IHC. GVI provided technical input in flow cytometry experiments.

6.8 Acknowledgements

The authors would like to thank Griet Van Imschoot technical assistance with the experiments. The authors are indebted to Tim Deceuninck for animal care. The plasmids used in this study were kindly provided by Dr. Barry Gumbiner, Dr. Frank McCormick, Dr. Osamu Tetsu, Dr. Kelly McLaughlin and Dr. Eric Bellefroid.

6.9 Supplemental information

Expression pattern of additional Notch signaling factors is illustrated in Figure S6.1. Additional images of expression pattern of Notch signaling factors upon Wnt signaling interference are shown in Figure S6.2. Gating strategy for cell cycle analysis is illustrated in Figure S6.3. Primer sequences used for generation of *in situ* hybridization RNA-probes are listed in Supplemental table 6.1. Target sequences of gRNA targeting Wnt ligands and their respective deep sequencing primers are listed in Supplemental table 6.2.

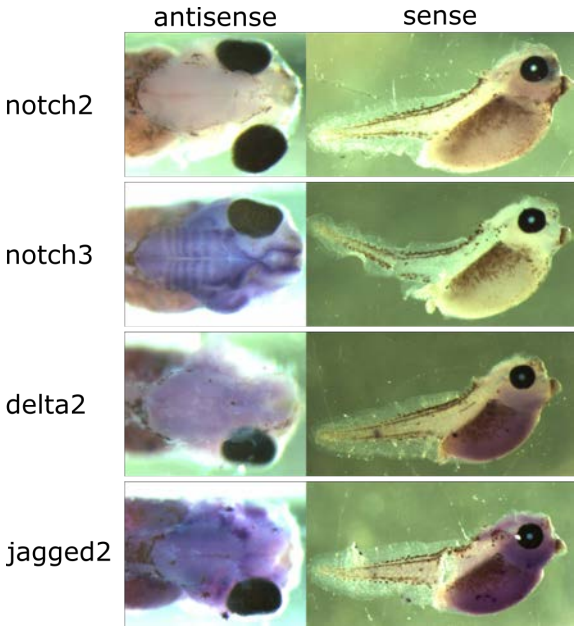

Figure S6.1 Expression of Notch factors in the hindbrain. Dorsal view of the *X. tropicalis* brain at stage 41. *Notch3* shows a similar expression pattern as *notch1. Notch2, delta2* and *jagged2* are not specifically expressed in the hindbrain. Sense probes were used as a negative control.

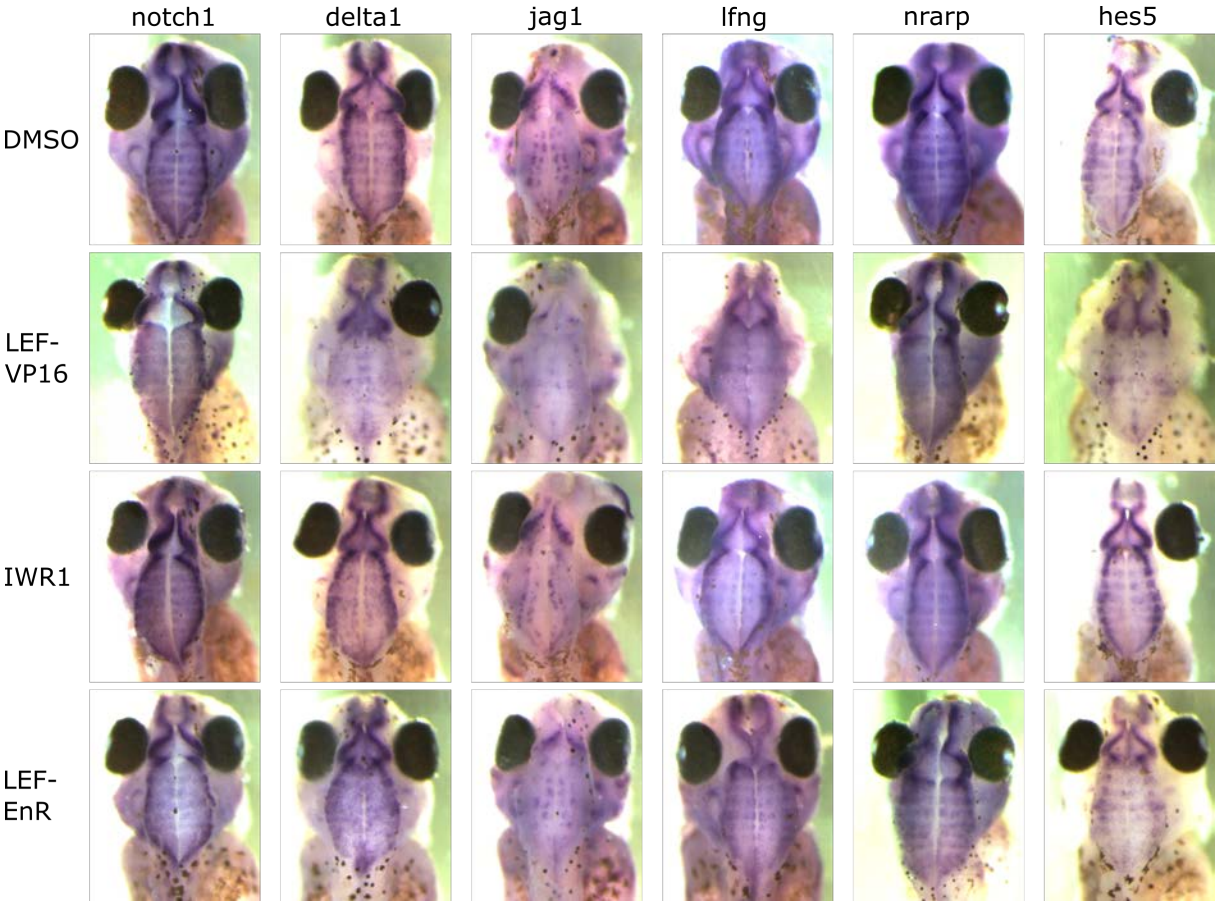

Figure S6.2 Effect of Wnt signaling interference on expression of Notch signaling factors. Embryos expressing the Wnt-activating construct LEF-VP16 show reduced expression of Notch signaling factors in the hindbrain. Wnt signaling inhibition through treatment with IWR1 or expression of LEF-EnR leads to no obvious changes in expression of Notch signaling factors.

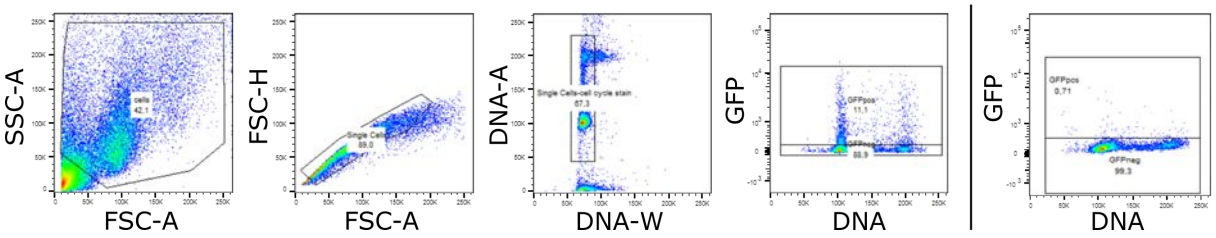

Figure S6.3 Gating strategy for cell cycle analysis. Cells were first identified through forward scatter (FSC) versus side scatter (SSC). Single cells were gated in two different ways: FSC height versus area and Hoechst signal area (DNA-A) versus Hoechst signal width (DNA-W). GFP positive cells were gated based upon hindbrains from GFP negative sibling tadpoles (panel on the right).

Supplemental table 6.1 Sequences of primers used for production of *in situ* hybridization probes.

gene		Primer sequence (5' → 3')
wnt1	F	CCCTGTCTCCCAGCAATGAG
	R	CATCCATCTAGTCCCAATGAAGTG
wnt2b	F	ACTCATCCTGGTGGTATATTGGT
	R	ACTTGAAGGGCTCATGTTTGG
wnt3	F	TTACACTTCCTCTGGATCTTCTC
	R	GACACTTCTCCTTGCGTTTCTC
wnt3a	F	GGGCTGCTTTGGATATTTCC
	R	TTCTTGACAGCTGACGTAGCA
wnt4	F	CATGTAACGGGACCTTAGGA
	R	GCAACTACACCTTTCTATGATCTC
wnt5a	F	GATCCCTGAGGTTTATATCATTGG
	R	TTGAAACCGAGGAGTAAGTG

wnt5b	F	TACTGTTGGTCACTTCTCTACTG
	R	CTTGGACCGTCTTGAATTGG
wnt8a	F	GTTTGTCCTTTCAACTCTTCTC
	R	ATTAGAATCCCTTTCCCTTCTG
wnt8b	F	TAGCGTCTCAGGGTATTCCA
	R	GTACCCAGAAGTCCCAAAGTC
wnt10b	F	ATGAAGAAAGAGCCTCACCATCTG
	R	GCCAAGCGTTTCTTGTTTAACC
wnt11	F	GGATCTGCCAAGGAATTAAATGGT
	R	TAGCAACACCAGTGGTACTTACAG
wnt11b	F	ACTGTGTCACCCTACTACTC
	R	GTCCGCTCACATTTCTTACAC
notch1	F	AACGAGTGCTTATCCAATCC
	R	CGCTTCTTATTCACGATGAC
notch2	F	CGGATACATTTGCCATTGCT
	R	ATTCATTCACATCGCCTTCAC
notch3	F	CTCTGGATATGAAGGGAAGAACTG
	R	GCTTTGATTGGATAGGGAAACTG
delta1	F	CCCACTTTCAGCAATCCT
	R	ACCCTTACACAGACAACCA
delta2	F	GAAGTCCTGTTTACCCAACTG
	R	TTCACACCTGTAACCATTCTC
jagged1	F	GACAAAGCCCTCCATTCTG
	R	TTGCCCTCGTAGTCTTCTG
jagged2	F	GAGTTTCAGGCCAAGATTACC
	R	ATAGCACCGAGCTTTGTTCTG
lfng	F	GGTGCTCATGGTGGATCAG
	R	CAGGGAAACTTGGGACGA
nrarp	F	CCTTCTTGGTGGACCTTCTC
	R	AAACTCACACTCACGCTCAC
hes5	F	CAAGCAGGAACCCAATGTC
	R	GGGAACAGCCATCTACAG
hes1	F	CCTTGGTGTTCAGTTGGT
	R	AGAAGTCCCAAAGTCATTTCC
sox3	F	CTGACTGGAAGTTGTTGAG
	R	ATAAAGAACACCTGGAACCT
myt1	F	CATAGCCAATTCCCTTCTAAACCT
	R	ACACTTCAGCACATTCTCGT

Supplemental table 6.2 Oligonucleotide sequences for Wnt ligand gRNA generation and deep sequencing primers. gRNA target sites are captilized in the oligonucleotide sequences.

Wnt ligand	**Oligonucleotide sequence (5' → 3')**	**Primer sequence (5' → 3')**
reverse oligo	aaaagcaccgactcggtgccacttttcaagttgataacggactagccttattttaacttgctatttctag ctctaaaac	na
wnt3	gaattaatacgactcactataGGGCAGCTGAGAAGATCCAGgttttagagctagaaatagc	F: CCCTCGCCATAATCAGAC R: GTCCTGCTTCAAAGTAAATTGG
wnt3a	gaattaatacgactcactataGGAGATCATGCCCAGCGTGGgttttagagctagaaatagc	F: GCCGAAACAATAGCATTTACTG R: CCACCGCAATCTGACATCTG
wnt4	gaattaatacgactcactataGGTAATGGATTCGGTCCGACGgttttagagctagaaatagc	F: AGTAGGGCTCTTCTCATTCTG R: ACCAAACGCAGATGTAACAC

6.10 REFERENCES

1. Alexander, T., C. Nolte, and R. Krumlauf, *Hox genes and segmentation of the hindbrain and axial skeleton.* Annu Rev Cell Dev Biol, 2009. **25**: p. 431-56.
2. Wizenmann, A. and A. Lumsden, *Segregation of rhombomeres by differential chemoaffinity.* Mol Cell Neurosci, 1997. **9**(5-6): p. 448-59.
3. Xu, Q., et al., *In vivo cell sorting in complementary segmental domains mediated by Eph receptors and ephrins.* Nature, 1999. **399**(6733): p. 267-71.
4. Calzolari, S., J. Terriente, and C. Pujades, *Cell segregation in the vertebrate hindbrain relies on actomyosin cables located at the interhombomeric boundaries.* EMBO J, 2014. **33**(7): p. 686-701.
5. Guthrie, S., M. Butcher, and A. Lumsden, *Patterns of cell division and interkinetic nuclear migration in the chick embryo hindbrain.* J Neurobiol, 1991. **22**(7): p. 742-54.
6. Heyman, I., A. Faissner, and A. Lumsden, *Cell and matrix specialisations of rhombomere boundaries.* Dev Dyn, 1995. **204**(3): p. 301-15.
7. Martinez, S., et al., *Reduced junctional permeability at interrhombomeric boundaries.* Development, 1992. **116**(4): p. 1069-76.
8. Straka, H., R. Baker, and E. Gilland, *Rhombomeric organization of vestibular pathways in larval frogs.* J Comp Neurol, 2001. **437**(1): p. 42-55.
9. Gilland, E. and R. Baker, *Evolutionary patterns of cranial nerve efferent nuclei in vertebrates.* Brain Behav Evol, 2005. **66**(4): p. 234-54.
10. Lumsden, A. and R. Keynes, *Segmental patterns of neuronal development in the chick hindbrain.* Nature, 1989. **337**(6206): p. 424-8.
11. Riley, B.B., et al., *Rhombomere boundaries are Wnt signaling centers that regulate metameric patterning in the zebrafish hindbrain.* Dev Dyn, 2004. **231**(2): p. 278-91.
12. Weisinger, K., et al., *Analysis of expression and function of FGF-MAPK signaling components in the hindbrain reveals a central role for FGF3 in the regulation of Krox20, mediated by Pea3.* Dev Biol, 2010. **344**(2): p. 881-95.
13. Nittenberg, R., et al., *Cell movements, neuronal organisation and gene expression in hindbrains lacking morphological boundaries.* Development, 1997. **124**(12): p. 2297-306.
14. Peretz, Y., et al., *A new role of hindbrain boundaries as pools of neural stem/progenitor cells regulated by Sox2.* BMC Biol, 2016. **14**: p. 57.
15. Logan, C.Y. and R. Nusse, *The Wnt signaling pathway in development and disease.* Annu Rev Cell Dev Biol, 2004. **20**: p. 781-810.
16. Noelanders, R. and K. Vleminckx, *How Wnt Signaling Builds the Brain: Bridging Development and Disease.* Neuroscientist, 2016.
17. Kopan, R. and M.X. Ilagan, *The canonical Notch signaling pathway: unfolding the activation mechanism.* Cell, 2009. **137**(2): p. 216-33.
18. Cheng, Y.C., et al., *Notch activation regulates the segregation and differentiation of rhombomere boundary cells in the zebrafish hindbrain.* Dev Cell, 2004. **6**(4): p. 539-50.
19. Duncan, R.N., et al., *Identification of Wnt Genes Expressed in Neural Progenitor Zones during Zebrafish Brain Development.* PLoS One, 2015. **10**(12): p. e0145810.
20. Amoyel, M., et al., *Wnt1 regulates neurogenesis and mediates lateral inhibition of boundary cell specification in the zebrafish hindbrain.* Development, 2005. **132**(4): p. 775-85.
21. Gerety, S.S. and D.G. Wilkinson, *Morpholino artifacts provide pitfalls and reveal a novel role for pro-apoptotic genes in hindbrain boundary development.* Dev Biol, 2011. **350**(2): p. 279-89.
22. Troost, T. and T. Klein, *Sequential Notch signalling at the boundary of fringe expressing and non-expressing cells.* PLoS One, 2012. **7**(11): p. e49007.
23. Tran, H.T. and K. Vleminckx, *Design and use of transgenic reporter strains for detecting activity of signaling pathways in Xenopus.* Methods, 2014. **66**(3): p. 422-32.

24. Garriock, R.J., et al., *Census of vertebrate Wnt genes: isolation and developmental expression of Xenopus Wnt2, Wnt3, Wnt9a, Wnt9b, Wnt10a, and Wnt16.* Dev Dyn, 2007. **236**(5): p. 1249-58.
25. Rossi, A., et al., *Genetic compensation induced by deleterious mutations but not gene knockdowns.* Nature, 2015. **524**(7564): p. 230-3.
26. LeBon, L., et al., *Fringe proteins modulate Notch-ligand cis and trans interactions to specify signaling states.* Elife, 2014. **3**: p. e02950.
27. Yun, T.J. and M.J. Bevan, *Notch-regulated ankyrin-repeat protein inhibits Notch1 signaling: multiple Notch1 signaling pathways involved in T cell development.* J Immunol, 2003. **170**(12): p. 5834-41.
28. Issack, P.S. and E.B. Ziff, *Genetic elements regulating HES-1 induction in Wnt-1-transformed PC12 cells.* Cell Growth Differ, 1998. **9**(10): p. 827-36.
29. Kubo, F. and S. Nakagawa, *Hairy1 acts as a node downstream of Wnt signaling to maintain retinal stem cell-like progenitor cells in the chick ciliary marginal zone.* Development, 2009. **136**(11): p. 1823-33.
30. Wall, D.S., et al., *Progenitor cell proliferation in the retina is dependent on Notch-independent Sonic hedgehog/Hes1 activity.* J Cell Biol, 2009. **184**(1): p. 101-12.
31. Shimojo, H., T. Ohtsuka, and R. Kageyama, *Oscillations in notch signaling regulate maintenance of neural progenitors.* Neuron, 2008. **58**(1): p. 52-64.
32. Baek, J.H., et al., *Persistent and high levels of Hes1 expression regulate boundary formation in the developing central nervous system.* Development, 2006. **133**(13): p. 2467-76.
33. Denayer, T., et al., *Canonical Wnt signaling controls proliferation of retinal stem/progenitor cells in postembryonic Xenopus eyes.* Stem Cells, 2008. **26**(8): p. 2063-74.
34. Myers, C.T., S.C. Appleby, and P.A. Krieg, *Use of small molecule inhibitors of the Wnt and Notch signaling pathways during Xenopus development.* Methods, 2014. **66**(3): p. 380-9.
35. Wettstein, D.A., D.L. Turner, and C. Kintner, *The Xenopus homolog of Drosophila Suppressor of Hairless mediates Notch signaling during primary neurogenesis.* Development, 1997. **124**(3): p. 693-702.
36. McLaughlin, K.A., M.S. Rones, and M. Mercola, *Notch regulates cell fate in the developing pronephros.* Dev Biol, 2000. **227**(2): p. 567-80.
37. Dodge, M.E., et al., *Diverse chemical scaffolds support direct inhibition of the membrane-bound O-acyltransferase porcupine.* J Biol Chem, 2012. **287**(27): p. 23246-54.
38. Hayward, P., T. Kalmar, and A.M. Arias, *Wnt/Notch signalling and information processing during development.* Development, 2008. **135**(3): p. 411-24.
39. Munoz Descalzo, S. and A. Martinez Arias, *The structure of Wntch signalling and the resolution of transition states in development.* Semin Cell Dev Biol, 2012. **23**(4): p. 443-9.
40. Buceta, J., et al., *Robustness and stability of the gene regulatory network involved in DV boundary formation in the Drosophila wing.* PLoS One, 2007. **2**(7): p. e602.
41. Peres, J.N. and A.J. Durston, *Role of X-Delta-2 in the early neural development of Xenopus laevis.* Dev Dyn, 2006. **235**(3): p. 802-10.
42. Qiu, X., et al., *Temporal Notch activation through Notch1a and Notch3 is required for maintaining zebrafish rhombomere boundaries.* Dev Genes Evol, 2009. **219**(7): p. 339-51.
43. Kobayashi, T. and R. Kageyama, *Hes1 regulates embryonic stem cell differentiation by suppressing Notch signaling.* Genes Cells, 2010. **15**(7): p. 689-98.
44. Johnston, S.H., et al., *A family of mammalian Fringe genes implicated in boundary determination and the Notch pathway.* Development, 1997. **124**(11): p. 2245-54.
45. Collu, G.M., et al., *Dishevelled limits Notch signalling through inhibition of CSL.* Development, 2012. **139**(23): p. 4405-15.
46. Acosta, H., et al., *Notch destabilises maternal beta-catenin and restricts dorsal-anterior development in Xenopus.* Development, 2011. **138**(12): p. 2567-79.
47. Lawrence, N., et al., *Notch signaling targets the Wingless responsiveness of a Ubx visceral mesoderm enhancer in Drosophila.* Curr Biol, 2001. **11**(6): p. 375-85.

48. Collu, G.M., A. Hidalgo-Sastre, and K. Brennan, *Wnt-Notch signalling crosstalk in development and disease.* Cell Mol Life Sci, 2014. **71**(18): p. 3553-67.
49. Tian, H., et al., *Opposing activities of Notch and Wnt signaling regulate intestinal stem cells and gut homeostasis.* Cell Rep, 2015. **11**(1): p. 33-42.
50. Chenn, A. and C.A. Walsh, *Regulation of cerebral cortical size by control of cell cycle exit in neural precursors.* Science, 2002. **297**(5580): p. 365-9.
51. Munji, R.N., et al., *Wnt signaling regulates neuronal differentiation of cortical intermediate progenitors.* J Neurosci, 2011. **31**(5): p. 1676-87.
52. Poschl, J., et al., *Constitutive activation of beta-catenin in neural progenitors results in disrupted proliferation and migration of neurons within the central nervous system.* Dev Biol, 2013. **374**(2): p. 319-32.
53. Woodhead, G.J., et al., *Cell-autonomous beta-catenin signaling regulates cortical precursor proliferation.* J Neurosci, 2006. **26**(48): p. 12620-30.
54. Megason, S.G. and A.P. McMahon, *A mitogen gradient of dorsal midline Wnts organizes growth in the CNS.* Development, 2002. **129**(9): p. 2087-98.
55. Du, Z., X. Tong, and X. Ye, *Cyclin D1 promotes cell cycle progression through enhancing NDR1/2 kinase activity independent of cyclin-dependent kinase 4.* J Biol Chem, 2013. **288**(37): p. 26678-87.
56. Tetsu, O. and F. McCormick, *Beta-catenin regulates expression of cyclin D1 in colon carcinoma cells.* Nature, 1999. **398**(6726): p. 422-6.
57. Shtutman, M., et al., *The cyclin D1 gene is a target of the beta-catenin/LEF-1 pathway.* Proc Natl Acad Sci U S A, 1999. **96**(10): p. 5522-7.
58. Hindley, C. and A. Philpott, *Co-ordination of cell cycle and differentiation in the developing nervous system.* Biochem J, 2012. **444**(3): p. 375-82.
59. Suh, H., et al., *In vivo fate analysis reveals the multipotent and self-renewal capacities of Sox2+ neural stem cells in the adult hippocampus.* Cell Stem Cell, 2007. **1**(5): p. 515-28.
60. Adachi, K., et al., *Beta-catenin signaling promotes proliferation of progenitor cells in the adult mouse subventricular zone.* Stem Cells, 2007. **25**(11): p. 2827-36.
61. Imura, T., et al., *Adenomatous polyposis coli is essential for both neuronal differentiation and maintenance of adult neural stem cells in subventricular zone and hippocampus.* Stem Cells, 2010. **28**(11): p. 2053-2064.
62. Piccin, D. and C.M. Morshead, *Wnt signaling regulates symmetry of division of neural stem cells in the adult brain and in response to injury.* Stem Cells, 2011. **29**(3): p. 528-38.
63. Janssens, S., et al., *Direct control of Hoxd1 and Irx3 expression by Wnt/beta-catenin signaling during anteroposterior patterning of the neural axis in Xenopus.* Int J Dev Biol, 2010. **54**(10): p. 1435-42.
64. Brade, T., et al., *The amphibian second heart field: Xenopus islet-1 is required for cardiovascular development.* Dev Biol, 2007. **311**(2): p. 297-310.
65. Monsoro-Burq, A.H., *A rapid protocol for whole-mount in situ hybridization on Xenopus embryos.* CSH Protoc, 2007. **2007**: p. pdb prot4809.
66. Vize, P.D., K.E. McCoy, and X. Zhou, *Multichannel wholemount fluorescent and fluorescent/chromogenic in situ hybridization in Xenopus embryos.* Nat Protoc, 2009. **4**(6): p. 975-83.
67. Lauter, G., I. Soll, and G. Hauptmann, *Sensitive whole-mount fluorescent in situ hybridization in zebrafish using enhanced tyramide signal amplification.* Methods Mol Biol, 2014. **1082**: p. 175-85.
68. Moreno-Mateos, M.A., et al., *CRISPRscan: designing highly efficient sgRNAs for CRISPR-Cas9 targeting in vivo.* Nat Methods, 2015. **12**(10): p. 982-8.
69. Bassett, A.R., et al., *Highly efficient targeted mutagenesis of Drosophila with the CRISPR/Cas9 system.* Cell Rep, 2013. **4**(1): p. 220-8.
70. Naert, T., et al., *CRISPR/Cas9 mediated knockout of rb1 and rbl1 leads to rapid and penetrant retinoblastoma development in Xenopus tropicalis.* Sci Rep, 2016. **6**: p. 35264.

71. Boel, A., et al., *BATCH-GE: Batch analysis of Next-Generation Sequencing data for genome editing assessment.* Sci Rep, 2016. **6**: p. 30330.
72. De Leeneer, K., et al., *Flexible, scalable, and efficient targeted resequencing on a benchtop sequencer for variant detection in clinical practice.* Hum Mutat, 2015. **36**(3): p. 379-87.

PART IIIB

RESULTS

WNT SIGNALING IN THE HINDBRAIN: CANCER

CHAPTER 7

A *XENOPUS TROPICALIS* WNT-TYPE MEDULLOBLASTOMA MODEL FOR FUNCTIONAL ANALYSIS OF TUMOR MODULATORY GENES

Rivka Noelanders, Dionysia Dimitrakopoulou, Suzan Demuynck and Kris Vleminckx
Manuscript in preparation

7.1 ABSTRACT

The fast advancement of sequencing technology has generated vast amounts of data, but with limited functional validation. This is especially true for cancer research in which next generation sequencing has provided researchers with massive lists of genetic changes in any tumor type. However, the great challenge remains to identify driver events, essential for tumor formation and progression. Identification of these events could in turn guide development of effective targeted therapies.

Medulloblastoma is the most prevalent pediatric brain malignancy. Current standard-of-care includes surgical resection with adjuvant chemo- and radiotherapy. Treatment-related toxicity heavily affects quality of life. Recent large-scale genomics and transcriptomics efforts identified four medulloblastoma subtypes based on molecular characteristics: Wnt-type, Shh-type, group 3 and group 4. This has initiated the search for targeted therapies and revealed a need for representative preclinical models for each subtype.

We created a *Xenopus tropicalis* model for Wnt-type medulloblastoma based on CRISPR/Cas9-mediated editing of *apc*, a negative regulator of the Wnt/β-catenin pathway. The obtained tumors closely resemble the clinical presentation of Wnt-type medulloblastoma. Furthermore, our results reveal some obstacles encountered by targeting tumor suppressor genes with important embryological functions. We also show that targeting additional tumor suppressor genes can increase tumor incidence and thereby provide a proof-of-principle that multiplexing of CRISPR/Cas9 in *Xenopus* is fast and cost-effective for functional assessment of potential tumor modulatory genes.

7.2 BACKGROUND

Central nervous system tumors are the second most common cancer type in children and are responsible for most of the cancer-related mortalities in childhood [1]. Medulloblastoma (MB) is the most prevalent pediatric brain malignancy [2-4]. It arises in the posterior fossa, which is composed of the cerebellum, brainstem and fourth ventricle [5]. Current treatment protocols consist of maximal surgical resection and adjuvant chemotherapy and craniospinal irradiation [6, 7]. Overall 5-year survival is around 70 percent, but long-term quality of life is severely affected by the aggressiveness of the treatment applied to the immature brain [3, 4, 7, 8]. Decreased intellectual capacity, neurocognitive impairment and neuro-endocrinological dysfunction are common consequences of MB treatment [9-11]. Moreover, treatment-induced secondary malignancies have been described [3, 4, 12]. In the latest decennia long-term survival rates have increased significantly, stressing the need for reduced treatment-related toxicity.

In the clinic, prognosis varies significantly between patients that present with similar clinical features (tumor size, histology,…) and share demographic factors (age, sex,…). Around 2010, large-scale genomic profiling finally revealed that MB is not a single disease entity [2, 4, 13-15]. Instead there are four different subtypes based on the molecular mechanism driving tumor formation and their gene expression profile. Wnt-type and Shh-type MB show hyperactivation of the Wnt- and Shh signaling pathway, respectively. Group 3 (g3) and group 4 (g4) medulloblastoma are characterized by *MYC* amplifications, but are not linked to a specific signaling pathway [16]. Current consensus is that epigenetic regulators drive g3 and g4 MB [4, 17, 18]. Stratification of patients according to the molecular subtypes correlates well with prognosis. Wnt-type MB show the best prognosis with a 90% cure rate, while prognosis is worst for g3 MB with cure rates only around 40-60% [3, 15]. The differential clinical features of the MB subgroups clearly stress the insufficiency of the current treatment protocol. Therapies need to be tailored to reflect the heterogeneity of the disease they are targeting. A first step in this process is a clear understanding of molecular events that drive tumorigenesis and tumor progression. Only then is identification of new therapeutic targets possible. Valuable preclinical research is totally dependent on model systems that accurately reflect the human disease. MB cell lines do not meet this criterion as they diverge from their original molecular subtype *in vitro* [19, 20]. Several mouse models have been developed for Shh-type MB [21-23], Wnt-type MB [17, 24], g3 MB [25-28] and g4 MB [29]. However, most of these models are based on either knockout of multiple genes or on patient-derived xenografts complicating functional assessment of potential tumor modulatory genes.

The rapid evolution of next generation sequencing has produced large datasets detailing the genetic profile of countless tumor types. Also for MB, new mutations and copy number variations are continuously being discovered [1, 18, 30-32]. However, it is unclear which of the genetic mutations or changes in expression are essential for tumor formation and survival. To be able to distinguish

these driver events, functional assays are needed. Targetable nucleases, like CRISPR/Cas9, have emerged as a promising tool to identify essential cancer genes *in vitro* through high-throughput library screens [33, 34]. However, since MB cell lines insufficiently represent the clinical situation, *in vivo* functional assessment is needed [20]. Recently, *in vivo* screens employing CRISPR/Cas9 in mice have identified tumor-modulating genes [35, 36]. However, semi-high throughput functional assays are expensive and time consuming in mice. Therefore, more primitive vertebrates like *Xenopus* and zebrafish have gained interest because of their accessibility for modeling human disease, including cancer, through genome editing [37, 38]. Our research group created the very first tumor models in *Xenopus* through TALEN- and CRISPR/Cas9-mediated genome editing [39, 40]. TALEN-mediated mosaic knockout of *apc* results in the development of a variety of tumors phenocopying the tumor syndrome familial adenomatous polyposis through constitutive activation of Wnt signaling [39]. FAP is mainly associated with colorectal cancer, but increased risk for multiple extracolonic malignancies like adenomas and adenocarcinomas in other regions of the gastrointestinal system, desmoid tumors and brain tumors [41]. Brain tumors, resembling MB, were also observed in *apc* gene edited animals indicating usefulness of *Xenopus* for modeling Wnt-type MB [39].

Since prognosis for Wnt-type MB is so favorable compared to other subgroups, current clinical trials for treatment of Wnt-type MB are mainly focused on therapy de-escalation to improve long-term functional outcomes. However, huge improvements could still be obtained by introducing targeted therapies and this should thus maintain an important focus in MB research. Injection of sgRNA and Cas9 in *Xenopus* embryos gives rise to mosaic animals in which the desired gene is disrupted in some cells while a wild type copy is maintained in other cells [42-44]. This is an advantage when assessing tumor-modulatory function of essential genes for embryonic development. Moreover, this more closely resembles the natural occurrence of cancer, in which one cell gains a proliferation advantage through genetic variation, while the surrounding cells remain homeostatic. Since gRNA/Cas9 ribonucleoprotein complexes (RNPs) are injected directly in the embryo, multiplexing is straightforward by the addition of multiple RNPs to the injection mixture [42, 45-47]. Moreover, the system becomes functional early after injection since no endogenous translation machinery is required as opposed to other genome editing techniques. This may in part explain the higher mutagenesis rate observed in F0 animals using CRISPR/Cas9 compared to other genome editing techniques [48].

In this work, we have created a model for Wnt-type MB through CRISPR/Cas9-mediated editing of *apc* in *Xenopus tropicalis.* Furthermore, we show that this model can be used for functional assessment of potential tumor-modulatory genes.

7.3 RESULTS

7.3.1 THE XENOPUS POSTERIOR FOSSA

Historically, *Xenopus* has mainly been used in developmental biology studies. As a result embryonic development and anatomy have been characterized in detail. However, detailed histological characterization of late tadpoles, froglets and adults is limited. The posterior fossa is composed of the brainstem, cerebellum and IVth ventricle. These structures are responsible for most vital functions like breathing, heartbeat, consciousness and motor coordination and as a consequence are well conserved throughout evolution [49]. All arise from the embryonic hindbrain, a structure that during embryonic stages is very similar in mammals and lower vertebrates. While the adult

mammalian hindbrain is composed of the pons, medulla oblongata and cerebellum, the adult *Xenopus* hindbrain still closely resembles the embryonic hindbrain in mammals. Even though the *Xenoupus* hindbrain thus represents a more primitive version of the mammalian hindbrain, all the same cell types are present. Most striking is the very small cerebellum in *Xenopus.* In mammals the granule neuron precursors (GNPs) undergo massive expansion in the embryo, resulting in them becoming the most prevalent neuron type in the human brain. However, in *Xenopus* the GNPs do not undergo this expansion phase, explaining the smaller size of the cerebellum [50]. However, Gibson et al. showed that Wnt-type MB originates from a progenitor cell population in the lower rhombic lip, so the different morphology of the cerebellum should not interfere with the creation of a Wnt-type MB model [24].

As a reference for normal brain histology, brains from wild type adult frogs were isolated and processed for histology (Figure 7.1). Fore-, mid- and hindbrain can easily be distinguished by the constrictions on the transitions. In the hindbrain a series of bulges, the rhombomeres, is present, a feature that in mammals is only present during embryonic development. The cavity in the medial hindbrain is the fourth ventricle. This is filled with cerebrospinal fluid, produced by the choroid plexus, a highly vascularized structure on the dorsal side of the hindbrain. The cerebellum can be most easily distinguished on a sagittal section as a small bulb at the transition between mid- and hindbrain.

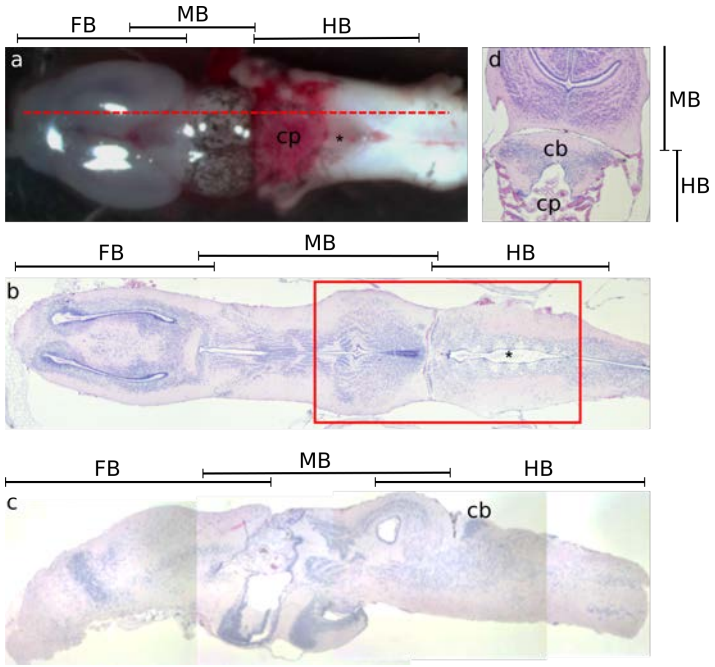

Figure 7.1 The *Xenopus* brain. (a) Dorsal view of a dissected brain from a 4 month old *Xenopus tropicalis.* Forebrain (FB), midbrain (MB) and hindbrain (HB) can easily be distinguished. The highly vascularized structure in the dorsal hindbrain is the choroid plexus. The fourth ventricle is indicated by an asterisk (*). (b) Haematoxylin and eosin staining of a coronal section through the brain of a 4 month old *Xenopus tropicalis.* Red square represents brain area portrayed in following figures. (c) Sagittal section through the brain of a 4 month old *Xenopus tropicalis.* The cerebellum is visible as a small bulb on the transition between the mid- and hindbrain (cb). The section plane is indicated as a red dashed line in panel a. (d) Close-up of the dorsal midbrain-hindbrain transition showing the cerebellum and choroid plexus.

7.3.2 CRISPR/Cas9- mediated mosaic knockout of APC leads to hyperproliferation in the Xenopus brain

The original FAP model was generated by TALEN-mediated knock out of *apc* [39]. However, a gRNA targeting almost the same location was generated and shown to replicate the phenotype observed

by TALEN-mediated gene editing (Naert et al., in preparation and this research). CRISPR/Cas9 has the advantage of very fast generation of gRNAs and ease of multiplexing (see Chapter 10). Moreover, when combined with recombinant Cas9 protein, there is no need for the endogenous transcriptional machinery. The CRISPR/Cas9 machinery is thus immediately functional in the cell, leading to high genome editing efficiencies [48]. We thus employed CRISPR/Cas9 for the generation of a *Xenopus tropicalis* Wnt-type MB model.

Furthermore, mosaic knockout of *apc* in the whole embryo results in the development of many different malignancies [39]. A second adjustment to the FAP model was injection of *apc* RNPs only in the animal-dorsal blastomeres of an eight-cell stage embryo. Consequently, based on the *Xenopus* fate map developed by Moody S.A. [51], mosaic knockout of *apc* will be mainly targeted to neural structures. This allows us to specifically assess constitutive activation of the Wnt signaling pathway in the brain. Three days post-injection pools of 3-5 embryos were lysed for genomic DNA (gDNA) extraction and the region around the target site was PCR amplified and sequenced by next generation sequencing to assess gene editing efficiency. Since only two out of eight blastomeres were injected the maximum achievable editing efficiency in the whole embryos is about 25%. Editing efficiency for *apc* reached 15%. Injected and control non-injected sibling embryos were sacrificed every two weeks starting from 4 weeks post-injection (Figure 7.2). The experiment was ended at eight weeks post-injection because of high lethality. The majority of the tadpoles showed no obvious external abnormalities. Most of the tadpoles presented with epidermal cysts around the brain region as has been described by Van Nieuwenhuysen et al. [39] (Figure S7.1). Histology revealed highly disrupted brain morphology already at 4 weeks post-injection and a similar phenotype was observed in 6- and 8-week old tadpoles. The subventricular zone is thickened and bulbs of brain tissue almost completely fill the cavity of the fourth ventricle. Also in the midbrain extra undulation of the brain tissue is observed with expansion of the subventricular zone. Moreover, lateral brain areas, which are almost devoid of nuclei in non-injected animals, show cell dense foci, which form small tubular structures or rosettes. Rosette formation is a characteristic of MB. However even though cell density is obviously increased indicating overproliferation, no brain tumors were observed in this experiment (n = 19) (Figure 7.2). We did observe tumor formation at the nostrils in 5% of the tadpoles (Figure S7.1).

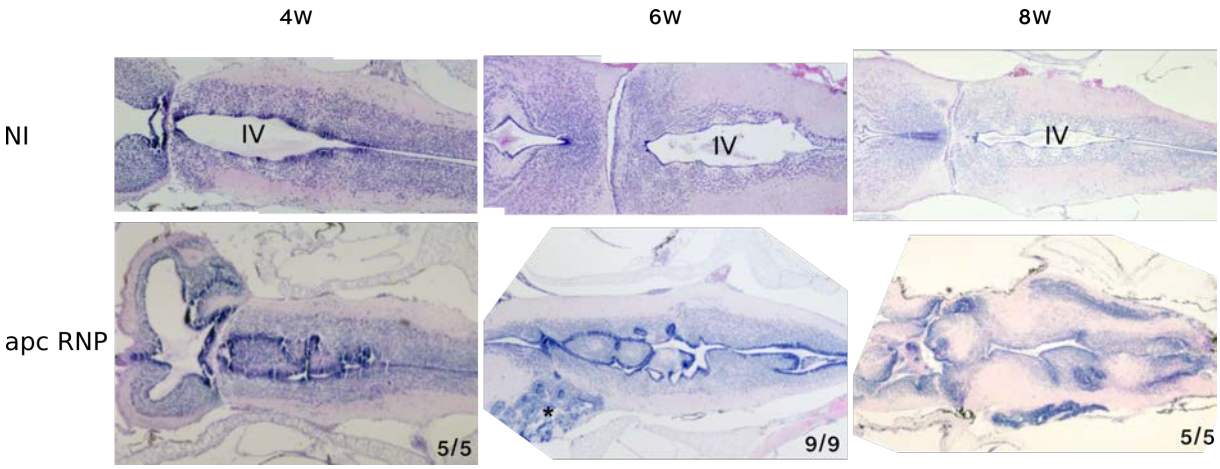

Figure 7.2 Mosaic *apc* knockout in the brain results in hyperproliferation but no tumor formation. Haematoxylin and eosin staining of coronal sections through the mid- and hindbrain with anterior to the left. *Apc* and Cas9 ribonucleoprotein complex (RNP) injected tadpoles and sibling non-injected tadpoles were sacrificed every two weeks and processed for histology. Injected tadpoles showed severe disturbance of brain morphology with outgrowths of brain tissue filling the fourth ventricle (IV). Extra undulations in the brain tissue indicate increased cell counts. Ectopic foci of cell nuclei forming rosettes in the lateral brain were also observed (*).

The experiment was repeated, this time yielding an editing efficiency in *apc* of only 4%. Tadpoles were sacrificed at a fixed time point 6 weeks post-injection (Figure 7.3). Lower gene editing efficiency was apparent in brain morphology, as overall histology more closely resembled that of non-injected animals with milder signs of increased proliferation. However 2 out of 13 (15%) tadpoles showed small tumors located at the midbrain-hindbrain boundary. These tumors had the typical characteristics of a small, blue round cell tumor and due to their localization were defined as MB by a clinical pathologist (Dr. David Creytens, University Hospital Ghent) (Figure 7.3).

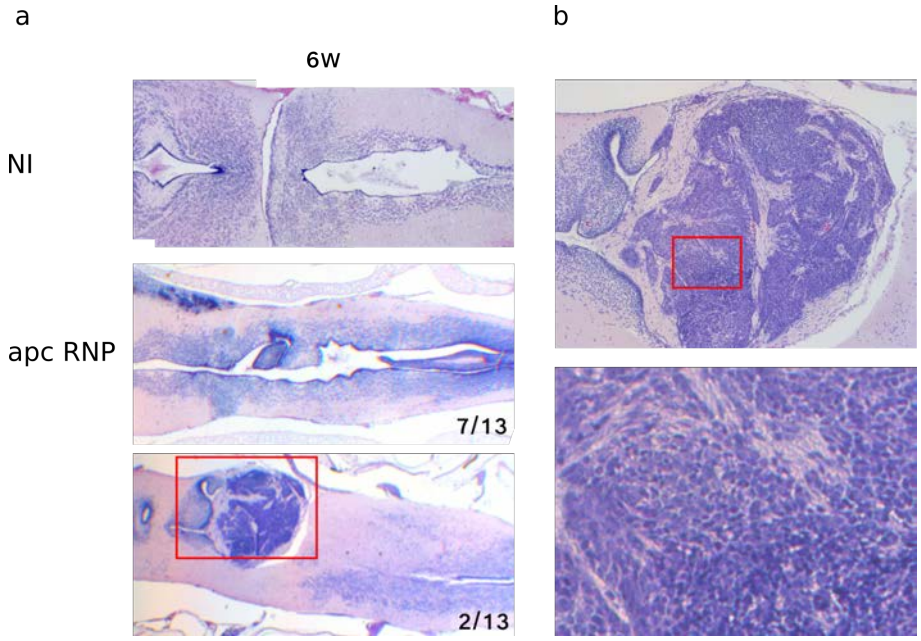

Figure 7.3 Wnt-type medulloblastoma upon lower efficiency of mosaic *apc* knockout. (a) Haematoxylin and eosin staining of coronal sections through the mid- and hindbrain with anterior to the left. *Apc* and Cas9 ribonucleoprotein complex (RNP) injected tadpoles and sibling non-injected tadpoles were sacrificed 6 weeks post-injection and processed for histology. Majority of tadpoles showed normal histology (not shown) or milder signs of increased proliferation (middle panel). 2 out of 13 tadpoles presented with tumors located on the transition between mid- and hindbrain. (b) Close-up of tumor shown in a. Red squares show magnified areas. Tumors show high density of cells with little cytoplasm characteristic of a small, blue round cell tumor like medulloblastoma.

It seems contradicting that tumors are observed in animals with lower gene editing efficiency. However, this closely resembles natural disease progression in which only a few cells will acquire a mutation giving them a survival advantage and of these even fewer cells will transform and truly give rise to a malignancy. Moreover, Wnt signaling activity has numerous functions during brain development including proliferation of neural progenitor cells [52]. It is thus possible that the observed overproliferation in the first experiment is mainly a consequence of Wnt signaling activation during embryonic stages and not of malignant transformation. Furthermore, this large-scale induction of proliferation might prevent acquirement of survival advantage and transformation of one specific cell or lead to lethality due to increased cranial pressure before malignant transformation occurs. In conclusion, constitutive Wnt signaling activation can induce MB formation in the *Xenopus* hindbrain, but also induces high lethality early in life due to hyperproliferation and brain malformation, probably resulting from an embryonic signaling function.

7.3.3 Combined apc/tp53 RNP injection induces Wnt-type medulloblastoma

Low *apc* editing efficiency can induce Wnt-type MB formation, be it at low penetrance. Since brain tumor formation cannot be observed externally, higher incidence is needed. This way, animals can be

sacrificed at a fixed time point and smaller sample sizes need to be sacrificed to get sufficient amount of tumors for statistical power. In order to increase tumor incidence, injection of *apc* RNPs was combined with *tp53* RNP injections. Tp53 is a well-known tumor suppressor and *Tp53* mutations are common in Wnt-type MB [30, 53, 54]. *Tp53* loss of function (LOF) was needed for MB formation in a mouse model of Wnt-type MB [24]. Furthermore, *Tp53* LOF has also been shown to increase incidence and reduce latency in a mouse model of Shh-type MB [21]. Moreover, upregulation of Tp53 in Wnt-driven tumors has been described [55]. Tp53 in turn promotes phosphorylation and degradation of β-catenin creating a negative feedback loop. Additional knockout of *Tp53* could thus further increase Wnt signaling activity in the hindbrain.

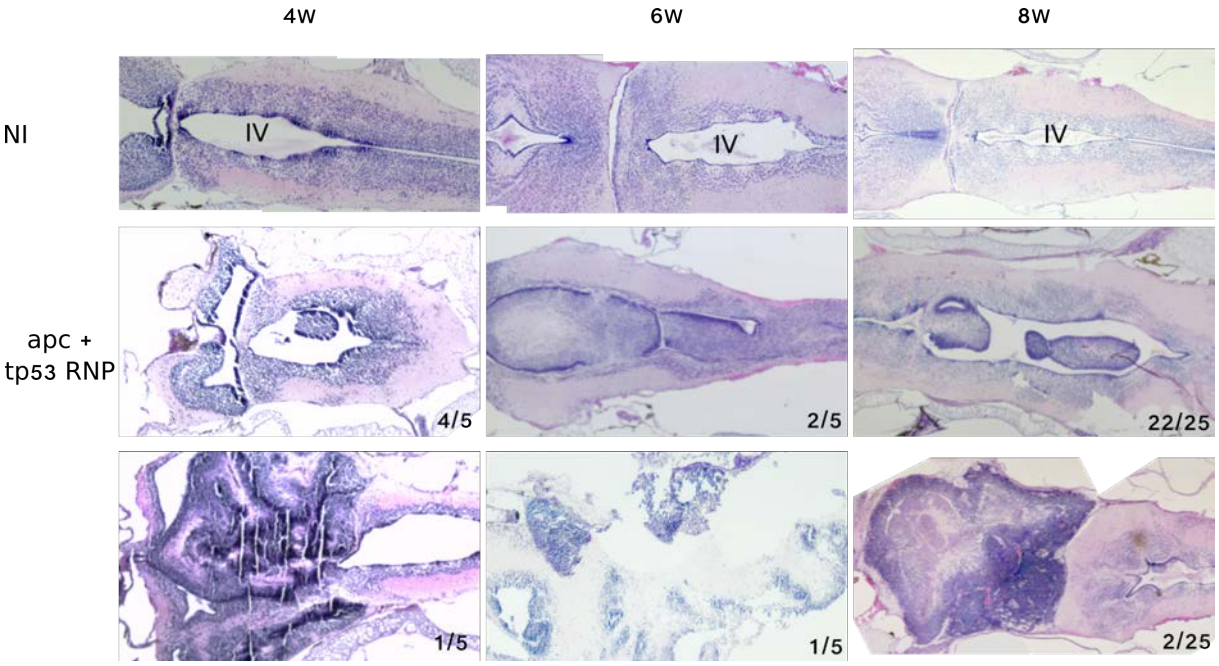

Figure 7.4 Wnt-type medulloblastoma formation upon combined mosaic *apc* and *tp53* knockout. Haematoxylin and eosin staining of coronal sections through the mid- and hindbrain with anterior to the left. *Apc* and *tp53* RNP injected tadpoles and sibling non-injected tadpoles were sacrificed every two weeks and processed for histology. More severe malformation of the midbrain was observed upon additional *tp53* knockout (left, lower panel). Outgrowths of in the fourth ventricle were also observed (middle panels). 3 out of 35 tadpoles presented with large tumors (middle and right, lower panel).

Injection of RNPs was again targeted to the brain and editing efficiency was 6% for *apc* and 1% for *tp53.* Animals were sacrificed every two weeks with end of the experiment at 8 weeks post-injection (Figure 7.4). Despite the low *tp53* editing efficiency, some differences were observed in brain histology compared to the *apc* single injected embryos. Midbrains were more severely malformed showing numerous undulations, completely disrupting normal tissue architecture. Outgrowths of brain tissue in the fourth ventricle were still observed, even though complete disappearance of the fourth ventricle cavity was less frequent. Importantly, 3 out of 35 (8.6%) tadpoles presented with large tumors, again located on the midbrain-hindbrain boundary (Figure 7.4). Tumors contained both areas with high density of round cells and areas with more spindle-like cells and fascicular appearance of the tissue (Figure 7.5). Large necrotic areas were observed in the center of the tumors, indicative of a fast growing tumor. Combined with the mixed histology this is characteristic for of a highly malignant tumor. Additional mutation of *tp53* thus induces formation of a more aggressive, fast growing Wnt-type MB as compared to only apc LOF.

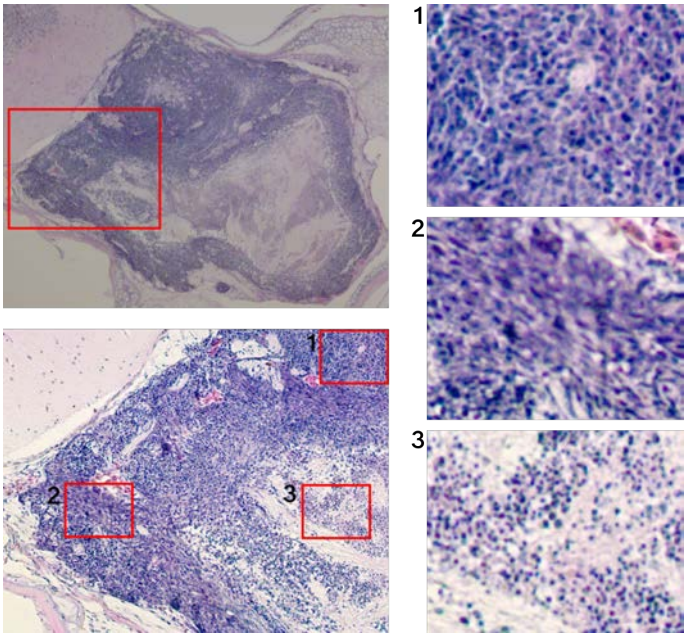

Figure 7.5 Haematoxylin and eosin staining of tumors upon combined *apc* and *tp53* knockout. Section through Wnt-type medulloblastoma after *apc* and *tp53* knockout. Tumors show mixed histology indicative of high grade of malignancy. Red rectangles indicate enlarged areas. Panel 1 shows high density of round cells, panel 2 contains spindle-like cells and panel 3 shows a necrotic area.

7.3.4 *TP53 MUTATION STATUS INFLUENCES WNT-TYPE MEDULLOBLASTOMA FORMATION*

In order to increase Wnt-type MB incidence, we employed two different approaches. A first one was generation of a full *tp53* homozygous knockout line, while a second approach entailed immediate delivery of RNPs to the brain at tadpole stages via electroporation (see 7.3.5).

For generation of a *tp53 homozygous* knockout line, adult mosaic *tp53* knockout animals were first mated to check for germ line transmission of frame shift inducing mutations. Genomic DNA from pools of offspring was checked by heteroduplex mobility assay for presence of mutated sequence. Two out of three males showed germ line transmission of *tp53* mutation. Next generation sequencing revealed that both males transmitted a 4 bp mutation at different locations. Both are thus frame shift mutations leading to a LOF of *tp53.* Furthermore, mutation frequencies of 11.3% and 16.8% were observed indicating transmission frequency of 1/5 and 1/3, respectively. Both males were outbred with wild type females to generate $tp53^{+/446-}$ and $tp53^{+/447-}$ offspring. Finally, $tp53^{+/446-}$ and $tp53^{+/447-}$ were mated to generate compound heterozygous knockout animals ($tp53^{446-/447-}$).

To verify an inducing effect of *tp53* loss on tumor formation $tp53^{+/446-}$ and $tp53^{+/447-}$ animals were mated and offspring was injected with *apc* RNPs or *ctnnb1* RNPs targeting the T41 phosphorylation site of β-catenin in exon 3. Small in frame mutations will disrupt β-catenin phosphorylation while maintaining protein function. This would result in a stabilized version of β-catenin that is resistant to degradation. TALENs directed to the S33 phosphorylation site of β-catenin replicated the FAP phenotype observed by mosaic *apc* knockout (Van Nieuwenhuysen et al., in preparation). Moreover, exon skipping upon CRISPR/Cas9 mediated targeting of β-catenin has been described *in vitro* [56]. Exon 3 skipping does not disrupt the reading frame but results in a stabilized protein resistant to phosphorylation-induced degradation. Loss of exon 3 is a well-known gain of function allele used in mice to achieve constitutive Wnt signaling activity [57].

Unfortunately, *apc* RNP injected embryos died within days after the injection and could not be analyzed. *Ctnnb1* T41 RNP injected embryos were raised up and assessed for tumor formation at two and four weeks post-injection on histology. Gene editing efficiency achieved was 7.6%. Since

heterozygous *tp53* animals were used for mating, offspring consisted of *tp53* wild type, heterozygous and compound heterozygous animals. This allowed us to assess the effect of *tp53* mutation status on Wnt-type MB formation. Tails from sacrificed animals were used for genomic DNA extraction and genotyping. Most tadpoles showed only mild signs of overproliferation, mostly around the midbrain-hindbrain boundary, 2 weeks post-injection (not shown). At 4 weeks post-injection, increased proliferation characteristics were more profound. This indicates that CRISPR/Cas9 mediated targeting of exon 3 of the *ctnnb1* gene results in constitutive activation of the Wnt signaling pathway. *Tp53* wild type tadpoles showed a milder phenotype, with only 1 out of 9 tadpoles showing profound overgrowth of the midbrain. Majority of $tp53^{+/-}$ and $tp53^{-/-}$ presented with undulation of the midbrain and ectopic cell dense areas. Some of these might correspond to pre-tumoric lesions as they show densely packed small round cells, but these are not clearly distinguishable from the normal brain tissue as was observed in Wnt-type MB bearing tadpoles. However, no tumors were observed and assessment at later time points is necessary. No difference could be observed between *tp53* heterozygous and homozygous animals. However, only 6 (15%) full knockout animals were recovered. This is below the expected Mendelian ratio (25%) and bigger sample size is needed to establish the effect of *tp53* heterozygous vs homozygous mutant status on medulloblastoma formation. Together this indicates that *tp53* mutation status influences the effect of constitutive Wnt signaling activation in the *Xenopus* hindbrain, but further experiments are needed to elucidate its effect on tumor incidence and latency.

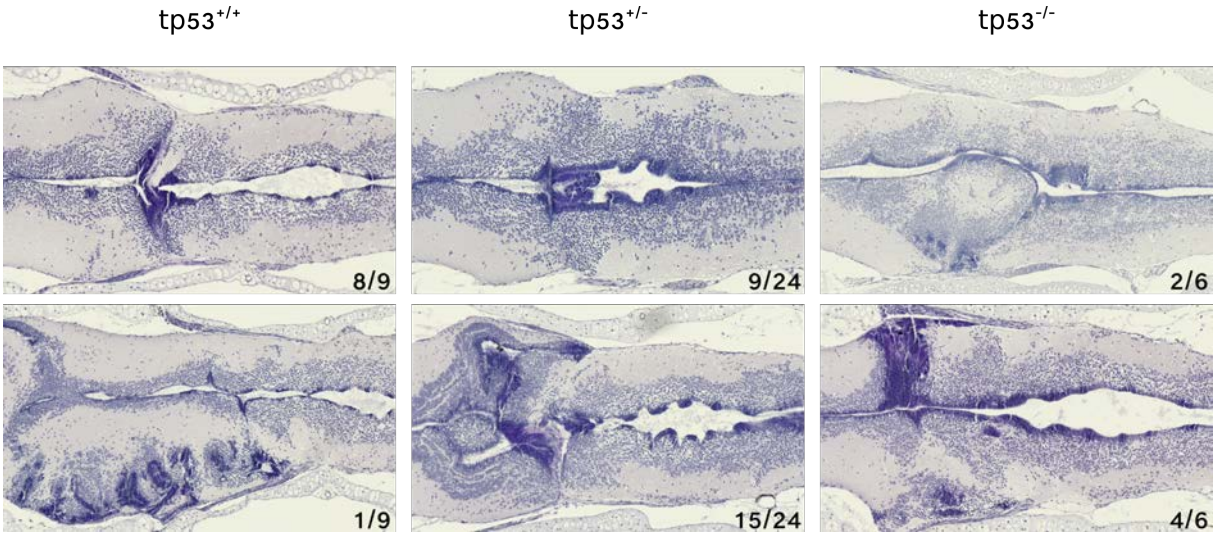

Figure 7.6 Influence of *tp53* mutation status on constitutive Wnt signaling activation in the *Xenopus* hindbrain. Haematoxylin and eosin staining of coronal sections through the mid- and hindbrain with anterior to the left. *Tp53* wildtype, heterozygous and homozygous knockout embryos were injected with RNPs targeting exon3 of *ctnnb1*. Observed phenotypes and their frequencies are shown. Heterozygous and homozygous knockout embryos showed a more severe overproliferation of the mid- and hindbrain compared to *tp53* wild type tadpoles. No tumors were observed.

7.3.5 Immediate delivery of RNPs to the brain via electroporation

A second approach to increase Wnt-type MB incidence was direct delivery of RNP to the tadpole brain via electroporation. In this way, constitutive Wnt activation would only occur after embryonic development thereby avoiding the embryonic hyperproliferation effect observed in injected embryos. Electroporation-mediated delivery of RNPs to the axolotl spinal cord and mouse zygotes was shown to be highly efficient [58, 59]. *Apc* RNPs alone or combined with *tp53* RNPs were delivered to the fourth ventricle of two week old tadpoles followed by the application of electric pulses to the hindbrain (18 V, 50 ms, 950 ms pulse interval, 5x to each side). Gene editing efficiency

in the mid- and hindbrain reached barely 1%. Tadpoles from two individual experiments were sacrificed three weeks after electroporation and showed no obvious abnormalities on external examination. Tadpoles were processed for histology, but no signs of hyperproliferation or tumor formation were observed (Figure S7.2). At this point we cannot draw any conclusions on tumor incidence after delayed *apc* gene-editing to tadpole stages. Electroporation efficiency needs to be optimized.

7.3.6 FUNCTIONAL ASSESSMENT OF TUMOR MODULATORY GENES

Our Wnt-type MB model would be ideally suited for functional analysis of potential tumor modulatory genes since simple multiplexing of RNPs and assessment of tumor characteristics can be applied. To identify potential tumor modulatory genes for Wnt-type medulloblastoma, we made use of publicly available datasets with expression profiles from human MB biopsies. We selected two datasets based on availability of molecular subclassification and because gene expression profiles were acquired on the same platform (Affymetrix GeneChip Human Genome U133 Plus 2.0 array) allowing immediate comparison [14, 17]. Pairwise comparison between expression in Wnt-type MB and other MB subtypes was done (performed by M. Vuylsteke). Selection of genes that were at least 8-fold higher expressed in Wnt-type MB compared to all other MB subtypes resulted in a list of about 80 genes (Supplemental table 7.1). Based on literature search these genes were divided in four categories: Wnt-pathway and target genes, genes with described oncogenic function, genes with described tumor suppressor function and genes of which no previous link to cancer has been found. Since tumor incidence was low in initial experiments, we decided to first try knockout of additional tumor suppressor genes (TSGs). Three known TSGs, *gad1.2, crabp2* and *bhmt* and 1 gene of unknown function *tmem51* were selected.

7.3.6.1 Gad1

Glutamate decarboxylase 1 (gad1) catalyzes the production of γ-aminobutyric acid (GABA), an inhibitory neurotransmitter, from glutamate, an excitatory neurotransmitter. GAD1 is highly expressed in Wnt-type MB and is used as a marker for its diagnosis [60]. Brain-targeted co-injection of *apc* and *gad1.2* RNPs achieved gene-editing efficiencies of 8.6% and 17.1%, respectively. Five tadpoles were sacrificed every two weeks and the experiment was ended after 8 weeks (Figure 7.7). Tadpoles with external signs of tumor formation or abnormal swimming behavior were sacrificed immediately. From 2 weeks post-injection significant disturbance of brain morphology was already observed with outgrowths in the fourth ventricle and additional undulations of the brain tissue, resembling gyri and sulci of the human brain. The observed surface expansion again indicates hyperproliferation of the brain tissue. At the midbrain-hindbrain boundary, foci of rosette formation were often observed on the lateral sides. Severity of the phenotype increased at later time points. The first tumor was observed after only 4 weeks (Figure 7.8). After 8 weeks 24% of the animals (n = 38) had developed MB. Tumors were very large, almost completely displacing the normal brain tissue. On histology tumors consisted mainly of rounded, epithelial-like cells and many rosettes were apparent, characteristic for classic MB histology. Gad1 thus seems to functions as a TSG in Wnt-type MB as its LOF increases tumor incidence.

7.3.6.2 Tmem51

Transmembrane protein 51 (tmem51) is a protein of unknown function. Since it was high on our list of Wnt-type MB specific genes, we decided tmem51 might be an interesting candidate for functional analysis in our model. Injection of *apc* and *tmem51* RNPs was again targeted to the brain and gene editing efficiencies were 6% and 11.5%, respectively. Two weeks post-injection, the majority of

tadpoles showed no gross abnormalities in brain morphology (Figure 7.7). Only minor signs of hyperproliferation were observed around the midbrain-hindbrain boundary in some tadpoles. Still at four weeks post-injection, hyperproliferation with outgrowths in the fourth ventricle was observed but milder than in the single *apc* injected tadpoles. However, one tadpole already presented with a tumor (Figure 7.8). After eight weeks total tumor incidence was 10% (n = 39).

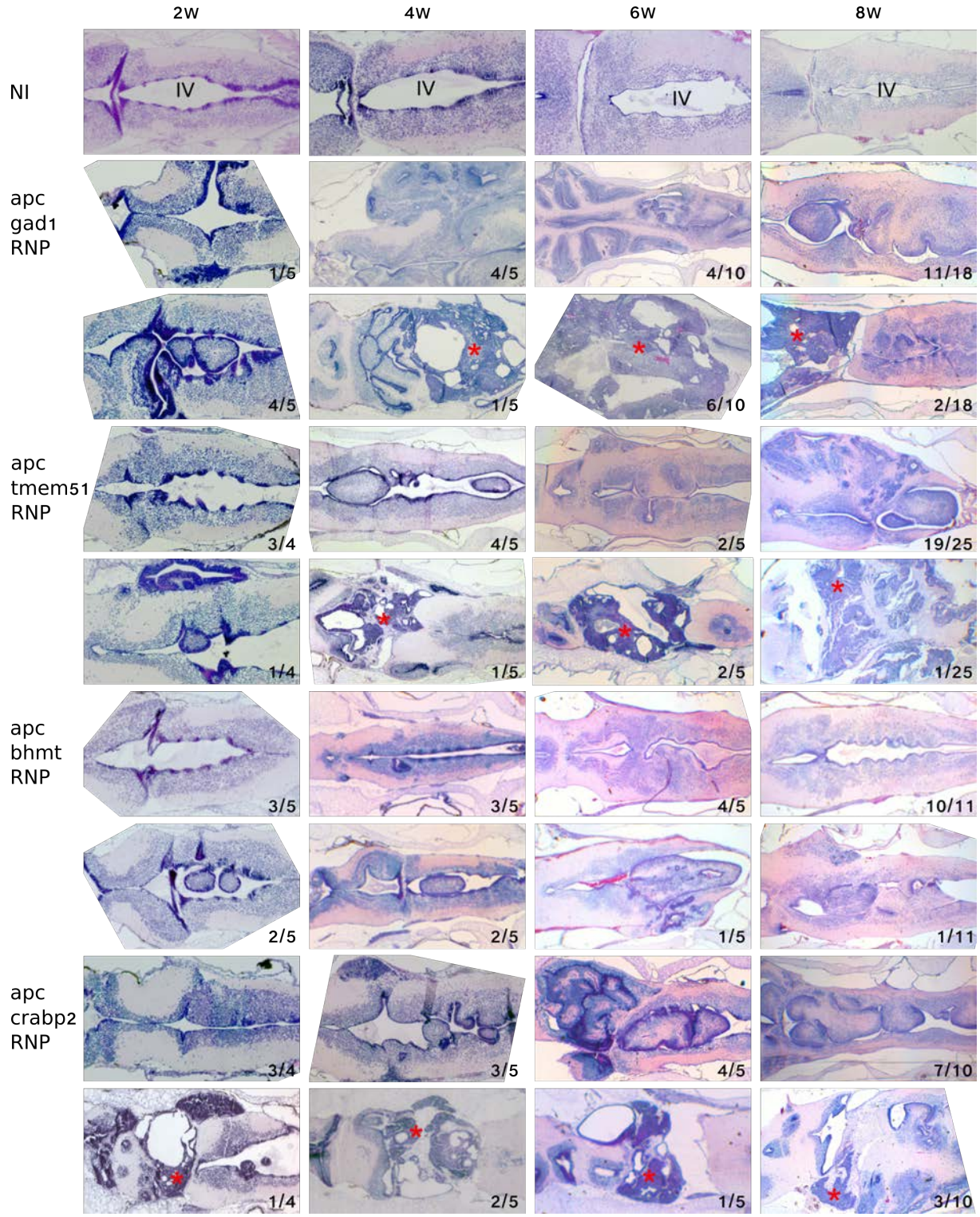

Figure 7.7 Functional assessment of potential tumor modulatory genes. Haematoxylin and eosin staining of coronal sections through the mid- and hindbrain with anterior to the left. Respective RNP injected tadpoles and non-injected tadpoles were sacrificed every two weeks and processed for histology. Different observed phenotypes are represented with their frequency. Red asterisk indicates presence of a brain tumor. IV, fourth ventricle.

7.3.6.3 Bhmt

Betaine-homocysteine methyltransferase (bhmt) is an enzyme that participates in the metabolism of the amino acids glycine, serine, threonine and methionine. Bhmt LOF results in liver cancer in mice and bhmt is often downregulated in human liver cancer [61, 62]. Editing efficiencies after brain-targeted co-injection of *apc* and *bhmt* RNPs reached 1.9% and 27.7%, respectively. Majority of the tadpoles showed normal gross morphology of the brain, while in others signs of hyperproliferation, of which outgrowths in the fourth ventricle were most pronounced, were observed (Figure 7.7). No tumors were observed (n = 26).

7.3.6.4 Crabp2

Cellular retinoic acid binding protein 2 (crabp2) plays a role in retinoic acid transport from the cytosol to the nuclear RA receptor. We previously identified *crabp2* as a Wnt target gene [63]. Crabp2 has been shown to function as a TSG in multiple malignancies [64]. Combined injection of *apc* and *crabp2* RNPs, targeted to the brain, resulted in gene-editing efficiencies of 11.9% and 12.8%, respectively. A first tumor was already detected 2 weeks post-injection, while other tadpoles only showed minor signs of hyperproliferation (Figure 7.7, Figure 7.8). By 4 weeks post-injection, all tadpoles showed typical signs of hyperproliferation observed in other condition set-ups with outgrowths in the fourth ventricle. Strikingly, like in the *apc+gad1.2* condition, foci of rosette formation on the lateral sides of the midbrain-hindbrain boundary were present in nearly all tadpoles. Total tumor incidence after 8 weeks reached 29% (n = 24). *Crabp2* thus seems to function as a TSG in Wnt-type MB and its LOF increases tumor incidence. Interestingly, tumors observed in *apc+crabp2* RNP injected were remarkably smaller than tumors observed in all other conditions, indicating that *crabp2* LOF induces tumor formation, but not tumor progression.

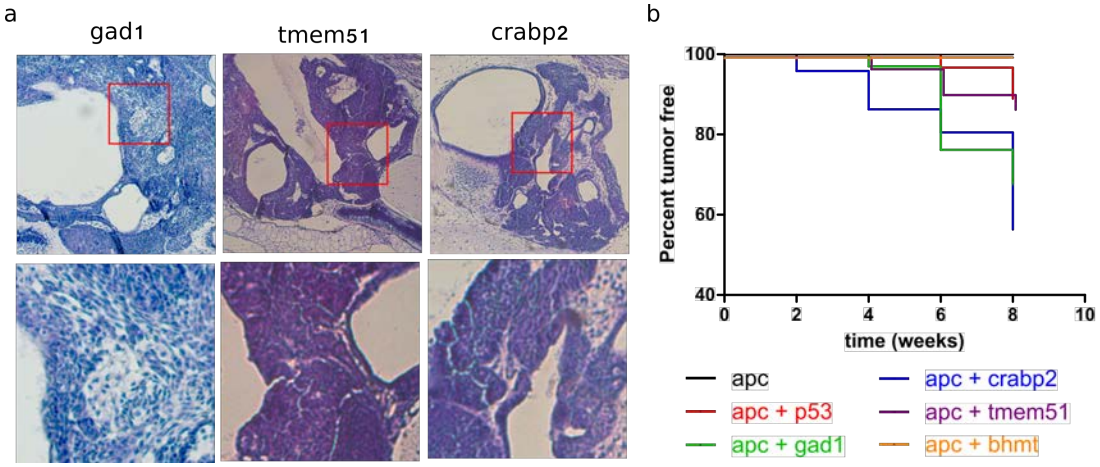

Figure 7.8 Altered tumor characteristics upon CRISPR/Cas9 multiplexing. (a) Haematoxylin and eosin staining of tumors obtained after multiplexing of *apc* RNPs with RNPs for the respective genes. Histology differs between different set-ups. Tumors obtained after additional *gad1* knockout show mixed histology of round and spindle-like cells. Tumors obtained after additional *tmem51* and *crabp2* knockout show only densely packed round cells. Tumors in the crabp2 set-up were consistently smaller. (b) Graph showing differences in tumor incidence and latency in the different injection set-ups. Tumor incidence was highest and tumor latency lowest in *apc* + *crabp2* injected tadpoles.

7.3.7 Validation of crabp2 as a tumor supressor gene in Wnt-type medulloblastoma

Our initial functional screen of potential tumor-modulatory genes in Wnt-type MB revealed three candidate tumor suppressors. We decided to validate *crabp2* as a TSG in Wnt-type MB since its involvement in retinoic acid signaling might have therapeutic relevance. Retinoic acid has been explored as a therapeutic agent in multiple malignancies with effects ranging from differentiation and apoptosis induction to tumor prevention [65].

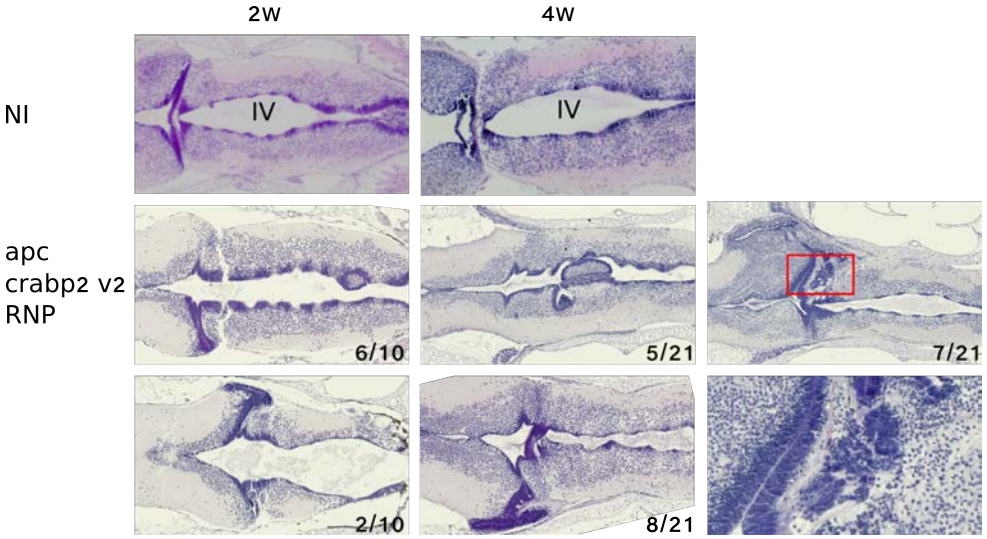

Figure 7.9 Pre-tumoral lesions upon *apc* and *crabp2* v2 RNP injection. Haematoxylin and eosin staining of coronal sections through the mid- and hindbrain with anterior to the left. Respective RNP injected tadpoles and non-injected tadpoles were sacrificed every two weeks and processed for histology. Different observed phenotypes and their frequency are represented. No tumors are observed only small ectopic cell dense areas that can correspond to pre-tumoral lesions (red rectangle and lower right panel). NI, non-injected; RNP, ribonucleoprotein complex.

We designed a second gRNA (v2) targeting a different region of the gene. This way we can exclude the influence of any off-target effects on the phenotype observed after injection of the first gRNA. Again injection of *apc* and *crabp2*v2 RNPs was targeted to the brain. Gene editing efficiencies achieved were 6.5% and 2.7%, respectively. Tadpoles ware sacrificed at two and four weeks post-injection and processed for histology. After 2 weeks most tadpoles showed only minor signs of increased proliferation with few tadpoles showing the typical cell dense outgrowths of the midbrain observed in previous experiments (see above). Four weeks post-injection overproliferation is clearer with 71% of the tadpoles (n = 21) showing increased undulations in the midbrain. Small cell dense areas around the midbrain-hindbrain transition are observed in 33% of tadpoles that might correspond to pre-tumoric lesions. We thus cannot formally identify *crabp2* as a TSG in Wnt-type medulloblastoma. However, the gene-editing efficiencies in this experiment, especially for *crabp2,* were low.

7.4 Discussion

The genetic profiling of the different medulloblastoma subtypes has initiated the search for molecular targeted therapies. This could lead to a dramatic decrease of treatment-related toxicity and significantly improve quality of life in MB patients. We generated a new model for Wnt-type medulloblastoma. Even though further optimization of the model is needed, we show that it could provide a straightforward and cost-effective platform for functional analysis of potential tumor modulatory genes.

7.4.1 A Xenopus tropicalis model for Wnt-type medulloblastoma

7.4.1.1 CRISPR/Cas9 mediated cancer modeling

Functional assessment of potential tumor modulatory genes requires models that accurately reflect the clinical presentation of the disease. Moreover, they should allow screening on a large-scale at a limited cost. Traditionally, these so-called essentiality screens have been conducted *in vitro* [33, 34]. Candidate genes identified in these screens move forward to preclinical testing in mammalian model

organisms, mostly mice. However, a lot of the candidate genes identified *in vitro* cannot be validated *in vivo.* Preclinical testing in mammalian model organisms is time-consuming and expensive leaving the necessity for an intermediate step. We propose that aquatic, lower vertebrates, like zebrafish and *Xenopus,* could fulfill this unmet need. Our research group generated the first cancer models in *Xenopus tropicalis* through targeted nuclease-mediated editing of TSGs [37, 39, 40]. These models were easily generated through microinjection of the genome-editing machinery in wild type embryos. Tumors arise in F0 animals with high penetrance and within 2 months [37]. This indicates that *Xenopus tropicalis* could be a valuable model organism for semi-high throughput *in vivo* functional analysis of tumor modulatory genes.

Previous research in the lab revealed the development of brain tumors upon mosaic knockout of *apc* [39]. We wanted to characterize this further and in this study we present the generation of a *Xenopus tropicalis* model for Wnt-type MB. Until now only one Wnt-type MB cell line for *in vitro* studies is available, however this is derived from a rare case of a recurrent Wnt-type MB with large cell-anaplastic histology and thus does not accurately reflect the clinical presentation of the disease [19]. Moreover, a recent study revealed that primary MB cells in culture lose subtype specific molecular characteristics [20]. A genetically engineered mouse model containing a stabilized β-catenin, together with homozygous loss of *tp53,* specifically in progenitor cells of the hindbrain (*Blbp-Cre*$^{+/-}$*;Ctnnb1*$^{+/lox(ex3)}$*;Tp53*$^{flx/flx}$) is available [24]. However only 15% of these mice develop MB after 500 days, which does not correlate with a pediatric malignancy. Tumor incidence was further increased by additional mutation of *Pik3ca* (*Blbp-Cre*$^{+/-}$*;Ctnnb1*$^{+/lox(ex3)}$*;Tp53*$^{flx/+}$*;Pik3ca*^{E545K}) to 100% by 3 months [17]. This creates a complicated genetic background hindering straightforward assessment of tumor modulatory genes. We made use of CRISPR/Cas9 mediated editing of *apc* targeted to the brain to drive tumorigenesis. CRISPR/Cas9 has emerged in recent years as a valuable technique to model human cancers [34, 66]. Moreover, it has already been employed to generate a model for Shh-type MB in the mouse [67]. Furthermore, CRISPR/Cas9 mainly induces small indels in its targets. Importantly, Wnt- and Shh-type MB are mainly characterized by small indels and SNVs targeting key signaling factors, underscoring the fitness of CRISPS/Cas9 for modeling of these tumor types [68]. CRISPR/Cas9 gene-editing machinery was injected in the animal dorsal blastomeres of an 8-cell stage embryo thereby limiting knockout to mostly neural tissues. This avoids lethality associated with development of other malignancies upon *apc* knockout [39]. Moreover, targeted injection allows editing of essential genes for embryonic development that would cause lethality upon complete knockout [69]. Moreover, microinjection based gene-editing results in mosaic animals in which some cells will have a complete loss of function of the targeted gene, while in others only one allele is affected and still other remain wild type also allowing targeting of essential genes. Furthermore, this actually more closely reflects the clinical progression of the disease than a complete gene knockout [70]. Injected tadpoles showed severe disruption of brain architecture with outgrowths of tissue in the fourth ventricle, surface expansion of the subventricular zone creating undulations in the brain tissue and ectopic foci of cell nuclei forming rosettes. This strongly indicates hyperproliferation in the tadpole brain. Only when gene-editing efficiency of *apc* was reduced, we observed brain tumors in 15% of the tadpoles. These tumors showed typical characteristics of a small, blue round cell tumor and based on their localization on the midbrain-hindbrain transition were identified as MB by a clinical pathologist. Even though tumor incidence was low indicating the need for additional mutation events, tumor formation occurred early (within 6 weeks) illustrating the potential of the model for semi-high throughput functional analysis.

To confirm Wnt subtype identity more advanced genetic profiling would be needed. Northcott et al. described a nanoString assay that could reliably identify MB subtype based on the expression level of 22 subgroup-specific signature genes [60]. For Wnt-type MB *wif1, tnc, gad1, dkk2* and *emx2* were included so further experiments that confirm elevated expression of these genes are needed to unequivocally validate our model. Laser capture microdissection of processed tumor tissue can be performed as described in [40]. This can then be followed by genomic DNA or RNA extraction to confirm frameshift mutations in the *apc* gene and assess gene expression changes in the tumor, respectively. Furthermore, detection of nuclear β-catenin could be performed to confirm Wnt subtype identity. Besides brain tumors, we also observed epidermoid cysts and tumors at the nostrils. Both features have been linked to constitutive Wnt signaling before [39, 71]. In mice, precursor cells of the olfactory epithelium were only susceptible to transformation if constitutive Wnt signaling activation occurred during embryonic development. This indicates that in *apc* RNP injected tadpoles constitutive Wnt signaling activation happens early in life, which confirms the value of our model for studying pediatric cancer development. However, this also confirms that the general hyperproliferation phenotype observed in the tadpole brain is most likely the result of disturbance of normal brain development. Wnt signaling has been shown to induce general overproliferation of neural progenitor cells in the early embryonic brain in mice [52, 72, 73], while probably a much smaller progenitor pool will be susceptible to Wnt signaling-induced malignant transformation.

Our results thus reveal that even though targeted injections can circumvent lethality from targeting genes with essential functions during embryonic development, developmental functions of these genes in the targeted organs can still interfere with analysis of their function in other processes, like tumorigenesis. We tried to postpone gene editing until after embryonic development by electroporation-mediated delivery of *apc* RNPs to the brain of 2-week old tadpoles. However, we failed to achieve efficient gene editing through this approach probably due to suboptimal electroporation conditions. Since electroporation mediated delivery of RNPs to the spinal cord of axolotl, another amphibian model organism, was shown to be highly efficient [58], we used similar experiment set-up and electroporation parameters. It remains unclear why in our hands gene-editing efficiency was low. Further optimization is necessary as *in vivo* delivery of RNPs could greatly expand the scope of *Xenopus tropicalis* for modeling human disease. An electroporation-based model for Shh-type MB has been created in mouse [67]. In this case, plasmids containing gRNA and Cas9 sequences were electroporated. Plasmids naturally possess a negative electrical charge as opposed to proteins. However, electroporation-mediated delivery was shown to be more efficient for RNPs than for plasmids [58]. Recently, also spontaneous uptake of RNPs in the mouse brain by using an engineered Cas9 variant containing multiple SV40 nuclear localization signals was described [74]. However, stereotactic delivery directly to the brain tissue was needed, which might be challenging to apply in a small *Xenopus* tadpole.

We also attempted gene editing of *ctnnb1* to create a Wnt-type MB model. Most Wnt-type MB in the clinic arise due to somatic mutation of β-catenin [1]. A model based on stabilized β-catenin would thus more closely reflect the clinical situation. CRISPR/Cas9 mediated gene-editing normally results in a LOF. However, small in frame deletions or insertions at the phosphorylation sites, that regulate protein degradation, could lead to a stabilized, functional protein. We hypothesized that there might be a positive selection for these mutations in tumor formation. Moreover, the phenotype obtained by mosaic *apc* knockout was reproduced through TALEN-mediated *β-catenin* editing (Van Nieuwenhuysen et al., unpublished results). Furthermore, exon skipping was described in vitro upon

CRISPR/Cas9 mediated-targeting of exon 3 in β-catenin [56]. Exon 3 encodes the phosphorylation sites that regulate β-catenin degradation and a skipped-exon 3 stabilized variant is highly used in mouse models of constitutive Wnt activation [24]. A gRNA targeting the T41 phosphorylation site in exon 3 of *ctnnb1* was designed. Brains of injected tadpoles showed similar symptoms of increased proliferation as observed in *apc* RNP injected tadpoles, indicating constitutive activation of the Wnt signaling pathway.

7.4.1.2 Tp53 in Wnt-type medulloblastoma

TP53 is a key TSG that is mutated in a lot of cancer types, including those malignancies characterized by constitutive Wnt signaling activation [75]. However, deregulated β-catenin has been also been shown to induce *Tp53* expression, which elicits an anti-proliferative response. Moreover, Tp53 was shown to downregulate β-catenin forming a negative feedback loop counteracting cancer development [55]. *Tp53* inactivation could thus be a necessary step in Wnt signaling induced tumor formation. In MB *TP53* mutation has been shown to either confer adverse prognosis or to have no negative impact on disease outcome [54, 76]. Two separate studies showed overrepresentation of *TP53* mutations in the Wnt subtype [53, 54]. However, this was not linked to poor survival in these patients [53, 54].

We employed additional *tp53* mutation as a strategy to increase tumor incidence in our Wnt-type MB model. Combined *apc* and *tp53* RNP injection resulted in only low editing efficiency for *tp53.* Tumor incidence was not increased, but histological features of the observed tumors differed dramatically compared to *apc* RNP single injected tadpoles. Tumors showed mixed histology and large necrotic areas indicating a more aggressive, highly malignant tumor. However, repetition of this experiment with increased editing efficiency of *tp53* is needed.

The influence of *tp53* mutation status on tumor formation was also checked by employing heterozygous *tp53* knockout animals. Mating between $tp53^{+/-}$ animals results in wild type, heterozygous and homozygous knockout offspring that was injected with *β-catT41* RNPs. An increase in severity of hyperproliferation was observed in *tp53* mutant animals (both heterozygous and homozygous) compared to *tp53* wild type tadpoles. However, no difference between *tp53* heterozygous or homozygous knockout animals was discerned. Since none of the tadpoles presented with a brain tumor, the influence of *tp53* mutation status on tumor incidence and latency could not be assessed. An increase in sample size and follow-up of the experiment is needed to determine the impact of *tp53* knockout on Wnt signaling induced tumor formation in the hindbrain.

7.4.2 Functional analysis of tumor modulatory genes through CRISPR/Cas9 multiplexing

Wnt-type MB has the best prognosis of the MB subtypes with 5-year overall survival rates exceeding 90% [4]. Clinical trials mainly focus on therapy de-escalation by significantly reducing or even eliminating craniospinal irradiation thereby diminishing treatment-related toxicity [4, 68]. However, huge improvements could still be achieved by molecular targeted therapies. Currently, no therapeutics that specifically target constitutive Wnt signaling activation are being explored for treatment of MB [4]. Direct therapeutic targeting of the Wnt signaling pathway holds significant risk for side effects given the many functions of Wnt signaling in tissue homeostasis of various organs (see Chapter 1). Also in the post-natal cerebellum, Wnt signaling was shown to be necessary for Purkinje cell maintenance [77]. It would thus be safer to target tumor-specific downstream genes. We made use of publicly available expression data from human MB samples to identify genes that are specifically overexpressed in Wnt-type MB. As expected, this list contained Wnt target genes and

signaling factors but also genes with described oncogenic or tumor suppressive function and genes with no known role in cancer. Moreover, some of the genes present in our list, like *ALK,* have already been shown to be associated with Wnt-type MB [78]. Since initial tumor incidence in our model was low, we decided to first target additional tumor suppressor genes to increase tumor incidence and as a proof-of-principle for functional analysis of tumor modulatory genes. The tumor transcriptome is not only characterized by oncogenic genes. The system will try to find a status-quo by simultaneous upregulation of TSGs. This might be especially true in Wnt-type MB given its good prognosis. Yogi et al. described the protective effect of miR-148a, a microRNA specifically upregulated in Wnt-type MB [79]. We thus selected four candidate TSGs that are overexpressed in Wnt-type MB: *gad1, tmem51, bhmt* and *crabp2.* Multiplexed targeting of the different genes was simply done by combined injection of *apc* and candidate TSG RNPs. Feasibility of CRISPR/Cas9 multiplexing based negative-selection screening and identification of driver genes had already been shown in mice for glioblastoma and pancreatic, liver and lung cancer [70, 80-82]. Combined mosaic knockout of *apc* with *gad1, tmem51* or *crabp2* increased tumor incidence to 24%, 10% and 29%, respectively. Tumor latency was also reduced with tumors arising as early as 2 weeks post-injection in *apc* + *crabp2* RNP injected embryos. We thus show that additional knockout of overexpressed TSGs specific for Wnt-type MB reduces tumor latency and increases tumor incidence in our model. A similar approach recently uncovered *ezh2* as a TSG in g3 MB. *Ezh2* is highly expressed in some g3 MBs in human. Inactivation of ezh2 accelerated MB development in a *myc*-driven mouse model of g3 MB [83]. Changes in tumorigenesis kinetics were also employed to identify new TSGs in another study of g3 MB mouse models [84].

Vo et al. revealed that ezh2 suppresses tumorigenesis through repression of *Gfi1,* an oncogenic driver of g3 MB thereby contributing to further understanding of g3 MB and giving a clue to new therapeutic strategies [83]. One of the candidate TSGs we assessed is *crabp2.* Crabp2 is involved in retinoic acid (RA) signaling for transport of RA from the cytoplasm to its nuclear receptor. RA has been explored as a therapeutic agent in multiple malignancies with effects ranging from differentiation and apoptosis induction to tumor prevention [65]. Moreover, a synthetic RA analogue was shown to inactivate Wnt signaling, induce cell cycle arrest and inhibit migration and invasion of MB cells *in vitro* [85]. Additional knockout of *crabp2* had the most dramatic effect on tumor formation kinetics and might thus be a newly identified tumor suppressor gene in Wnt-type MB. However, we failed to confirm the observed effect with a second gRNA, probably both due to low gene-editing efficiency and too short follow-up of the experiment. Furthermore, determination of mutation status of *crabp2* in the observed tumors is needed. Nevertheless we show that our model allows functional analysis of tumor modulatory genes. Importantly, a recent study described that even though molecular subtype is homogenous across the entire tumor in MB patients, MB demonstrates significant spatial heterogeneity in somatic mutations and copy number aberrations [86]. This could complicate functional assessment of tumor modulatory genes as different regions of each tumor need to be sampled to assess selection pressure for the candidate gene. Moreover, it implies that therapeutic targeting of a single gene will be insufficient. A previous study described divergence of recurrent tumors from the original tumors with a minor clone of the original tumor driving recurrence [87]. This implies the need to assess sensitivity of the whole tumor to the targeted therapy. Moreover, it further stresses the need for personalized treatment regimens composed of therapies targeting different mutation events. This increases the urgency of functional assessment of genetic variations within different tumor types.

7.5 CONCLUSIONS

With this research we fulfill a need for representative models for the different MB subtypes that can be used for preclinical testing. In conclusion, we show that CRISPR/Cas9- mediated editing of *apc* in the *Xenopus* brain results in the formation of brain tumors. These tumors highly resemble the clinical presentation of MB. Furthermore, we show that we can use this model for functional analysis of potential tumor modulatory genes through CRISPR/Cas9 multiplexing. We provide a proof-of-principle with the identification of a new TSG for Wnt-type MB, *crabp2.*

7.6 MATERIALS AND METHODS

7.6.1 ISOLATION OF THE XENOPUS BRAIN

Froglets or frogs are sedated in 0.05% benzocaine in 0.1x MMR (10 mM NaCl, 0.2 mM KCl, 0.1 mM $MgSO_4$, 0.2 mM $CaCl_2$, 0.5 mM HEPES (pH 7.8), 0.01 mM EDTA). An incision is made on the dorsal side of the frog and skin is peeled off towards the heads. All soft tissue surrounding the skull and anterior vertebrate column is removed. The dorsal bones of the skull are thinned by scraping with a scalpel. On the transition between mid- and hindbrain, there is an opening in the skull. Insert one arm of your tweezers in this opening, and apply some force to lift the dorsal bone thereby revealing the anterior brain. The hindbrain can be revealed by cutting the first 3 to 4 vertebrae and pulling them open to the lateral side. The brain is isolated by severing the spinal cord and the cranial nerves and gently scooping it out of the bottom of the skull with closed tweezers. The brain is fixed overnight in 4% PFA/PBS at 4 °C. For further processing see 7.6.2.

7.6.2 HISTOLOGY

Tadpoles are anesthetized in 0.01% MS-222 in 0.1x MMR. Tail is cut off and intestine removed. Heads are fixed overnight @ 4 °C in 4% PFA/PBS. Heads of tadpoles aged 4 weeks and older are incubated 6h in Morse's solution (10% sodium citrate, 20% formic acid) at room temperature. Heads are then transferred to cassettes and submersed in 70% EtOH. Further dehydration and embedding in paraffin is done by Thermo Shandon Citadel 2000 (Thermo scientific). Tissue sections of 5 µm are made with a microtome (Microm HM360). Rehydration and subsequent haematoxylin and eosin staining is performed by a Varistain™24-4 Automatic Slide Stainer (Thermo scientific). Images were acquired using an Olymus BX51 light microscope or an Axio Scan.Z1 (Zeiss) equipped with a 20x Plan-Apochromat 0.8 NA dry objective and Hitachi HV-F202SCL camera.

7.6.3 DESIGN AND GENERATION OF GUIDERNAS

Design of gRNAs was performed with the CRISPRScan algorithm [88]. Generation of DNA templates was done with a PCR-based method departing from one common oligonucleotide (AAAAGCACCGACTCGGTGCCACTTTTTCAAGTTGATAACGGACTAGCCTTATTTTAACTTGCTATTTCTAGCTCTAAAAC) and one partly complementary oligonucleotide containing the target site (GAATTAATACGACTCACTATA-target site-GTTTTAGAGCTAGAAATAGC) according to [89]. Hanging ends were filled in with a standard PCR reaction using Phusion high-fidelity polymerase (Thermo scientific). Target sites for the genes used in this study are listed in Supplemental table 7.2. Purification was done through phenol/chloroform extraction and sodiumacetate precipitation followed by dilution in RNAse-free water. RNA transcription was performed using HiScribe™ T7 High Yield RNA Synthesis Kit (New England Biolabs) and gRNAs were purified by phenol-chloroform

extraction/ammoniumacetate precipitation and diluted in RNAse-free water. Concentrations were determined by Nanodrop (Thermo-Scientific).

7.6.4 MICROINJECTION OF RNPS

Wild type *Xenopus tropicalis* males and females were primed +/- 36 h in advance with 10U and 20U of PREGNYL© human chorionic gonadotropine (hCG) (Merck), respectively. Natural matings were induced by boosting the male and female with 100U and 150U hCG, respectively. Embryos were collected and jelly coat removed using 2% cysteine solution in 0.1x MMR (pH 8.0). Injection mixture was prepared by combining 400 ng/µl total gRNA (for multiplexing: 200 ng/µl gRNA A + 200 ng/µl gRNA B) with 900 ng/µl recombinant NLS-Cas9-NLS protein (VIB Protein Service Facility, UGent) [40] and incubated at 37°C for 1 minute for ribonucleoprotein complex assembly. 1 nl of the injection mixture is injected in each animal-dorsal blastomere of an 8-cell stage embryo.

7.6.5 DETERMINATION OF GENE-EDITING EFFICIENCY

For analyzing gene-editing efficiency, minimum 2 pools of 3 stage 56 tadpoles were lysed overnight at 55°C in lysis buffer containing proteinase K (50 mM Tris pH 8.8, 1 mM EDTA, 0.5% Tween-20, 200 µg/ml proteinase K). The locus of interest was amplified by PCR using Phusion high-fidelity polymerase (Thermo scientific). Primer pairs are listed in Supplemental table 7.2. Targeted deep sequencing of PCR products was performed using a previously described workflow [90, 91].

7.6.6 GENOTYPING TP53$^{+/-}$ ANIMALS

Mosaic *tp53* knockout males were mated with wild type females. 5 pools of ten stage 46 tadpoles were lysed (see 7.6.5) for gDNA extraction. Germ line transmission was checked by heteroduplex mobility assay (HMA). The *tp53* RNP targeted region was PCR amplified (primers can be found in Supplemental table 7.2) using Phusion high-fidelity polymerase (Thermo scientific). At the end of the PCR samples are heated to 98°C and slowly cooled down to 4°C (1°C/s), allowing formation of heteroduplexes due to presence of mutated sequences. Amplicons are separated on an 8% polyacrylamide gel in 1x TBE buffer (90 mM Tris-borate, 1 mM EDTA) and stained with Ethidium Bromide. Samples that contained heteroduplexes were sent for targeted deep sequencing (see 7.6.5) to confirm frame shift mutation and to estimate transmission frequency. Males that showed germ line transmission of a frame shift mutation were used again for mating with a wild type female. Embryos were raised according to [92]. Stage 55 tadpoles were sedated in 0.01% MS-222 in 0.1x MMR and the tip of the tail was cut off by a scalpel and lysed for gDNA extraction (see 7.6.5). Individual tadpoles were kept in individual containers in 0.1x MMR supplemented with gentamycin to recover. *Tp53*$^{+/-}$ animals were identified by HMA the next day and raised to adulthood according to [92].

7.6.7 ELECTROPORATION

2 week old tadpoles were sedated in 0.01% MS-222 in 0.1x MMR. Tadpoles were transferred to a silicone dish with a tissue soaked in the sedation solution. Glass capillary needles with a short taper are pulled with a P-97 Pipette Puller (Sutter instruments): heat = ramp, pull = 100, velocity = 80, delay = 120, pressure = 500, 3 loops. Injection mixture was prepared by combining 400 ng/µl total gRNA (for multiplexing: 200 ng/µl gRNA A + 200 ng/µl gRNA B) with 900 ng/µl recombinant NLS-Cas9-NLS protein (VIB Protein Service Facility, UGent) [40] and incubated at 37°C for 1 minute for ribonucleoprotein complex assembly. FCF green was added to a final concentration of 0.4% to allow

easy assessment of injection location. The injection mixture was injected in the fourth ventricle until all ventricles and spinal canal were completely filled. Immediately after injection electrodes (Genetrodes, 3 mm L-Shape, BTX) were placed next to midbrain-hindbrain tranistion and 5 pulses (18 V, 50 ms, 950 ms interval) were applied to each side with an ECM830 Square Wave Electroporation System (BTX). Tadpoles were allowed to recover for 24h in 0.1x MMR supplemented with gentamycin and were then returned to normal rearing conditions (see 7.6.6).

7.7 Author contributions

RV and KV designed and conceived the study and wrote the manuscript. RN performed all the experiments. DD generated *tp53*$^{+/-}$ animals. SD provided technical assistance.

7.8 Acknowledgements

The authors would like to thank Imane El Fakhar for technical assistance with the experiments. The authors are indebted to Tim Deceuninck for animal care.

7.9 Supplemental information

Additional malignancies observed in *apc* RNP injected tadpoles are illustrated in Figure S7.1. Brain histology after electroporation-mediated delivery of *apc* RNPs to the brain is shown in Figure S7.2. Supplemental table 7.1 represents the list of potential tumor modulatory genes for Wnt-type MB considered in this study. Target sequences for all gRNAs and corresponding primers used to assess gene editing efficiency are listed in Supplemental table 7.2.

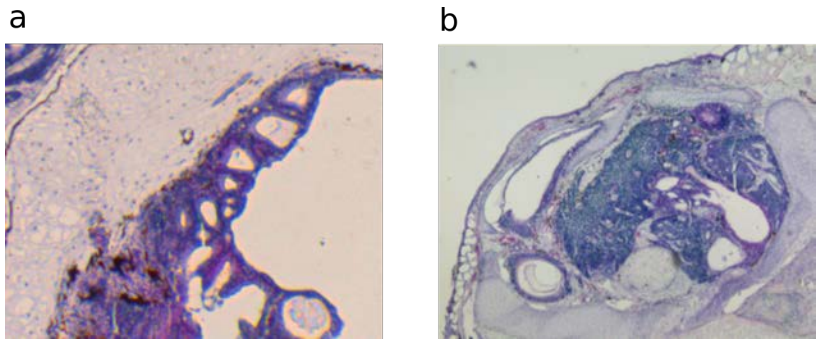

Figure S7.1 Epidermoid cysts and tumors at the nostrils after animal-dorsal *apc* RNP injection. (a) Haematoxylin and eosin staining of an epidermoid cysts on the skin after *apc* RNP injection. (b) Haematoxylin and eosin staining of a tumoral mass at the nostril of an *apc* RNP injected tadpole.

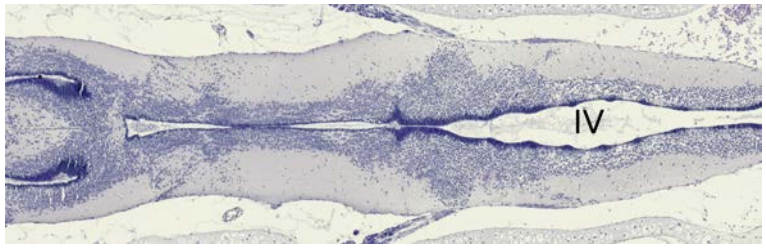

Figure S7.2 Brain histology after electroporation-mediated delivery of *apc* RNPs to the brain. Tadpoles show normal brain histology.

Supplemental table 7.1 List of potential tumor modulatory genes in Wnt-type medulloblastoma. Genes that are at least 8-fold higher expressed in Wnt-type MB compared to other MB subtypes are shown with expression difference (log2). Red genes are Wnt target genes or signaling factors, green genes are known tumor suppressor genes, blue genes are known oncogenes and orange genes have no known link to cancer.

Gene Symbol	Gene Title	S3 vs Wnt	S4 vs Wnt	Shh vs Wnt
NTN5	netrin 5	-5,003	-3,010	-5,058
VSTM2A	V-set and transmembrane domain containing 2A	-3,998	-3,060	-5,044
SLC1A3	solute carrier family 1 (glial high affinity glutamate transporter), member 3	-3,784	-3,375	-3,323
LHX8	LIM homeobox 8	-4,604	-4,063	-3,200
TNC	tenascin C	-6,125	-5,592	-5,532
CRABP2	cellular retinoic acid binding protein 2	-3,886	-3,611	-5,696
LOC101927705 /// P4HA2	uncharacterized LOC101927705 /// prolyl 4-hydroxylase, alpha polypeptide II	-3,260	-3,774	-4,619
SLC1A3	solute carrier family 1 (glial high affinity glutamate transporter), member 3	-3,889	-3,290	-3,432
DKK1	dickkopf WNT signaling pathway inhibitor 1	-4,503	-4,338	-4,533
WIF1	WNT inhibitory factor 1	-7,453	-7,267	-7,076
TNFRSF11B	tumor necrosis factor receptor superfamily, member 11b	-3,584	-3,326	-3,044
TGFA	transforming growth factor, alpha	-3,684	-3,473	-3,896
GAD1	glutamate decarboxylase 1 (brain, 67kDa)	-6,903	-6,333	-6,116
GPR64	G protein-coupled receptor 64	-4,406	-4,198	-4,200
EPHA3	EPH receptor A3	-4,783	-4,665	-4,277
EPHA3	EPH receptor A3	-3,659	-3,630	-3,322
BHMT	betaine--homocysteine S-methyltransferase	-4,268	-3,893	-4,635
DKK4	dickkopf WNT signaling pathway inhibitor 4	-5,113	-4,775	-5,109
GAD1	glutamate decarboxylase 1 (brain, 67kDa)	-4,585	-4,247	-4,549
GAD1	glutamate decarboxylase 1 (brain, 67kDa)	-5,273	-5,065	-5,214
EPHA7	EPH receptor A7	-5,190	-4,533	-4,821
AMHR2	anti-Mullerian hormone receptor, type II	-3,656	-3,630	-3,722
CNGA3	cyclic nucleotide gated channel alpha 3	-4,263	-3,571	-3,779
ALK	anaplastic lymphoma receptor tyrosine kinase	-4,327	-4,094	-3,652
SHOX2	short stature homeobox 2	-5,905	-5,122	-4,364
SHOX2	short stature homeobox 2	-6,696	-6,104	-4,698
MSX2	msh homeobox 2	-3,177	-3,073	-3,276
BMP4	bone morphogenetic protein 4	-3,391	-3,223	-3,431
TRBC1	T cell receptor beta constant 1	-3,686	-3,487	-3,655
C9orf3	chromosome 9 open reading frame 3	-3,335	-3,720	-3,437
OSR2	odd-skipped related transciption factor 2	-3,621	-3,389	-3,517
CEP112	centrosomal protein 112kDa	-3,686	-3,466	-3,557
ADAM12	ADAM metallopeptidase domain 12	-3,564	-3,091	-3,902
YME1L1	YME1-like 1 ATPase	-7,085	-5,551	-4,846
TNC	tenascin C	-5,223	-4,850	-4,797
TRDV3	T cell receptor delta variable 3	-6,665	-6,133	-4,767
RNF43	ring finger protein 43	-3,810	-3,292	-3,118
TMEM51	transmembrane protein 51	-5,277	-4,691	-4,692
RASL11B	RAS-like, family 11, member B	-4,461	-4,077	-3,213
LAMP5	lysosomal-associated membrane protein family, member 5	-4,296	-3,882	-4,445
MYOT	myotilin	-4,452	-3,914	-4,580
FZD10	frizzled class receptor 10	-5,288	-5,134	-4,824
DKK2	dickkopf WNT signaling pathway inhibitor 2	-7,202	-7,279	-6,752
FGF20	fibroblast growth factor 20	-3,233	-3,054	-3,326
LEF1	lymphoid enhancer-binding factor 1	-5,153	-4,758	-3,453
EMX2	empty spiracles homeobox 2	-6,443	-5,614	-6,280
AXIN2	axin 2	-3,288	-3,185	-3,135
DMRT2	doublesex and mab-3 related transcription factor 2	-5,664	-5,356	-5,283
WNT16	wingless-type MMTV integration site family, member 16	-3,973	-3,942	-3,926
EMB	embigin	-4,644	-4,062	-4,160
RTTN	rotatin	-3,063	-3,082	-3,483
PCSK9	proprotein convertase subtilisin/kexin type 9	-3,965	-3,504	-3,774
TNFRSF19	tumor necrosis factor receptor superfamily, member 19	-5,635	-5,296	-3,758
EPHA7	EPH receptor A7	-5,444	-4,681	-5,021

NKD1	naked cuticle homolog 1 (Drosophila)	-3,606	-3,440	-3,452
ADAMTSL1	ADAMTS-like 1	-4,419	-4,242	-4,453
RP11-401P9.4	---	-5,630	-5,340	-5,439
CCBE1	collagen and calcium binding EGF domains 1	-3,950	-3,744	-3,930
PIWIL4	piwi-like RNA-mediated gene silencing 4	-3,562	-3,523	-3,457
PGM5-AS1	PGM5 antisense RNA 1	-4,576	-4,159	-5,587
SLC35D3	solute carrier family 35, member D3	-4,943	-4,692	-4,288
PAX3	paired box 3	-4,733	-4,479	-3,438
NKD1	naked cuticle homolog 1 (Drosophila)	-4,716	-4,522	-4,612
SP5	Sp5 transcription factor	-4,614	-3,351	-4,308
LOC102659288	uncharacterized LOC102659288	-3,338	-3,153	-3,216
FAM179A	family with sequence similarity 179, member A	-3,850	-3,302	-4,358
TNC	tenascin C	-4,097	-3,716	-3,641
ADAMTSL1	ADAMTS-like 1	-3,441	-3,227	-3,219
PDE11A	phosphodiesterase 11A	-4,357	-4,256	-4,616
ABHD12B /// MIR4454	abhydrolase domain containing 12B /// microRNA 4454	-3,232	-3,037	-3,179
EPHA7	EPH receptor A7	-5,150	-4,605	-4,790
LOC440934	uncharacterized LOC440934	-3,910	-3,636	-3,421
ADAMTSL1	ADAMTS-like 1	-4,124	-4,184	-4,158
LOC101927760	uncharacterized LOC101927760	-3,156	-3,000	-3,160

Supplemental table 7.2 gRNA target sites and primers for deep sequencing. Target sites for the different genes and complementary primer pairs for targeted deep sequencing are shown.

Gene	Target sequence (5' → 3')	Primer sequence (5' → 3')
apc	GTTCTTCAGTACACCATACACGG	F: GCGGAAGATGAGATTGAAGGA R: ATGGACTGTTTGAGGAGGTG
ctnnb1 (T41)	ACTTAAAGATGGTGCTGTGG	F: TGCTGTAACTTTTGGGTTTCT R: ACTCGCTGGGCTCTTGT
tp53	CCTCAACTGAGGATTACGCA	F: CAGTGCTTATTGTTACCTCCA R: CATGGGAACTGTAGTCTATCAC
gad1	GAGCTGCTTGAAGGCTATAAAGG	F: CATCACCATCAAGGAACCA R: TCCACACTGATTCTAAAGCCA
tmem51	CGGAGTGGGAATGCTGGTCCTGG	F: CCCTGTGTTTCTTACTGTGTAGAG R: GTTTGTCTCTGTAGTGATTTCTGG
bhmt	GAGGTTGTCATCGGAGACGGCGG	F: AACTTCTGCTCCTCACTACTC R: CTGTTTATACTGCCTGTCTTTACC
crabp2	GGTGGTCCGAACCGTTGTTGAGG	F: AGGAGTGAATATGATGCTGAGG R: ATCTCGTACTGTTTGGAAGAC
crabp2 (v2)	AGTGGATGGGCGCCCTTGCAAGG	F: CCGCTTCTAAACCAGCAG R: GCACCCTATATTCCTGTATCC

7.10 References

1. Northcott, P.A., et al., *Medulloblastomics: the end of the beginning.* Nat Rev Cancer, 2012. **12**(12): p. 818-34.
2. Northcott, P.A., et al., *Medulloblastoma comprises four distinct molecular variants.* J Clin Oncol, 2011. **29**(11): p. 1408-14.
3. Coluccia, D., et al., *Medulloblastoma: Tumor Biology and Relevance to Treatment and Prognosis Paradigm.* Curr Neurol Neurosci Rep, 2016. **16**(5): p. 43.
4. Northcott, P.A., et al., *The clinical implications of medulloblastoma subgroups.* Nat Rev Neurol, 2012. **8**(6): p. 340-51.
5. Millen, K.J. and J.G. Gleeson, *Cerebellar development and disease.* Curr Opin Neurobiol, 2008. **18**(1): p. 12-9.
6. Raffel, C., *Medulloblastoma: molecular genetics and animal models.* Neoplasia, 2004. **6**(4): p. 310-22.

7. Roussel, M.F. and M.E. Hatten, *Cerebellum development and medulloblastoma.* Curr Top Dev Biol, 2011. **94**: p. 235-82.
8. Gajjar, A., et al., *Risk-adapted craniospinal radiotherapy followed by high-dose chemotherapy and stem-cell rescue in children with newly diagnosed medulloblastoma (St Jude Medulloblastoma-96): long-term results from a prospective, multicentre trial.* Lancet Oncol, 2006. **7**(10): p. 813-20.
9. Mulhern, R.K., et al., *Neurocognitive consequences of risk-adapted therapy for childhood medulloblastoma.* J Clin Oncol, 2005. **23**(24): p. 5511-9.
10. Moxon-Emre, I., et al., *Intellectual Outcome in Molecular Subgroups of Medulloblastoma.* J Clin Oncol, 2016. **34**(34): p. 4161-4170.
11. Uday, S., et al., *Endocrine sequelae beyond 10 years in survivors of medulloblastoma.* Clin Endocrinol (Oxf), 2015. **83**(5): p. 663-70.
12. Ning, M.S., et al., *Evidence of high mortality in long term survivors of childhood medulloblastoma.* J Neurooncol, 2015. **122**(2): p. 321-7.
13. Thompson, M.C., et al., *Genomics identifies medulloblastoma subgroups that are enriched for specific genetic alterations.* J Clin Oncol, 2006. **24**(12): p. 1924-31.
14. Kool, M., et al., *Integrated genomics identifies five medulloblastoma subtypes with distinct genetic profiles, pathway signatures and clinicopathological features.* PLoS One, 2008. **3**(8): p. e3088.
15. Cho, Y.J., et al., *Integrative genomic analysis of medulloblastoma identifies a molecular subgroup that drives poor clinical outcome.* J Clin Oncol, 2011. **29**(11): p. 1424-30.
16. Cavalli, F.M.G., et al., *Intertumoral Heterogeneity within Medulloblastoma Subgroups.* Cancer Cell, 2017. **31**(6): p. 737-754 e6.
17. Robinson, G., et al., *Novel mutations target distinct subgroups of medulloblastoma.* Nature, 2012. **488**(7409): p. 43-8.
18. Jones, D.T., et al., *Dissecting the genomic complexity underlying medulloblastoma.* Nature, 2012. **488**(7409): p. 100-5.
19. Ivanov, D.P., et al., *In vitro models of medulloblastoma: Choosing the right tool for the job.* J Biotechnol, 2016. **236**: p. 10-25.
20. Chlapek, P., et al., *Uniformity under in vitro conditions: Changes in the phenotype of cancer cell lines derived from different medulloblastoma subgroups.* PLoS One, 2017. **12**(2): p. e0172552.
21. Wetmore, C., D.E. Eberhart, and T. Curran, *Loss of p53 but not ARF accelerates medulloblastoma in mice heterozygous for patched.* Cancer Res, 2001. **61**(2): p. 513-6.
22. Zindy, F., et al., *Hemangiosarcomas, medulloblastomas, and other tumors in Ink4c/p53-null mice.* Cancer Res, 2003. **63**(17): p. 5420-7.
23. Briggs, K.J., et al., *Cooperation between the Hic1 and Ptch1 tumor suppressors in medulloblastoma.* Genes Dev, 2008. **22**(6): p. 770-85.
24. Gibson, P., et al., *Subtypes of medulloblastoma have distinct developmental origins.* Nature, 2010. **468**(7327): p. 1095-9.
25. Kawauchi, D., et al., *Novel MYC-driven medulloblastoma models from multiple embryonic cerebellar cells.* Oncogene, 2017.
26. Kawauchi, D., et al., *A mouse model of the most aggressive subgroup of human medulloblastoma.* Cancer Cell, 2012. **21**(2): p. 168-80.
27. Northcott, P.A., et al., *Enhancer hijacking activates GFI1 family oncogenes in medulloblastoma.* Nature, 2014. **511**(7510): p. 428-34.
28. Pei, Y., et al., *An animal model of MYC-driven medulloblastoma.* Cancer Cell, 2012. **21**(2): p. 155-67.
29. Swartling, F.J., et al., *Pleiotropic role for MYCN in medulloblastoma.* Genes Dev, 2010. **24**(10): p. 1059-72.
30. Pugh, T.J., et al., *Medulloblastoma exome sequencing uncovers subtype-specific somatic mutations.* Nature, 2012. **488**(7409): p. 106-10.

31. Lin, C.Y., et al., *Active medulloblastoma enhancers reveal subgroup-specific cellular origins.* Nature, 2016. **530**(7588): p. 57-62.
32. Northcott, P.A., et al., *Subgroup-specific structural variation across 1,000 medulloblastoma genomes.* Nature, 2012. **488**(7409): p. 49-56.
33. Munoz, D.M., et al., *CRISPR Screens Provide a Comprehensive Assessment of Cancer Vulnerabilities but Generate False-Positive Hits for Highly Amplified Genomic Regions.* Cancer Discov, 2016. **6**(8): p. 900-13.
34. Luo, J., *CRISPR/Cas9: From Genome Engineering to Cancer Drug Discovery.* Trends Cancer, 2016. **2**(6): p. 313-324.
35. Katigbak, A., et al., *A CRISPR/Cas9 Functional Screen Identifies Rare Tumor Suppressors.* Sci Rep, 2016. **6**: p. 38968.
36. Xu, C., et al., *piggyBac mediates efficient in vivo CRISPR library screening for tumorigenesis in mice.* Proc Natl Acad Sci U S A, 2017. **114**(4): p. 722-727.
37. Naert, T., T. Van Nieuwenhuysen, and K. Vleminckx, *TALENs and CRISPR/Cas9 fuel genetically engineered clinically relevant Xenopus tropicalis tumor models.* Genesis, 2017. **55**(1-2).
38. Liu, J., et al., *CRISPR/Cas9 in zebrafish: an efficient combination for human genetic diseases modeling.* Hum Genet, 2017. **136**(1): p. 1-12.
39. Van Nieuwenhuysen, T., et al., *TALEN-mediated apc mutation in Xenopus tropicalis phenocopies familial adenomatous polyposis.* Oncoscience, 2015. **2**(5): p. 555-66.
40. Naert, T., et al., *CRISPR/Cas9 mediated knockout of rb1 and rbl1 leads to rapid and penetrant retinoblastoma development in Xenopus tropicalis.* Sci Rep, 2016. **6**: p. 35264.
41. Clements, W.M., A.M. Lowy, and J. Groden, *Adenomatous polyposis coli/beta-catenin interaction and downstream targets: altered gene expression in gastrointestinal tumors.* Clin Colorectal Cancer, 2003. **3**(2): p. 113-20.
42. Guo, X., et al., *Efficient RNA/Cas9-mediated genome editing in Xenopus tropicalis.* Development, 2014. **141**(3): p. 707-14.
43. Blitz, I.L., et al., *Biallelic genome modification in F(0) Xenopus tropicalis embryos using the CRISPR/Cas system.* Genesis, 2013. **51**(12): p. 827-34.
44. Nakayama, T., et al., *Simple and efficient CRISPR/Cas9-mediated targeted mutagenesis in Xenopus tropicalis.* Genesis, 2013. **51**(12): p. 835-43.
45. Cong, L., et al., *Multiplex genome engineering using CRISPR/Cas systems.* Science, 2013. **339**(6121): p. 819-23.
46. Mali, P., et al., *RNA-guided human genome engineering via Cas9.* Science, 2013. **339**(6121): p. 823-6.
47. Wang, H., et al., *One-step generation of mice carrying mutations in multiple genes by CRISPR/Cas-mediated genome engineering.* Cell, 2013. **153**(4): p. 910-8.
48. Burger, A., et al., *Maximizing mutagenesis with solubilized CRISPR-Cas9 ribonucleoprotein complexes.* Development, 2016. **143**(11): p. 2025-37.
49. Parker, H.J., M.E. Bronner, and R. Krumlauf, *The vertebrate Hox gene regulatory network for hindbrain segmentation: Evolution and diversification: Coupling of a Hox gene regulatory network to hindbrain segmentation is an ancient trait originating at the base of vertebrates.* Bioessays, 2016. **38**(6): p. 526-38.
50. Butts, T., M.J. Green, and R.J. Wingate, *Development of the cerebellum: simple steps to make a 'little brain'.* Development, 2014. **141**(21): p. 4031-41.
51. Moody, S.A., *Fates of the blastomeres of the 16-cell stage Xenopus embryo.* Dev Biol, 1987. **119**(2): p. 560-78.
52. Noelanders, R. and K. Vleminckx, *How Wnt Signaling Builds the Brain: Bridging Development and Disease.* Neuroscientist, 2016.
53. Zhukova, N., et al., *Subgroup-specific prognostic implications of TP53 mutation in medulloblastoma.* J Clin Oncol, 2013. **31**(23): p. 2927-35.

54. Pfaff, E., et al., *TP53 mutation is frequently associated with CTNNB1 mutation or MYCN amplification and is compatible with long-term survival in medulloblastoma.* J Clin Oncol, 2010. **28**(35): p. 5188-96.
55. Levina, E., M. Oren, and A. Ben-Ze'ev, *Downregulation of beta-catenin by p53 involves changes in the rate of beta-catenin phosphorylation and Axin dynamics.* Oncogene, 2004. **23**(25): p. 4444-53.
56. Mou, H., et al., *CRISPR/Cas9-mediated genome editing induces exon skipping by alternative splicing or exon deletion.* Genome Biol, 2017. **18**(1): p. 108.
57. Harada, N., et al., *Intestinal polyposis in mice with a dominant stable mutation of the beta-catenin gene.* EMBO J, 1999. **18**(21): p. 5931-42.
58. Fei, J.-F., et al., *Tissue- and time-directed electroporation of CAS9 protein–gRNA complexes in vivo yields efficient multigene knockout for studying gene function in regeneration.* Npj Regenerative Medicine, 2016. **1**: p. 16002.
59. Chen, S., et al., *Highly Efficient Mouse Genome Editing by CRISPR Ribonucleoprotein Electroporation of Zygotes.* J Biol Chem, 2016. **291**(28): p. 14457-67.
60. Northcott, P.A., et al., *Rapid, reliable, and reproducible molecular sub-grouping of clinical medulloblastoma samples.* Acta Neuropathol, 2012. **123**(4): p. 615-26.
61. Pellanda, H., *Betaine homocysteine methyltransferase (BHMT)-dependent remethylation pathway in human healthy and tumoral liver.* Clin Chem Lab Med, 2013. **51**(3): p. 617-21.
62. Teng, Y.W., et al., *Deletion of betaine-homocysteine S-methyltransferase in mice perturbs choline and 1-carbon metabolism, resulting in fatty liver and hepatocellular carcinomas.* J Biol Chem, 2011. **286**(42): p. 36258-67.
63. Janssens, S., et al., *Direct control of Hoxd1 and Irx3 expression by Wnt/beta-catenin signaling during anteroposterior patterning of the neural axis in Xenopus.* Int J Dev Biol, 2010. **54**(10): p. 1435-42.
64. Vreeland, A.C., et al., *Cellular retinoic acid-binding protein 2 inhibits tumor growth by two distinct mechanisms.* J Biol Chem, 2014. **289**(49): p. 34065-73.
65. Schenk, T., S. Stengel, and A. Zelent, *Unlocking the potential of retinoic acid in anticancer therapy.* Br J Cancer, 2014. **111**(11): p. 2039-45.
66. Doudna, J.A. and E. Charpentier, *Genome editing. The new frontier of genome engineering with CRISPR-Cas9.* Science, 2014. **346**(6213): p. 1258096.
67. Zuckermann, M., et al., *Somatic CRISPR/Cas9-mediated tumour suppressor disruption enables versatile brain tumour modelling.* Nat Commun, 2015. **6**: p. 7391.
68. Holgado, B.L., et al., *Tailoring Medulloblastoma Treatment Through Genomics: Making a Change, One Subgroup at a Time.* Annu Rev Genomics Hum Genet, 2017. **18**: p. 143-166.
69. Blitz, I.L., M.B. Fish, and K.W. Cho, *Leapfrogging: primordial germ cell transplantation permits recovery of CRISPR/Cas9-induced mutations in essential genes.* Development, 2016. **143**(15): p. 2868-75.
70. Maresch, R., et al., *Multiplexed pancreatic genome engineering and cancer induction by transfection-based CRISPR/Cas9 delivery in mice.* Nat Commun, 2016. **7**: p. 10770.
71. Engel, N.W., et al., *Canonical Wnt Signaling Drives Tumor-Like Lesions from Sox2-Positive Precursors of the Murine Olfactory Epithelium.* PLoS One, 2016. **11**(11): p. e0166690.
72. Chenn, A. and C.A. Walsh, *Regulation of cerebral cortical size by control of cell cycle exit in neural precursors.* Science, 2002. **297**(5580): p. 365-9.
73. Woodhead, G.J., et al., *Cell-autonomous beta-catenin signaling regulates cortical precursor proliferation.* J Neurosci, 2006. **26**(48): p. 12620-30.
74. Staahl, B.T., et al., *Efficient genome editing in the mouse brain by local delivery of engineered Cas9 ribonucleoprotein complexes.* Nat Biotechnol, 2017. **35**(5): p. 431-434.
75. Baugh, E.H., et al., *Why are there hotspot mutations in the TP53 gene in human cancers?* Cell Death Differ, 2017.
76. Tabori, U., et al., *Universal poor survival in children with medulloblastoma harboring somatic TP53 mutations.* J Clin Oncol, 2010. **28**(8): p. 1345-50.

77. Huang, Y., et al., *Lrp5/6 are required for cerebellar development and for suppressing TH expression in Purkinje cells via beta-catenin.* Mol Brain, 2016. **9**: p. 7.
78. Lastowska, M., et al., *ALK Expression Is a Novel Marker for the WNT-activated Type of Pediatric Medulloblastoma and an Indicator of Good Prognosis for Patients.* Am J Surg Pathol, 2017. **41**(6): p. 781-787.
79. Yogi, K., et al., *MiR-148a, a microRNA upregulated in the WNT subgroup tumors, inhibits invasion and tumorigenic potential of medulloblastoma cells by targeting Neuropilin 1.* Oncoscience, 2015. **2**(4): p. 334-48.
80. Weber, J., et al., *CRISPR/Cas9 somatic multiplex-mutagenesis for high-throughput functional cancer genomics in mice.* Proc Natl Acad Sci U S A, 2015. **112**(45): p. 13982-7.
81. Rogers, Z.N., et al., *A quantitative and multiplexed approach to uncover the fitness landscape of tumor suppression in vivo.* Nat Methods, 2017. **14**(7): p. 737-742.
82. Chow, R.D., et al., *AAV-mediated direct in vivo CRISPR screen identifies functional suppressors in glioblastoma.* Nat Neurosci, 2017.
83. Vo, B.T., et al., *Inactivation of Ezh2 Upregulates Gfi1 and Drives Aggressive Myc-Driven Group 3 Medulloblastoma.* Cell Rep, 2017. **18**(12): p. 2907-2917.
84. Wei, L., et al., *Exome sequencing analysis of murine medulloblastoma models identifies WDR11 as a potential tumor suppressor in Group 3 tumors.* Oncotarget, 2017. **8**(39): p. 64685-64697.
85. Bassani, B., et al., *Fenretinide (4-HPR) Targets Caspase-9, ERK 1/2 and the Wnt3a/beta-Catenin Pathway in Medulloblastoma Cells and Medulloblastoma Cell Spheroids.* PLoS One, 2016. **11**(7): p. e0154111.
86. Morrissy, A.S., et al., *Spatial heterogeneity in medulloblastoma.* Nat Genet, 2017. **49**(5): p. 780-788.
87. Morrissy, A.S., et al., *Divergent clonal selection dominates medulloblastoma at recurrence.* Nature, 2016. **529**(7586): p. 351-7.
88. Moreno-Mateos, M.A., et al., *CRISPRscan: designing highly efficient sgRNAs for CRISPR-Cas9 targeting in vivo.* Nat Methods, 2015. **12**(10): p. 982-8.
89. Bassett, A.R., et al., *Highly efficient targeted mutagenesis of Drosophila with the CRISPR/Cas9 system.* Cell Rep, 2013. **4**(1): p. 220-8.
90. Boel, A., et al., *BATCH-GE: Batch analysis of Next-Generation Sequencing data for genome editing assessment.* Sci Rep, 2016. **6**: p. 30330.
91. De Leeneer, K., et al., *Flexible, scalable, and efficient targeted resequencing on a benchtop sequencer for variant detection in clinical practice.* Hum Mutat, 2015. **36**(3): p. 379-87.
92. Jafkins, A., et al., *Husbandry of Xenopus tropicalis.* Methods Mol Biol, 2012. **917**: p. 17-31.

PART IV
GENERAL DISCUSSION AND PERSPECTIVES

CHAPTER 8

GENERAL DISCUSSION AND PERSPECTIVES

8.1 INTRODUCTION

Embryonic development entails the careful orchestration of multiple simultaneous processes, like cell proliferation, differentiation and migration, leading to the formation of a fully autonomous organism from a single cell. Astonishingly, all these processes are regulated by a limited amount of highly conserved developmental signaling pathways that are reiteratively used throughout life. The Wnt/β-catenin pathway is responsible for a myriad of functions ranging from establishment of the dorsal organizer to proliferation of stem cells in the adult intestine. Deregulation of the Wnt/β-catenin signaling pathway has consequently been linked to a variety of human diseases, both congenital and acquired. This is especially true for the central nervous system where Wnt signaling has been linked to congenital disorders, like neural tube defects and autism, neurodegenerative disorders, like Alzheimer's and Parkinson's disease and to brain malignancies, like glioma and medulloblastoma [1]. Advancement in understanding of the spatiotemporal regulation of this multifaceted signaling pathway during development and disease can guide new research towards a cure for Wnt-related disorders.

In this work, we focused on the hindbrain. The hindbrain is responsible for most vital functions like breathing, heartbeat, consciousness and motor coordination and as a result is highly conserved throughout evolution [2]. We employed *Xenopus tropicalis* as a model organism, which due to its external development, large brood size, aquatic habitat and easy experimental manipulation allowed us take a unique approach to answer our biological questions.

8.2 WNT/β-CATENIN SIGNALING IN THE HINDBRAIN: THE RHOMBOMERE BOUNDARIES

One of the most remarkable features of the embryonic hindbrain is its subdivision in eight rhombomeres. This subdivision can be observed physically as a series of bulges, but more importantly also at the molecular level by segment-specific expression of transcription factors [3]. At the boundaries between these segments, a specialized cell population is formed that shows activity of multiple signaling pathways [4-6]. However, the precise function of these rhombomere boundaries (RBs) remains unclear.

A transgenic *Xenopus* Wnt reporter line, which reflects the spatiotemporal dynamics of Wnt signaling activity, was generated in our research group [7]. These animals show highly localized Wnt signaling activity in the RBs from tadpole stages on (Nieuwkoop stage 41). In zebrafish, a positive feedback loop between Notch and Wnt signaling at the RBs, similar to the dorso-ventral boundary in the *Drosophila* wing disc, was proposed [4]. However, our results contradict the proposed model and instead show an antagonistic relationship between both signaling pathways at the RBs. Expression of Notch signaling factors is excluded from the RBs, but is instead confined to a repetitive pattern in the rhombomere centers. Wnt signaling inhibition lead to a narrowing of the rhombomere boundaries and almost continuous expression of Notch signaling factors throughout the hindbrain. Conversely, Notch signaling inhibition resulted in widening of Wnt signaling activity around the RBs, while Notch signaling activation almost eradicated Wnt signaling activity in the hindbrain. We thus revealed opposing activities of both signaling pathways in the hindbrain (Figure 8.1).

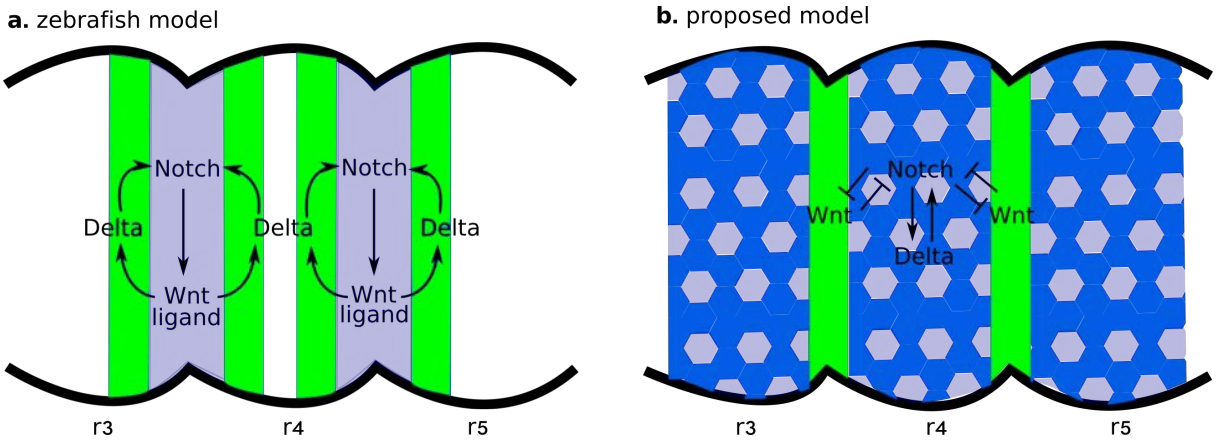

Figure 8.1 Comparison zebrafish model and proposed model. (a) Previous model describing Wnt-Notch signaling interaction in the zebrafish hindbrain. A positive feedback loop was proposed in which active Notch signaling at the rhombomere boundaries induces expression of Wnt ligands in the boundaries. Wnt signaling, in turn, induces expression of Notch ligands (Delta) adjacent to the boundaries. Delta-Notch interaction maintains Notch signaling activation in the boundaries. (b) Proposed model based on experimental data in *Xenopus.* Notch signaling factors are exclusively expressed in the rhombomere centers, while Wnt signaling is specifically activated in the rhombomere boundaries. Both pathways counteract each other's expression maintaining two distinct cell populations. An antagonistic relationship thus exists between both pathways. In the rhombomere centers Notch signaling activity regulates neurogenesis via lateral inhibition.

Many questions still remain about the mechanism behind the observed Wnt-Notch antagonism. Interplay between Notch and Wnt signaling has been extensively described [8]. Interaction between both pathways can be either agonistic or antagonistic, transcription dependent or -independent and can occur at multiple levels of the signaling cascade. Since most of the RNA constructs used in this study interfered at the transcriptional endpoint of either pathway, a transcription-dependent mechanism seems most plausible. This is further supported by the long-range effect of Wnt signaling activation to the whole rhombomere, which indicates involvement of another factor downstream of Wnt signaling. Specific interference on different levels of each pathway, e.g. by knockdown or

knockout of specific signaling factors, is needed to elucidate the interaction between both pathways. Importantly, the signaling pathways are often involved in binary cell fate decisions in which mutually exclusive signaling states guide cells along the right lineage and refine initially crude patterns [8]. This indicates that the signaling antagonism in the hindbrain assures localized Wnt signaling activation in the RBs. Not surprisingly, the tight interaction between Wnt and Notch signaling also has clinical implications. *In vitro* directed differentiation of embryonic stem cells or induced pluripotent cells for therapeutic intervention is highly dependent upon recapitulation of endogenous signaling events, stressing the need to understand signaling crosstalk under physiological conditions [8, 9]. Furthermore, signaling interaction in cancer has also been described [10-14]. This implies that we have to consider the effects on both pathways when therapeutically targeting either Wnt or Notch signaling. Interference with one signaling pathway may have unwanted effects on signaling activity of the other pathway or, on the contrary, the interplay can be exploited to simultaneously target both pathways.

Only one Notch signaling factor was expressed in the RBs, the Notch target gene *hes1.* We show that *hes1* expression in the RBs is induced by Wnt signaling. Wnt signaling induced expression from the *Xenopus tropicalis hes1* promoter in vitro to a similar extent as Notch signaling. However, we could not observe a synergistic effect. While Wnt signaling activation induced widening of the *hes1* expression domain in the hindbrain, Wnt signaling inhibition eradicated *hes1* expression in the RBs. Other studies have already described Notch-independent regulation of *hes1* expression, including regulation by Wnt signaling [15-17]. We provide a new example of Wnt-signaling dependent *hes1* expression. Moreover, the β-catenin ChIP experiment strongly indicates that *hes1* is a direct target gene of Wnt signaling. Interestingly, *hes1* expression is associated with neural progenitor cells in which elevated *hes1* expression prevents neural differentiation through direct repression of proneural genes [18, 19]. A recent study in chick identified the RBs as pools of self-renewing and multipotent neural stem or progenitor cells that serve as a source of progenitors and differentiating neurons for the rhombomeres [20]. Furthermore, Wnt signaling in the RBs is specifically active on the ventricular side. The subventricular zone is a well-described source of neural progenitor cells. We evaluated the proliferation characteristics of Wnt-active cells in the *Xenopus* hindbrain. Cell cycle analysis shows that Wnt-active boundary cells are actively cycling cells and indicates increased proliferation compared to Wnt-inactive cells. Moreover, we find that Wnt signaling activation induces G1- to S-phase transition, possibly due to induction of its target gene *cyclinD1* [21-23]. IdU labeling also showed clear enrichment of S-phase cells at the RBs. Together this indicates that Wnt signaling prevents cell cycle exit and induces proliferation in at least a subset of RB cells. Wnt signaling has been shown to promote proliferation of different progenitor cell populations in the brain during development, in the adult and upon disease or injury [24-28]. However, Peretz et al. describe the chick boundary cells as a slow cycling population with proliferation occurring immediately adjacent to the RBs [20]. No Wnt signaling activity has been described in the chick indicating species-specific signaling networks. Based on the current observations we would like to propose a new model for Wnt signaling function in the hindbrain (Figure 8.2). According to this model, during early development, the rhombomere boundaries function as a barrier separating autonomous units. They are a population of quiescent, inert cells that aid patterning of the hindbrain through its subdivision in smaller compartments. However, at this stage these boundary cells already show signaling activity and act as a source of morphogens to pattern the adjacent tissue. During later stages, when crude neural circuitry is formed, Wnt signaling is activated in the rhombomere boundary cells and induces their self-renewal. The rhombomere boundaries now functions as a

reservoir of naïve progenitor cells or stem cells that will further contribute to neural circuitry formation in the hindbrain. Wnt-Notch signaling antagonism confines Wnt signaling mediated self-renewal to the boundaries and prevents depletion of this progenitor population through Notch-mediated neurogenesis.

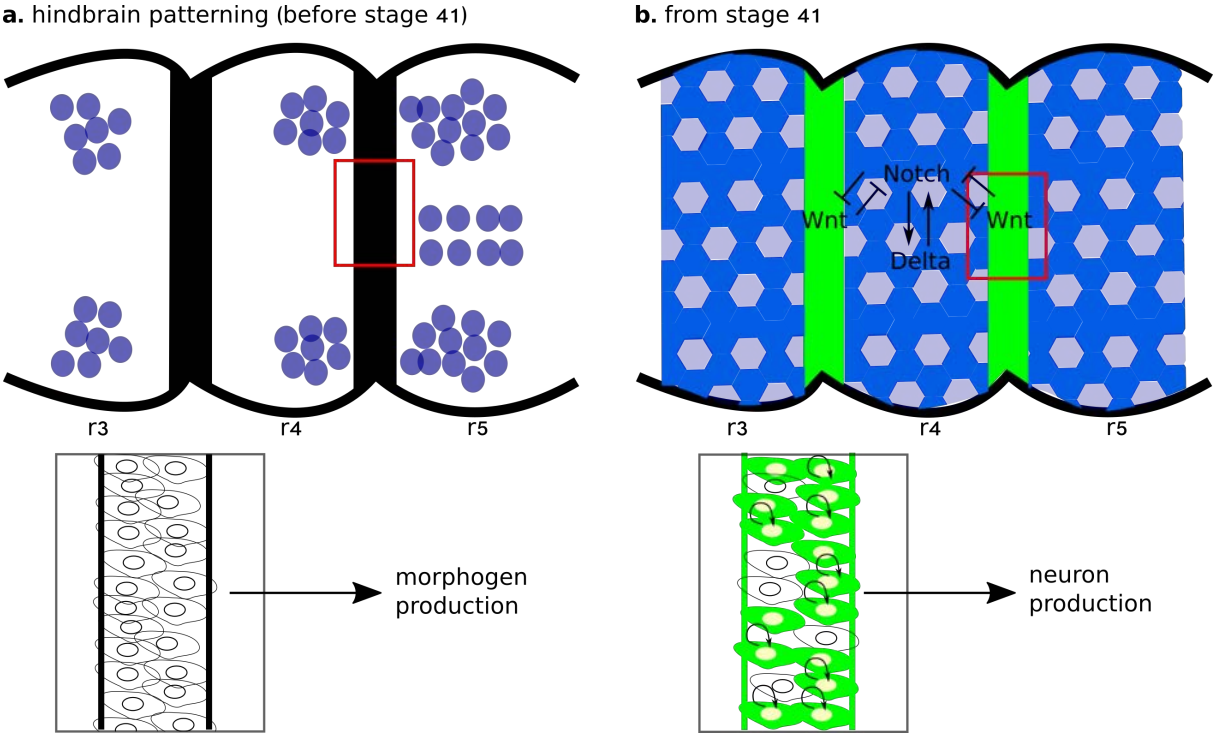

Figure 8.2 Proposed model for Wnt signaling function in the rhombomere boundaries. (a) During early hindbrain development the rhombomere boundary cells are a quiescent, inert cell population. The rhombomere boundaries produce morphogens that further pattern the adjacent tissue. At this time crude patterning of hindbrain neural circuits occurs as depicted here for the nuclei of cranial motorneurons. (b) Wnt signaling is activated in the *Xenopus* rhombomere boundaries from stage 41 and induces proliferation of the rhombomere boundary cells. The boundaries now actively contribute to new neuron formation in the rhombomere centers. At the same time Wnt-Notch signaling antagonism exists, separating the self-renewing boundary cells from the rhombomere centers, where Notch mediated neurogenesis occurs through lateral inhibition. Red rectangles show boundary areas enlarged in lower panels.

However, further research is necessary to confirm the assumptations made in this model. More detailed analysis of the cell cycle upon Wnt interference, for instance cell cycle length by double halogenated thymidine analogue labeling or length of each cell cyle phase by separation of all five cell cycle phases, would provide more insight on proliferation characteristics of the boundary cells. Furthermore, cell fate of the Wnt active boundary cells has to be determined to define them as stem cells. Especially long-term consequences of Wnt signaling interference need to be elucidated. We already showed that Wnt signaling inhibition leads to increased cell-cycle exit through an increase in the immature neuron marker *myt1*, which indicates importance of Wnt signaling for progenitor maintenance. Its inhibition may thus lead to depletion of neural progenitor cells, which could influence neuronal circuit formation in the hindbrain. Thorough analysis of neural circuit formation after Wnt signaling interference during different time frames could elucidate the contribution of RB cells to different neuron populations of the hindbrain. However, the limited availability of specific neuron markers in *Xenopus* hinders this analysis. Furthermore, it might be interesting to induce injury to the hindbrain and investigate contribution of Wnt active RB cells to tissue regeneration.

The continued value of *Xenopus* for embryology studies was confirmed by this research. The extensive expression analysis of Notch signaling factors was made possible through the large brood

size and ease of experimental manipulation of signaling pathways in *Xenopus* through microinjection of RNA constructs. On average 300 embryos were used for each experiment a feat that would no be possible in mice. Furthermore, for cell cycle analysis again 180 – 270 hindbrains were dissected. This is possible due to the external development and relatively large size of *Xenopus* embryos. Zebrafish embryos are considerably smaller making tissue dissections very challenging.
Research on hindbrain development has mainly focused on the initial segmentation process and the formation of boundaries creating lineage-restricted compartments. A recent study [20] and our work presented here reveal the rhombomere boundaries as pools of neural stem cells after embryonic development. Further research is needed to elucidate their role in maturation of the hindbrain.

8.3 WNT/β-CATENIN SIGNALING IN THE HINDBRAIN: MEDULLOBLASTOMA

Next generation sequencing has created vast libraries of genomic alterations in human cancer. However, correlating these changes with their function in tumor formation and progression holds the major challenge for modern cancer research. Cancer cells in culture display extensive genetic and epigenetic changes and completely eliminate influence from the tumor microenvironment, thereby limiting their value for providing new insights in tumor biology *in vivo.* Many genetically engineered mouse models of human cancers have been generated and have yielded invaluable insight in tumor growth in an *in vivo* setting. However, generation of these models is time-consuming and expensive, making them insufficient for large-scale functional screening [29]. CRISPR/Cas9 has quickly gained value in cancer research as a tool to more rapidly generate complex genetic models [30]. It also made it possible to apply factual reverse genetics in lower vertebrates, like *Xenopus,* thereby creating a new toolbox for modeling human disease. Our research group created the first *Xenopus* cancer models by targeted-nuclease mediated editing of known tumor suppressor genes [31, 32]. In this work we generated a model for Wnt-type medulloblastoma (MB) and assessed its applicability for functional analysis of tumor modulatory genes.
MB is the most common pediatric brain malignancy. Four subtypes exist based on the molecular variation driving tumor formation. Wnt-type MB is characterized by constitutive activation of the Wnt signaling pathway. Targeted injection of *apc* gRNA/Cas9 ribonucleoprotein complexes (RNPs) to the brain resulted in the formation of brain tumors highly resembling the clinical presentation of medulloblastoma. Tumors appeared early (after 6 weeks), as we observed with the other *Xenopus* cancer models [31, 32]. However, incidence was low (15%). Given the important role for Wnt signaling in multiple processes during brain development we believe that developmental defects somehow interfere with tumor formation. Indeed, upon high editing efficiency brain architecture is severely disrupted, showing clear signs of hyperproliferation. Another possibility is that constitutive Wnt signaling activation is needed but not sufficient to drive tumor formation. Additional mutational events might be necessary, however it is highly likely that these events are patient-specific. The firstly developed mouse model for Wnt-type MB, solely based on Wnt signaling activation and *Tp53* loss of function, only results in 15% tumor formation after 500 days [33]. Addition of a mutation in *pik3ca* found in a single patient increased tumor incidence to 100% after 3 months [34]. 85% of Wnt-type MB show monosomy 6 [35-38]. This indicates that (a) factor(s) on chromosome 6 are important for Wnt-type MB progression.
We attempted to increase tumor incidence through electroporation-mediated delivery of RNPs directly to the tadpole brain. In this way we postpone gene-editing until after embryonic development thereby avoiding the impact of embryonic defects on analysis of tumor formation. We

were not yet successful in achieving high gene-editing efficiency after electroporation, but further optimization of this technique could expand the scope of *Xenopus* for human genetic disease modeling, especially for genes with important developmental functions. Furthermore, we tried to increase tumor incidence through additional knockout of *tp53,* a well-known tumor suppressor that is often mutated in Wnt-type MB [39, 40]. Even though editing efficiency for *tp53* and tumor incidence was low, we observed a dramatic change in tumor histology. Tumors showed a more aggressive, malignant phenotype. When comparing tumor formation in $tp53^{-/-}$, $tp53^{+/-}$ and $tp53^{+/+}$ animals we saw no real genotype-phenotype correlation. Importantly, *tp53* LOF is not associated with worse prognosis in Wnt-type MB [39, 40]. Further experiments are needed to elucidate the role of *tp53* in Wnt-type MB initiation and progression.

The ultimate goal is to use our *Xenopus* model for negative-selection based screening of tumor dependency factors. These are factors that are essential for either tumor formation or survival. Tumor formation is a process during which high selective pressure arises for genetic variations that will give the tumor a survival advantage. Simultaneously, there is a negative selection pressure for LOF of dependency factors as tumor formation or survival would not be possible without their functional gene product. An interesting candidate dependency factor for Wnt-type MB would be *ALK.* This is a receptor tyrosine kinase that is frequently altered in human cancer [41]. *ALK* is highly expressed in Wnt-type MB, partly through activation of *ALK*-specific enhancers [42]. Importantly, ALK inhibitors are already available in the clinic for the treatment of non-small cell lung cancer [41]. Since further optimization of the model to increase tumor incidence was still needed to commence negative-selection based screening, we decided to first conduct functional analysis of Wnt-type MB specific potential tumor suppressor genes through CRISPR/Cas9 multiplexing. This would provide a proof-of-principle of our experimental set-up. CRISPR/Cas9 multiplexing based functional annotation of cancer genomes has been done in mice [43-45]. However, this was done by simultaneous targeting of >10 genes to maintain economic feasibility. Large deletions and chromosomal rearrangements have been described by using this approach [43, 44, 46]. Furthermore, this significantly complicates analysis of the essentiality of each gene separately. Due to the advantages of using *Xenopus,* like large brood size, aquatic habitat and low tumor latency, we could screen the same amount of genes separately in a similar time frame. We identified three genes that modified tumor characteristics in our Wnt-type MB model. Two of these, *gad1* and *crabp2,* increased tumor incidence and reduced tumor latency, identifying them as new potential tumor suppressor genes. Further validation is evidently needed, but these experiments prove the applicability of our model for straightforward functional analysis of potential tumor modulatory genes.

This research underscores some important advantages of using *Xenopus* for cancer modeling. *Xenopus* can tolerate a wide range of living conditions, are obligatory aquatic and can be simply held in aquaria. Brood size is large, generating several thousand embryos and development occurs extra-uterine [47]. These characteristics are shared with zebrafish and make disease modeling in these lower vertebrates economically feasible for semi-high throughput functional screening of disease genes compared to mammalian model systems. The discovery of novel genome editing tools, like CRISPR/Cas9, has permitted the induction of targeted mutations, thereby allowing reverse genetics in these non-murine animal models. Furthermore, using injection of CRISPR/Cas9 components results in tumor formation in F0 animals without the requirement of time-consuming breeding. Moreover, compared to zebrafish, *Xenopus tropicalis* holds some advantages. *X. tropicalis,* has a true diploid genome [47-49]. Importantly, the *X. tropicalis* genome also shows great homology with the human genome, while the zebrafish genome is paleotetraploid [48, 50]. The genome of *X. tropicalis* was

published in 2010 and is highly syntenic with the human genome [47, 49]. This allows easy identification of orthologs of human disease genes [47]. Furthermore, translation of findings in zebrafish directly to mammals has limitations, while amphibians, like *Xenopus,* are evolutionary closer to humans. In fact, amphibians are the highest order animals having free-living offspring, thus permitting high-throughput chemical screening. Firstly, they are tetrapods and thus, unlike fish, develop limbs and lungs [47]. Organ organization and structure of the heart, kidneys and immune system are more similar to their mammalian counterparts [51, 52]. Second, due to the availability of a fate map and the relatively large size of the embryos, injections of experimental molecules can be targeted to specific blastomeres [53]. This allows assessment of tissue-specific functions and functional examination of genes that are lethal in a full knockout context.

Molecular stratification of MB patients is not yet routine practice in the clinic [54]. Any progress made in identification of new therapeutic targets and their advancement to clinical trials could boost implementation of molecular stratification in the clinic. This would in turn lead to a more personalized medicine with improved outcomes and reduced impact on long-term quality of life. We generated a new *Xenopus tropicalis* model for Wnt-type MB and show the fitness of this model for functional analysis of tumor modulatory genes.

8.4 REFERENCES

1. Noelanders, R. and K. Vleminckx, *How Wnt Signaling Builds the Brain: Bridging Development and Disease.* Neuroscientist, 2016.
2. Parker, H.J., M.E. Bronner, and R. Krumlauf, *The vertebrate Hox gene regulatory network for hindbrain segmentation: Evolution and diversification: Coupling of a Hox gene regulatory network to hindbrain segmentation is an ancient trait originating at the base of vertebrates.* Bioessays, 2016. **38**(6): p. 526-38.
3. Kiecker, C. and A. Lumsden, *Compartments and their boundaries in vertebrate brain development.* Nat Rev Neurosci, 2005. **6**(7): p. 553-64.
4. Riley, B.B., et al., *Rhombomere boundaries are Wnt signaling centers that regulate metameric patterning in the zebrafish hindbrain.* Dev Dyn, 2004. **231**(2): p. 278-91.
5. Cheng, Y.C., et al., *Notch activation regulates the segregation and differentiation of rhombomere boundary cells in the zebrafish hindbrain.* Dev Cell, 2004. **6**(4): p. 539-50.
6. Weisinger, K., et al., *Analysis of expression and function of FGF-MAPK signaling components in the hindbrain reveals a central role for FGF3 in the regulation of Krox20, mediated by Pea3.* Dev Biol, 2010. **344**(2): p. 881-95.
7. Tran, H.T., et al., *Wnt/beta-catenin signaling is involved in the induction and maintenance of primitive hematopoiesis in the vertebrate embryo.* Proc Natl Acad Sci U S A, 2010. **107**(37): p. 16160-5.
8. Collu, G.M., A. Hidalgo-Sastre, and K. Brennan, *Wnt-Notch signalling crosstalk in development and disease.* Cell Mol Life Sci, 2014. **71**(18): p. 3553-67.
9. Mussmann, C., et al., *HES5 is a key mediator of Wnt-3a-induced neuronal differentiation.* Stem Cells Dev, 2014. **23**(12): p. 1328-39.
10. Balint, K., et al., *Activation of Notch1 signaling is required for beta-catenin-mediated human primary melanoma progression.* J Clin Invest, 2005. **115**(11): p. 3166-76.
11. Hanlon, L., et al., *Notch1 functions as a tumor suppressor in a model of K-ras-induced pancreatic ductal adenocarcinoma.* Cancer Res, 2010. **70**(11): p. 4280-6.
12. Kim, H.A., et al., *Notch1 counteracts WNT/beta-catenin signaling through chromatin modification in colorectal cancer.* J Clin Invest, 2012. **122**(9): p. 3248-59.
13. Kwon, C., et al., *Notch post-translationally regulates beta-catenin protein in stem and progenitor cells.* Nat Cell Biol, 2011. **13**(10): p. 1244-51.

14. Nicolas, M., et al., *Notch1 functions as a tumor suppressor in mouse skin.* Nat Genet, 2003. **33**(3): p. 416-21.
15. Issack, P.S. and E.B. Ziff, *Genetic elements regulating HES-1 induction in Wnt-1-transformed PC12 cells.* Cell Growth Differ, 1998. **9**(10): p. 827-36.
16. Kubo, F. and S. Nakagawa, *Hairy1 acts as a node downstream of Wnt signaling to maintain retinal stem cell-like progenitor cells in the chick ciliary marginal zone.* Development, 2009. **136**(11): p. 1823-33.
17. Wall, D.S., et al., *Progenitor cell proliferation in the retina is dependent on Notch-independent Sonic hedgehog/Hes1 activity.* J Cell Biol, 2009. **184**(1): p. 101-12.
18. Taelman, V., et al., *Sequences downstream of the bHLH domain of the Xenopus hairy-related transcription factor-1 act as an extended dimerization domain that contributes to the selection of the partners.* Dev Biol, 2004. **276**(1): p. 47-63.
19. Kobayashi, T., et al., *The cyclic gene Hes1 contributes to diverse differentiation responses of embryonic stem cells.* Genes Dev, 2009. **23**(16): p. 1870-5.
20. Peretz, Y., et al., *A new role of hindbrain boundaries as pools of neural stem/progenitor cells regulated by Sox2.* BMC Biol, 2016. **14**: p. 57.
21. Tetsu, O. and F. McCormick, *Beta-catenin regulates expression of cyclin D1 in colon carcinoma cells.* Nature, 1999. **398**(6726): p. 422-6.
22. Shtutman, M., et al., *The cyclin D1 gene is a target of the beta-catenin/LEF-1 pathway.* Proc Natl Acad Sci U S A, 1999. **96**(10): p. 5522-7.
23. Amoyel, M., et al., *Wnt1 regulates neurogenesis and mediates lateral inhibition of boundary cell specification in the zebrafish hindbrain.* Development, 2005. **132**(4): p. 775-85.
24. Chenn, A. and C.A. Walsh, *Regulation of cerebral cortical size by control of cell cycle exit in neural precursors.* Science, 2002. **297**(5580): p. 365-9.
25. Adachi, K., et al., *Beta-catenin signaling promotes proliferation of progenitor cells in the adult mouse subventricular zone.* Stem Cells, 2007. **25**(11): p. 2827-36.
26. Imura, T., et al., *Adenomatous polyposis coli is essential for both neuronal differentiation and maintenance of adult neural stem cells in subventricular zone and hippocampus.* Stem Cells, 2010. **28**(11): p. 2053-2064.
27. Piccin, D. and C.M. Morshead, *Wnt signaling regulates symmetry of division of neural stem cells in the adult brain and in response to injury.* Stem Cells, 2011. **29**(3): p. 528-38.
28. Lie, D.C., et al., *Wnt signalling regulates adult hippocampal neurogenesis.* Nature, 2005. **437**(7063): p. 1370-5.
29. Rogers, Z.N., et al., *A quantitative and multiplexed approach to uncover the fitness landscape of tumor suppression in vivo.* Nat Methods, 2017. **14**(7): p. 737-742.
30. Luo, J., *CRISPR/Cas9: From Genome Engineering to Cancer Drug Discovery.* Trends Cancer, 2016. **2**(6): p. 313-324.
31. Naert, T., et al., *CRISPR/Cas9 mediated knockout of rb1 and rbl1 leads to rapid and penetrant retinoblastoma development in Xenopus tropicalis.* Sci Rep, 2016. **6**: p. 35264.
32. Van Nieuwenhuysen, T., et al., *TALEN-mediated apc mutation in Xenopus tropicalis phenocopies familial adenomatous polyposis.* Oncoscience, 2015. **2**(5): p. 555-66.
33. Gibson, P., et al., *Subtypes of medulloblastoma have distinct developmental origins.* Nature, 2010. **468**(7327): p. 1095-9.
34. Robinson, G., et al., *Novel mutations target distinct subgroups of medulloblastoma.* Nature, 2012. **488**(7409): p. 43-8.
35. Clifford, S.C., et al., *Wnt/Wingless pathway activation and chromosome 6 loss characterize a distinct molecular sub-group of medulloblastomas associated with a favorable prognosis.* Cell Cycle, 2006. **5**(22): p. 2666-70.
36. Jones, D.T., et al., *Dissecting the genomic complexity underlying medulloblastoma.* Nature, 2012. **488**(7409): p. 100-5.
37. Northcott, P.A., et al., *The whole-genome landscape of medulloblastoma subtypes.* Nature, 2017. **547**(7663): p. 311-317.

38. Northcott, P.A., et al., *Medulloblastoma comprises four distinct molecular variants.* J Clin Oncol, 2011. **29**(11): p. 1408-14.
39. Zhukova, N., et al., *Subgroup-specific prognostic implications of TP53 mutation in medulloblastoma.* J Clin Oncol, 2013. **31**(23): p. 2927-35.
40. Pfaff, E., et al., *TP53 mutation is frequently associated with CTNNB1 mutation or MYCN amplification and is compatible with long-term survival in medulloblastoma.* J Clin Oncol, 2010. **28**(35): p. 5188-96.
41. Hallberg, B. and R.H. Palmer, *Mechanistic insight into ALK receptor tyrosine kinase in human cancer biology.* Nat Rev Cancer, 2013. **13**(10): p. 685-700.
42. Lin, C.Y., et al., *Active medulloblastoma enhancers reveal subgroup-specific cellular origins.* Nature, 2016. **530**(7588): p. 57-62.
43. Maresch, R., et al., *Multiplexed pancreatic genome engineering and cancer induction by transfection-based CRISPR/Cas9 delivery in mice.* Nat Commun, 2016. **7**: p. 10770.
44. Weber, J., et al., *CRISPR/Cas9 somatic multiplex-mutagenesis for high-throughput functional cancer genomics in mice.* Proc Natl Acad Sci U S A, 2015. **112**(45): p. 13982-7.
45. Chow, R.D., et al., *AAV-mediated direct in vivo CRISPR screen identifies functional suppressors in glioblastoma.* Nat Neurosci, 2017.
46. Shin, H.Y., et al., *CRISPR/Cas9 targeting events cause complex deletions and insertions at 17 sites in the mouse genome.* Nat Commun, 2017. **8**: p. 15464.
47. Schmitt, S.M., M. Gull, and A.W. Brandli, *Engineering Xenopus embryos for phenotypic drug discovery screening.* Adv Drug Deliv Rev, 2014. **69-70**: p. 225-46.
48. Hirsch, N., L.B. Zimmerman, and R.M. Grainger, *Xenopus, the next generation: X. tropicalis genetics and genomics.* Dev Dyn, 2002. **225**(4): p. 422-33.
49. Hellsten, U., et al., *The genome of the Western clawed frog Xenopus tropicalis.* Science, 2010. **328**(5978): p. 633-6.
50. Howe, K., et al., *The zebrafish reference genome sequence and its relationship to the human genome.* Nature, 2013. **496**(7446): p. 498-503.
51. Raciti, D., et al., *Organization of the pronephric kidney revealed by large-scale gene expression mapping.* Genome Biol, 2008. **9**(5): p. R84.
52. Ny, A., et al., *A genetic Xenopus laevis tadpole model to study lymphangiogenesis.* Nat Med, 2005. **11**(9): p. 998-1004.
53. Moody, S.A., *Fates of the blastomeres of the 16-cell stage Xenopus embryo.* Dev Biol, 1987. **119**(2): p. 560-78.
54. Northcott, P.A., et al., *Medulloblastomics: the end of the beginning.* Nat Rev Cancer, 2012. **12**(12): p. 818-34.

CURRICULUM VITAE

Rivka Noelanders

Stationsstraat 48, 9860 Scheldewindeke, Belgium
10-03-1989 | +32 (0) 494 91 58 34 | rivka.noelanders@irc.ugent.be

Professional Experience

Oct 2012 – current

PhD in Biotechnology | Ghent University | Prof. Dr. K. Vleminckx

Topic: *Wnt/β-catenin signaling in the Xenopus hindbrain during development and tumorigenesis*

Funded by scholarship of the Research Foundation – Flanders (FWO Vlaanderen)

Education

Sept 2007 – June 2012

BSc and MSc in Biomedical Sciences | Ghent University | Prof. Dr. C. Ampe
major Neuroscience | Greatest distinction

Thesis title: *de rol van beta-actine in migratie en differentiatie van neurale kamcellen (Function of beta-actin during migration and differentiation of neural crest cells)*

Additional education

2017	Leadership foundation course	Dan Steer, Ghent University
2012	International developmental biology course	UPMC, Paris
2011	Laboratory Animal Science: FELASA C	Ghent University

Teaching and Research Training Activities

Guidance of practical exercises

2013-2017 assistance lab session developmental biology
Bachelor biochemistry and biotechnology

2013 guidance internship Tieneke Ruts: *Analysis of Wnt target genes during organogenesis*
Master biochemistry and biotechnology

Supervision of MSc theses

2012-2013 Dmitry Khalenkow: *Investigating the mechanisms underlying organ-specific transcriptional responses to Wnt signaling*
Master biochemistry and biotechnology

2014-2015 Bart Dequeker: *Genome editing by CRISPR/Cas9 to analyze the Wnt pathway in the rhombomere boundar*ies
Master biochemistry and biotechnology

2014-2016 Imane El Fakhar: *Een medulloblastoma-model in Xenopus tropicalis door middel van de CRISPR/Cas9 techniek (A Xenopus tropicalis medulloblastoma model through CRISPR/Cas9-mediated gene editing)*
Master biomedische wetenschappen

Supervision of foreign exchange programme internships

2013-2014 Andrzej Kozlowski: *The role of the Wnt signaling pathway in the regulation of proliferation of neural progenitors in the embryonic Xenopus hindbrain*

Publications

Wnt/β -catenin signaling antagonizes Notch signaling and induces proliferation in the *Xenopus* rhombomere boundaries
BMC Biology (under revision)
Noelanders R, Dequeker B, Kozlowski A, Van Isterdael G and Vleminckx K.

How Wnt signaling builds the brain: bridging development and disease
The Neuroscientist. 2016 Sept 13;23(3):314-29.
Noelanders R and Vleminckx K.

Beta-actin is required for proper mouse neural crest ontogeny
PLoS One. 2014 Jan 7;9(1):e85608.
Tondeleir D, Noelanders R, Bakkali K, Ampe C.

Presentations

Oral presentation

2016	Hot Science, Cool talks	*Ghent, Belgium*
2015	IUAP meeting DevRepair	*Leuven, Belgium*

Poster presentation

2017	European Amphibian Club	*Rennes, France*
2017	Brain Tumor meeting	*Berlin, Germany*
2016	Oncopoint meeting	*Ghent, Belgium*
2015	BSCDB meeting	*Leuven, Belgium*
2014	International Xenopus meeting	*Monterey, USA*
2014	BSCDB meeting	*Antwerp, Belgium*
2013	Morphogen gradients meeting	*Oxford, UK*
2013	BSCDB meeting	*Liege, Belgium*